

EMSEV 2018

Electro-Magnetic Studies of Earthquakes and Volcanoes

International Workshop

Potenza, Italy

September 17-21, 2018

ABSTRACTS

Integrating Geophysical
Observations
from Ground to Space
for Earthquake and
Volcano Investigations



EMSEV 2018 International Workshop

Potenza, Italy
September 17-21, 2018



ABSTRACTS

Integrating
Geophysical
Observations
from Ground to Space
for Earthquake and
Volcano Investigations

***Video Message of Prof. Uyeda (first EMSEV Chair)
to the EMSEV 2018 participants***



... EMSEV was established in early days of the century by rather a few colleagues. However, ever since EMSEV has been recognized as one of the most active working groups in IUGG, mainly thanks to our friends like Jacques Zlotnicki, Malcolm Johnston and Toshi Nagao.

I'm told this year hundred scientists will get there in Potenza. I have to thank Prof. Tramutoli and Lapenna for that, and I wish a good success of the meeting.

Scientific Committee:

Jacques ZLOTNICKI, (*Chairperson*) - National Centre for Scientific Research, France

Malcolm JOHNSTON, (*co-Chair*) - US Geological Survey, USA

Toshiyasu NAGAO, (*co-Chair*) - Tokai University, Japan

Xuhui SHEN, (*co-Chair*) - Center of Earthquake Observation from Space, China

Valerio TRAMUTOLI, (*co-Chair*) - University of Basilicata, Italy

Honorary Chairperson:

Antonio MELONI, Institute of Geophysics and Volcanology, Italy

Domenico PATELLA, University Federico II of Naples, Italy

Seiya UYEDA, University of Tokyo, Japan

Scientific Committee Members (National):

Roberto BATTISTON, Italian Space Agency - ASI (*President*)

Carlo DOGLIONI, National Institute of Geophysics and Volcanology - INGV (*President*)

Maria Cristina PEDICCHIO, National Institute of Oceanography and Experimental Geophysics - OGS (*President*)

Aurelia SOLE, University of Study of Basilicata - UNIBAS (*Rector*)

Francesca BIANCO, Vesuvius Observatory, Napoli (*Director*)

Riccardo LANARI, Institute for Electromagnetic Sensing of the Environment - IREA-CNR (*Director*)

Vincenzo LAPENNA, Institute of Methodologies for Environmental Analysis - IMAA-CNR (*Director*)

Pier Francesco BIAGI, University of Bari

Vincenzo CUOMO, Institute of Methodologies for Environmental Analysis - IMAA-CNR

Angelo DE SANTIS, National Institute of Geophysics and Volcanology - INGV

Maurizio FEDI, University Federico II of Naples

Fabrizio FERRUCCI, University of Calabria

Francesco MARCHESE, Institute of Methodologies for Environmental Analysis - IMAA-CNR

Nicola PERGOLA, Institute of Methodologies for Environmental Analysis - IMAA-CNR

Piergiorgio PICOZZA, University of Rome Tor Vergata

Carmine SERIO, University of Basilicata

Agata SINISCALCHI, University of Bari

Roberto SULPIZIO, University of Bari

Luciano TELESCA, Institute of Methodologies for Environmental Analysis - IMAA-CNR

Umberto VILLANTE, University of L'Aquila

Scientific Committee Members (International):

Alik ISMAIL-ZADEH, IUGG Secretary-General, Azerbaijan

Brijesh K. BANSAL, Ministry of Earth Sciences, Geoscience Division, India

Jan BLECKI, Polish Academy of Sciences - PAS, Poland

Xuebin DU, Lanzhou Institute of Seismology, CEA, China

Friedemann FREUND, NASA Ames Research Center, USA

Mikhail B GOHKBERG, Russian Academy of Sciences - RAS, Russia

Takeshi HASHIMOTO, Hokkaido University, Japan

Katsumi HATTORI, Chiba University, Japan

Masashi KAMOGAWA, Tokyo Gakugei University, Japan

Yuri KOPYTENKO, Russian Academy of Sciences - RAS, Russia

Valery KOREPANOV, Lviv Centre Institute for Space Research of National Academy of Sciences, Ukraine

Jean-Louis LE MOUEL, Institute de Physique du Globe de Paris - IPGP, France

Jann Yenq LIU, National Central University, Taiwan

Mioara MANDEA, IAGA GENERAL Secretary, France

Dimitar OUZOUNOV, Chapman University, USA

Michel PARROT, Centre National de la Recherche Scientifique LPC2E/CNRS, France

Sergey Alexander PULINETS, Russian Academy of Sciences - RAS, Russia

Nicholas SARLIS, University of Athens, Greece

Ramesh SINGH, Chapman University, USA

Dimitru STANICA, Romanian Academy, Romania

Filippos VALLIANATOS, Technological Educational Institute of Crete, Greece

Panayiotis VAROTSOS, University of Athens, Greece

Local Organizing Committee

Valerio TRAMUTOLI, (Chair) University of Basilicata

Nicola PERGOLA, (co-Chair) Institute of Methodologies for Environmental Analysis - IMAA-CNR

Angelo DE SANTIS, National Institute of Geophysics and Volcanology - INGV

Agata SINISCALCHI, University of Bari

Livio CONTI, Uninettuno University and INFN

Gianfranco CIANCHINI, National Institute of Geophysics and Volcanology - INGV

Gilda CURRENTI, National Institute of Geophysics and Volcanology - INGV-CT

Domenico DI MAURO, National Institute of Geophysics and Volcanology - INGV

Carolina FILIZZOLA, Institute of Methodologies for Environmental Analysis -- IMAA-CNR

Nicola GENZANO, University of Basilicata

Teodosio LACAVA, Institute of Methodologies for Environmental Analysis - IMAA-CNR

Mariano LISI, University of Basilicata

Rosalba NAPOLI, National Institute of Geophysics and Volcanology - INGV-CT

Zaccaria PETRILLO, National Institute of Geophysics and Volcanology - INGV

Sabatino PISCITELLI, Institute of Methodologies for Environmental Analysis - IMAA-CNR

Gerardo ROMANO, University of Bari

Enzo RIZZO, Institute of Methodologies for Environmental Analysis - IMAA-CNR

Preface**EMSEV 2018 - Potenza, Italy**

Early in the 1960's the international community began to organize meetings related to electromagnetic phenomena related to earthquakes and volcanoes. In 1995, The University of Napoli and the National Institute of Geophysics and Volcanology organized a first international meeting called 'Magnetic, Electric and electromagnetic Methods in Seismology and Volcanology (MEEMSEV)' at Positano, Italy. A second MEEMSEV meeting was located at Chania, Greece, in 1999. Then, meetings were merged in EMSEV activities.

The strong interest in Electromagnetic Studies related to Earthquakes and Volcanoes shown by a large multi-disciplinary international community motivated the International Union of Geodesy and Geophysics ([IUGG](http://www.iugg.org), <http://www.iugg.org>) to create an international Inter-Association Working Group called EMSEV for "Electromagnetic Studies of Earthquakes and Volcanoes" (<http://www.emsev-iugg.org/emsev/>). Professor Seiya Uyeda from Japan became the first chair and managed EMSEV for many years. He brought into light the best observations in the monitoring of earthquakes and volcanoes and promoted the key results regarding the physical processes leading to the genesis of earthquakes and volcanic eruptions.

Since its foundation in 1999 at the Birmingham IUGG meeting, the International Union of Geodesy and Geophysics (IUGG, <http://www.iugg.org>), and the three International IUGG Associations of Geomagnetism (IAGA, <http://www.iugg.org/iaga/>), Volcanology and Chemistry of the Earth's Interior (IAVCEI, <http://www.iavcei.org/>), and Seismology and Physics of the Earth's Interior (IASPEI, <http://www.iaspei.org/>) strongly support EMSEV and promote its activities.

Within this framework, EMSEV is focused on investigating the tectonic and geological setting of active faults and active volcanoes as well as the physical and dynamical processes leading to fault rupture and volcanic eruptions.

EMSEV supports new research and findings in electromagnetism, integration of new methodologies and inclusion of other geophysical data to describe, monitor, analyze, and model fault systems and volcanoes.

EMSEV objectives are:

- evaluation and the promotion of advanced studies in the electromagnetic field through international cooperation, conferences and workshops, and high levels international publications
- integration of electromagnetic methods together with other geophysical techniques to identify physical processes on all scales before, during and after earthquakes and volcanic eruptions

- organization and management of international and regional workshops including sponsorship of sessions at international meetings that describe these results and
- participation in educational programs relating observed results to reduction of earthquake and volcanic hazards.

The EMSEV International meetings are held every two years and are organized by many teams around the world who are actively involved in electromagnetic studies: Moscow (Russia) in 2002, La Londe les Maures (France) in 2004, Agra (India) in 2006, Sinaia (Romania) in 2008, Chapman (USA) in 2010, Shizuoka (Japan) in 2012, Konstancin (Poland) in 2014, Lanzhou (China) in 2016.

Today, it is an immense pleasure to come back to Italy where a large scientific community is working hard on the understanding of earthquakes and volcanic eruptions as well as on the possible methods to foresee the onset of these events.

This meeting involves a very large community (more than 300 researchers, 100 speakers coming from 25 different countries and 4 continents) as the high level communications written in this book attests it. New findings and perspective will emerge from this meeting.

Jacques Zlotnicki (EMSEV Chair)

Malcolm Johnston (EMSEV co-Chair)

Toshiyasu Nagao (EMSEV Secretary)

Nicola Pergola and Valerio Tramutoli (EMSEV 2018 LOC chairs)

Index

Chapter 1 CSES Mission concept and preliminary results

Preliminary Results of the CSES Mission	
<i>X. Shen, S. Yuan, J. Huang, X. Zhu, X. Zhang, Y. Yang, S. Zhao</i>	16
The Italian contribution to the CSES satellite missions	
<i>G. Ambrosi, R. Battiston, L. Conti, A. Contin, A. De Santis, C. De Santis, R. Iuppa, G. Osteria, P. Picozza, M. Ricci, R. Sparvoli, P. Ubertini, S. Zoffoli, CSES-LIMADOU Collaboration.....</i>	18
Result analysis on electron density inverted by GNSS occultation of CSES	
<i>Y. Cheng, Z. Zhou, X. Wan, J. Huang, J. Han.....</i>	19
HEPD: the instrument, the first data and the analysis method for investigating seismo-associated perturbations	
<i>L. Conti, G. Ambrosi, R. Battiston, A. Contin, A. De Santis, C. De Santis, R. Iuppa, G. Osteria, P. Picozza, M. Ricci, R. Sparvoli, P. Ubertini, S. Zoffoli, CSES-LIMADOU Collaboration.....</i>	20
The Italian electric field detector for space observations	
<i>L. Conti, R. Ammendola, D. Badoni, I. Bertello, P. Cipollone, C. De Santis, P. Diego, F. Fiorenza, G. Masciantonio, P. Picozza, R. Sparvoli, P. Ubertini, G. Vannaroni, CSES-LIMADOU Collaboration.</i>	21
Plasma analyzer package onboard CSES satellite	
<i>Y. Guan, A. Zhang, X. Zheng, C. Liu, Z. Tian, W. Wang, L. Kong, J. Ding, Y. Sun.....</i>	22
Electric response to ground-based signals	
<i>J. Huang, W. Li, S. Zhao</i>	23
A Cross-Validation Method for Electromagnetic Sensors on the Same Platform	
<i>Z. Li, J. Zhang, C. Li, G. Liu, X.H. Zhu, X. Li, P. Du.....</i>	24
The Langmuir probe payload on CSES: Scientific Objectives, Methods and Preliminary result	
<i>C. Liu, Y. Guan, A. Zhang, X. Zheng, Y. Sun.....</i>	25
The introduction of data processing and products of the Tri-Band Beacon onboard the China Seismo-electromagnetic Satellite (CSES)	
<i>H.X. Lu, S.F. Zhao, J. Huang, X. Shen.....</i>	27
Seismo-magnetic measurements from the Coupled Dark State Magnetometer (CDSM) aboard the China Seismo-Electromagnetic Satellite (CSES) mission	
<i>K. Schwingenschuh, G. Prates, W. Magnes, X. Shen, J. Wang, A. Pollinger, Ch. Hagen, R. Lammegger, M. Ellmeier, H.U. Eichelberger, D. Wolbang, M.Y. Boudjada, B.P. Besser, A.A. Rozhnoi, M. Delva, I. Jernej, Ö. Aydogar, R. Leonhardt</i>	28
The preliminary results of the search coil magnetometer (SCM) onboard the CSES	
<i>Q. Wang, L. Zeng, J. Huang.....</i>	32
The Langmuir Probe Onboard ZH-1: inversion analysis method commission test and preliminary results	
<i>R. Yan, X. Shen, J. Huang, Y. Guan, C. Liu</i>	33

The Data Quality Evaluation System for China Seismo-Electromagnetic Satellite <i>J. Zhang, X. Li, C. Li, Z. Li, P. Du, G. Liu, X.H. Zhu, X. Yuan</i>	34
The new application results on CSES <i>X. Zhang, S. Zhao, X. Ouyang, Z. Zeren, Y. Wu, Y. Wang, X. Shen, J. Huang</i>	35
Chapter 2 Electromagnetic methods for seismicity and volcano monitoring	
Electromagnetic observation addressed to the short-term earthquake prediction research in VLF band <i>T. Nagao, J. Izutsu, M. Kamogawa, Y. Orihara, S. Sugiura, H. Kondo</i>	37
Volcanic activity over 40 years of la Soufrière of Guadeloupe inferred by electromagnetic studies. Teaching for other volcanoes <i>J. Zlotnicki, G. Vargemezis, J.L. Le Mouël</i>	38
A review of recent attempts on natural time analysis as well as on Seismic Electric Signals worldwide <i>N.V. Sarlis, E.S. Skordas, M.S. Lazaridou-Varotsos, P.A. Varotsos</i>	41
Simultaneous Radiation Belt Electron Precipitation and broad band (~1-20kHz) VLF activity in the Ionosphere as an Earthquake precursor <i>G. Anagnostopoulos, A. Karli</i>	45
Space Weather and Seismicity (1993-2015) <i>G. Anagnostopoulos, A. Karli, A. Rigas, I. Spyroglou</i>	46
Application of a robust analysis for the detection and characterization of the Seismo-Electromagnetic Signals observed in Southern Italy <i>M. Balasco, A.E. Pastorella, G. Romano, A. Siniscalchi</i>	47
Active seismo-electromagnetic experiment in the Solfatara crater (Campi Flegrei, Italy) <i>M. Balasco, G. Romano, A. Siniscalchi, S. Tripaldi</i>	48
Geophysical observations for the shallow structure reconstruction of the Stracciacappa maar (Sabatini Volcanic District, central Italy) <i>J. Bellanova, G. Calamita, A. Perrone, I. Gaudiosi, S. Giannini, M. Mancini, M. Moscatelli, F. Polpetta, R. Razzano, M. Simionato, P. Sirianni, G. Sottilli, G. Vignaroli, A. Pagliaroli, G. Lanzo, A. Avalle, S. Piscitelli</i>	50
Integration of geophysical and engineering analysis of the possible causes of different damage observed after the 2016 Central Italy Earthquakes: the case of Pescara del Tronto and Vezzano villages <i>G. Calamita, J. Bellanova, L. Chiauzzi, M.R. Gallipoli, A. Masi, A. Perrone, S. Piscitelli, G. Santarsiero, T.A. Stabile, L. Vignola</i>	51
Recurrence plot measures of complexity and its applications to self-potential time series arising from a Mexican seismic zone <i>F. Cervantes-De La Torre, J.I. Gonzalez-Trejo, C.A. Real-Ramirez</i>	52
Tectonic plate tension as the source of noise in the geomagnetic field, measured at the PIA geomagnetic observatory (Piran, Slovenia) <i>R. Čop</i>	61
Features of earthquake preparation in the Central and South-Western parts of the Baikal rift according to the tectonomagnetic monitoring data <i>P. Dyadkov, A. Duchkova, D. Kuleshov, L. Tsibizov, M. Kozlova, Y. Romanenko</i>	66

An electric cloud model for the signals recorded in Central Italy during intense seismic swarms <i>C. Fidani</i>	68
New Deep Electrical Resistivity Tomography in the High Agri Valley basin (Basilicata, Southern Italy) <i>V. Giampaolo, L. Capozzoli, E. Rizzo</i>	72
Statistical Analysis and Assessment of ULF Magnetic Signals in Japan as Potential Earthquake Precursors <i>K. Hattori, P. Han</i>	76
Groundwater Electrical Conductivity signal processing and earthquake precursors <i>N. Inbar, Y. Reuveni, S. Agibayev</i>	77
Quality Assessment of Long Term Magnetometer Array Data: Lessons Learned from the QuakeFinder Dataset <i>K.N. Kappler, T.B. Bleier, L.S. MacLean, D.D. Schneider</i>	82
Investigation of lower ionosphere properties in correlation with Romanian seismic activity using VLF/LF radio waves propagation and GPS/GNSS analysing techniques <i>I.A. Moldovan, C. Oikonomou, A. Muntean, V.E. Toader, P.F. Biagi, A. Constantin, D.D. Toma, E. Nastase, A. Moldovan</i>	83
Modelling magnetic pulse swarms that anticipated the 2016 Norcia, and 2017 Capitignano, Central Italy earthquakes <i>M. Orsini, C. Fidani</i>	87
Progress in VHF pre-seismic emission studies <i>Yu. Ruzhin, V.M. Sorokin</i>	90
Anomalous Changes in the MT impedances during February 2015 Seismo-Volcanic Crisis in Taal Volcano (Philippines): Recurrence of the 2010-2011 Event? <i>Y. Sasai, P.K.B Alanis, P. Reniva , M. Uyeshima, T. Nagao, J. Zlotnicki, M.J.S. Johnston, PHIVOLCS EM Team</i>	94
Model for generation of geomagnetic perturbation in the ionosphere due to tsunami <i>V.M. Sorokin, A.K. Yashchenko, V.V. Surkov</i>	98
Ground-Based Geomagnetic Signature related to the Mw 8.1 Earthquake (Chiapas, Mexico), on September 8 th 2017 <i>D.A. Stănică, D. Stănică</i>	99
Identification and Prediction of Destructive Earthquakes <i>X. Zeng, Y. Zeng, L. Shi, J. Zeng</i>	103

Chapter 3 Investigation of active faults and volcanoes based on satellite remote sensing

New perspectives on regional and national scale surface deformation analysis through advanced space-borne radar interferometry techniques <i>R. Lanari</i>	109
From ERS-1 to Sentinel-1: 25 years of radar interferometry investigations on the Neapolitan active volcanic district surface deformations <i>M. Bonano, F. Casu, C. De Luca, R. Lanari, M. Manunta, M. Manzo, G. Onorato, I. Zinno</i>	113

Swarm satellite constellation to study the possible effect of large earthquakes to the ionosphere <i>A. De Santis, D. Marchetti, G. Cianchini, R. Di Giovambattista, L. Perrone, A. Piscini, A. Ippolito, C. Cesaroni, L. Spogli.....</i>	117
Investigating the possible correlation of atmospheric ozone variability with earthquakes: The case of Greece <i>M.N. Efstathiou, P.K. Varotsos</i>	118
Is there a precursory signal of the surface air-temperature variability for earthquakes? <i>M.N. Efstathiou, P.K. Varotsos</i>	121
Investigating volcanic ash phenomena from space by means of Himawari-8 data <i>A. Falconieri, F. Marchese, N. Pergola, V. Tramutoli.....</i>	123
Correlations between VAB electron loss detected by NOAA and strong seismic activity used to improve forecasting of $M \geq 6$ earthquakes <i>C. Fidani.....</i>	124
On the potential of Robust Satellite Techniques (RST) to investigate TIR signatures associated to impending earthquakes <i>N. Genzano, C. Filizzola, M. Lisi, N. Pergola, V. Tramutoli</i>	128
Monitoring Mt. Etna thermal activity by means of RST _{VOLC} system <i>F. Marchese, A. Falconieri, T. Lacava, G. Mazzeo, N. Pergola, V. Tramutoli.....</i>	129
Pre-earthquake chain processes in occasion of the 2016-2018 seismic sequence in Central Italy from ground and space observations <i>D. Marchetti, A. De Santis, A. Piscini, S. D'Arcangelo, F. Poggio</i>	130
Integration of field surveys and remote sensing techniques for seismic damage assessment <i>A. Masi, L. Chiauzzi, G. Nicodemo</i>	131
Research on electron density of Swarm satellites based on DWT <i>K. Zhu, M. Fan, K. Li, C. Chi, Z. Yu</i>	133

Chapter 4 Magnetospheric, ionospheric and atmospheric phenomena associated with seismic activities

Seismo-ionospheric precursors of the 2017 M7.3 Iran-Iraq Border Earthquake and the 2018 M5.9 Osaka Earthquake observed by FORMOSAT-5/AIP <i>J.Y. Liu, iSTEP/CAPE groups</i>	138
Electromagnetic field observations by the DEMETER satellite in connection with the 2009 L'Aquila Earthquake <i>I. Bertello, M. Piersanti, M. Candidi, P. Diego, P. Ubertini.....</i>	139
The INFREP Cooperation: Recent Results <i>P.F. Biagi, R. Colella, L. Schiavulli, A. Ermini, M. Boudjada, H. Eichelberger, K. Schwingenschuh, K. Katzis, M. Kachakhidze, M.E. Contadakis, C. Skeberis, I.A. Moldovan, H.G. Silva</i>	140
The new algorithm for the complex modeling of seismoionospheric coupling (SIC) <i>P.F. Biagi, V.V. Grimalsky, A. Gritsay, V.N. Fedun, A. Krankowski, Yu.G. Rapoport, A. Rozhnoi, M. Solovieva</i>	142
Disturbances in the ionosphere above seismic and thunderstorm areas - Swarm satellite registrations <i>J. Błęcki, J. Ślomiński, R. Wronowski, E. Ślomińska, R. Haagmans</i>	146

A study of the correlation between hazard of large aftershocks and GPS TEC measured after the main shock	
<i>Y. Chen, J.Y. Liu</i>	150
Investigation of Very Low Frequency range of radio waves for the sub-ionospheric perturbations associate with Turkey earthquakes	
<i>Su. Choudhary, A.K. Gwal, G. Lather, R. Gour, J. Lohiya</i>	151
Development and assessment of a robust GPS-TEC data analysis (RST_{TEC}) for the identification of ionospheric perturbations possibly related to impending earthquakes: the case of L'Aquila (April 6 th , 2009, Mw=6.1) earthquake	
<i>R. Colonna, V. Tramutoli</i>	152
Observation of the Ionospheric turbulence modulation by intense seismic activity	
<i>M.E. Contadakis, D.N. Arabelos, G.S. Vergos</i>	154
Some aspects of low-latitude upper atmosphere response to impact from above and below	
<i>A. Depueva, V. Depuev, Yu. Ruzhin, M. Devi, A.K. Barbara</i>	155
Atmospheric waves as Earthquake Precursive Index	
<i>M. Devi, A.K. Barbara, A. Depueva</i>	157
Perturbation features imprinted on ionosphere by successive clusters of strong earthquakes with epicenters in the East-West Pacific zone: Role of atmospheric coupling dynamics	
<i>M. Devi, S. Patgiri, A.K. Barbara, V. Depuev, A. Depueva, Yu. Ruzhin</i>	159
A tsunami early warning system using GNSS-TEC data	
<i>M. Kamogawa, T. Nagao, Y. Orihara</i>	161
Origin of Pre-seismic whistler wave intensity attenuation observed by DEMETER satellite	
<i>M. Kamogawa, T. Nagao, Y. Orihara, J.J. Berthelier</i>	162
D-region ionospheric precursors and its earthquake predictability	
<i>M. Kamogawa, T. Nagao, Y. Orihara, J.J. Berthelier</i>	163
Atmospheric Parameter Measurements for Earthquake Forecast at Kanto, Japan: Case studies for regional earthquakes and the 2018 Boso Slowslip Event	
<i>H. Kojima, J. Omura, C. Yoshino, K. Hattori, M. Shimo, T. Konishi, R. Furuya, K. Ninagawa, D. Ouzounov</i>	164
Space weather and earthquakes	
<i>V. Novikov, Yu. Ruzhin, V. Sorokin, A.K. Yashchenko</i>	165
The lower ionospheric perturbations related to the strong earthquakes in Southern Europe in 2014 and 2016	
<i>A. Rozhnoi, M. Solovieva, P.F. Biagi, M.Y. Boudjada, K. Schwingenschuh, H.U. Eichelberger, M. Hayakawa, V. Fedun</i>	169
Pre-seismic Ionospheric Anomalies Detected Before the 2016 Taiwan Earthquake with M=6.4	
<i>K. Umeno, S. Goto, R. Uchida, K. Igarashi, C.H. Chen</i>	173

Chapter 5 Theoretical and laboratory studies for understanding seismic and volcanic phenomena

Landslide monitoring test based on self-potential method <i>K.Y. Hu, Q.H. Huang</i>	175
Integrated GPR and Structural surveys at the Consoli Palace of Gubbio (Italy) <i>I. Catapano, N. Cavalagli, F. Ubertini, F. Soldovieri, G. Padeletti</i>	176
Modeling of gravity and magnetic anomalies to reduce the general geophysical ambiguity <i>M. Fedi</i>	180
Self-potential, Ground-tilt and Infra-Red Emission Associated with Geyser Eruptions: Implications for Monitoring Volcanic Activity <i>M.J.S. Johnston</i>	181
Multifractal analysis of telluric time series along the Hellenic Subduction Zone <i>G. Michas, J. Makris, F. Vallianatos</i>	183
Micro-ERT laboratory measurements for seismic liquefaction study <i>R. Mollica, R. de Franco, G. Caielli, G. Boniolo, G.B. Crosta, R. Castellanza, A. Villa, A. Motti</i>	185
New algorithms as robust procedure for Geohazards climatological precursor assessment <i>A. Piscini, D. Marchetti, A. De Santis</i>	189
A complexity view into the physics of precursory accelerating seismicity <i>F. Vallianatos, G. Chatzopoulos</i>	190
On the way to electromagnetic earthquake control: Results of forty-year field and lab experiments on injection of DC electrical pulses into the Earth crust <i>V. Zeigarnik, A. Avagimov, V. Novikov, A. Rybin, G. Schelochkov, V. Bragin, V. Sychev, L. Bogomolov, N. Tarasov</i>	191

Chapter 6 Earthquake and volcano related phenomena investigation by multidisciplinary and multi-parametric approaches

Intergeospheres interaction as a source of earthquake precursor's generation <i>S. Pulinets, D. Ouzounov</i>	195
Local and regional stress-forecasting from Covasna fault, Romania <i>A. Apostol, I.A. Moldovan, V. Toader, A. Muntean, A. Mihai</i>	196
Earthquake Prediction Preparedness and Disaster Management Studies in an around Nepal region <i>Sh. Choudhary, Su. Choudhary</i>	198
A multidisciplinary geophysical approach to unravel geothermal processes in volcanic areas <i>G. Currenti, R. Napoli</i>	199
Characteristics of Optical and Microwave responses of land and meteorological parameters Associated with Earthquakes <i>F. Jing, R.P. Singh</i>	202
Are deep-sea fish appearances an earthquake precursor? <i>Y. Orihara, M. Kamogawa, Y. Noda, T. Nagao</i>	203

Experimental study of Radon activity associated with pre-earthquake phenomena observed in the Earth atmosphere-ionosphere environment <i>D. Ouzounov, S. Pulinets, L.C. Lee, C.C. Fu, V. Karastathis, K. Tsinganos, M. Kafatos, N. Hatzopoulos, G. Eleftheriou, K. Hattori</i>	204
Multi-parameter assessment of pre-earthquake atmospheric -ionospheric signals and their potential for short-term prediction <i>D. Ouzounov, S. Pulinets, J.Y. Liu, K. Hattori, P. Han</i>	205
Transient Effects in Atmosphere and Ionosphere preceding the 2015 M7.8 and M7.3 Gorkha–Nepal earthquakes <i>D. Ouzounov, A. Rozhnoi, S. Pulinets, D. Davidenko, M. Solovieva, V. Fedun, A. Srivastava, A. Rybin</i>	206
Ground geochemical observations for Earthquake and Volcano investigations: the example of the Geochemical Monitoring Network of Tuscany <i>L. Pierotti, G. Facca, F. Gherardi</i>	207
Compatibility of different electromagnetic precursors in terms of critical dynamics <i>S.M. Potirakis, Y. Contoyiannis, T. Asano, A. Schekotov, M. Hayakawa, K. Eftaxias</i>	212
A decision making system using Deep Learning for earthquake prediction by means of electromagnetic precursors <i>S.M. Potirakis, P. Kasnesis, C.Z. Patrikakis, Y. Contoyiannis, N.A. Tatlas, S.A. Mitilineos, T. Asano, M. Hayakawa</i>	217
Constraining seismic sources using electromagnetic geothermometry: Hengill volcano (Iceland) case study <i>V. Spichak, O. Zakharova, A. Goidina</i>	222
Reliability of precursor phenomena in Vrancea seismic zone <i>V.E. Toader, I.A. Moldovan, C. Ionescu, A. Marmureanu</i>	227
Long-term air ion monitoring applied to earthquake forecasting <i>S. Warden, T. Bleier, K. Kappler</i>	230
Progress and development trend of comprehensive prediction Method for large earthquakes in China <i>Z. Zeng, Y. Deng, Q. Dai, F. Li, G. Hao, Q. Du, V. Sibgatulin</i>	234

Chapter 1

CSES Mission concept and preliminary results

Preliminary Results of the CSES Mission

X. Shen¹, S. Yuan², J. Huang¹, X. Zhu², X. Zhang³, Y. Yang¹, S. Zhao³

¹*Institute of Crustal Dynamics, CEA;* ²*DFH satellite Co. Ltd.;* ³*Institute of Earthquake Forecast, CEA*

China Seismo-Electro Magnetic Satellite (hereafter called ‘CSES’), is the first space-based platform for the earthquake stereo-monitoring system and also the first launched satellite for the national geophysical field detecting mission in China.

CSES uses the CAST2000 micro-platform with the 3-axis stability. Its orbit is solar synchronization circle with descending local time (LT) at 14:00, 5-day revisiting period and 5-year life time. There are 3 types of payloads including 8 payloads onboard CSES: High Precision Magnetism (HPM), Electric Field Detector (EFD), Search Coil Magnetism (SCM), Plasma Analyzer Package (PAP), Langmuir Probe (LAP), High Energetic Particle Package (HEPP), GNSS Radio Occultation (GRO) and Tri-Band Beacon (TBB). In which, the higher energy detector of HEPP was manufactured by Italian National Institute Nuclear Physics, and the scalar detector of HPM was manufactured by Austrian Space Institute. CSES will offer the following products: Geomagnetic field, electromagnetic wave and spectrum; In-situ electron and ion density/temperature, ion drifting velocity; ionospheric structure parameters; Energetic Particle’s flux and counts. These products will strong benefit the related scientific activities, such as the earthquake science and earthquake monitoring, the global magnetism and ionosphere model construction, great earthquake/volcano and magnetic storm analysis and multi-layers coupling mechanism research.

At 15:51 on February 2, 2018, CSES was launched at China Jiuquan Satellite Launching Center. According to the plan, the in-orbit test will last 6 months and be delivered in August, 2018. Up to now, CSES has finished satellite platform test, payloads functional test and part of the performance tests. According to the draft results after a few months commission test, we reach the following points:

(1) The capabilities of CSES meet the general requirement of the project. Besides the common test, some special tests for CSES have been done, including the orbit-seismic belts matching, electromagnetic cleanliness of the platform, mutual interference among the platform and payloads, and different working modes switch, etc. All results are as expectation.

(2) Up to now, the performance test can be concluded that: the electromagnetic cleanliness of the platform meets the design index, and the effect to the payload is limited and could be distinguished clearly; function of each payload generally meet the general requirement of the project; the link and transfer are stable and reliable among satellite-ground measurement and control, data up and downlink, data transformation; data processing progress are updated continuously and the data products come to stable; data management ability almost meet the design.

(3) Based on those data, the global geomagnetic field and ionosphere was achieved which is coherent to IGRF model and IRI model and also to the SWARM observatory. The effect of global VLF signals could also be found clearly from CSES with good space-temporal correspondence.

(4) The in-orbit test of CSES will go on till the end of July. During these time, work will be arranged to better performance, satellite-ground jointly observatory and data quality assessment by the international in-orbit satellite and ground-based resource, earthquakes and geomagnetic storms.

(5) Following the “Announcement on strengthen the China Seismo-Electromagnetic Satellite data arrangement by CNSA and CEA”, CSES data will be open to people in the fields of earthquake, geophysics, space physics, electromagnetic propagation. In August2018, the manual for data products will be distributed and then the data will be announced in succession.

The Italian contribution to the CSES satellite missions

G. Ambrosi¹, R. Battiston^{2,3}, L. Conti^{4,5}, A. Contin⁶, A. De Santis⁷, C. De Santis⁵, R. Iuppa³, G. Osteria⁸, P. Picozza^{9,4,5}, M. Ricci¹⁰, R. Sparvoli^{9,5}, P. Ubertini¹¹, S. Zoffoli²,
CSES-LIMADOU Collaboration

¹*INFN - Sezione of Perugia, V.A. Pascoli, 06123, Perugia, Italy;* ²*Agenzia Spaziale Italiana, Rome,*

Italy; ³*University of Trento and INFN -TIFPA, Povo (TN), Italy;* ⁴*Uninettuno University, Rome, Italy,*

livio.conti@uninettunouniversity.net; ⁵*INFN - Sezione of Roma Tor Vergata, Rome, Italy;* ⁶*University of Bologna*
and INFN - Sezione of Bologna, Bologna, Italy; ⁷*INGV, Rome, Italy;* ⁸*INFN - Sezione of Napoli, Napoli, Italy;*

⁹*University of Tor Vergata, Rome, Italy;* ¹⁰*INFN - LNF, Frascati (RM), Italy;* ¹¹*INAF - IAPS, Rome, Italy.*

The Italian LIMADOU Collaboration participates to the CSES mission for studying seismo-electromagnetic phenomena in space, launched on February 2nd, 2018 , with a 3-axes stabilized spacecraft. The orbit is circular Sun-synchronous, altitude of about 500 km, inclination of about 98°, descending node at 14:00 LT. The payload includes nine instruments: two particle detectors, a Search-Coil Magnetometer, a High Precision Magnetometer, an Electric Field Detector, a Plasma analyzer, a Langmuir probe, a GNSS Occultation Receiver and a Tri-Band Beacon. The LIMADOU collaboration has built the HEPD particle detectors, contributed to develop the EFD electric field detector and participated to the several tests in the plasma chamber in Rome. We summarize the characteristics of the developed instruments and draw the prospective of the CSES-LIMADOU collaboration for the second CSES mission.

Result analysis on electron density inverted by GNSS occultation of CSES

Y. Cheng¹, Z. Zhou¹, X. Wan¹, J. Huang², J. Han¹

¹ Space Star Technology Co., Ltd, Wuhan, China, chengyan_nuc@163.com; ² The Institute of Crustal Dynamics, Beijing, China, 18834815348@163.com;

The CSES which called “Zhang Heng-1” successfully launched on February 2nd, 2018, loaded with GNSS occultation receiver used to detect ionosphere total electron content and electron density. GNSS occultation receiver receives occultation data for ionosphere inversion, which getting a profile of electron density with variety of height. After more than three months of on-orbit testing, more than 40,000 ionosphere occultation events have been generated. The ionosphere electron density profile was compared with the query result of IRI reference model, the COSMIC publication result, and the ionosphere vertical sounding results. Making the day and night coverage picture of global ionosphere occultation events, then analyses it. Preliminary analyzed of ionosphere disturbances at high latitudes and low latitudes. Ionosphere occultation events can cover the globe and reflect the global ionosphere distribution better.

HEPD: the instrument, the first data and the analysis method for investigating seismo-associated perturbations

L. Conti^{1,2}, G. Ambrosi³, R. Battiston^{4,5}, A. Contin⁶, A. De Santis⁷, C. De Santis², R. Iuppa⁵, G. Osteria⁸, P. Picozza^{9,2,1}, M. Ricci¹⁰, R. Sparvoli^{9,2}, P. Ubertini¹¹, S. Zoffoli⁴,
CSES-LIMADOU Collaboration

¹*Uninettuno University, Rome, Italy, livio.conti@uninettunouniversity.net;* ²*INFN - Sezione di Roma Tor Vergata, Rome, Italy;* ³*INFN - Sezione di Perugia, V.A. Pascoli, 06123, Perugia, Italy;* ⁴*Agenzia Spaziale Italiana, Rome, Italy;* ⁵*University of Trento and INFN -TIFPA, Povo (TN), Italy;* ⁶*University of Bologna and INFN - Sezione di Bologna, Bologna, Italy;* ⁷*INGV, Rome, Italy;* ⁸*INFN - Sezione di Napoli, Napoli, Italy;* ⁹*University of Tor Vergata, Rome, Italy;* ¹⁰*INFN - LNF, Frascati (RM), Italy;* ¹¹*INAF - IAPS, Rome, Italy.*

CSES (China Seismo-Electromagnetic Satellite) is a Chinese-Italian space mission dedicated to monitoring electromagnetic fields, plasma parameters and particle fluxes induced by natural sources and artificial emitters in the near-Earth space. The mission aims at extending the DEMETER observations of seismic precursors and in particular the existence of possible (temporal and spatial) correlations between the precipitation of particles from the inner Van Allen belts and the occurrence of seismic events pointed out by analyzing SAMPEX and NOAA data. However, a careful analysis is needed in order to distinguish measurements possibly associated to earthquakes from the large background. Data collected by the mission will also allow to studying solar-terrestrial interactions and phenomena of solar physics, namely CME, flares and cosmic ray solar modulation. CSES has been launched on February 2nd, 2018 with nine instruments (for measuring electric and magnetic fields, plasma parameters and charged particles) for an expected mission lifetime of 5 years. Italy participates to the CSES mission with the LIMADOU Collaboration that has built the High Energy Particle Detector (HEPD) conceived for optimizing detection of high-energy charged particles precipitating from the inner Van Allen belts and participated in developing the electric field detector of the CSES mission. We will present the first preliminary analyses of HEPD data in the calibration procedure and we discuss the method for studying the correlations to be investigated.

The Italian electric field detector for space observations

L. Conti^{1,2}, R. Ammendola², D. Badoni², I. Bertello³, P. Cipollone², C. De Santis², P. Diego³, F. Fiorenza³, G. Masciantonio², P. Picozza^{4,2,1}, R. Sparvoli^{4,2}, P. Ubertini³, G. Vannaroni^{1,3}, CSES-LIMADOU Collaboration

¹*Uninettuno University, Rome, Italy, livio.conti@uninettunouniversity.net;*²*INFN - Sezione di Roma Tor Vergata, Rome, Italy;*³*INAF - IAPS, Rome, Italy;*⁴*University of Tor Vergata, Rome, Italy.*

Within the CSES mission, the LIMADOU collaboration has developed a new high-performance electric field detector for space applications. On the pathway of the observations carried out by DEMETER, the CSES mission can clarify the scenario with a long-term investigation of seismo-electromagnetic phenomena on a global scale. In this framework, we have developed, built and fully tested in laboratory a new electric field detector conceived for measurement in space of signals from quasi DC up to several MHz that is candidate to be installed on the second CSES satellite mission. The new electric field detector can ensure the characteristics need for investigation the seismo-electromagnetic elusive phenomena such as high sensitivity, dynamic range, bit resolution, frequency resolution, number of channels, (hardware and software) redundancy, data reduction and real-time data processing. We present the electric field detector in details together with the tests in laboratory.

Plasma analyzer package onboard CSES satellite

Y. Guan¹, A. Zhang^{1,2}, X. Zheng¹, C. Liu¹, Z. Tian¹, W. Wang¹, L. Kong¹, J. Ding¹, Y. Sun¹

¹*National Space Science Center, Chinese Academy of Science, Beijing, China, gyb@nssc.ac.cn;* ²*University of Chinese Academy of Science, Beijing, China*

Recent tens of years' investigations showed that the earthquake could induce some disturbances in the ionosphere, but the correlation between the seism and the ionosphere perturbations is still poorly understood. The Chinese Seismo Electromagnetic Satellite (CSES), which launched on Feb2, 2018, gives a big opportunity to learn the earthquake in the space view.

The plasma analyzer package (PAP) is one of the scientific payloads of CSES to measure main ion parameters of the ionosphere with three main objectives: (1) Survey the global parameters of the ionosphere in situ, accumulate the data of the ionosphere plasma environment for further research. (2) Provide data for studies of the coupling between earthquake and ionosphere, the dynamics of the ionosphere, the model of the ionosphere and prediction or forecast of the space weather. (3) Try to detect and identify the ionosphere abnormality, which may be coupled with earthquake, and cooperate with the other payloads and ground based observation station to search after the new ways to forecast the severe earthquake.

The PAP includes 3 classic in-situ sensors: retarding potential analyzer (RPA), ion drift meter (IDM), ion capture meter (ICM). The RPA is used to measure ion density, ion temperature; ion composition and ion drift velocity (parallel to the direction of the satellite flight on orbit). The IDM is used to measure ion drift velocity perpendicular to the direction of the satellite flight on orbit. The ICM is used to measure the fluctuation of the ion density.

Before launch, the electronics of the PAP has been calibrated carefully in NSSC. And it has been tested in the plasma chamber of IAPS-INAF, which could produce plasma environment most like the ionosphere environment on the orbit of CESE. All the test results show that PAP works well and its' performances meet the requirements of CSES.

By now, the PAP has been worked about 3 months, and first results showed it works well, but it is still need more work for in-orbit commissioning.

The PAP onboard the CSES satellite is the first plasma analyzer package as a payload on a satellite in China, and it would make a great contribution for the earthquake research

Electric response to ground-based signals

J. Huang¹, W. Li¹, S. Zhao²

¹*Institute of Crustal Dynamics, China Earthquake Administration, Beijing, China, xhhjp@126.com;* ¹*Institute of Crustal Dynamics, China Earthquake Administration, Beijing, China, lwj34329922@163.com;* ¹*Institute of Earthquake Forecasting, China Earthquake Administration, Beijing, China, zsf2008bj@126.com*

The first CSES, named ZH-1, was launched on February 2, 2018. On the satellite, one of the payloads was the Electric Field Detector (EFD), which measures the spatial electric field from DC-3.5MHz. After 6 six months test, EFD payload works smoothly. From February to August, there are some strong earthquakes with magnitude more than 7.0 around the world. And at the same time, there are some VLF transmitters around the globe. It seems that EFD has measured some response to the ground-based signals. Here was also compared with the CSES and DEMETER, which showed the similar trend.

A Cross-Validation Method for Electromagnetic Sensors on the Same Platform

Z. Li^{1,2}, J. Zhang^{1,2}, C. Li^{1,2}, G. Liu^{1,2}, X.H. Zhu^{1,2}, X. Li^{1,2}, P. Du^{1,2}

¹*Key Laboratory of Quantitative Remote Sensing Information Technology, Chinese Academy of Sciences*

²*Academy of Opto-Electronics, Chinese Academy of Sciences*

With the development of earth observation technology, the research on the electromagnetic ionosphere disturbance has become a critical science area. It is the most effective approach to measure the ionospheric disturbance with on-borne instruments. The accuracy of the electromagnetic sensor data directly affects the reliability of earthquake prediction. Similar to the cross-calibration of spaceborne optical payload, a cross-validation method for electromagnetic sensors on the same platform is proposed. Taking DEMETER satellite for example, some same types of data from different sensors (i.e. Langmuir probe and plasma analyzer package) were analyzed. The method supports the cross-validation of electromagnetic sensors on the same platform both in normal and specific space electromagnetic environment. The method has been successfully applied in on-orbit cross-validation for China Seismo-Electromagnetic Satellite (CSES).

The Langmuir probe payload on CSES: Scientific Objectives, Methods and Preliminary result

C. Liu¹, Y. Guan², A. Zhang³, X. Zheng⁴, Y. Sun⁵

¹National Space Science Center, CAS, Beijing, china, liuch@nssc.ac.cn; ²National Space Science Center, CAS, Beijing, china, gyb@nssc.ac.cn; ³National Space Science Center, CAS, Beijing, china, zab@nssc.ac.cn;

⁴National Space Science Center, CAS, Beijing, china, zxz@nssc.ac.cn; ⁵National Space Science Center, CAS, Beijing, china, syq@nssc.ac.cn;

Massive research results show that the ionospheric changes caused by earthquakes are real, and the electromagnetic anomaly is the most sensitive precursor phenomenon. The change of space plasma is the precursor of ionosphere change. The seismic ionosphere disturbances include four aspects: low-frequency electromagnetic disturbances, plasma changes, high-energy particle disturbances, and planetary radiation flux changes. The plasma changes are mainly represented by the abnormal parameters of total electron content (TEC), electron density (Ne), ion density (Ni), electron temperature (Te) and ion temperature (Ti). Langmuir probe (LP) is one scientific payload of The China Seismo-Electromagnetic satellite (CSES). The scientific objective of LP is to measure the electron density and electron temperature of ionospheric plasma, and to obtain ionospheric plasma anomaly information.

The Langmuir probe (LP) consists of sensor 1, sensor 2 and electronics box. The instrument configuration is integrated, as shown in figure 1. The sensor extension bar which length is 50cm is designed to support the sensor away from the satellite surface and to reduce the interference of the satellite. The Langmuir probe is designed to load the scan voltage at the sensor and collect the current to obtain the I-V characteristic curve. The electron density and electron temperature can be obtained by fitting the I-V characteristic curve.

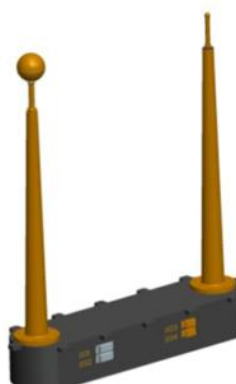


Fig 1. The Langmuir probe diagram

During the development of Langmuir probe, the verify test has been carried out at Institute for Space Astrophysics and Planetology of the Italian National Institute of Astrophysics (INAF-IAPS). The test results of electron density and ion density were consistent with the trend in the plasma chamber, and were close to the test results of the IAPS chamber's diagnostic sensor.

The China Seismo-Electromagnetic satellite (CSES) has been launched and Langmuir probe has been working on track. The preliminary results of Langmuir probe show that the electron density and the electron temperature are within a reasonable range and are consistent with seasonal changes in the ionosphere.

The introduction of data processing and products of the Tri-Band Beacon onboard the China Seismo-electromagnetic Satellite (CSES)

H.X. Lu¹, S.F. Zhao², J. Huang¹, X. Shen¹

¹*Institute of Crystal Dynamic, CEA, Beijing, China, lhx_icd@163.com;* ²*Institute of Earthquake Forecasting, CEA, Beijing, China, zsf2008bj@126.com;*

Tri-Band Beacon(TBB) is one of the main payloads of the CSES mission. It is used to detect the TEC, electron density, and NmF2 of ionosphere in China. The detection principle is to launch three coherent carrier signals from the TBB transmitter on the satellite, the signals will be received by the TBB receiver set up on the ground. Through a certain data processing and inversion, some ionospheric parameters will be inverted over the station chain.

The TBB transmitter works in China area. Before the arrival of the satellite arrival chain, the TBB transmitter works in advance. And the ground TBB receiving system is ready to receive the signal in advance according to the forecast track information. We now have 9 receive station in China.

This report will focus on the data classification of TBB data, the process and algorithm of data processing, and the data products we have now after a period of time running.

Seismo-magnetic measurements from the Coupled Dark State Magnetometer (CDSM) aboard the China Seismo-Electromagnetic Satellite (CSES) mission

K. Schwingenschuh¹, G. Prattes¹, W. Magnes¹, X. Shen², J. Wang³, A. Pollinger¹, Ch. Hagen¹, R. Lammegger⁵, M. Ellmeier¹, H.U. Eichelberger¹, D. Wolbang¹, M.Y. Boudjada¹, B.P. Besser¹, A.A. Rozhnoi⁴, M. Delva¹, I. Jernej¹, Ö. Aydogar¹, R. Leonhardt⁶

¹*Space Research Institute, Austrian Academy of Sciences, Graz, Austria, konrad.schwingenschuh@oeaw.ac.at*

²*Institute of Earthquake Administration, Beijing, China, ³Center for Space Science and Applied Research Chinese Academy of Sciences, Beijing, China, ⁴Institute of the Earth Physics, RAS, Moscow, Russia, ⁵Institute of Experimental Physics, Graz University of Technology, Graz, Austria, ⁶Central Institution for Meteorology and Geodynamics (ZAMG), Vienna, Austria*

We investigate first seismo-magnetic measurements obtained with the new type of scalar magnetometer – the Coupled Dark State Magnetometer (CDSM) [1] – aboard the China Seismo-Electromagnetic Satellite (CSES), launched Feb. 2nd, 2018, from the Jiuquan Satellite Launch Center, China. The total magnetic field data are from the commissioning phase of the CDSM instrument, a characteristic segment of ~35 min. within the geographical latitude range from -65° to 65° is depicted in Fig.1. As an example a whole day with 23 segments is shown in Fig.2.

The CDSM can measure the total magnetic field B_t with a noise level of about 50 pT/sqrt(Hz) from 1000 nT up to 100000 nT in the frequency range between DC and 30 Hz [2; 3]. In order to minimize the stray field of the satellite, the sensor of the scalar magnetometer is mounted at the tip of a 5 m boom. The satellite operates in a Sun synchronous polar orbit, at an altitude of about 550 km, inclination of 97°, and is three axes stabilized [4; 5].

The main scientific objective is the identification of earthquake precursors by the study of ionospheric electromagnetic and plasma phenomena.

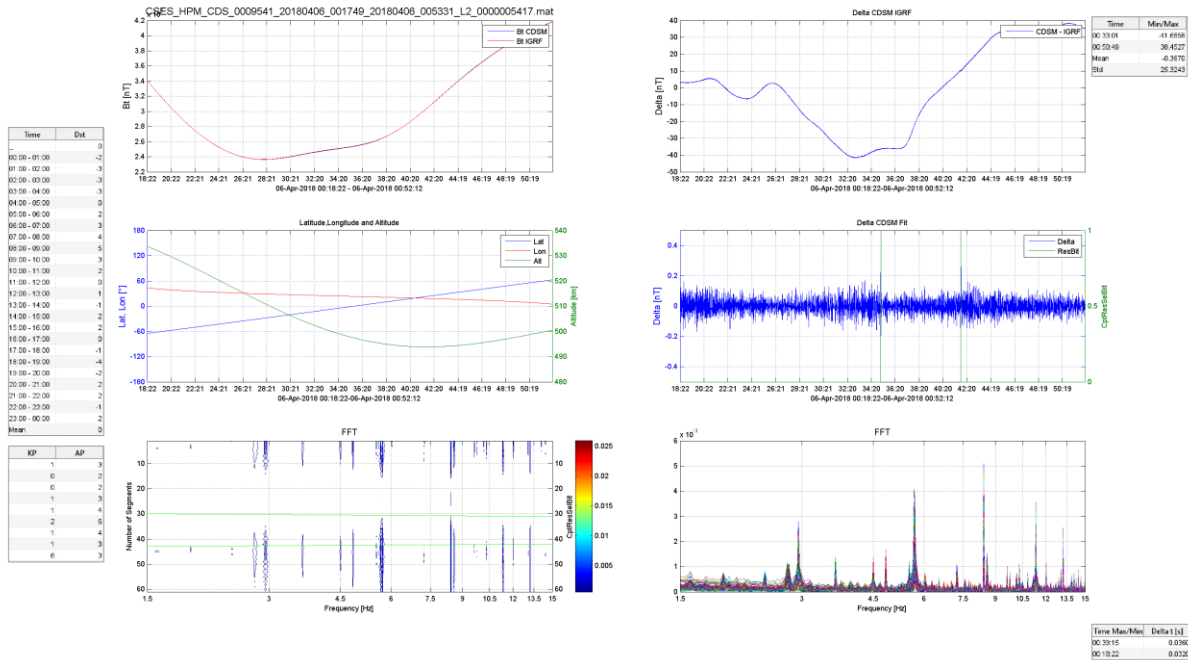


Fig. 1. One of the first CDSM magnetic field measurements aboard CSES from April 6, 2018. Top left: Measured B_t (blue color) compared to the International Geomagnetic Reference Field (IGRF). Top right: Residual from CDSM and IGRF. Centre left: CSES orbital parameters latitude [deg], longitude [deg], and altitude [km]. Centre right: High pass filtered residual signal (polynomial fits for 62 segments); the green lines correspond to switches of the CDSM modes. Bottom left: 62 FFT segments of the high pass filtered residual signal. Bottom right: Individual 62 FFT segments with characteristic peaks from the spacecraft and the environment.

A snapshot of commissioning scalar magnetic field data B_t is shown in Fig.1. The CDSM magnetic field data is in accordance with the IGRF model data. The remaining low frequency component is removed with a polynomial fit (62 segments, 1000 points each, 30 Hz sampling frequency) in order to get variations in sub-nT range. In particular, in the FFT a characteristic non-seismic pattern is visible, this behavior will be considered in the analysis of seismic signals. Since beginning of the CDSM commissioning phase the scalar magnetic fields are constantly monitored and evaluated in order to get knowledge about the systematic behaviour of the instrument.

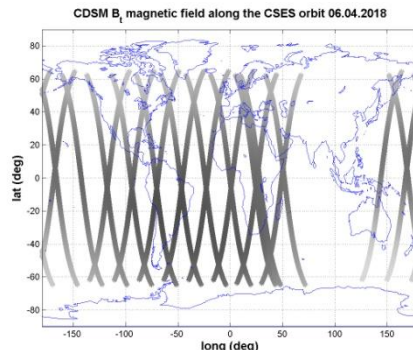


Fig. 2. CDSM magnetic field data (color coded in gray) for all 23 tracks, April 6, 2018. Emphasis is on

the spatial coverage (China is excluded).

In Fig.2. all 23 tracks (April 6, 2018) are visible in color coded format (gray). We consider the data in the mentioned latitude range -65° to 65° except China. In principle, the data coverage is without losses. In scientific terms, the comparison with the French DEMETER (Detection of Electro-Magnetic Emissions Transmitted from Earthquake Regions) mission data, epoch 2004-2010, is of particular interest.

In the science phase of CDSM combined investigations with the CSES instruments and ground based facilities are planned, like past studies [6; 7; 8; 9; 10] related to seismo-electromagnetic topics.

References

- [1] R. Lammegger, WO 2008/151344 A3, Method and Device for Measuring Magnetic Fields, (Patent)
- [2] A. Pollinger, M. Ellmeier, W. Magnes, C. Hagen, W. Baumjohann, E. Leitgeb, R. Lammegger: Enable the inherent omni-directionality of an absolute coupled dark state magnetometer for e.g. scientific space applications. In: Proc. 2012 IEEE International Instrumentation and Measurement Technology Conference (I2MTC), IEEE, Piscataway, NJ, 33-36, doi:10.1109/I2MTC.2012.6229247 (2012)
- [3] A. Pollinger, R. Lammegger, W. Magnes, M. Ellmeier, W. Baumjohann, L. Windholz, CDSM - a new scalar magnetometer, EGU General Assembly 2010, Vienna, May 2010
- [4] W. Lanwei, Analysis on the Payloads of China Seismo-Electromagnetic Satellite, presented at the magnetometer workshop in Jizerka, Czech Republic, March 2014
- [5] X. Shen, X. Zhang, L. Wang, H. Chen, Y. Wu, S. Yuan, J. Shen, S. Zhao, J. Qian, J. Ding, The earthquake-related disturbances in ionosphere and project of the first China seismo-electromagnetic satellite, *Earthquake Science*, 24, 6, 639–650, 2011
- [6] G. Prates, K. Schwingenschuh, H. U. Eichelberger, W. Magnes, M. Boudjada, M. Stachel, M. Vellante, U. Villante, V. Wesztergom, and P. Nenovski, Ultra Low Frequency (ULF) European multi station magnetic field analysis before and during the 2009 earthquake at L'Aquila regarding regional geotechnical information, *NHESS*, 11, 1959-1968, 2011
- [7] O. A. Molchanov, M. Hayakawa, V. A. Rafalsky, Penetration characteristics of electromagnetic emissions from an underground seismic source into the atmosphere, ionosphere and magnetosphere, *JGR*, 100, A2, 1691–1712, 1995
- [8] G. Prates, K. Schwingenschuh, H. U. Eichelberger, W. Magnes, M. Boudjada, M. Stachel, M. Vellante, V. Wesztergom, and P. Nenovski, Multi-point ground-based ULF magnetic field observations in Europe during seismic active periods in 2004 and 2005, *Nat. Hazards Earth Syst. Sci.*, 8, 501–507, 2008
- [9] O. Molchanov, and M. Hayakawa, On the generation mechanism of ULF seismogenic electromagnetic emissions, *Phys. of the Earth and Planet. Int.*, 105, 201-210, 1998
- [10] K. Schwingenschuh, W. Magnes, S. Xuhui, J. Wang, A. Pollinger, Ch. Hagen, R. Lammegger, M. Ellmeier, G. Prates, H. U. Eichelberger, D. Wolbang, M. Y. Boudjada, B.

P. Besser, A. A. Rozhnoi, M. Delva, I. Jernej, Ö. Aydogar, and R. Leonhardt, First seismo-magnetic measurements aboard the China Seismo-Electromagnetic Satellite (CSES) mission, Geophysical Research Abstracts, 20, EGU2018-19013, 2018

The preliminary results of the search coil magnetometer (SCM) onboard the CSES

Q. Wang¹, L. Zeng², J. Huang¹

¹*Institute of Crustal Dynamics, Beijing, China, wangqiaochn@163.com;* ²*Beihang University, Beijing, China, lzeng@buaa.edu.cn;*

Search coil magnetometer (SCM) is a payload onboard the China Seismo-electromagnetic Satellite (CSES), launched on 2nd February 2018.

Its data acquisition system collects the fast variation of geomagnetic vector field at the orbit height, based on the Faraday's Law and the orthogonal tri-axial magnetic sensor design. In order to reduce interference suffering from the satellite platform, the distance from magnetic sensors to the platform is 4.5 meter.

During the Commission Test of six months from February to August, 2018, SCM has accumulated certain amounts of global data. It showed that the instrument is working at a good status and has a good big events acquisition, such as space weather and ionospheric disturbances of ground VLF transmitters and possibly related to large earthquakes of Mexico M7.1 and New Guinea M7.5 in February.

In this talk, its preliminary results including the onboard calibration results, level-2 to level-4's waveform and time-frequency profile, detections of ground VLF transmitters, and ionospheric disturbances possibly related with large earthquakes.

The Langmuir Probe Onboard ZH-1: inversion analysis method commission test and preliminary results

R. Yan¹, X. Shen², J. Huang³, Y. Guan⁴, C. Liu⁵

¹*The Institute of Crustal Dynamics, China Earthquake Administration, Beijing, China.*

Yanxiaoxiao_best@163.com; ²*The Institute of Crustal Dynamics, China Earthquake Administration, Beijing, China, shenxh@seis.ac.cn;* ³*The Institute of Crustal Dynamics, China Earthquake Administration, Beijing, China. xhhjp@126.com;* ⁴*National Space Science Center, China Academy of Sciences, Beijing, China. gyb@nssc.ac.cn;* ⁵*National Space Science Center, China Academy of Sciences, Beijing, China. liuch@nssc.ac.cn*

The ZH-1 (CSES, the China seismic electromagnetic satellite) Langmuir probe experiment, called “LAP”, has been designed for in situ measurements of the bulk parameters of the ionosphere plasma. The two main parameters measured by LAP are the electron density and temperature. In this paper, a brief description of the LAP and of its work mode and of capabilities is provided. Based on the characteristic of the LAP, under the assumptions of ideal plasma environment, the LAP data calibration and analysis method has been discussed and given in use of the approximate theoretical formulas. The commission test and data verification are introduced. Finally, some examples of ‘classical’ ionospheric features and phenomena probably with earthquakes as being observed by LAP are discussed.

The Data Quality Evaluation System for China Seismo-Electromagnetic Satellite

J. Zhang^{1,2}, X. Li^{1,2}, C. Li^{1,2}, Z. Li^{1,2}, P. Du^{1,2}, G. Liu^{1,2}, X.H. Zhu^{1,2}, X. Yuan^{1,2}

¹*Key Laboratory of Quantitative Remote Sensing Information Technology, Chinese Academy of Sciences*

²*Academy of Opto-Electronics, Chinese Academy of Sciences*

The China Seismo-Electromagnetic Satellite (CSES), also called ZHANGHENG-1, is the first satellite for both earthquake observation and geophysical field measurement in China. The satellite was launched successfully on February 2nd, 2018. Quality evaluation of the data product is of importance for satisfying the application requirements. Up to now, Data Quality Evaluation System (DQES) of CSES is designed to support eight instruments data evaluation, such as Search-Coil Magnetometer (SCM), Electric Field Detector(EFD), High Precision Magnetometer (HPM), GNSS Occultation Receiver (GOR), Plasma Analyzer Package(PAP), Langmuir Probe (LAP), High Energetic Particle Package (HEPP), and Tri-Band Beacon (TBB). DQES has two patterns, which are automatic and manual model, and supports three kinds of cross-validations, including cross-validation of different instruments on the same platform, cross-validation of same instrument on different platforms and cross-validation between CSES data and the ground site data. Also, the system implements objective quality evaluation for CSES products.

The new application results on CSES

X. Zhang¹, S. Zhao¹, X. Ouyang¹, Z. Zeren¹, Y. Wu¹, Y. Wang¹, X. Shen², J. Huang²

¹*Institute of Earthquake Forecasting China Earthquake Administration, Beijing, China, zhangxm96@126.com*

²*Institute of Crustal Dynamics, CEA, Beijing, China, shenxh@seis.ac.cn*

The China Seismo-Electromagnetic satellite (CSES, also named as *Zhangheng-1*) has been launched on February 2, 2018, and the recording data has been sent to the ground application center since Feb. 13. During February to July 2018, the in-orbit test has been carried out continuously. There are eight payloads, including high precision magnetometer, Search-coil magnetometer, Electric field detector, GNSS radio occultation receiver, High energetic particle package, Langmuir probe, Tri-band beacon. Three main products are obtained, such as vector and scalar electromagnetic field, in-situ plasma parameters, and electron density profiles. Here we will show some preliminary and new results by using this satellite data.

- 1) As for the in-situ plasma parameters, the research includes: their spatial and temporal evolutional features in northern spring and summer seasons, their comparison and correlation among different parameters, the comparison with ground-based, other satellites observations and IRI model, to illustrate the observing quality of in-situ plasma parameters on CSES;
- 2) As for electromagnetic field and waves, the study consists of: their background spital features at different frequency bands (ULF, ELF, VLF, HF), the artificial source signal selection and analysis, the natural signal analysis from geomagnetic storms, lightning, comparison with IGRF model, other satellite and ground-based geomagnetic field observations, to demonstrate the sensitivity of electromagnetic detection on CSES;
- 3) About the ionospheric profiles, the main research includes: the inversion technique development and optimization, the comparison with ground-based and other satellite observations.
- 4) As for the energetic particles, the research focuses on: the spatial distribution features in electrons and protons, the comparison with other satellite data and models as AP9 or AE9, analysis on wave-particle interaction in particle flus at different energy band with ground-based transmitters.

Chapter 2

Electromagnetic methods for seismicity and volcano monitoring

Electromagnetic observation addressed to the short-term earthquake prediction research in VLF band

T. Nagao¹, J. Izutsu², M. Kamogawa³, Y. Orihara¹, S. Sugiura⁴, H. Kondo⁴

¹*Institute of Oceanic Research and Development, Tokai University, Japan, nagao@scc.u-tokai.ac.jp;* ²*College of Engineering, Chubu University, Japan;* ³*Tokyo Gakugei University;* ⁴*Genesis Research Institute, Inc., Japan*

There have been many reports electromagnetic (EM) waves preceding earthquakes have existed since the 1980s. The late Professor Toshi Asada and his colleagues focused on the VLF band and developed devices and made observations at the Tokai University in the 1990s. As a result, in the apparent arrival direction analysis, the electromagnetic waves, which comes from the epicenter direction were observed. However, after that, the observation was interrupted due to the death of Professor Asada. It seemed promising results, therefore we resumed research from FY 2014. The feature of the present apparatus is that not only the apparent arrival direction analysis but also the wave source determination can be performed using the time difference of arrival (TDOA) of EM waves. Because apparent arrival direction method can only apply when the observed EM wave has a linear polarization. In the wave source determination using TDOA, the arrival time of the EM wave was determined by using the autoregressive model and AIC. We observed EM waves coming from the epicentral region, two days before the earthquake, which occurred in the southern part of Nagano Prefecture on June 25, 2017 (M5.6). This earthquake was the largest one occurred in the vicinity of our observation network at this moment. However, it is highly likely that the EM environment is getting worse even in the VLF band over the past two decades, and by further reviewing the measurement environment, eliminating noise, and improving the program, more accurate wave source position determination will be possible.

Acknowledgments

Concerning the determination program of the arrival time of the EM wave, Dr. Tetsuo Takanami of former Faculty of Science, Hokkaido University, kindly provided us the basic program. We express our sincere thanks here. This study was partly supported by the Ministry of Education, Culture, Sports, Science and Technology (MEXT) of Japan, under its Earthquake and Volcano Hazards Observation and Research Program, research fund of the core-project of Institute of Oceanic Research and Development (IORD), Tokai University and Genesis Research Institute, Inc.

Volcanic activity over 40 years of la Soufrière of Guadeloupe inferred by electromagnetic studies. Teaching for other volcanoes.

J. Zlotnicki¹, G. Vargemezis², J.L. Le Mouël³

¹CNRS, UMR6524-OPGC, Clermont-Ferrand, France, Email: jacques.zlotnicki@wanadoo.fr; ²Aristotle's University of Thessaloniki, Thessaloniki, Greece, Email: varge@geo.auth.gr; ³IPGP, Paris, France, Email: lemouel@ipgp.jussieu.fr.

Soufrière of Guadeloupe volcano is one of the active andesitic stratovolcanoes located along the recent Lesser Antilles arc. The present day activity is surrounded to a 1467 m high mineralized dome built during the last magmatic eruption dated around 1530 AD. The dome is set inside nested horse-shoe shaped Carmichael and Amic craters formed 11,500 and 3,100 years ago (Boudon et al., 1987). During the past 500 years, seven phreatic eruptions have occurred and opened radial fissures and pits craters on the dome. During these eruptions, vertical and laterally-directed blasts, ash fall, debris flows have happened. After the 1956 phreatic eruption, the volcano recovered a very quite state characterized by a low level of seismic and degassing activities. In July 1975, 30 volcano-tectonic earthquakes were recorded and the seismicity gradually increased. Two major swarms of 296 and 2713 events were respectively recorded in November-December 1975 and in March-June 1976. Up to that time, no noticeable raise in the surface activity was noticed (Dorel and Feuillard 1980; Feuillard et al., 1983). After minor landslides along the regional Ty fault and opening of small fissures to the South of the dome in June 1976, the first phreatic explosion started on July 8. 26 explosions were recorded between July 8, 1976 and March 1, 1977, when the seismicity started to recede (Figure 1). The seismicity returned back to the background level after June 15, 1977 (Hincks et al., 2014).



Fig. 1. One of the explosions during the 1976-1977 activity

After the 1976-1977 phreato-magmatic eruption, the seismicity progressively returned to almost a zero level till 1992. During this period of time the degassing activity, the temperature in wells and in the ground, and the surface activity decreased. Mainly, this epoch was characterized by the strong argillization of the blocks forming the dome and its basis stuck up by the surrounding Amic crater walls. The mineralization of rocks is produced by the infiltration of the average 9 m annual rainfalls, the leaching of faults and pits and the upward release of hot magmatic fluids through faults and warm thermal ground fluids emerging at lower altitude (800 to 1200 m in altitude)(Zlotnicki et al., 1994).

Year 1992 was marked by a strong renew of seismic activity which has evolved sporadically, since then. Further seismicity was recorded in February 2018 with earthquakes located between 1.5 and 2 km depth which turned to a large energy release during April and May (Soufrière of Guadeloupe 2018 bulletins, Figure 2).

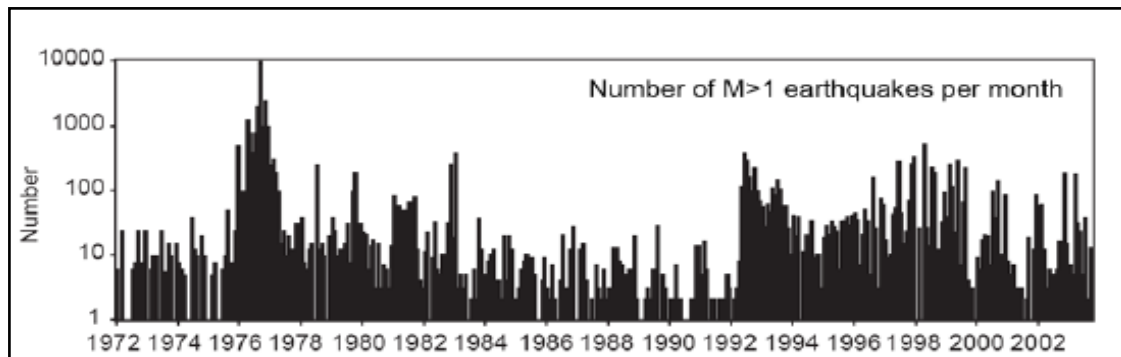


Fig. 2. Monthly number of volcanic earthquakes of magnitude above 1 between 1972 and 2003

Before the 1976-1977 volcanic activity, few geophysical instrumentations were available on the edifice, and it is only during and after the crisis that geophysical prospecting's and monitoring devices were intensely implemented. In particular, magnetic monitoring, self-potential surveys, magnetotelluric, resistivity and VLF soundings have been temporarily carried out (Figure 3). These observations made over 40 years allow to depict the spatial and temporal activity of La Soufrière which seems to enter in a new pre-eruptive stage.

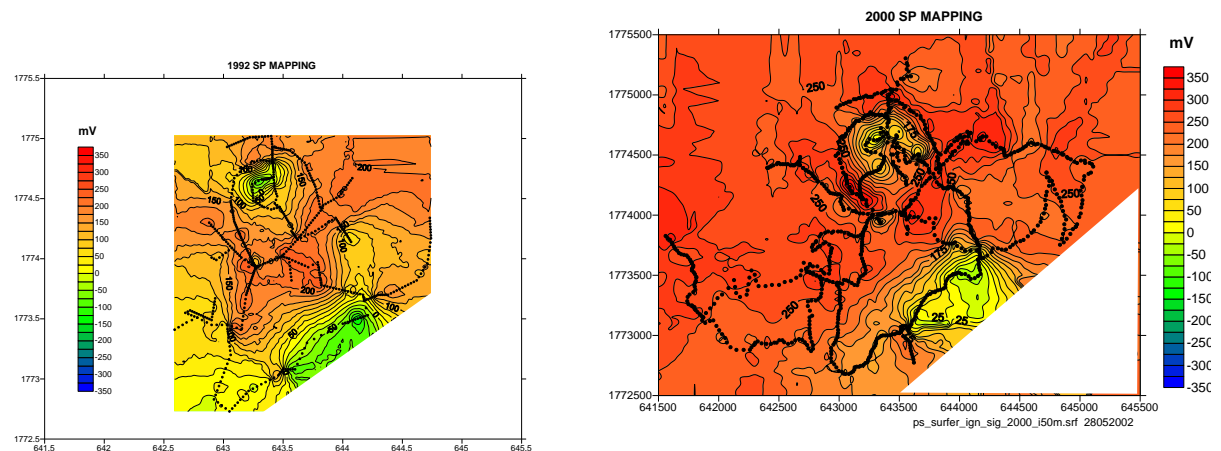


Fig. 3. Self-potential mappings performed in 1992 (left) and 2000 (right).

Beyond the outcomes on the hydrothermal activity of La Soufrière of Guadeloupe along the last 40 years mainly based on electromagnetic methods, it appears that the features of electromagnetic observations may contribute to a better understanding of the on-going hydrothermal activities of some other volcanoes (i.e. Mount Pelée, Miyake-jima, La Fournaise, Taal ...).

A review of recent attempts on natural time analysis as well as on Seismic Electric Signals worldwide

N.V. Sarlis¹, E.S. Skordas¹, M.S. Lazaridou-Varotsos², P.A. Varotsos^{1,2}

¹*Section of Solid State Physics, Department of Physics, School of Science, National and Kapodistrian University of Athens, Panepistimiopolis, Zografos 157 84, Athens, Greece;* ²*Solid Earth Physics Institute, Department of Physics, School of Science, National and Kapodistrian University of Athens, Panepistimiopolis, Zografos 157 84, Athens, Greece, e-mail: pvaro@otenet.gr*

The present paper is far from being an in depth review of the research efforts on Seismic Electric Signals (SES) activities [1,2] (VAN method) and on Natural Time Analysis [3,4] worldwide that have been introduced in the 1980's and 2000's, respectively. Here, we will solely focus on the advances that have been achieved during the last years. Furthermore, we will not deal with relevant efforts worldwide, but we will restrict ourselves to recent research activities carried out, beyond Greece, in USA, Japan, China, Mexico and Russia. These could be summarized as follows:

1) USA: A collaboration of several eminent experts from USA led to the suggestion [5-8] of a new method for estimating the current level of earthquake hazard in a region termed “nowcasting”, which is based on the concept of natural time. The proponents of this method state [5] that they preferred to use natural time since it has at least the following two advantages when applied to earthquake seismology: (a) It is not necessary to decluster the aftershocks. The natural time is uniformly valid when aftershocks dominate, when background seismicity dominates and when both contribute. (b) Natural time statistics are independent of the level of the seismicity as long as the b value is approximately constant. In computing nowcasts, the concept of natural time, counts of small earthquakes, is used as a measure of the accumulation of stress and strain between large earthquakes in a defined geographic region.

This new method of “nowcasting” has been used along various interesting directions. For example: First to show that large global earthquakes are temporally clustered [6]. Second, to make a comparison of induced earthquakes in Oklahoma and at the Geysers, California [7]. Third, to make an estimation of seismic risk to global megacities, e.g., Tokyo, Los Angeles, San Francisco, Taipei, etc. [8].

Concerning the electric and magnetic field measurements, we clarify that magnetic field variations have been reported [9] to be detectable for earthquakes of magnitude 6.5 or larger

accompanying SES activities by monitoring the magnetic field by three component induction coil magnetometers [9]. Such variations have been detected almost 30 years ago by Fraser-Smith and coworkers [10] before the M7.1 Loma Prieta earthquake in California in 1989. Along these lines, 124 stations have been installed mostly along the San Andreas fault monitoring the magnetic field via the Quake Finder network for approximately 10 years [11].

2) Japan: By analyzing the seismicity in natural time, it was shown [12] that the fluctuations of the order parameter κ_1 of seismicity exhibits a minimum β_{\min} at the time of the initiation of the SES activity observed by Uyeda and coworkers [13] almost two months before the onset of the volcanic-seismic swarm activity in 2000 in the Izu Island region, Japan. It was also shown [12] that these two phenomena (SES activity and seismicity) are also linked in space, which opened the window for an estimation of the epicentral area of an impending earthquake. This has been subsequently confirmed in Ref. [14] (see also Ref. [15]) for all major mainshocks of magnitude larger than 7.6 that occurred in Japan during 1984-2011 (cf. for all these mainshocks the existence of β_{\min} has been verified in Ref.[16], see also Ref. [17]). Thus, once the epicentral area becomes known the natural time of seismicity in this candidate area that occurs after β_{\min} may lead to the identification of the occurrence time of the impending earthquake (i.e., within one week or so after the condition $\kappa_1=0.070$ is satisfied). This was verified [18] for example for the case of M9 Tohoku earthquake in Japan that occurred in 2011. Furthermore, in ULF magnetic field variations detected before earthquakes in Japan, criticality features have been identified [19,20] by means of natural time analysis.

3) China: Referring to the devastating Wenchuan Ms8 earthquake that occurred on 12 May 2008, Huang [21] reported that the preliminary analysis of the extremely low frequency data during January-June 2008 at the Hanwang station (which is the nearest station to the epicenter, i.e., around ~300km) showed that the power spectra of electric and magnetic fields enhanced significantly [22] during 1-12 May 2008. Furthermore, it was observed [23] that during around 50 days (i.e., from 21 March to 9 May 2008) before the Wenchuan earthquake, large geoelectric field changes similar to SES of the VAN method were recorded at the Songshan station of China-France cooperation lying ~684km from the epicenter. More recently (e.g., see Ref.[24]), independent studies reported encouraging results concerning geoelectric anomalies before strong earthquakes that occurred during the period 2008-2016. In addition, natural time analysis has been recently applied to the seismicity of China, for example see Ref. [25], where the κ_1 values were calculated before the 30 stronger earthquakes contained in the catalogue of China Earthquake Networks Center during the period 1978-

2014.

4) Mexico: Here, emphasis will be given on the deadly M8.2 earthquake that struck the Mexico's Chiapas state on 7 September 2017. This is Mexico's largest earthquake in more than a century and, although it was characterized as an extremely strange event [26] and "unexpected" by seismologists, we discuss here that it was preceded by clear precursory phenomena [27, 28].

As for the research on SES activities, SES-like geoelectric disturbances have been observed in several cases, for example, before the M7.4 Guerrero-Oaxaca earthquake [29] that occurred on 14 September 1995 as well as before the M6.6 earthquake in the Pacific coast of Mexico on 24 October 1993 (see Fig. 5 of Ref. [30]).

5)Russia: Several studies on SES as well as on natural time analysis have been published by various groups in Russia (see pp. 198 and 199 of Ref. [31]; see also Ref. [32]). Here, we only restrict ourselves to the collaboration between EMSEV and the Bishkek Research Station of the Russian Academy of Science in Kyrgyzstan which started on November 2011 with the installation of two autonomous geoelectric stations. During the subsequent period possible SES of dichotomous nature have been recorded almost two months and 22 days before two earthquakes that occurred on 5 February 2012 (M5.2) and 1 January 2015 (M4.9), respectively [33].

References

1. Varotsos P and Alexopoulos K, *Tectonophysics* 110, 73-98, 1984.
2. Varotsos P and Alexopoulos K, *Tectonophysics* 110, 99-125, 1984
3. Varotsos PA, Sarlis NV, Skordas ES, *Phys. Rev. E* 66, 011902, 2002.
4. Varotsos PA, Sarlis NV, Skordas ES, *Natural Time Analysis: The new view of time. Precursory Seismic Electric Signals, Earthquakes and other Complex Time-Series*, Springer-Verlag, Berlin Heidelberg (2011) 449 pages.
5. Rundle JB, Turcotte DL, Donnellan A, Grant Ludwig L, Luginbuhl M, Gong G, *Earth and Space Science* 3, 480–486, 2016.
6. Luginbuhl M, Rundle JB, Turcotte DL, *Pure Appl. Geophys.* 175, 661-670, 2018.
7. Luginbuhl M, Rundle JB, Hawkins A, Turcotte DL, *Pure Appl. Geophys.* 175, 49-65, 2018.
8. Rundle JB, Luginbuhl M, Giguere A, Turcotte DL, *Pure Appl. Geophys.* 175, 647-660. 2018.
9. Varotsos P, Sarlis N, Skordas E, *Phys. Rev. Lett.* 91, 148501, 2003; Sarlis N and Varotsos P, *J. Geodyn.* 33, 463-476, 2002.
10. Fraser-Smith AC, Bernardi A, McGill PR, Ladd ME, Helliwell RA, Villard, Jr. OG, *Geophys. Res. Letters* 17, 1465-1468, 1990.
11. Kappler KN, Schneider DD, MacLean LS, Bleier TE, *Earthq Sci* 30, 193-207, 2017.

12. Varotsos PA, Sarlis NV, Skordas ES, Lazaridou MS, *Tectonophysics* 589, 116-125, 2013
13. Uyeda S, Hayakawa M, Nagao T, Molchanov O, Hattori K, Orihara Y, Gotoh K, Akinaga Y, Tanaka H, *Proc. Natl. Acad. Sci. U.S.A.* 99, 7352–7355, 2002.
14. Sarlis NV, Skordas ES, Varotsos PA, Nagao T, Kamogawa M, Uyeda S, *Proc. Natl. Acad. Sci. U.S.A.* 112, 986-989, 2015.
15. Huang Q, *Proc. Natl. Acad. Sci. U.S.A.* 112, 944-945, 2015.
16. Sarlis NV, Skordas ES, Varotsos PA, Nagao T, Kamogawa M, Tanaka H, Uyeda S, *Proc. Natl. Acad. Sci. U.S.A.* 110, 13734–13738, 2013.
17. Varotsos PA, Sarlis NV, Skordas ES, Lazaridou MS, *Earthq. Sci.* 30, 183-191, 2017.
18. Varotsos PA, Sarlis NV, Skordas ES *Earthq. Sci.* 30, 209-218, 2017.
19. Hayakawa M, Schekotov A, Potirakis S, Eftaxias K, *Proc. Jpn. Acad. Ser. B* 91, 25–30, 2015.
20. Potirakis SM, Asano T, Hayakawa M, *Entropy* 20, 199, 2018.
21. Huang Q, *J. Asian Earth Sci.* 41, 421-427, 2011.
22. Gao SD, Tang J, Du XB, Liu XF, Su YG, Chen YP, Di GR, Mei DL, Zhan Y, Wang LF, *Chinese J. Geophys.* 53, 512 –525, 2010.
23. Fan YY, Du XB, Zlotnicki J, Tan DC, An ZH, Chen JY, Zheng GL, Liu J, Xie T, *Chinese J. Geophys.* 53, 997–1010, 2010.
24. Tan DC, Xin JC, *Earthq. Sci.* 30, 173-181, 2017.
25. Gao Y, An, Z, Fan Y, Liu J, Wang J, *Acta Seismologica Sinica* 39, 593-603, 2017.
26. Wade L, *Science* 357 (6356) 1084– 1084, 2017
27. Ramírez-Rojas A, Flores-Márquez EL, *Physica A* 392, 2507-2512, 2013.
28. Sarlis NV, Skordas ES, Varotsos PA, Ramírez-Rojas A, Flores-Márquez EL, *Physica A* 506C, 625-634, 2018.
29. Ramírez-Rojas A, Flores-Márquez EL, Guzmán-Vargas L, Gálvez-Coyt G, Telesca L, Angulo-Brown F, *Nat. Hazards Earth Syst. Sci.* 8, 1001-1007, 2008.
30. Ramírez-Rojas A, Telesca L, Angulo-Brown F, *Nat. Hazards Earth Syst. Sci.* 11, 219-225, 2011.
31. Lazaridou-Varotsos MS, *Earthquake Prediction by Seismic Electric Signals*, Springer-Verlag, Berlin Heidelberg (2011) 254 pages.
32. Chmel A, Smirnov V, Golovanov O, *Physica A* 389, 2617-2627, 2010.
33. Sarlis NV, Varotsos PA, Skordas ES, Uyeda S, Zlotnicki J, Nagao T, Rybin A, Lazaridou-Varotsos MS, Papadopoulou KA, *Earthq. Sci.* 31, 44-51, 2018.

Simultaneous Radiation Belt Electron Precipitation and broad band (~1-20kHz) VLF activity in the Ionosphere as an Earthquake precursor

G. Anagnostopoulos,¹ A. Karli¹

¹*Demokritos University of Thrace, Sector of Telecommunications and Space Science, Xanthi, Greece,
ganagno@ee.duth.gr*

Many authors have provided significant evidence that Radiation Belt electron precipitation (RBEP) precedes great earthquakes (EQs). In the present study we present more detailed features of the EQ-related RBEP phenomenon as inferred from the analysis of observations obtained by the DEMETER and POES satellites. (1) These energetic ($>\sim 70$ keV) electron events are characterized by a time duration of $\sim 0.5\text{-}3$ min. (2) They are accompanied by broad band ($\sim 1\text{--}20$ KHz) VLF (bVLF) wave activity. (2) A statistical study of 63 big ($M \geq 7$) EQs between 11.8.2004-31.12.2008 suggests RBEP events precede some ($\sim 2\text{-}6$) days the EQ occurrence at a percentage as high as $\sim 90\%$ (Figure 1; L'Aquila). (3) A further examination of the EQ-related RBEP events ceases shortly ($<\sim 4$ hours) before the EQ occurrence (Figure 2; L'Aquila).

Characteristic features of RBEP events before some catastrophic great EQs, as for instance, the EQs in *Wenchuan* (China), L'Aquila (Italy), Methoni / Andavida (Greece) will be reported in some detail. Finally, a case with the presence electromagnetic EQ precursors (RPEP etc) will be reported in the case of a Greek EQ, when not a strong EQ was followed. Our studies suggest that the RPEP associated with bVLF wave activity is an important earthquake precursor. In particular, the *silence* observed a few hours before great EQs might be shown a short-time alarm signal. Definitely, further work is needed (a) to verify our present statistical results and (b) to fully understand the physical relationship between seismic activity and the RPEP phenomenon.

Space Weather and Seismicity (1993-2015)

G. Anagnostopoulos¹, A. Karli, A. Rigas¹, I. Spyroglou¹

¹*Demokritos University of Thrace, Sector of Telecommunications and Space Science, Xanthi, Greece,
ganagno@ee.duth.gr*

Earth is in general highly dependent on the presence of Sun. Important Sun's electromagnetic influences on Earth have been recognized by modern Science. On these lines we examine the possible influence of Space Weather on Seismicity. We performed several statistical and case studies during the time interval of 22 years (1993 to 2015) and we have found some important results. (1) The yearly values of the number of great ($M \geq 6$) EQs and of the amount of the total seismic energy released E are higher during the inclining (2010-201) and the declining phases (1994-1996, 2003-2005) of the solar cycles 23 and 24. (2) A power spectrum analysis performed on binary time series of $M \geq 6$ EQ energy release values, during the inclining and the declining phases, shows a significant peak at the Solar rotational period of ~ 27 days. For instance, during the years 2004-2010, a significant peak was found at 26.6 days (significant level 5%). (3) We have studied in extend the Space Weather along with Seismicity about 1 month before the Sumatra big ($M9.1$) Earthquake (EQ) of December 26, 2004. We found that the Sumatra EQ occurred at the end of a sequence of 8 fast solar wind streams, followed by a series of great EQs, with an average time delay of ~ 1.5 days (Anagnostopoulos and Papandreou, 2012). Our results suggest that the space weather may be a significant parameter for the (time) prediction of great EQs, in particular, during (the inclining and) the declining phase of a solar cycle, when Corotating Interaction Regions are more steady in space.

Application of a robust analysis for the detection and characterization of the Seismo-Electromagnetic Signals observed in Southern Italy

M. Balasco², A.E. Pastorella¹, G. Romano¹, A. Siniscalchi¹

¹*Dipartimento di Scienze della Terra e Geoambientali, Università degli Studi di Bari “Aldo Moro”, Bari, Italy*

²*Istituto di Metodologie per l’Analisi Ambientale –IMAA, Consiglio Nazionale delle Ricerche, Tito, Italy*

Seismo-ElectroMagnetic signals (SES) are anomalous ElectroMagnetic signals generated as a response to the propagation of a mechanical perturbation within the subsoil. Fluid presence plays a key role in determining SES generation and characteristics therefore SES study could be useful for subsoil characterization. In a more general framework, it can give insight on the role of fluids in the earthquake generation and seismic waves propagation.

A systematic study on the SES and on the related data analysis techniques is fundamental in order to define the characteristics of these signals which are superimposed to the natural electromagnetic field induced by the external variable magnetic field. To this aim, the Pollino seismic swarm was a great opportunity because continuous MagnetoTelluric (MT) data were recorded in a period in which numerous seismic events of various magnitudes occurred. During the observational period, SES were also recorded in correspondence to earthquakes distant from the MT stations over 800km.

We adopted an innovative procedure aimed to improve the SES detectability and to gather the maximum information possible on these signals.

The procedure is especially tuned for the analysis of MT time series and it is based on the application of the Continuous Wavelet Transform and frequency filters.

We will present the results of the application of the operational scheme to the MT time series collected in the Pollino area. As it will be shown, a minimization of the background variability of the MT signal is obtained allowing an easier detection and characterization of SES in terms of amplitude and duration.

Active seismo-electromagnetic experiment in the Solfatara crater (Campi Flegrei, Italy)

M. Balasco², G. Romano¹, A. Siniscalchi¹, S. Tripaldi¹

¹*Dipartimento di Scienze della Terra e Geoambientali, Università degli Studi di Bari “Aldo Moro”, Bari, Italy*

²*Istituto di Metodologie per l’Analisi Ambientale –IMAA, Consiglio Nazionale delle Ricerche, Tito, Italy*

The integration between electromagnetic and seismic geophysical methods has always been considered as a desirable target. The joint inversion and, mostly, the joint interpretation are now routinely applied to get a better characterization of the subsoil status. The above mentioned strategies are based on the integration, at a certain stage of the data modelling/interpretation, of totally independent electromagnetic and seismic data. The upcoming frontier is the acquisition of an “integrated seismoelectric dataset”. To understand what should be considered as an “integrated dataset”, it is necessary to define the “Seismo-electromagnetic” signal (Seismo- SES, in what follow). SES are anomalous ElectroMagnetic signals generated as a response to the propagation of a mechanical perturbation within the subsoil. Fluid presence, and more in general, propagating medium characteristics play a key role in determining SES generation and characteristics. Several research papers (i.e Pride, 1994, Gao & Hu, 2010) allow, theoretically speaking, to predict the SES produced by a seismic wave knowing the characteristics of the medium in which the seismic propagation takes place. Reversing the point of view, knowing the characteristics of the SES and of the seismic source, it should be plausible and possible the characteristics of the subsoil. the first steps in this direction, have been already made (i.e Warden et al. 2012), but there is still a lot to do in order to make really feasible the use of the SES.

To this aim, ElectroMagnetic signal were recorded during an active seismic experiment (performed in the framework of the RICEN project) in the campi Flegrei area. By using MagnetoTelluric (MT) instruments, the SES generated by the controlled seismic source have been detected for a their future characterization and to define a reliable and objective analysis technique.

In this work we present some of the results obtained by analysing the collected data. SES attenuation maps will be shown an compared with seismic dispersion tomography.

The presented results will show the strengths and weaknesses of using a SES based integrated dataset for subsoil characterization.

References

- Gao, Y., and Hu H.; 2010: Seismoelectromagnetic waves radiated by a double couple source in a saturated porous medium. *Geophys. J. Int.*, 181, 873–896.
- Pride, S. R.; 1994: Governing equations for the coupled electromagnetics and acoustics of porous media. *Phys. Rev. B*, 50, 15,678–15,696
- Warden S., Garambois S., Sailhac P., Jouniaux L. and Bano M.; 2012: Curvelet-based seismoelectric data processing. *Geophys. J. Int.*, 190, 1533–1550

Geophysical observations for the shallow structure reconstruction of the Stracciacappa maar (Sabatini Volcanic District, central Italy)

J. Bellanova¹, G. Calamita¹, A. Perrone¹, I. Gaudiosi², S. Giallini², M. Mancini², M. Moscatelli², F. Polpetta², R. Razzano², M. Simionato², P. Sirianni², G. Sottilli², G. Vignaroli², A. Pagliaroli³, G. Lanzo⁴, A. Avalle⁵, S. Piscitelli¹

¹CNR IMAA - Istituto di Metodologie per l'Analisi Ambientale, Tito (PZ), Italy, jessica.bellanova@imaa.cnr.it

²CNR IGAG - Istituto di Geologia Ambientale e Geoingegneria, Rome, Italy ³Università degli Studi di Chieti-

Pescara - Dipartimento di Ingegneria e Geologia, Pescara, Italy ⁴Università di Roma "La Sapienza"-

Dipartimento di Ingegneria Strutturale e Geotecnica, Rome, Italy ⁵Università degli Studi Roma 3, Rome, Italy

This work deals with the application of different geophysical techniques in a circular shaped volcanic setting: the Stracciacappa maar (Sabatini Volcanic District, central Italy). Its pyroclastic succession records phreatomagmatic eruptive phases ended about 0.09 Ma ago. Its present-day crater has a diameter of about 1 km and a crater floor about 30–40 m below the crater rim. A composite interfingering between lacustrine and epiclastic debris sediments fills the crater floor. Heterogeneous characteristics of the Stracciacappa maar (stratification, structural setting, lithotypes, and thickness variation of depositional units) make it an ideal case history for understanding mechanisms and processes leading to modifications of amplitude-frequency-duration of seismic waves generated in volcanic settings.

Electrical Resistivity Tomography tests were carried out for constraining the geometry of the maar, while HVSR noise measurements were collected in order to studying the characteristics of the noise field, obtaining inferences of the local heterogeneities. 2D seismic passive arrays were gathered and analysed both with SPAC and F-k techniques and used to infer the profiles of the S-waves (Vs). Together with the aforementioned extensive geophysical fieldwork, new geological map and cross sections illustrate the complex geometric relationships between the thick pyroclastic succession and even meter-sized lava ballistic. A continuous coring borehole was drilled inside the crater, 45 meters deep from the wellhead, with sampling of undisturbed samples. Regarding the non-linear properties of soils, the cyclic soil behaviour was investigated through simple shear tests. The collected dataset was used to define the shallow subsoil model useful for 2D\3D site response analyses. Our results may be a start point in the assessment of local seismic response in similar volcanic settings in highly urbanised environments elsewhere.

Integration of geophysical and engineering analysis of the possible causes of different damage observed after the 2016 Central Italy Earthquakes: the case of Pescara del Tronto and Vezzano villages

G. Calamita¹, J. Bellanova¹, L. Chiauzzi², M. R. Gallipoli¹, A. Masi², A. Perrone¹, S. Piscitelli¹, G. Santarsiero², T.A. Stabile¹, L. Vignola³

¹CNR IMAA - Istituto di Metodologie per l'Analisi Ambientale, Tito (PZ), Italy, giuseppe.calamita@imaa.cnr.it;

²School of Engineering, University of Basilicata, Potenza (Italy); ³National Association for Public Assistance (ANPAS), Marsicovetere, Italy,

On 24th August 2016 a ML=6.0 earthquake occurred in Central Italy destroying several villages. In the aftermath of the main event, the authors surveyed many damaged villages located in the epicentral area and some unexpected situations were found like, for example, the very different damage occurred to the villages of Vezzano and Pescara del Tronto (both districts of Arquata del Tronto). Despite these two villages are spaced just about 1300 m from each other, Pescara del Tronto undergoes very heavy damage with many collapses of masonry buildings and 48 fatalities, while Vezzano was subjected to very light damage to few buildings. Indeed, possible causes of the different damage distribution were analysed from the engineering and geophysics point of view. To evaluate the contribution of site amplifications for the damage increase in Pescara del Tronto respect to Vezzano, a geophysical survey was carried out. In particular, five geophysical techniques were performed (Electrical Resistivity Tomography, noise single station measurements, bi-dimensional passive and active seismic arrays, foreshocks recorded in four sites). The results of the geophysical survey highlight a strong lateral variation: three sites analyzed in Pescara del Tronto show amplification in frequency range between 3-7 Hz (range of interest of built environmental), whereas Vezzano has flat amplification function, although, the two village lies on the same geological sequence (Laga Formation, consisting of arenaceous-pelitic and pelitic-arenaceous lithofacies). This different behavior, probably, can be due to different local geological factors, such as the presence of a different thickness of the cover deposits and a travertine slab underlying Pescara del Tronto settlement. Further geological and geophysical investigations are currently ongoing to better understanding this peculiar behavior.

Recurrence plot measures of complexity and its applications to self-potential time series arising from a Mexican seismic zone.

F. Cervantes-De La Torre¹, J.I. Gonzalez-Trejo², C.A. Real-Ramirez³

¹Departamento de Sistemas UAM-AZCAPOTZALCO, México, CDMX, fcdt@correo.azc.uam.mx; ²Departamento de Sistemas UAM-AZCAPOTZALCO, México, CDMX, jesus.glez.t@gmail.com; ³Departamento de Sistemas UAM-AZCAPOTZALCO, México, CDMX, cesar.real@gmail.com

Since several years ago, electro-telluric stations located in several sites of Mexico records signals of the self-potential of the ground. Some of these stations are located along the coast of Guerrero state, near the Middle American Trench, which is the border between Cocos and North American tectonic plates. In this work, we study time series of self-potential signals arising from Acapulco station (16.85°N , 99.9°W), linked to the Middle American Trench. This work analyzes time series corresponding to the 1993 year. An earthquake of magnitude Mw 6.6 occurred in this year. The theory of dynamical systems allows to appreciate the richness of behavior of the world around us. The self-potential time series show a complex behavior, but the Recurrence Plots (RP) theory provides a valuable tool for studying this kind of systems.

1 Introduction

The Mexico City is vulnerable to seismic waves whose epicenter is located in the distant Pacific coast, but that propagate across the entire country. The Cocos Plate is one of the dozen or so tectonic plates that make up the outer layer of the Earth. Most of the earthquakes that hit Mexico are the result of the subduction of the Cocos Plate under the North American Plate. The Cocos Plate moves from the southwest with a speed of just over 2 inches a year (Fig.1). Upon colliding with the North American Plate, the Cocos Plate bends downwards and begins to sink into the Earth's hot mantle. The mechanical stresses associated with the bending and the temperature change cause the earthquakes.

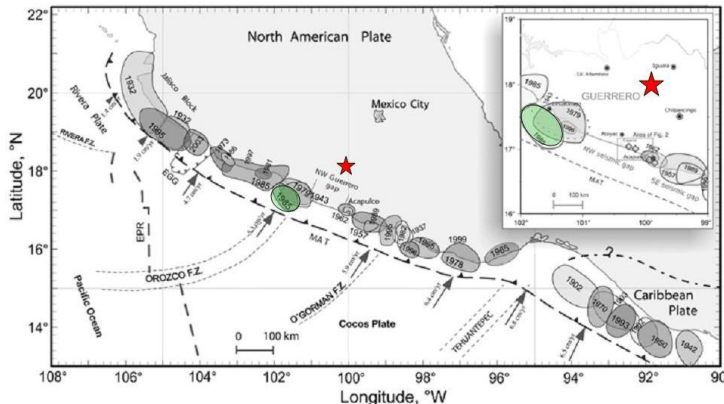


Fig. 1 Seismic setting of the Pacific coast of Mexico. Small dashed lines indicates fracture zones, shaded circles indicate rupture areas and numbers the years of most important subduction seismic events of last century. Thick dash with arrowheads shows subduction zone. Figure from Ramírez-Herrera et al [1].

The Cocos Plate diverges from the Pacific Plate along the East Pacific Rise. In the past century, some of the earthquakes that hit Mexico occurred along this subduction zone. Among them, one of magnitude Mw 8.2, cost thousands of lives and produced severe damages in Mexico City. The epicenter of this earthquake was located near the Michoacan Coast and occurred in the year of 1985. The absence of significant earthquakes in a region along a tectonic front for a long period is named as a “seismic gap”. During this time gap, the fear that an earthquake of great consequences occurs increases as the period lengthens. There are several locations along the Cocos subduction zone where tectonic stresses have been released by earthquakes over the last century. Nevertheless, during that time, nothing happened in the Guerrero Gap. The area near the southeast of the Michoacan state is certainly empty. For more than 100 years, no significant quakes with a magnitude greater than Mw 7.8 have occurred in the immediate vicinity of the Acapulco City, in the Mexican state of Guerrero. The absence of earthquakes means that the stresses caused by subduction of the Cocos Plate have been accumulated for a long period. Therefore, many seismologists expect a huge earthquake in this region. This earthquake would not only affect Acapulco City but as the earthquake occurred in 1985, it would cause significant damage in Mexico City too.

2. Description of the time series for study

In this work, we study self-potential time series measured at the Acapulco electro telluric station (16.85°N , 99.9°W), which is linked to the Middle American Trench. In this station as in others with similar characteristics, thousands of data were taken each two (or four) seconds, along intervals ranging from months to years. We restrict our analysis to a time series corresponding to the 1993 year because a strong earthquake of magnitude Mw 6.6 occurred

on October 24, and its epicenter was near the Acapulco station. Two typical segments of the self-potential time series are depicted in Fig. #2. The behavior of these time series shows any dependence on the rainfall seasons [6].

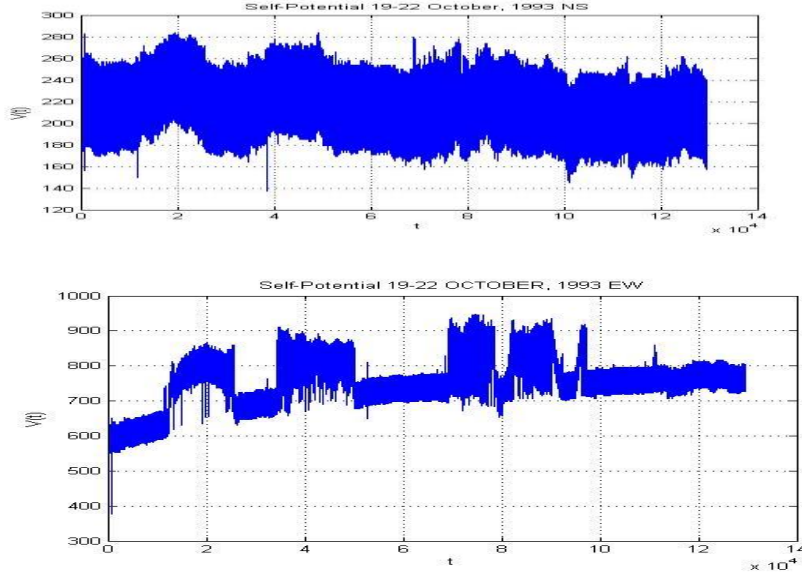


Fig. 2. Typical segments of Self-Potential time series collected at Acapulco station. The superior series is the N-S one and the down series corresponds to the E-W line.

3. Recurrence quantification analysis for self-potential time series

Now, the recurrence quantification analysis is applied to a self-potential time series from measurements along four days, October 19 to 22, 1993. To reconstruct the phase space, the time delay, τ , and the dimension embedding, d_E , were calculated by taking the first minimum of the Mutual Info function (**MI**) and the **FNN** algorithm, respectively.

Figures 3 to 10 show the results of the analysis applied to the four self-potential time series using the RP and RQA methodologies. We observed a complex behavior for these four self-potential time series. Several crossovers appear, indicating underlying dynamics. This behavior has a complex structure and this means that the analyzed self-potential time series has a multifractal behavior, rather than a monofractal.

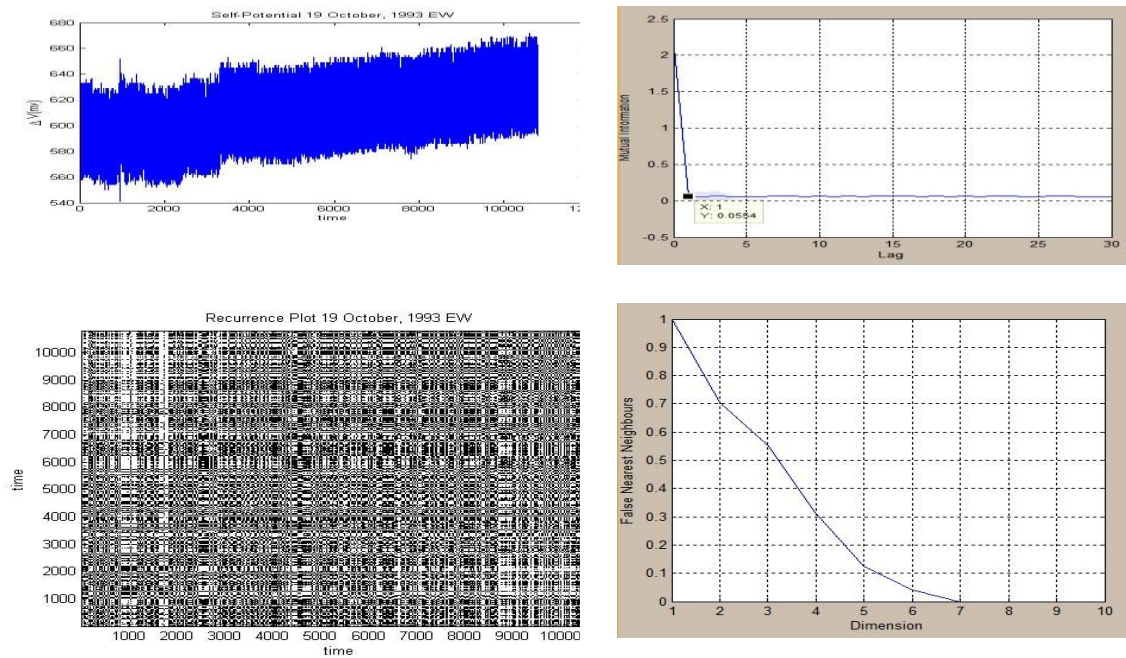


Fig. 3 Self-potential time series and RP for October 19, 1993. E-W line.

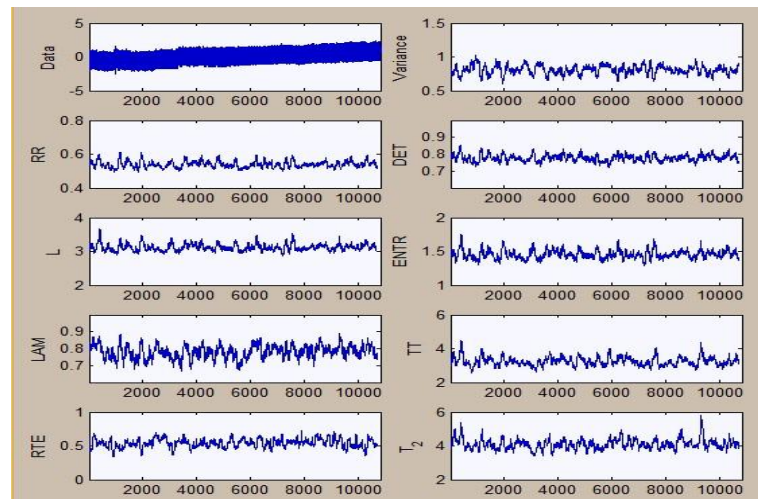


Fig. 4 RQA for self-potential time series for October 19, 1993. E-W line.

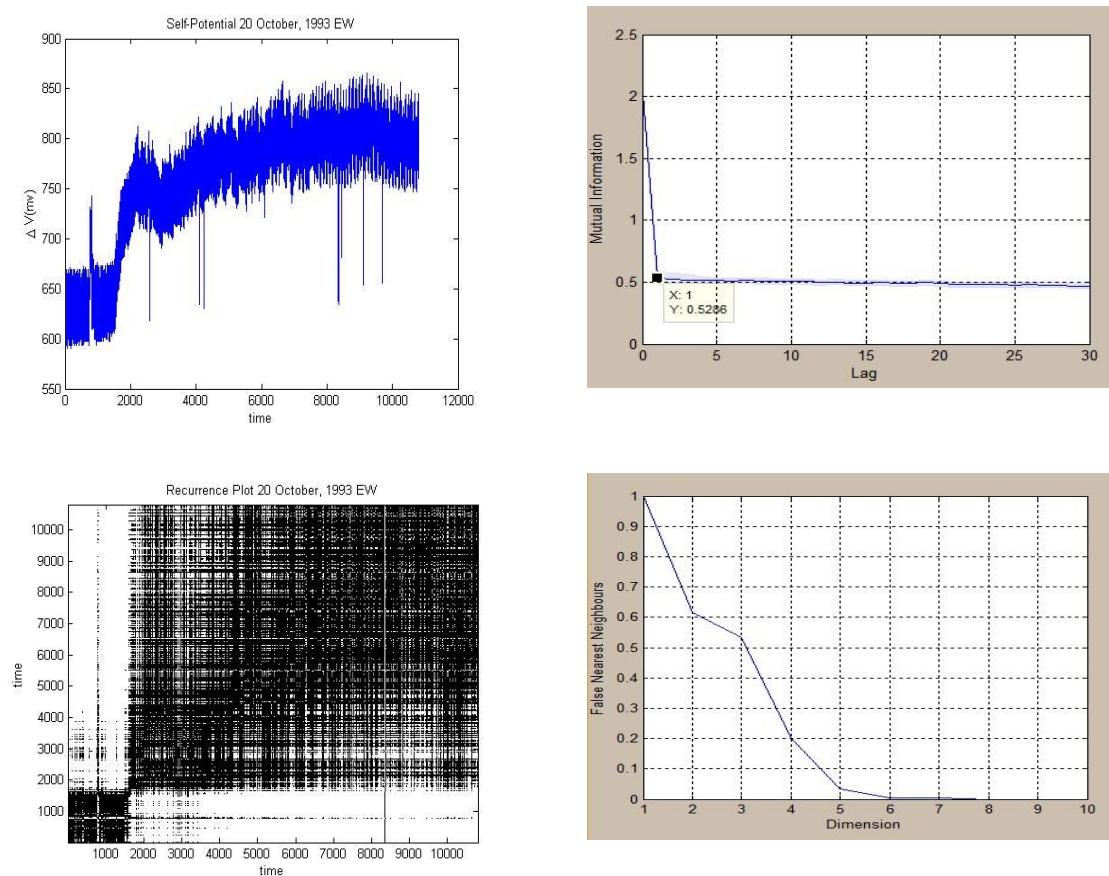


Fig. 5 Self-potential time series and RP for October 20, 1993. E-W line.

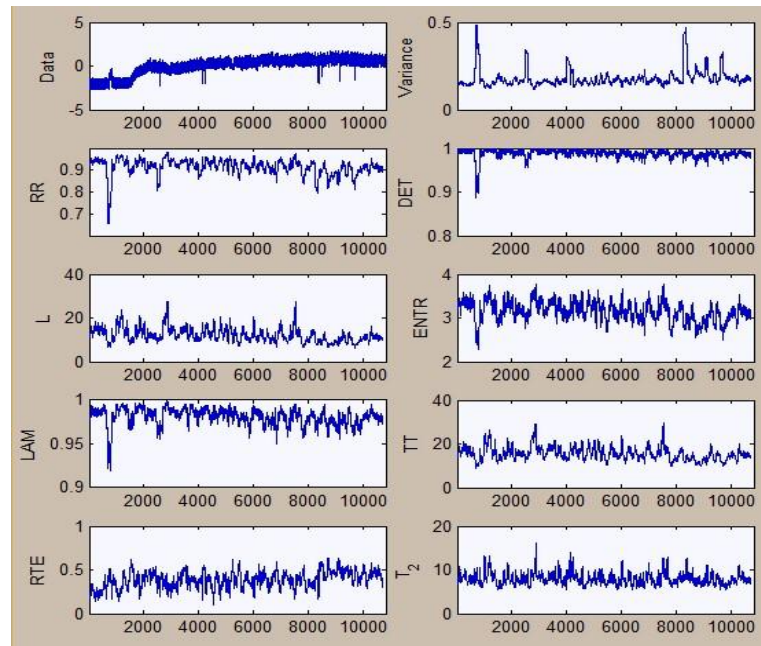


Fig. 6 RQA for self-potential time series for October 20, 1993. E-W line.

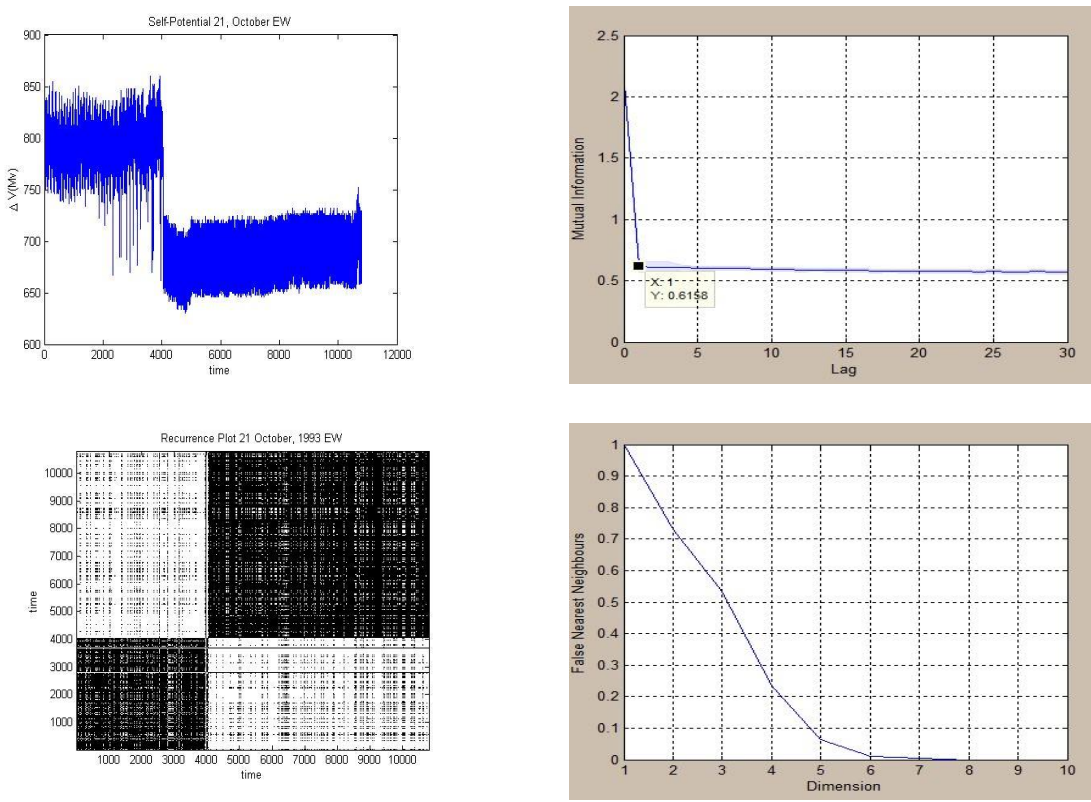


Fig. 7 Self-potential time series and RP for October 21, 1993. E-W line.

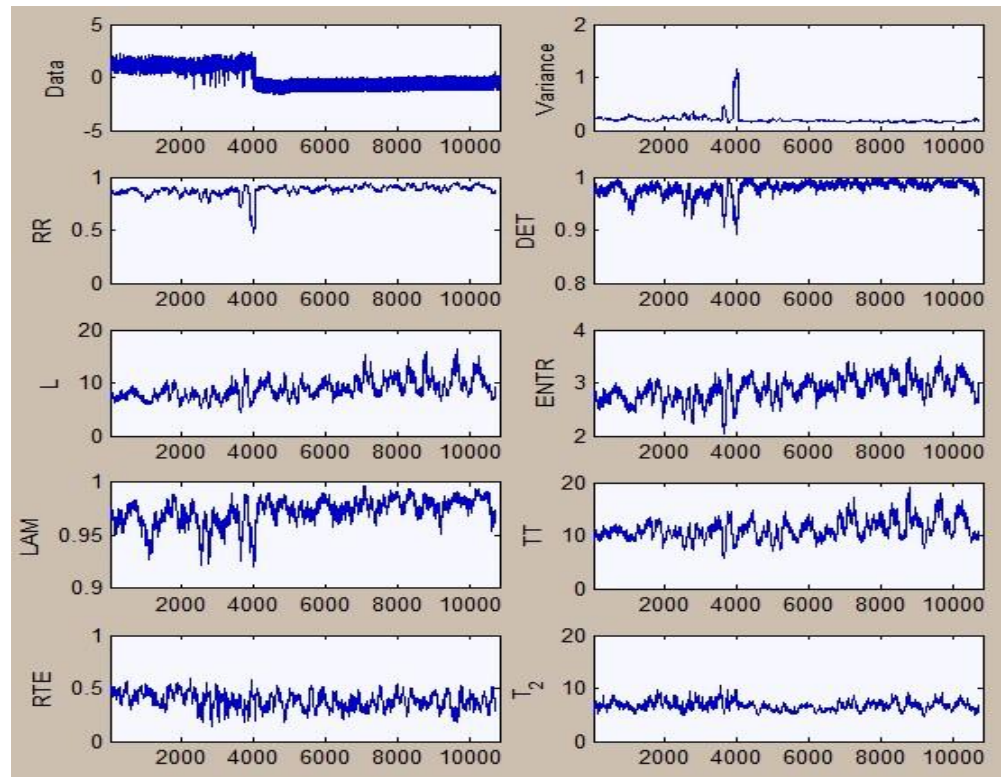


Fig. 8 RQA for self-potential time series for October 21, 1993. E-W line.

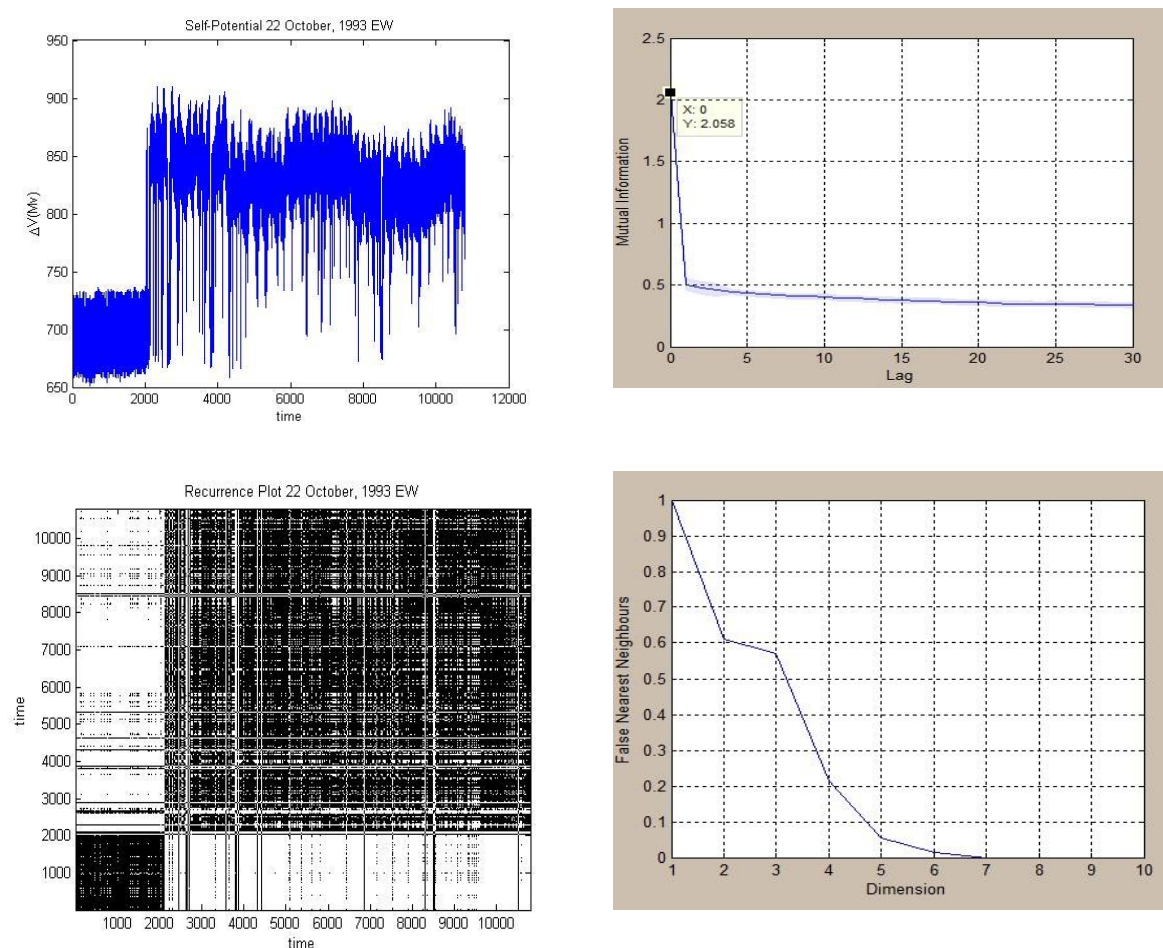


Fig. 9 Self-potential time series and RP for October 22, 1993. E-W line.

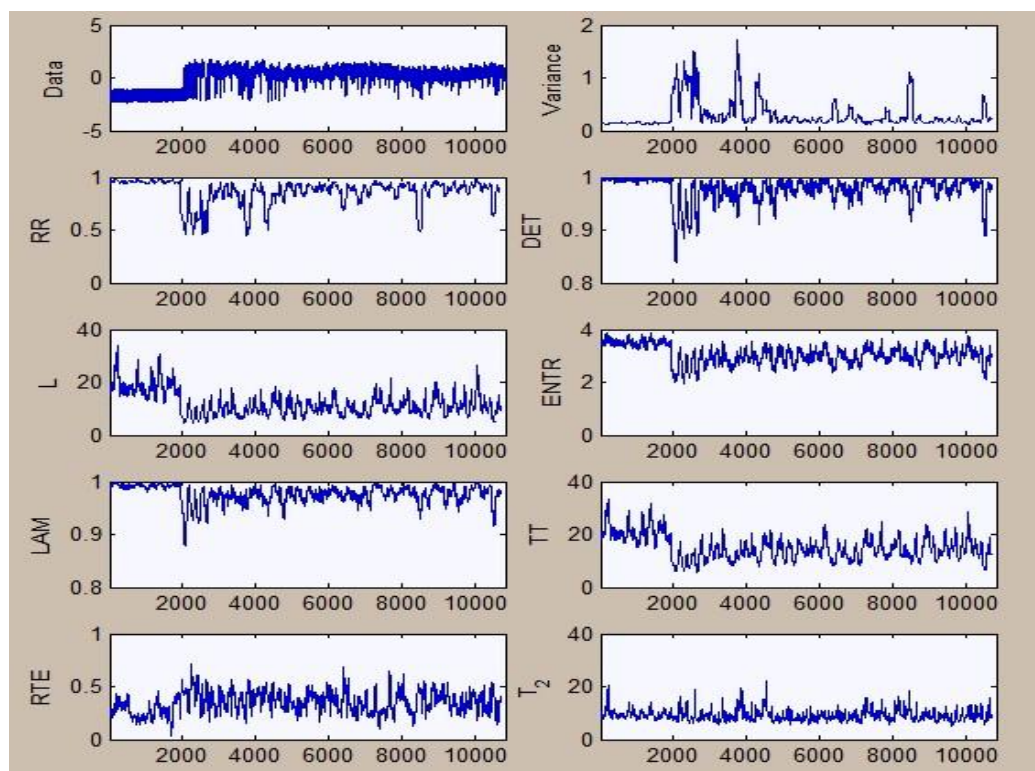


Fig. 10 RQA for self-potential time series for October 22, 1993. E-W line.

4 Conclusion

The analysis performed using RP and RQA methods showed that the self-potential time series previous the earthquake occurred on October 24, 1993, display a very complex behavior. This fact confirms previous results where fractal structures have been found in time series from a wide range of geophysical phenomena. The multifractal behavior identifies deviations in fractal structure within time periods with large and small fluctuations. Monofractal and multifractal structures of the studied self-potential series are particular examples of systems whose dynamics displays scale invariance. A single power law defines the monofractal structure of a time series. On the contrary, spatial and temporal variations indicate a multifractal structure, as was observed in the analysis carried out using the RP and RQA of the self-potential signals studied in this work.

Acknowledgments

The RP and RQA analysis were conducted using TOCSY toolbox (<http://www.recurrence-plot.tk/rqa.php>).

References

- 1) Ramírez-Herrera M. T., A. B. Cundy, V. Kostoglodov, and M. Ortiz., Late Holocene tectonic land-level changes and tsunamis at Mitla lagoon, Guerrero, Mexico. *Geofísica Internacional* 48 (2), 195-209 (2009).
- 2) Hayakawa M., editor *Atmospheric and Ionospheric Electromagnetic Phenomena Associated with Earthquakes*, TERRAPUB, Tokyo, 996 pp. 1999.
- 3) Varotsos P., Alexopoulos K., Physical properties of the variations of the electric field of the Earth preceding earthquakes I. *Tectonophysics* , 110, 73-98, 1984a.
- 4) Varotsos P., Alexopoulos K., Physical properties of the variations of the electric field of the Earth preceding earthquakes II. *Tectonophysics* , 110, 99-125, 1984b.
- 5) Varotsos P. and Lazaridou M., Latest aspects of earthquake prediction in Greece base don seismic electric signals, *Tectonophysics*, 188, 321-347, 1991.
- 6) Yépez E., Angulo-Brown F., Peralta J. A., Pavía-Miller C. G., and Gonzalez-Santos G., Electric field patterns as seismic precursors, *Geophys Res. Lett.*, 22, 3087-3090, 1995.
- 7) F. Cervantes-De la Torre, A. Ramírez-Rojas, C. G. Pavía-Miller, F. Angulo-Brown, E. Yépez, and J. A. Peralta, A comparison between spectral and fractal methods in electrotelluric time series, *Revista Mexicana de Física*, 45 (3), 298-302.
- a. F. Cervantes-De la Torre, C. G. Pavía-Miller, A. Ramírez-Rojas, F. Angulo-Brown, Time Evolution of the Fractal Dimension of Electric Self-Potential Time Series., *Nonlinear Dynamics in Geosciences*, Edited by Anastasios A. Tsonis and James B, Elsner, 407-418,2007 Springer.
- 8) T. Higuchi, Approach to an irregular time series on the basis of the fractal theory. *Physica D*, 31 (1988), 277-283.

- 9) Turcote D. L., Fractals and chaos in geology and geophysics, Cambridge University Press, 1992.
- 10) Hayakawa Masashi, Ito Tesuya and Smirnova Natalia. Fractal analysis of ULF geomagnetic data associated with the Guam earthquake on August, 8,1993. Geophysical Research Letters, Vol. 26, No. 18. 2797-2800, September 1999.
- 11) N. Marwan. A historical review of recurrence plots Eur. Phys. J. Special Topics 164, 3-12 (2008).
- 12) Eckman J. P., Oliffson Kamphorst N. S. and Ruelle D., Recurrence Plot of Dynamical Systems, Europhys. Lett., 4 (91), 973-977, 1987:
- 13) Takens F. Detecting strange attractors in fluid turbulence. In Dynamical systems and turbulence. Rand D, Young LS, editors. Springer, Berlin, 1981.
- 14) Andrew M. Fraser and Harry L. Swinney, Independent coordinates for strange attractors from mutual information, Physical Review A, Vol. 33 Number 2,1134-1140, 1986.
- 15) M. B. Kennel, R. Brown, and H. D. I. Abarbanel, *Determining embedding dimension for phase-space reconstruction using a geometrical construction*, Phys. Rev. A **45**, 3403 (1992).
- 16) Marwan N., Encounters with Neighbors: Current Developments of Concepts Based on Recurrence Plots and Their Applications [PhD Thesis]. Potsdam: University of Potsdam; 2003. Available from: <http://www.recurrence-plot.tk/furtherreading.php>
- 17) Norbert Marwan, M. Carmen Romano, Marco Thiel, Jürgen Kurths, Recurrence plots for the analysis of complex systems. Physics Reports 438 (2007) 237-329.
- 18) Edward N. Lorenz. Deterministic Nonperiodic Flow, Journal of The Atmospheric Sciences, Vol. 20, 130-141, 1963.

Tectonic plate tension as the source of noise in the geomagnetic field, measured at the PIA geomagnetic observatory (Piran, Slovenia)

R. Čop¹

¹Institute Terra Viva, Sv. Peter 115, 6333 Sečovlje, Slovenia; E-mail: rudi@artal.si

Slovenia lies in the central part of Europe. It is at the juncture of three important tectonic formations: the Alps in the northwest and the north, the Dinarides in the south and the Pannonian Plain in the east. In the southwest it includes a part of Istria, which geologically consists of flysch sedimentary rocks. This part of Slovenia ends on the short coastline of the northern Adriatic Sea. On the basis of extensive measurements of the Z component of geomagnetic field, carried out in the early 1960s, the territory of Slovenia is divided into the Alpides in the northeast, the Pannonian Plate in the east and the Dinarides in the entire western and central part. This division is not the same as on the topographic map or on the geologic map of this territory.

The territory of Slovenia is gravimetrically unbalanced: the Alps rise faster than the Pannonian Plain descends. Slovenia lies in the far northeastern part of the Adriatic tectonic micro plate. Due to the pressure of the Eurasian tectonic plate from the north and the African tectonic plate from the south, the Adriatic micro plate rotates in anticlockwise direction. The territory of Slovenia is geologically very diverse and also seismologically active. There are over a hundred tectonic cracks and gaps, which, however, are seismologically active only in relatively short sections. The vast majority of earthquakes have shallow epicenters, 5 to 15 km deep in the Earth's crust. The only volcanic mountain range in Slovenia is Smrekovec in its northeastern part, which was last active in the tertiary geological period about 30 million years ago. Due to these natural features of Slovenia, it is very appropriate to study the influence of the increased tectonic plate tension in the geomagnetic field on this territory.

PIA Geomagnetic Observatory (hereinafter: the Observatory) lies in Slovenian Istria. On 1 January 2015 it began to regularly send measurement data to the INTERMAGNET (International Real-Time Magnetic Observatory Network), the network for the exchange of measurement data on the state of the geomagnetic field in the near real time. Due to the natural characteristics of its surroundings it is a unique construction. All measuring places for

the continuous registration of changes in the geomagnetic field are in underground shafts. The measuring places are therefore more stable in temperature and at the same time better protected against the effects of atmospheric discharges. The Observatory is located on the edge of the southern part of Slovenia with the highest density of atmospheric discharges in Europe. In its construction, it was also necessary to take into account that Slovenia is a seismically active area, and has some local features, including, above all, flows of underground and surface waters.

At the Observatory, the measured changes in the Earth's magnetic field contain more noise than in the neighboring countries. This noise is of natural and/or artificial origin. The first discovered natural sources of noise in the geomagnetic field were the transition of the weather fronts MCS (mesoscale convective system). The tectonic plate tension change is also a natural source of noise in the geomagnetic field. Therefore, an analysis of the relative change in the density of the geomagnetic field energy and the comparison with changes in seismic activity in 2015 was made.

The increased energy in the geomagnetic field due to the increased tectonic plate tension was determined on the basis of measurements at the Observatory and on the basis of the data provided by ARSO (Slovenian Environment Agency). In 2015, the automatic network of seismographers of the Republic of Slovenia registered 1944 earthquakes or 5.3 in average per day (Figure 1). Among them, 378 or 19.4% were with magnitudes greater than $M_L = 1.0$. In 2015, the most seismologically active month was November, with 291 registered earthquakes or 15.0% of all, and the least active was June with 110 registered earthquakes or 5.7% of all.

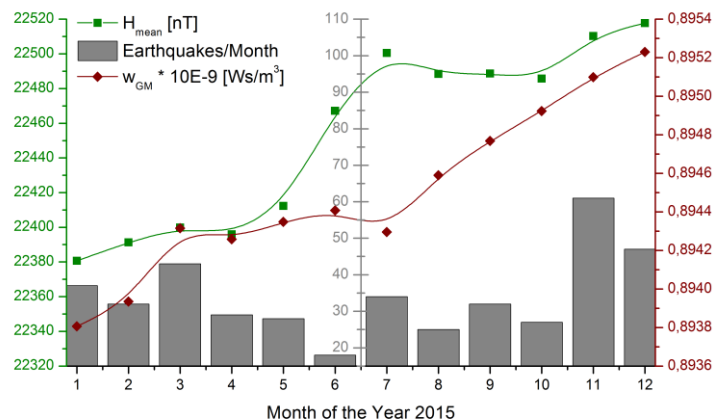


Fig 1: Monthly number of earthquakes with magnitude $M \geq 1$ on the territory of Slovenia in comparison with changes in the horizontal component of the geomagnetic field H and the change in the energy density in the geomagnetic field w_{GM} measured at the Observatory.

On Sunday, 1 November 2015 at 07:52 UTC, an earthquake in the southeast of Slovenia reached the magnitude of $M_L = 4.2$. Magnetometers at the Observatory recorded a geomagnetically calm day. A more detailed analysis of the magnetograms of that day did not show any additional changes due to earthquakes. This was the first earthquake since 2012, which was reliably felt by the inhabitants of Slovene Istria. Therefore, it was possible to reliably check the behavior of magnetometers in such an event at the Observatory.

In variometric measurements, the triaxial magnetometer typically measures changes of all three components XYZ (north, east, nadir) of the earth magnetic field at the same time. The measurement of all three components makes it possible to calculate the horizontal component of the geomagnetic field H as well as the geomagnetic index K . Index K gives a relative deviation of a single day compared to a geomagnetically calm day. It is calculated for a single three-hour measurement period and has a logarithmic scale. The geomagnetic index A or the equivalent daily amplitude is the arithmetic mean of all eight linear geomagnetic indices a (average) of a day, which are calculated from the indexes K .

Table 1: Comparisons of two periods of 14 days in the year 2015.

Period of 14 days in 2015	Samples per day	Windows per day	Average A	Act *E-6
9 June – 22 June	1440	24	12.1	-15.038
25 October – 7 November	1440	24	12.4	6.366
Difference:	0	0	0.3	21.404

The equation for the energy density w in the geomagnetic field derives from the equation for energy in the magnetic field of the coil: $w = \frac{1}{2\mu_0}B^2$. When processing digital data, the width of the selected time windows is important. Also the measurement data of a geomagnetically calm day include daily variations generated by the Sun. In order to exclude this daily influence of the Sun, the used width of the time windows should be less than 24 hours. At the same time a sufficient number of samples must be provided in each window.

The standard deviation of the X component of the geomagnetic field is given by its mean X_{avg} value in the selected time window with the number of samples i :

$$X_w = \sqrt{\frac{1}{N} \sum_{i=1}^N \left(\frac{X_i - X_{avg}}{X_{avg}} \right)^2}$$

The standard deviations of all three components of the geomagnetic field form an index of the geomagnetic activity Act (w) for each window and for a given Act (day) day, consisting of all windows w on that day:

$$Act(w) = \sqrt{\Delta X_w^2 + \Delta Y_w^2 + \Delta Z_w^2} \quad Act(day) = \frac{1}{w} \sum_{n=1}^w Act(w)_n$$

Comparison of the index of the geomagnetic activity of each day Act (day) with index of the previous day Act (day-1) gives the relative geomagnetic activity index Act:

$$Act = f [Act(day) - Act(day-1), A * k]$$

The effect of geomagnetic storms is eliminated in the relative geomagnetic activity index of the Act by the equivalent of the daily amplitude A of the individual day.

During the two periods considered in 2015, the change in energy in the geomagnetic field increased sharply over the period around 1 November 2015 compared to that in June 2015 (Table 1). From a very negative value it turned into a positive one for over 21 value units. The index of relative magnetic field energy could be used for the short-term forecasting of earthquakes.

Conclusions:

1. Geomagnetic observatories in the seismologically active areas must be equipped with such types of magnetometers that do not become bad seismographs after seismic shocks. Their installation cannot be carried out completely according to standard international recommendations for the construction of geomagnetic observatories. The operator of the observatory must know the marginal magnitude of the earthquake to which magnetometers are still working normally.

2. From the analysis of the relative change in the energy of the geomagnetic field, the energy is increased in the periods with increased seismological activity. It constantly grows two to three days before the earthquake and then drops. However, an increased index of change in the energy of the geomagnetic field is not a serious indicator of the earthquake. When the earthquake has actually occurred, the energy of the geomagnetic field is increased in advance, but with the increased energy an earthquake does not necessarily occur. In addition to geomagnetism, seismology, volcanology and other areas of geophysics should be involved in the successful forecasting of earthquakes from the increased relative change of geomagnetic field energy.

3. The current measurements of the changes in the geomagnetic field are primarily focused on monitoring the conditions in the Earth's interior and in the Sun's wind near the planet Earth. To monitor changes in the local geomagnetic field on the Earth's surface, further development of suitable measuring instruments, measurement methods and procedures for the processed measurement results and their explanations are needed.

Features of earthquake preparation in the Central and South-Western parts of the Baikal rift according to the tectonomagnetic monitoring data

P. Dyadkov^{1,2}, A. Duchkova¹, D. Kuleshov¹, L. Tsibizov^{1,2}, M. Kozlova^{1,2}, Y. Romanenko^{1,2}

¹*Trofimuk Institute of Petroleum Geology and Geophysics of SB RAS (IPGG SB RAS), 630090, Novosibirsk, Russia, e-mail: DyadkovPG@ipgg.sbras.ru;* ²*Novosibirsk State University, 630090, Novosibirsk, Russia, e-mail: dpg07@mail.ru*

Tectonomagnetic monitoring in the central and southern regions of the Baikal rift zone is carried out at 150 points of repeated annual observations by the Trofimuk Institute of Petroleum Geology and Geophysics of SB RAS, Novosibirsk.

This region is distinguished by high seismic activity and a high degree of seismic hazard. For example at southern end of the Baikal basin earthquakes with a magnitude from 6 to 7.7 for the last 300 years there occurred at least ten.

The purpose of the research is to develop a tectonomagnetic method for monitoring changes in the stressed state of rock massifs, which is important for studying the processes of preparing strong earthquakes and identifying on this basis medium- and short-term seismic-prognostic criteria.

The method and results of the tectonomagnetic observations at the central part and near a southwest end of the Baikal basin are considered.

The main interfering factors for detection of tectonomagnetic anomalies are the inductive effects of geomagnetic variations and secular variation. Special methods of accounting and exclusion of these factors are developed.

Preparation of earthquakes with $M \sim 4.5 - 5$ in the central part of the Baikal rift was accompanied by a bay-like decrease 20-40 days before the event and a subsequent increase in the values of modulus of the magnetic induction vector F 5-10 days before the earthquake. The amplitude of these anomalous changes usually does not exceed 0.5 - 1 nT, which makes it difficult to allocate them in real time.

The change of the anomalous magnetic field in the Central part of the Baikal basin in the early 2000s coincided with a increase in the b-value in this area, which may be due to changes in the state of the seismogenic medium associated with its decompression.

At southern end of the Baikal basin such effects as stabilization of changes in magnetic field for 2 – 3 years before the strong Kultuk earthquake of 2008 with M=6.3, and also gradual relaxation after it are registered. High magnetization of rock massifs in this area allows to consider a source of these changes the piezomagnetic (magnetoelastic) mechanism. Theoretical calculations of a direct problem of a magnetoelasticity with use of a prime model of the magnetic body with relatives to actual magnetic properties allowed to estimate the changes of a stress state which were equal to the first units of MPa. The stabilization effect of magnetic field changes before the Kultuk earthquake in 2005-2008 coincided with seismic quiescence on southeast segment of the Main Sayan fault that gives the grounds to assume existence of "coupling" of one of rigid blocks of the Amur plate with the Siberian platform during this period.

Acknowledgements

Research is partially supported by RFBR 17-05-01234, SB RAS Interdisciplinary project 34 and FSI program IX.128.2.

An electric cloud model for the signals recorded in Central Italy during intense seismic swarms

C. Fidani¹

¹*Central Italy Electromagnetic Network, Fermo, Italy, c.fidani@virgilio.it*

A first step of the test for wide band electromagnetic detectors that continuously recorded the electric components of the electromagnetic field, ranging from a few of Hz to tens of kHz, was concluded. The detectors realised the Central Italy Electromagnetic Network (CIEN) that has been operating for more than twelve years. CIEN started to record in 2006 with the first station at San Procolo, Fermo, reached a maximum of 16 stations in 2015 – 2017, and is presently composed of 8 stations. The active CIEN stations are Fermo, Chieti, Camerino, Colfiorito, Avigliano Umbro, Trasacco, Faenza and Narni. The recent decreasing number of active stations was due to the need to publish the results of the first step test and waiting to install new detectors. The first step test consisted in verifying the presence of electromagnetic radiation in connection with strong earthquakes using electric detectors. In fact, occasional observations centuries ago up until today of earthquake lights in Central Italy suggested the occurrence of electric phenomena in the atmosphere (Fidani, 2005).

A relevant probability of strong earthquake occurrence was calculated in recent studies for Central Italy (Cinti et al., 2004) and, in fact, three periods of major earthquakes have occurred throughout three different regions of Central Italy over the last decade, leading to deaths and extensive damage. The April 6 L'Aquila earthquake in 2009, the May 20 Modena earthquake in 2012 and the Amatrice – Norcia – Capitignano sequence which occurred August 24, October 30 in 2016 and January 18 in 2017, respectively. Four earthquakes occurred at these times having reached the magnitude of 6: L'Aquila Mw = 6.3, Modena Mw = 6.0, Amatrice Mw = 6.0 and Norcia Mw = 6.6. Whereas, 14 earthquakes overcame magnitude 5 in Central Italy during the same period, including the July 23 Ancona earthquake in 2013 with Mw = 5.0 and the October 26 Castelsantangelo sul Nera earthquakes in 2016 with Mw = 5.9 and Mw = 5.4.

Oscillations in electric amplitudes were recorded during all these three periods with amplitudes greater than normally measured. These oscillations are well discriminated from other natural and anthropogenic signals in spectrograms, see Figure 1 up. Patterns recorded during all three periods were generally the same: they lasted from a few minutes up to two

hours, and concerned frequencies between 40 Hz and 350 Hz. The electrical oscillation intensities observed during strong seismic activity in all the CIEN stations ranged between -80 dB to -50 dB. Electric oscillation intensities started to increase weeks or months before the main shocks, reached a maxim around the main shocks which were maintained for days or weeks, and then started to decrease returning to normal values in few weeks. The pattern of intensity observed during the 2009 L'Aquila swarm (Fidani, 2011) is reproduced in Figure 1.

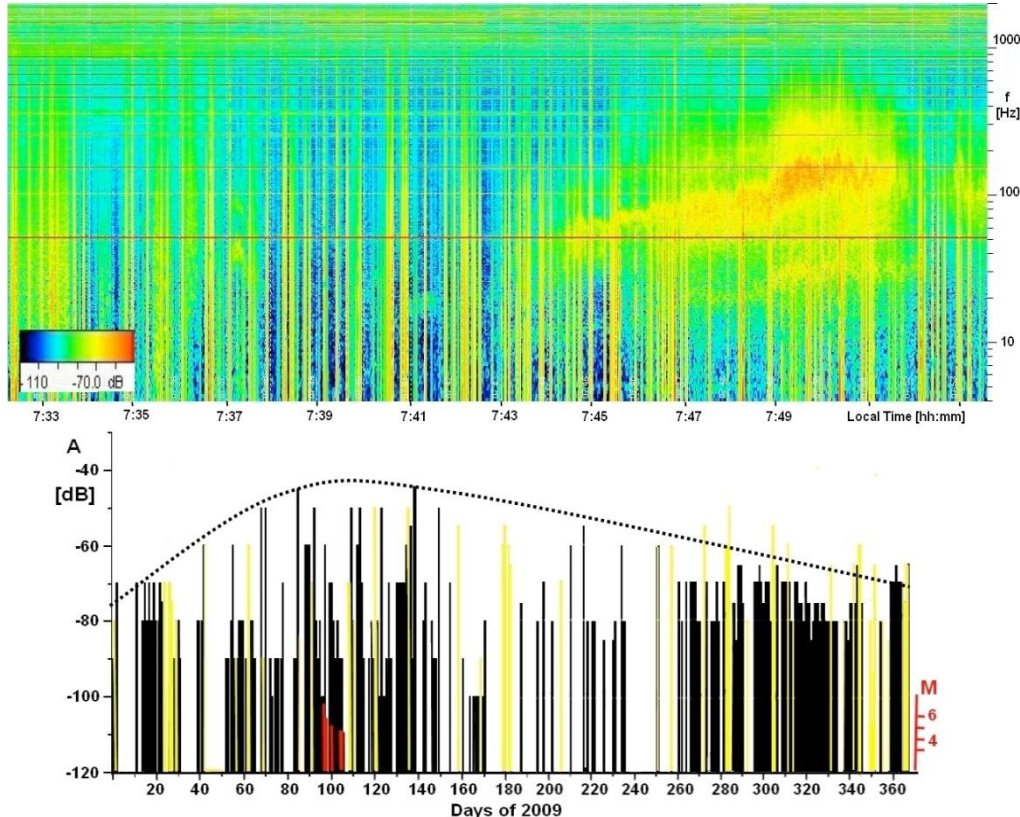


Fig. 1. up: The spectrogram for the ELF band recorded at Fermo Station on 2 April 2009, from 7:33LT to 7:53LT; down: The maximum amplitude power spectrum in dB of oscillations in ELF band recorded at the Fermo Station in 2009. Yellow bars refer to data influenced by meteorology while red bars indicate strong earthquakes in Central Italy.

The same pattern of intensity was observed also during the Modena swarm (Fidani and Martinelli, 2015) and the Norcia – Capitignano swarms (Fidani, 2017). However, until now, there was no evidence for the same pattern of intensity to be observed during the Amatrice swarm. Furthermore, not all the CIEN stations have shown the same intensity modulation. Even if such behavior was observed in three of the main shocks with $Mw \geq 6$ out of four in the same way, there is not sufficient data to obtain a statistical correlation. Electrical oscillations, such as those described above were also detected by other CIEN stations during low and moderate seismic activity. Specifically, electrical oscillations were recorded on many occasions where earthquake magnitudes comprised between 2.0 – 3.7 in the Umbria territory after 2013 (Fidani and Marcelli, 2017). A statistical analysis was possible on electric data in

relation to low and moderate seismic activity. Correlation plots were calculated on about one years of data at Avigliano Umbro and are shown on Figure 2. Electric oscillations statistically preceded low and moderate seismic activity for about 6 days in these limited examples.

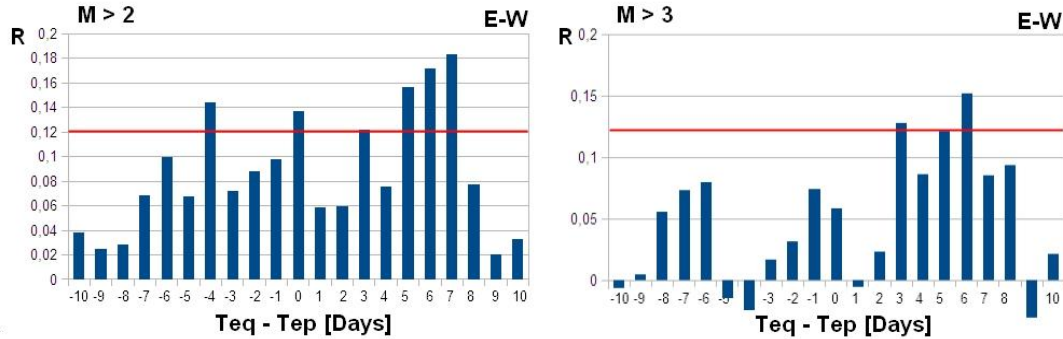


Fig. 2. Statistical correlations between earthquakes and electric oscillations at Avigliano Umbro Station, left plot with $M > 2$ was calculated considering seismic events within 30 km, right plot with $M > 3$ was calculated considering seismic events within 70 km; red lines indicate a probability greater than 95%.

Results of the increasing in amplitude of electric oscillations around strong earthquakes and the statistical correlations between electric oscillations and low and moderate seismic activity support the possibility of an association between earthquakes and electric signals. To describe a physical model able to generate the observed electric field oscillations and to be able to link them with earthquakes is the essential confirmation for such an hypotheses. Measurements suggested localised floating sources in the atmosphere of limited dimensions able to generate local horizontal electric fields. Recordings of electric oscillations shown relatively stable phenomena the duration of which go on for up to several hours. For these reasons the physical model of electrically charged clouds where electric forces are balanced by gas pressure forces, was taken into consideration (Tennakone, 2011). It can be associated with a well known mathematical problem for spherical symmetry which produces simple solutions describing stable oscillations of the cloud.

One of the charge distributions correspondent to the charged cloud stability can be calculated in

$$\rho(r) = (2 \Delta P \varepsilon_o / r_o^2)^{0.5} (3 - r/r_o) \exp(-r/r_o),$$

which indicates that a positive charge is confined in a spherical volume of radius $3r_o$, where $\varepsilon_o = 8.85 \cdot 10^{-12}$ F/m is the dielectric constant and ΔP is the pressure difference between the centre and a point far outside of the charged cloud. With $\Delta P/P = 0.5$ the oscillation frequency of charged sphere can be linked to its radius $f = 20.5/r_o$ and the charge inside the sphere to the frequency $Q = 6.7/f^2$, so that for oscillation frequency of 50 Hz a sphere of 2.46

m must be considered which contains $2.7 \cdot 10^{-3}$ C. With $\Delta P/P = 0.1$ oscillation frequency of 50 Hz requires a sphere of 1.08 m which contains $2.3 \cdot 10^{-4}$ C and an oscillation frequency of 200 Hz requires a sphere of 0.27 m which contains $1.4 \cdot 10^{-5}$ C. This model is attractive because it suggests that with high charge concentrations, corona discharges in the spaces between the separate charges can render the cloud luminous and this explains some recordings of earthquake lights such as luminous spheres.

The charged cloud model does not contradict any experimental measurement made by CIEN. It can be linked to seismic activity by crustal fluid migration which transport charges escaping into the atmosphere, at different temperatures and pressures with respect to the atmospheric ones. Pressure and electric forces balanced between themselves in the atmosphere generate stable structures which must pass near the CIEN stations to be revealed. To further confirm this model other types of physical measurements are now necessary and will form the next CIEN stations. For example, an air ion detector could reveal increased ion numbers when electric oscillations are detected. Moreover, experimental proof is needed to demonstrate fluid electrification escaping from the ground. Finally, the influence of meteorological activity on charged cloud movements such as wind direction and velocity must be investigated.

References

- Cinti F.R., Faenza L., Marzocchi W., Montone P.; 2004: Probability map of the next M 3 5.5 earthquakes in Italy. *Geochemistry Geophysics Geosystems*, Volume 5, Number 11, 1-15.
- Fidani C.; 2005: Ipotesi sulle anomalie elettromagnetiche associate ai terremoti. Libreria Universitaria Benedetti L'Aquila, L'Aquila, Italy, 300pp.
- Fidani C.; 2011: The Central Italy Electromagnetic Network and the 2009 L'Aquila earthquake: observed electric activity. *Geoscience*, 1, 3-25.
- Fidani C. and Martinelli G.; 2015: A possible explanation for electric perturbations recorded by the Italian CIEN stations before the 2012 Emilia earthquakes, *Bollettino di Geofisica Teorica ed Applicata*, 56, 2, 211-226.
- Fidani C. and Marcelli D.; 2017: Ten Years of the Central Italy Electromagnetic Network (CIEN) Continuous Monitoring, *Open Journal of Earthquake Research*, 6, 73-88.
- Fidani C.; 2017: Electricity perturbations observed around the October 30, 2016 Norcia earthquake, $M = 6.5$, 36th GNGTS, November 14 – 16, Trieste, 314-316.
- Tennakone K.; 2011: Stable spherically symmetric static charge separated configurations in the atmosphere: Implications on ball lightning and earthquake lights. *J. Electrostat.*, 69, 638-640.

New Deep Electrical Resistivity Tomography in the High Agri Valley basin (Basilicata, Southern Italy)

V. Giampaolo¹, L. Capozzoli¹, E. Rizzo¹

¹CNR-IMAA, Laboratory Hydrogeosite, Italy, enzo.rizzo@imaa.cnr.it

A deep longitudinal high-resolution image of the fault-controlled High Agri Valley Basin obtained with the electrical resistivity tomography is presented. The aim of the present work was to characterize the superficial morphology of the pre-Quaternary substrate, the thickness of the Quaternary alluvial deposits and to contribute to the knowledge of the geological-structural structure of the basin of the high Agri Valley, using Deep Electrical Resistivity Tomography (DERT) method.

The high Agri valley (Basilicata) is one of the intermontane depressions of tectonic origin of the Southern Apennines and it is one of the most complex component of the Quaternary fault network of the Apennine chain. The basin represents an active neotectonic area and one of the higher seismic and environmental hazard sectors of southern Apennines. In fact, the basin was affected by recurrent and destructive earthquakes, such as the 1857 Basilicata earthquake (Gasperini et al., 1999; Burrato and Valensise, 2008), as well as it is one of the most important areas for hydrocarbon extraction in Europe. Finally, the area was characterized by the development of important historical settlements in the past and by dense urbanization in recent times. The geometry of the pre-Quaternary bedrock, the location and dip of the master fault and the tectonic evolution of the basin are still debated. The geological complexity of the study area has led to the use of geophysical techniques, in fact, geophysical methods have been effective tools over the years for studying tectonically active areas.

Several recent works focus on geophysical survey (seismic and Magnetotelluric surveys) for deep geological and tectonic High Agri Valley characterization, mostly in the quaternary basin southern portion (Impronta et al., 2010; Stabile et al., 2014; Balasco et al., 2015; Buttinelli et al., 2016; Impronta et al., 2017). They provided images of fault systems and gave a relevant support to seismologists and structural geologists.

In this frame only few applications concerning the use of unconventional geoelectrical methods (investigation depth greater than 200 m), such as Deep Electrical Resistivity Tomography (DERT) method, have been presented. However, it is an excellent geophysical tool to the study of the sedimentary basin (Rizzo et al., 2004; Giocoli et al., 2008; Balasco et

al., 2011; Pucci et al., 2016). In detail, the remarkable resolution obtained through this technique allows to discriminate much more effectively the resistivity contrasts present in the subsoil.

In this paper, we focus our attention on the analysis of a new acquired Deep Electrical Resistivity Tomography giving a first deep geoelectrical longitudinal section of the Agri Valley and thus providing more reliable information on the basin characteristics, on the presence of surfaces of structural discontinuities, and development of aquifers and/ or fluids of various origins. The geological complexity of the study area and the depth of the basin led to the use of the Dipole-type. In contrast to previous studies (Colella et al., 2004; Rizzo et al., 2004), in the present work the DERT was acquired through a new instrumentation designed and built at the Geophysical Laboratory of the Institute of Methodologies for Environmental Analysis (IMAA) of the CNR. These instruments introduces many innovations compared to the instrumentation used in the past. It also allows the expansion and the adaptability of this system to the most varied logistical conditions, both as regards the number of data that can be acquired (greatly increasing the number) and in optimizing the survey times. In addition, the DERT profile measured during this work reaches a length of about 21 km along the longitudinal section of the valley and a depth of investigation of about 1 km, giving new insight of the deep structure of the studied basin.

Finally, by integrating the geological-structural data present in the literature and the new geophysical ones, it was possible to elaborate a new and more detailed geological-structural-paleomorphological model of the basin in depth. In particular, it is possible to observe, under several metres of quaternary deposits (more than 500 m), buried structures probably as the result of the combined action of the pre-quaternary and fragile quaternary deformations. The buried pre-quaternary bedrock structural highs are bordered by anti-Apennine faults (NE-SW), probably characterized by a Strike-slip component (Figure 1).

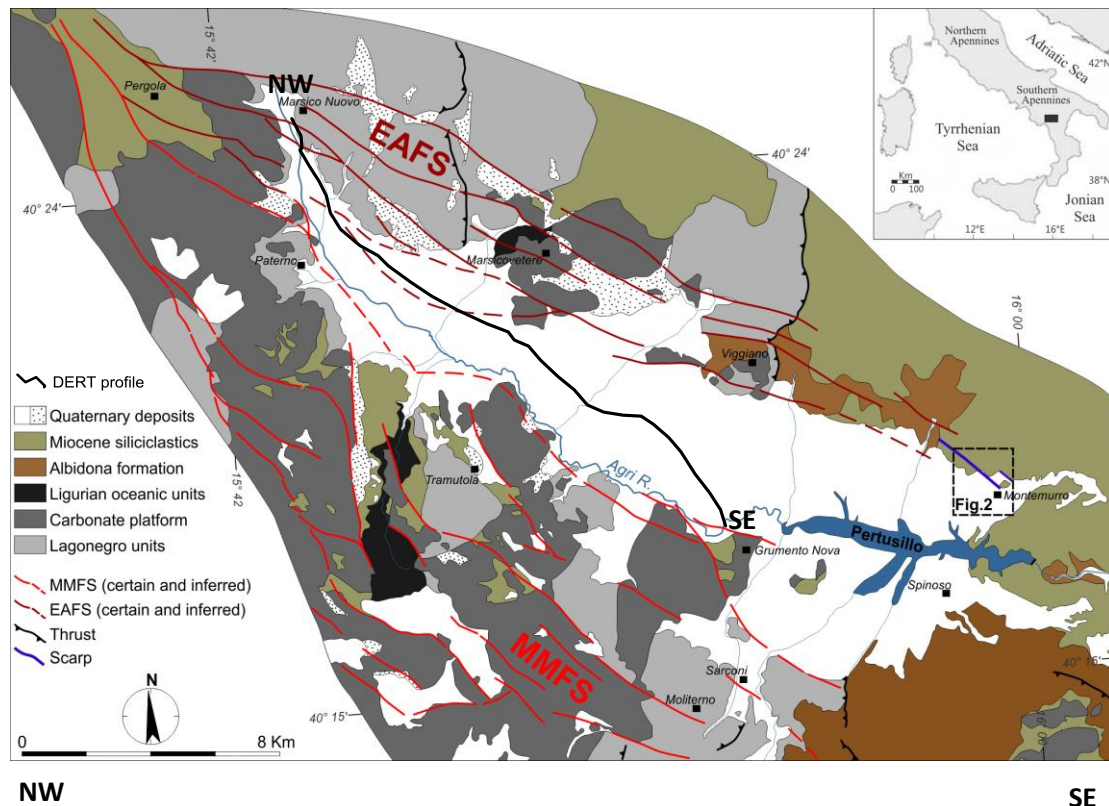


Fig. 1 - Geological map of the High Agri Valley (modified from Giocoli et al., 2015) and the location and geological interpretation of DERT profile.

References

- M. Balasco, P. Galli, A. Giocoli, E. Gueguen, V. Lapenna, A. Perrone, S. Piscitelli, E. Rizzo, G. Romano, A. Siniscalchi, M. Votta (2011). Deep geophysical electromagnetic section across the middle Aterno Valley (central Italy): preliminary results after the April 6, 2009 L'Aquila earthquake. doi:10.4430/bgta0028
- M. Balasco, A. Giocoli, S. Piscitelli, G. Romano, A. Siniscalchi, T. A. Stabile, and S. Tripaldi (2015), Magnetotelluric investigation in the High Agri Valley (southern Apennine, Italy). Nat. Hazards Earth Syst. Sci., 15, 843–852.
- P. Burrato, G. Valensise (2008), Rise and fall of a hypothesized seismic gap: source complexity in the 16 December 1857, Southern Italy earthquake (Mw 7.0). Bull. Seism. Soc. Am. 98 (1), 139-148, doi:10.1785/0120070094.
- M. Buttinelli, L. Imrota, S. Bagh, C. Chiarabba (2016), Inversion of inherited thrusts by wastewater injection induced seismicity at the Val d'Agri oilfield (Italy). Scientific Reports, 6:37165, DOI: 10.1038/srep37165.
- Colella, V. Lapenna, E. Rizzo (2004), High-resolution imaging of the High Agri Valley Basin (Southern Italy) with electrical resistivity tomography. Tectonophysics 386 (2004) 29–40.
- P. Gasperini, F. Bernardini, G. Valensise, E. Boschi (1999), Defining seismogenic sources from historical earthquake felt reports, Bull. Seism. Soc. Am. 89, 94-110.
- Giocoli, C. Magrì, S. Piscitelli, E. Rizzo, A. Siniscalchi, P. Burrato, P. Vannoli, C. Basso, S. Di Nocera (2008), Electrical Resistivity Tomography investigations in the Ufita Valley

- (southern Italy), *Ann. Geophys.*, 51, 213–223.
- L. Imrota, S. Baghi, P. De Gori, L. Valoroso, M. Pastori, D. Piccinini, M. Buttinelli (2017), Reservoir structure and wastewater-induced seismicity at the Val d'Agri oilfield (Italy) shown by three-dimensional Vp and Vp/Vs local earthquake tomography. *Journal of Geophysical Research: Solid Earth*, 122, 9050–9082. <https://doi.org/10.1002/2017JB014725>.
 - L. Imrota, L. Ferranti, P. M. De Martini, S. Piscitelli, P. P. Bruno, P. Burrato, R. Civico, A. Giocoli, M. Iorio, G. D'Addazio, L. Maschio (2010), Detecting young, slow-slipping active faults by geologic and multidisciplinary high-resolution geophysical investigations: A case study from the Apennine seismic belt, Italy, *J. Geophys. Res.*, 115, B11307, doi:10.1029/2010JB000871.
 - S. Pucci, R. Civico, F. Villani, T. Ricci, E. Delcher, A. Finizola, V. Sapia, P. M. De Martini, D. Pantosti, S. Barde-Cabusson, E. Brothelande, R. Gusset, C. Mezon, S. Orefice, A. Peltier, M. Poret, L. Torres, B. Suski (2016), Deep electrical resistivity tomography along the tectonically active Middle Aterno Valley (2009 L'Aquila earthquake area, central Italy). *Geophys. J. Int.* (2016) 207, 967–982 Imrota, L., Bagh, S., De Gori, P., Valoroso, L., Pastori, M., Piccinini, D., ... Buttinelli, M. (2017). Reservoir structure and wastewater-induced seismicity at the Val d'Agri oilfield (Italy) shown by Three-dimensional Vp and Vp/Vs local earthquake tomography. *Journal of Geophysical Research: Solid Earth*, 122, 9050–9082. <https://doi.org/10.1002/2017JB014725> Imrota, L., Bagh, S., De Gori, P., Valoroso, L., Pastori, M., Piccinini, D., Buttinelli, M. (2017). Reservoir structure and wastewater-induced seismicity at the Val d'Agri oilfield (Italy) shown by three-dimensional Vp and Vp/Vs local earthquake tomography. *Journal of Geophysical Research: Solid Earth*, 122, 9050–9082. <https://doi.org/10.1002/2017JB014725>
 - E. Rizzo, A. Colella, V. Lapenna, S. Piscitelli (2004), High-resolution images of the fault-controlled High Agri Valley basin (Southern Italy) with deep and shallow electrical resistivity tomographies. *Physics and Chemistry of the Earth*, 29, 321–327.
 - T. A. Stabile, A. Giocoli, A. Perrone, S. Piscitelli, V. Lapenna (2014), Fluid injection induced seismicity reveals a NE dipping fault in the south-eastern sector of the High Agri Valley (southern Italy), *Geophys. Res. Lett.*, 41, 5847–5854, doi:10.1002/2014GL060948.

Statistical Analysis and Assessment of ULF Magnetic Signals in Japan as Potential Earthquake Precursors

K. Hattori¹, P. Han²

¹*Graduate School of Science, Chiba University, Japan, hattori@earth.s.chiba-u.ac.jp;* ²*Southern University of Science and Technology, China*

In order to clarify the ULF seismomagnetic phenomena, a sensitive geomagnetic network has been installed in the Kanto region of Japan. In this study, we have analyzed geomagnetic data observed during the past decade in Izu and Boso Peninsulas, and at the Kakioka station. Energy of ULF geomagnetic signals at the frequency around 0.01 Hz has been investigated by wavelet transform analysis. Statistical studies by SEA have indicated that before a sizeable earthquake there are clearly higher probabilities of ULF anomalies than after the earthquake. Meanwhile, we have used Molchan's error diagram to evaluate the potential earthquake precursory information in the ULF magnetic data recorded in the Kanto region of Japan during 2000–2010. The results show that the earthquake detections based on magnetic anomalies are clearly better than a random guess, indicating that the magnetic data contain potentially useful information on earthquake forecasts. We have also demonstrated the influences of Δ and L on short - term earthquake forecasting. To find out the best prediction parameters, a modified area skill score was introduced to assess the efficiency of different prediction strategies. The detailed results will present in the talk.

Groundwater Electrical Conductivity signal processing and earthquake precursors

N. Inbar^{1,2}, Y. Reuveni^{1,2}, S. Agibayev¹

¹*Eastern R&D Center, Geophysics and Space Sciences, Ariel, Israel;* ²*Physics Department, Ariel University, Israel*

Correlation between groundwater Electrical Conductivity (EC) and $Mw > 2.9$ earthquakes has been found (Fig. 1), using a newly developed algorithm, based on frequency domain signal analysis applied with six months of data collected in four different monitoring wells at the northern part of Israel. Data were measured at a sampling resolution of 1/60 Hz (1 measurement/minute) both in phreatic and confined parts of the cretaceous carbonates. All earthquakes of $Mw > 2.9$, and with sufficient forgoing data, occurring along the Dead Sea Transform as far as 500 km, are preceded by a clear indication with the processed EC signal in the time frame of several days. Conversely, earthquakes with epicenter located on the Cyprus Arc subduction zone, as far as 200 km from the monitoring stations show no effect on the processed EC signal. We conclude that groundwater EC precursory signs for earthquakes with magnitude larger than 2.9 Mw might be detectable using such algorithm. However, it seems that detection is strictly related to the tectonic system on which continues monitoring is performed.

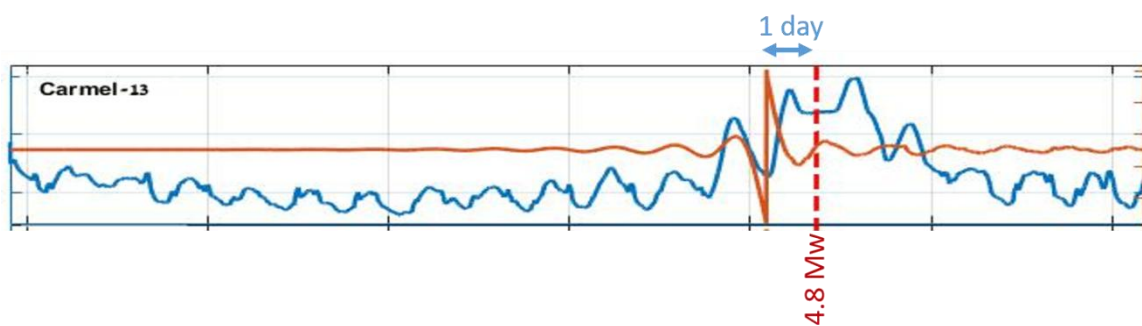


Fig. 1. Processed signal (orange) Vs. raw data (blue). The Epicentre of the 4.8 Mw Earthquake was >400 km from the monitoring station.

Introduction

Changes in groundwater prior to seismic events is considered to be related to several aspects of pre-seismic crustal deformation. Both increases and decreases in groundwater, oil, or gas pressure and flow rate have been interpreted as possible precursors, at distances up to

several hundred kilometers from the earthquake epicenter (Roeloffs, 1988). At the fault zone, episodic flow of high pressure water between local compartments was suggested to precede earthquake occurrence generating electrical and/or magnetic signal (Byerlee, 1993). Aquifer breaching of various scales was considered as the mechanism leading to mixing of different water type from adjacent lateral source (Cicerone *et al.*, 2009) and adjacent vertical source (Wang *et al.*, 2016). Chemical precursory changes were attributed also to exposure of fresh rock surfaces to groundwater by expansion of the rock volume (dilation) and enhanced permeability (Skelton *et al.*, 2014). Additionally, pre-seismic electrical signal was attributed to physio-electrical processes (Freund, 2011).

Based on statistical analysis of reported observations, Cicerone *et al.* (2009) concluded that, (1) large amplitude precursory anomalies tend to occur before the large magnitude earthquake, (2) the number of precursory anomalies tends to increase the closer in time to the occurrence of the earthquake and (3) the precursory anomalies tend to occur close to the eventual epicenter of the earthquake. Our findings imply that the tectonic settings should be taken into account as well.

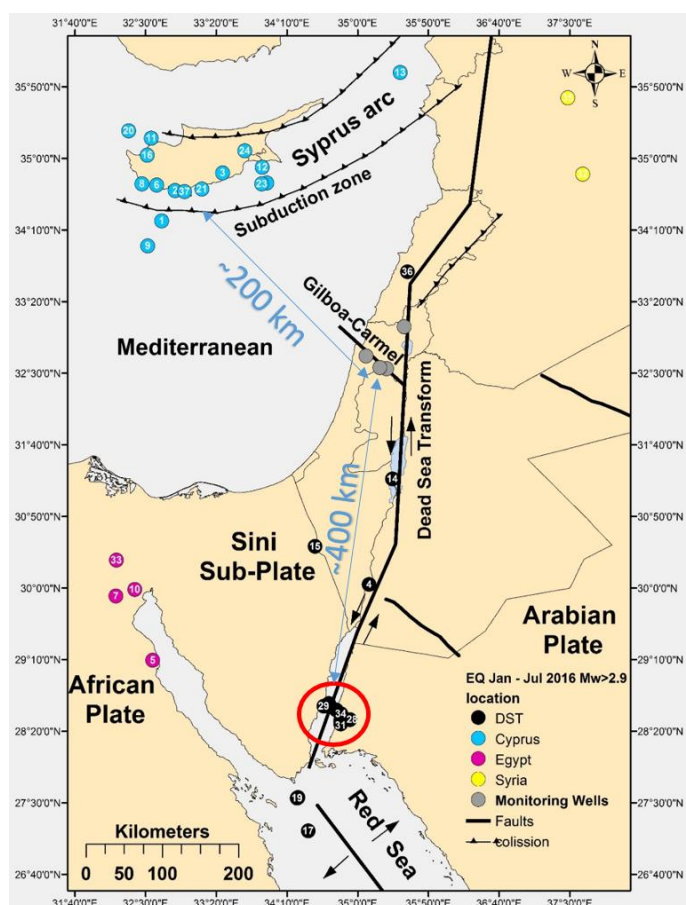


Fig. 2 Location map. Monitoring wells marked with grey circles. All earthquakes above 2.9 Mw in the area at the time of the processed signal marked with color-coded circles according to tectonic settings.

Data and methodology

In the current research, four water wells in northern Israel were continuously monitored between January and July 2016 (fig. 2). The wells were drilled into the Cenomanian-Turonian carbonate aquifer. Two of the wells are located on the phreatic part of the aquifer (Carmel-13 and Hindaj-2) and in the other two are under confined conditions (Ta'anach-4 and Nurit-1). Three wells (Carmel-13, Ta'anach-4 and Nurit-1) are located along the Gilboa-Carmel Fault (GCF). Another well (Hindaj-2) is located north of the

Hula Basin, close to the Dead Sea Transform (DST). All monitoring

stations are located in observation wells with no adjacent pumping or injecting wells (*Inbar et al.*, 2017).

Earthquakes information was obtained from the Geophysical Institute of Israel (<http://seis.gii.co.il/heb/earthquake/searchEQS.php>). The database was screened to include all events above 2.9 Mw in the area defined by the rectangle 27.0 – 36.0 Latitude and 32.0 – 38.0 Longitude. Altogether 37 events were recorded between 1/1/2016 and 3/7/2016, the period of analyzed dataset (Fig. 2). For each seismic event, the epicenter distance for each monitoring station was calculated.

Data Analysis

The raw EC signal has been analyzed both in time and frequency domain followed by de-trending procedure. Preliminary analysis indicated a diurnal dominant frequency which seems to be strongly linked with earth tides.

Raw data was collected at a sampling resolution of 1/60 Hz. However, due to equipment failure, GPRS connection loss and server malfunction, raw data is not entirely continues.

Those gaps in raw data poses preliminary challenge in data processing. Hence, small data gaps (<90 min) were interpolated. Larger gaps were left out of analysis and filtering (Fig .3).

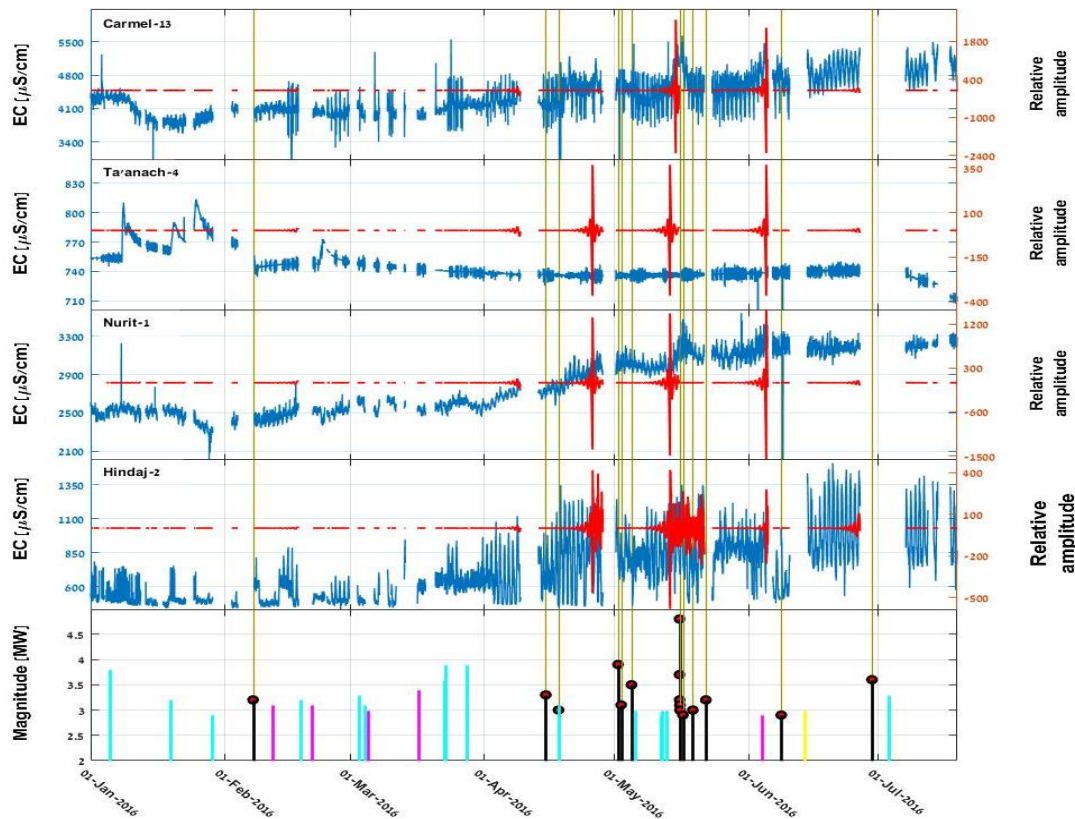


Fig. 3 Electrical conductivity raw data (blue) and de-trended signal (red) obtained from all four monitoring stations. At the base, all seismic events color-coded according to tectonic settings (as in Fig. 2).

Conclusions

Following data analysis, we obtained a de-trended signal which starts rippling a few days prior to a seismogenic activity along the Dead Sea Transform (DST) and peaking about 24 hours prior to the main shock. It seems that tectonic settings influence the measured signal as earthquakes show precursory signs at our monitoring stations only if epicentre is located at the DST. Closer and similar or higher magnitude events with epicentre located at the Cyprus arc was not detected.

The mechanism behind the fluctuating electrical conductivity of groundwater is unclear. For the diurnal fluctuation we suggest exploring the possibility of gravity driven mixing of stratified groundwater due to earth tides effect. Whereas the precursory change in fluctuation might be attributed to local deformation at monitoring site or fast traveling electric field generated by stress applied at the area of future earthquake.

Time and frequency domain analysis followed by de-trending procedure of the raw Electrical Conductivity signal measured in four water wells show encouraging and convincing earthquake precursors. However, further data collection and additional signal processing approaches are needed in order to gain a robust, real time, operational methodology for earthquake forecasting.

References

- Byerlee, J. D. (1993), Model for episodic flow of high-pressure water in fault zones before earthquakes, *Geology*, 21(4), 303-306.
- Cicerone, R. D., J. E. Ebel, and J. Britton (2009), A systematic compilation of earthquake precursors, *Tectonophysics*, 476(3), 371-396, doi:<http://dx.doi.org/10.1016/j.tecto.2009.06.008>.
- Freund, F. (2011), Pre-earthquake signals: Underlying physical processes, *Journal of Asian Earth Sciences*, 41(4), 383-400, doi:<http://dx.doi.org/10.1016/j.jseaes.2010.03.009>.
- Inbar, N., Y. Reuveni, S. Agibayev, Y. Anker, and J. Guttman (2017), A New Approach for Analyzing Continuous Groundwater Physicochemical Measurements Related to Earthquake Precursor Studies, *Judea and Samaria Research Studies*, 26(2), 83-91.
- Roeloffs, E. A. (1988), Hydrologic precursors to earthquakes: A review, *pure and applied geophysics*, 126(2), 177-209, doi:10.1007/bf00878996.
- Skelton, A., et al. (2014), Changes in groundwater chemistry before two consecutive earthquakes in Iceland, *Nature Geosci*, 7(10), 752-756, doi:10.1038/ngeo2250

- <http://www.nature.com/ngeo/journal/v7/n10/abs/ngeo2250.html#supplementary-information>.
- Wang, C.-Y., X. Liao, L.-P. Wang, C.-H. Wang, and M. Manga (2016), Large earthquakes create vertical permeability by breaching aquitards, *Water Resources Research*, 52(8), 5923-5937, doi:10.1002/2016WR018893.

Quality Assessment of Long Term Magnetometer Array Data: Lessons Learned from the QuakeFinder Dataset

K.N. Kappler¹, T.B. Bleier¹, L.S. MacLean¹, D.D. Schneider¹

¹*Quakefinder, Palo Alto, USA, kkappler@quakefinder.com*

Since 2005 QuakeFinder (QF) has acquired via a distributed array of remote measuring stations, a unique dataset with outstanding spatial and temporal sampling of earth's magnetic field variations along several active fault systems. This QF network consists of 124 stations in California and an additional 45 stations along fault zones in Greece, Taiwan, Peru, Chile and Indonesia. Each station is equipped with three feedback induction magnetometers, two ion sensors (one for detection of positive ions and one for the detection of negative ions), a horizontal geophone, a temperature sensor, and a humidity sensor. The data is continuously recorded at 50 samples per second with GPS antennas supplying pulse-per-second reference time stamps and transmitted daily to the QF data center in California for analysis. A 24h segment of data from these sensors from an arbitrary but fixed QF station we refer to a "station day". We have acquired approxiamtely 300,000 station days to date. QF is attempting to detect and characterize anomalous EM activity occurring ahead of earthquakes. This presentation provides a status report of our effort.

Investigation of lower ionosphere properties in correlation with Romanian seismic activity using VLF/LF radio waves propagation and GPS/GNSS analysing techniques

I.A. Moldovan¹, C. Oikonomou², A. Muntean³, V.E. Toader⁴, P.F. Biagi⁵, A. Constantin⁶, D.D. Toma⁷, E. Nastase⁸, A. Moldovan⁹

¹National Institute for Earth Physics, Magurele, Romania, irenutza_67@yahoo.com, ²Frederick Research Center, Nicosia, Cyprus, res.ec@frederick.ac.cy, ³National Institute for Earth Physics, Magurele, Romania, muntean@infp.ro, ⁴National Institute for Earth Physics, Magurele, Romania, asyst@asystech.ro, ⁵Department of Physics, University of Bari, Bari, Italy, pf.biagi@gmail.com, ⁶National Institute for Earth Physics, Magurele, Romania, angela@infp.ro, ⁷National Institute for Earth Physics, Magurele, Romania, toma@infp.ro, ⁸National Institute for Earth Physics, Magurele, Romania, eduard_nastase@infp.ro, ⁹Terrasingna Ltd, Bucharest, Romania, amold03@yahoo.com

The understanding and interpretation of the relation between seismic activity and ionospheric disturbances has received significant attention the last three decades. In the present study, we follow a multi-techniques and multi-parameters approach aiming to observe possible ionospheric precursors related to six medium sized ($M_L \geq 5$) earthquakes that took place in Romania during 2013–2017 (Table 1) in Vrancea seismogenic zone, both at normal and intermediate depth (VRN and VI in Figure 1).

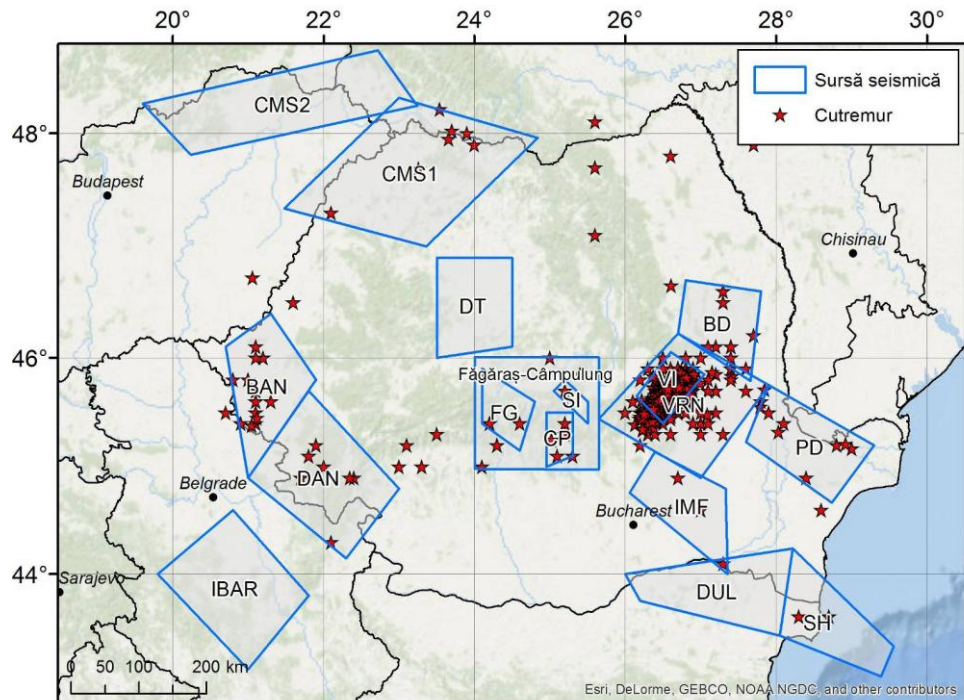


Fig. 1. Seismic zonation in Romania

Table 1. Recent seismicity ($M_L > 5.0$) from Vrancea zone (crustal and intermediate depth)

No	Date	Time (UTC)	Latitude	Longitude	Depth	M_L	M_w	Io
R1	2013/10/06	01:37:21	45.6423	26.6928	134	5.6	5.3	V
R2	2014/11/22	19:14:17.11	45.8683	27.1517	40.9	5.7	5.4	VI
R3	2016/09/23	23:11:20.06	45.7148	26.6181	92.0	5.8	5.5	VI
R4	2016/12/27	23:20:55.94	45.7139	26.5987	96.9	5.8	5.6	VI
R5	2017/02/08	15:08:20.89	45.4874	26.2849	123.2	5.0	4.8	IV
R6	2017/08/02	02:32:12.68	45.5286	26.4106	131.0	5.0	4.6	IV

In detail, we applied spectral analysis on GNSS TEC data, as well as the terminator time method on VLF/LF subionospheric signal amplitude data deriving from the Romanian receivers of INFREP European network (Table 2).

Table 2. Romanian VLF/LF radio receivers from INFREP and NIEP

Ri	Code	Location	Lat	Long	Start	LFi	VLFi
R11	Dob-RO	Eforie Nord, Romania	44.08	28.63	9/2009	T11, T8,T7, T4	T10,T13,T14,T12, T5, AWT25
R12	Bir-RO	Barlad	46.23	27.64	06/2017	T11, T8,T7, T4	T10,T13,T14,T12, T5, AWT25
R13	PLOR-RO	Plostina	45.85	26.65		New receivers (not installed)	
R15	MAG-RO	Magurele	44.35	26.03		New receivers (not installed)	

The INFREP network consists of 11 digital radio receivers that measure the amplitude of the radio signals on 10 frequencies distributed in the VLF/LF bands, since February 2009. In Figure 2 (right side) are shown the locations of the Romanian INFREP receivers (Moldovan et al., 2015) and the monitored transmitters as well as the Vrancea earthquakes epicentres R1-6 and also of the European earthquakes with $M_L > 6.0$.

The modern Romanian NIEP GNSS/GPS network started in 2001 when the first permanent station was installed on the Lacauti peak in the mountainous zone of the Carpathian Bending Zone, west of the Vrancea epicentral area. Now the network has 27 operational stations, <http://gps.infp.ro> (Figure 2 – left side).

The major objectives of the network are (Muntean et al., 2016 and 2017 and Nastase et al., 2016):

- monitoring the surface expressions of the crustal changes occurring in and around the

Romanian Carpathians and the neighboring tectonic units, as direct expression of the tectonic processes viewed at a larger scale, for example on the northeastern flank of the Africa-Europe interaction);

- observation the crustal motions in order to better understand the surface-to-depth interconnections of intermediate deep earthquakes with shallow expressions in the Vrancea zone;
- real time mapping of TEC and ionospheric studies.

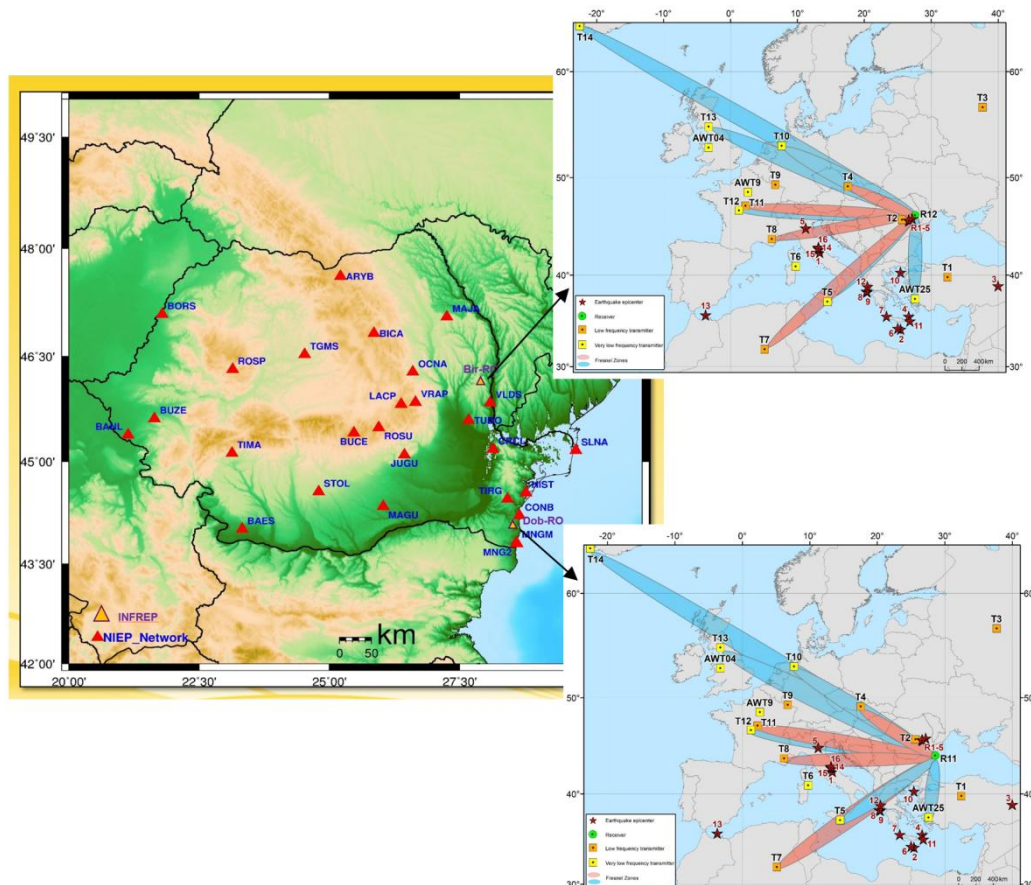


Fig 2. GPS/GNSS network and INFREP Romanian receivers

The analysis of six seismic events in Romania with magnitudes $M_L > 5.0$ by utilizing TEC data obtained from the Romanian permanent GPS station network has shown that ionospheric precursory phenomena can be observed one day up to few hours prior to the crustal $M_L = 5.7$ earthquake (R2) and especially for the stations from the vicinity of the epicenter, whereas preseismic TEC anomalies were not identified in case of deeper or lower magnitude earthquakes and during the occurrence of small sized geomagnetic storms. In addition, this study demonstrates that in order to increase the credibility on the presence of ionospheric precursory phenomena associated with an earthquake and to provide more safe conclusions, it is of high importance to simultaneously apply different techniques such as the Cross-

Correlation Analysis and the Spectral Analysis (Oikonomou, et al., 2017).

The analysis of the same seismic events by applying terminator time method on VLF/LF signal data demonstrated that in all events the sunrise terminator times were delayed approximately 20–40 min few days prior and during the earthquake day.

The multi-technique and multi-parameter approach which was adopted in this study is a requirement for the precise identification of earthquake ionospheric precursors and is highly recommended it for ionospheric-earthquake related studies.

Acknowledgements

This paper was carried out within Nucleu Program, supported by ANCSI, project no. PN 16 35 03 01/2016 and PN 18 15 01 01/2018

References

- Moldovan, I.A., A.P. Constantin, P.F. Biagi, D. Toma Danila, A.S. Moldovan, P. Dolea, V.E. Toader, T. Maggipinto. The Development of the Romanian VLF/LF Monitoring System as Part of the International Network for Frontier Research on Earthquake Precursors (INFREP), *Rom. Journ. Phys.*, 60, 7–8, 1203–1217 (2015)
- Muntean, A., V. Mocanu, B. Ambrosius, (2016) A GPS study of land subsidence in the Petrosani (Romania) coal mining area. *Nat. Hazards*, 80:797-810
- Muntean, A., B.A.C Ambrosius, V. Mocanu, E.I. Nastase, C. Ionescu (2017) Surface motions in Romania derived from 15 years of continuous GNSS measurements. 17th International Multidisciplinary Scientific GeoConference SGEM2017, Conference Proceedings, ISBN 978-619-7408-00-3/ISSN 1314-2704, Vol. 17. Issue 14, 429-436pp, DOI: 10.5593/sgem2017/14/SO5.054
- Nastase, E.I., Oikonomou, C., Toma-Danila, D., Haralambous, H., Muntean, A., & Moldovan, I. A., Investigation Of Ionospheric Precursors Of Earthquakes In Romania Using The Romanian GNSS/GPS Network, *Rom. Journ. Phys.*, 61(7-8), 1426-1436, 2016
- Oikonomou, C., Haris Haralambous, Iren Adelina Moldovan, Razvan Greculeasa, Investigation of Pre-Earthquake Ionospheric Anomalies Using VLF/LF INFREP European and GNSS Global Networks, *Romanian Journal of Physics*, Volume 62, Number 7-8, 2017.

Modelling magnetic pulse swarms that anticipated the 2016 Norcia, and 2017 Capitignano, Central Italy earthquakes

M. Orsini¹, C. Fidani¹

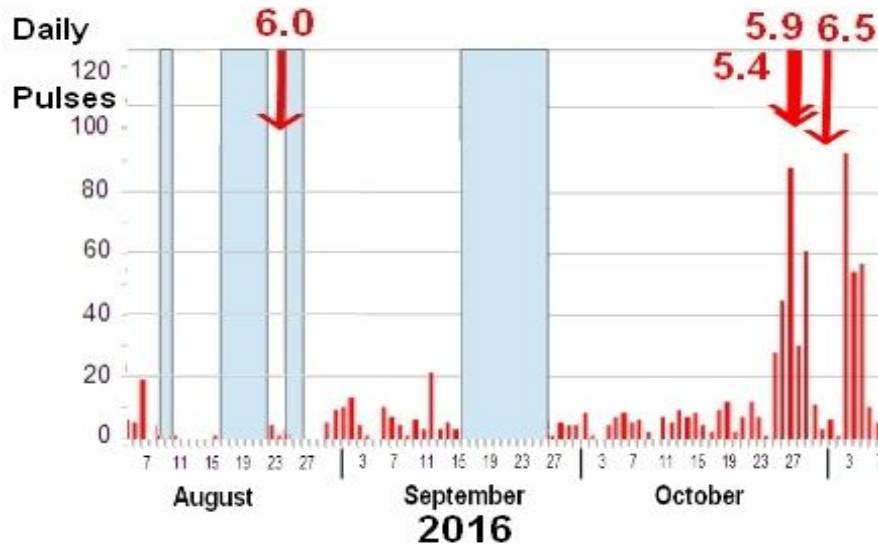
¹*Central Italy Electromagnetic Network, Fermo, Italy, c.fidani@virgilio.it*

Magnetic recordings were made at five Central Italy Electromagnetic Stations (CIEN) stations after 2011. They were made by induction coils of a diameter of about 80 – 100 cm, with the objective of detecting the magnetic component of electric oscillations already revealed during strong seismic activity. The recordings confirmed the absence of magnetic radiation correspondent to electric field oscillation measurements and this result was described according to the charged cloud model (Fidani and Marcelli, 2017). CIEN stations where magnetic field detectors were installed are: Chieti, Città di Castello, Avigliano Umbro, Norcia and Narni, and only the first three were active in 2016. Even if the magnetic component of the electric field oscillations did not appear, a large number of intense magnetic pulses were detected during 2016 - 2017 at Chieti station. Magnetic pulses had a time length of 0.1 sec and were concentrated around the time of the Norcia and the Capitignano seismic swarms.

The hardware architecture for magnetic measurements at the Chieti Station (Orsini, 2011) was composed of three main functional blocks: amplifier, low pass filter and signal discriminator. The low pass filter and the voltage discriminator were two virtual instruments realised on a Labview platform; this platform analysed the digital signal coming from the audio sound card. The coil magnetometer was designed to receive audio signals below 3 KHz using a pre-amplified 80 cm loop antenna. The direction of the antenna had been previously fixed to reduce magnetic noises coming from electric power lines. The pre-amplified signal was connected to two sound cards of two different PCs. In one of two PCs a software saved the spectrum of the received signals in ascii format for 24 hours, only when they went beyond a fixed voltage threshold. This acquisition process archives the time stamp of the events only when the frequency of the signal is lower than 30 Hz and greater than a voltage threshold of 110 mV. In another PC, the spectrogram of the magnetic signal was saved between 1 and 450 Hz in a logarithmic scale. Spectrograms of magnetic components were recorded every 80 minutes as for electric recording, so to obtain a simple comparison between electric and magnetic components.

Magnetic recordings evidenced regular shapes that were interrupted a few times every day by vertical lines, which denoted pulses. Daily pulse numbers increased suddenly on October 26, when two strong earthquakes, $M_w = 5.4$ and $M_w = 5.9$, struck Central Italy about 100 km from the Chieti Station. Pulse rates increased about four hours before the quakes (Orsini and Fidani, 2017). The number of magnetic pulses was equal to 30 on October 26, 45 on October 27, around 90 on October 28, returning to 30 on October 29 and increased to 60 on October 30, when a strong earthquake struck Norcia. Daily numbers of pulses continued to increase up until November 3, reaching a peak of 94 counts. Recordings were completely similar also for the Labview analysis. There was no evidence of daily pulse number increases from both the analysis around the Amatrice main event on August 24, 2016. Unfortunately, data was not available for the week prior this event. There was evidence of daily pulse number increases from both the analysis around the Capitignano seismic swarm which manifested four strong earthquakes with magnitudes between 5.0 and 5.7 on January 18, 2017. Increases in pulse numbers began on January 17, 2017, and reached a maximum on January 19, 2017.

Fig. 1. Distribution of daily magnetic pulse numbers around the four strong quakes striking Central



Italy. An unexpected increase in the number of daily magnetic pulses occurred on October 26, 2016, no increases were observed around the Amatrice earthquake; the blue colored areas indicate unavailable data.

Methodologies as performed by two computers were essentially different, as the first was based on the Fast Fourier Transform with a threshold chosen from the signal power, whereas the other was based on a threshold chosen from the signal amplitude after filtering in signal periods. However, they produced identical results regarding significant variations in pulse rates. Contemporary recordings of electric detectors operating at the same location in Chieti did not evidence correspondent pulses of the electric fields to those of the magnetic field. To

have an initial estimate of the minimal electrical current flowing in the earth's crust, a simple model was used through the Biot-Savart law which considers an infinitely long line conductor that is at some depth in the earth's crust

$$|B| = \mu_0 |I| / (2 \pi r)$$

Given that the loop have the axis oriented approximately N-S, the idealised current flowing parallel to the ground plane able to induce in the loop will have approximately an E-W direction, which is perpendicular to the faults strike of Central Italy. However, this configuration required currents of at least 1.7 MA for the Norcia earthquake, which the E-W line is about 90 km away from Chieti, and 1.1 MA for the Capitignano earthquakes, which the E-W line is about 60 km away from Chieti, to produce the magnetic induction recorded from the loop at Chieti. These extremely high current values are difficult to justify and constitute a challenge to model electric currents in the earth's crust.

References

- Fidani C. and Marcelli D.; 2017: Ten Years of the Central Italy Electromagnetic Network (CIEN) Continuous Monitoring, Open Journal of Earthquake Research, 6, 73-88.
- Orsini M.; 2011: Electromagnetic anomalies recorded before the earthquake of L'Aquila on April 6, 2009. Bollettino di Geofisica Teorica e Applicata, 52, 1, 123-130.
- Orsini M. and Fidani C.; 2017: Magnetic perturbations observed around the October 30, 2016, Norcia, 36th GNGTS, November 14 – 16, 2017, Trieste, 316-318.

Progress in VHF pre-seismic emission studies.

Yu. Ruzhin¹, V.M. Sorokin¹

¹*Pulkov Institute of Terrestrial Magnetism, Ionosphere and Radio Wave Propagation (IZMIRAN), Russian Academy of Sciences, Moscow, Troitsk, 142190, RUSSIA. ruzhin@izmiran.ru*

For the first time, the regular observation of pre-EQ anomalies in VHF electromagnetic radiation had been carried out on Create Island for three years starting from 1992. This observation was carried out using receivers with two frequencies 41 and 53 MHz located on the four sites (*Vallianatos and Nomicos, 1998*), and the pre-EQ VHF radiation had been registered. The center of EQs was located both on the ground and under the sea bottom. Based on the obtained data *Ruzhin et al. (2000)* have shown that the possible VHF radiation source is located in the atmosphere (Fig.1) at altitudes of several km above the epicenter of preparing EQs. It was suggested (*Ruzhin et al. 2000; Ruzhin and Nomicos, 2007*) that the generation of VHF radiation could be occurred as a result of electric discharges connected with convective transport of the charged aerosols at altitudes of 1–10 km in the zone of EQ preparation. Later, *Yamada et al. (2002)* confirmed this conclusion that VHF radiation sources are located in the atmosphere at altitudes over several kilometers. VHF radiation (52.1–52.5 MHz) related to an EQ was obtained as a result of long-term observations from July 1999. Direction to the EQ epicenters was in the limits of antenna diagram. The distance to epicenters was several hundreds of kilometers, and therefore it was possible to register radiation if its source was located in the atmosphere at altitude of several kilometers.

Possible candidate was soon discovered and intensively studied at present (*Rakov and Uman, 2003*). This is a special class of lightning activity - compact intracloud discharges (in English literature, this phenomenon is known as the Compact Intracloud Discharge, CID). Compact discharges occur substantially higher than normal lightning in a range of heights from 8 to 17 km. Unusual also is the power (up to tens GWt) emitted by them in the radio - the level considered to be the most intense in the world natural sources of radio emission at HF - VHF bands. Independent optical and radio measurements CID effects on the satellite FORTE give the possibility to estimate the effective radiation power of VHF (ERP - Effective Radiated Power) in the 26-49 MHz frequency band, which is greater than 140 kW.

It were proposed and substantiated the theory of generation VHF earthquake precursor (*Sorokin et al. 2011*), which is based on the assumption that the formation of charged clouds in

the atmosphere over an area of earthquake preparation and subsequent electric discharges, which are the source of radiation in the VHF band. Enhancement of the DC electric field up to the value of the order of 10 mV/m in the ionosphere is observed by the satellite during the same period. The occurrence of such a strong DC electric field in the ionosphere is related to the electric current flowing into the atmosphere–ionosphere circuit. The current source is an electromotive force (*Sorokin and Ruzhin, 2015*) in the ground-air layer occurring by injection of charged aerosols with soil gases in the atmosphere during seismic activity. The electric field of conducting current flowing between the atmosphere and ionosphere can reach the breakdown value in the lower atmosphere. Electric field forms the electric discharges in this region of the atmosphere which are the source of VHF radiation (*Sorokin et al. 2011*). The theory-based calculations of the spatial distribution of the ratio of the electric field to its breakdown value showed that the troposphere may have areas under some conditions where the field reaches the breakdown value.

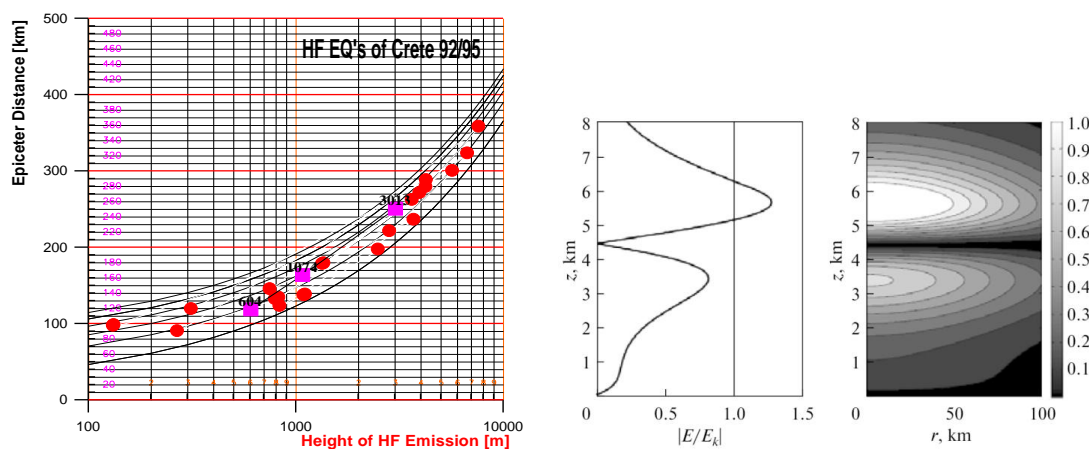


Fig.1. The minimum VHF emitting heights (left). **Fig.2.** Spatial distribution of the ratio of the vertical component of the electric field to its breakdown value.

Figure 2 shows an example of the spatial distribution of the electric field with an indication of the area (for $E/E_k > 1$) where the field reaches the breakdown value. This area contains one or two layers of a thickness of 1–2 km located at a height of 10 km. The characteristics of these layers are determined by atmospheric and aerosol parameters. With an increasing rate of vertical convection of the atmosphere, the height of the breakdown field area in the lower troposphere increases and then a second layer appears above (at a height of 10 km). In this case, the lower layer disappears.

As an example, the earthquake anomalies associated with the Mw 6.3 L'Aquila earthquake have been widely reported (see overview - *Fidani, 2010*).

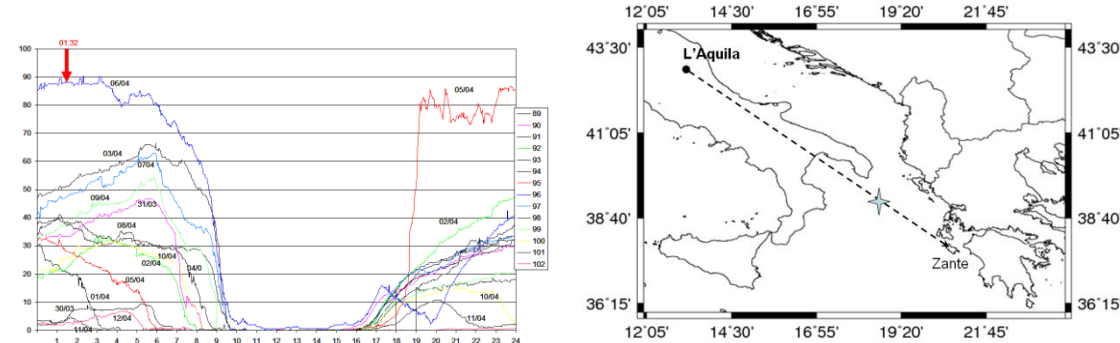


Fig.3. VHF amplitude of 41 MHz (left) and map (right) of Zante- L'Aquila location.

Since 1994, a station has been installed and operating at a mountainous site of Zante Island in the Ionian Sea (Western Greece). Its purpose is the detection of EM precursors (*Eftaxias et al., 2010*). VHF electromagnetic (EM) anomalies were recorded prior to the L'Aquila catastrophic earthquake that occurred on 6 April 2009. The figure 3 shows the progress of the signal received at a frequency of 41 MHz. Time period is taken from 30 March to 12 April. In this time interval, namely the 06 April at 1:32 UTC, there was an earthquake in Italy a magnitude M=6.3. It is shown by the red arrow in the picture. As the graph shows, the maximum surge around the time of the earthquake, after which the signal decreases with a 225mv at the time of the earthquake, to 10mv. Also, the graph shows that over the three days to push bursts of signal that reaches up to 125mv that can be taken for a precursor of the earthquake. It should be noted that the daily course of the signal is quite regular. By April 12, the signal weakens, going down to the lowest levels. Daily max occur at night, and minima are marked by day.

From Fidani report (*Fidani, 2010*) the complex pre-earthquake events were observed. The main part of them were phenomena that can be accompanying random electrical discharges in the lower atmosphere: (1) random electrical discharges, (2) atmospheric heating in the discharge area and generation of outgoing microwave radiation, (3) wide_band VHF radio emission observed on the Earth and in space, (4) glow in the visible range of the spectrum, (5) refraction and scattering of VHF radiowaves in the troposphere, leading to receipt of transmitted signals beyond the horizon on the Earth and on the satellite.

As a result, our model makes it possible to couple the satellite data of electromagnetic and plasma measurements with electrophysical and meteorological characteristics of the lower atmosphere at the stage of earthquake preparation and typhoon initiation. The model explains the numerous effects on cosmic plasma by a single cause: the change in the conduction current flowing in the atmosphere-ionosphere circuit. At the initial stage of seismic activity and typhoon formation (until the catastrophic phase), aerosol injection or vapor condensation

over the ocean surface occurs with a redistribution of charge carriers and a change in their mobility, which, together with vertical convection, leads to the effect described above in the Earth–ionosphere electric circuit.

References

1. Vallianatos, F. and Nomicos, K., Seismogenic radioemissions as earthquake precursors in Greece, *Phys. Chem. Earth*, 1998, vol. 23, nos. 9–10, pp. 953–957.
2. Ruzhin, Yu.Ya., Nomicos, C., Vallianatos, F.(2000). High frequency seismoprecursor emissions. In: Proceedings of 15th Wroclaw EMC Symposium, pp. 512–517.
3. Ruzhin Yu., Nomicos C. (2007). Radio VHF precursors of earthquakes. *Natural Hazards*. V. 40. 573-583. DOI 10.1007/s11069-006-9021-1.
4. Yamada, A., Sakai, K., Yaji, Y., Takano, T., Shimakura, S.(2002). Observation of natural noise in VHF band which relates to earthquakes. In: Hayakawa, M., Molchanov, O.A. (Eds.), *Seismo Electromagnetics: Lithosphere–Atmosphere–Ionosphere Coupling*. TERRAPUB, Tokyo, pp. 255–257.
5. Rakov V.A. and M.A. Uman (2003), *Lightning: Physics and Effects*. Cambridge University Press, 687 p.
6. Sorokin V.M., Yu.Ya. Ruzhin, V.D. Kuznetsov, A.K. Yaschenko. (2011) Generation of VHF radio emissions by electric discharges in the lower atmosphere over a seismic region. *Jour. Atm. STP*, 73, N5-6, 664–670
7. V. M. Sorokin and Yu. Ya. Ruzhin.(2015). Electrodynamic Model of Atmospheric and Ionospheric Processeson the Eve of an Earthquake. *Geomagnetism and Aeronomy*, 2015, Vol. 55, No. 5, pp. 626–642.
8. Eftaxias K. et al. (2010). Unfolding the procedure of characterizing recorded ultra low frequency, kHZ and MHz electromagnetic anomalies prior to the L'Aquila earthquake as pre-seismic ones. *Nat. Hazards Earth Syst. Sci.*, 10, 275–294, 2010
9. C. Fidani (2010). The earthquake lights (EQL) of the 6 April 2009 Aquila earthquake, in Central Italy.
10. *Nat. Hazards Earth Syst. Sci.*, 10, 967–978, 2010

Anomalous Changes in the MT impedances during February 2015 Seismo-Volcanic Crisis in Taal Volcano (Philippines): Recurrence of the 2010-2011 Event?

Y. Sasai¹, P. K. B Alanis², P. Reniva² M. Uyeshima³, T. Nagao¹, J. Zlotnicki⁴, M. J. S. Johnston⁵, PHIVOLCS EM Team²

¹Tokai University, Shizuoka, Japan, yosasai@zag.att.ne.jp; ²PHIVOLCS, Manila, Philippines, paulkarsonalanis@gmail.com; paolo.reniva@gmail.com; ³ERI, Univ. Tokyo, Tokyo, Japan, Uyeshima@eri.u-tokyo.ac.jp, ⁴CNRS, Toulouse, France, JacquesZlotnicki@wanadoo.fr; ⁵USGS, Menlo Park, U.S.A., mal@usgs.gov

Taal volcano is located in the island of Luzon and 60 km south of the capital city of Manila. It is one of the most active volcanoes in the Philippines. The first recorded eruption was in 1573 and since then it has erupted a total of 33 times, with the last eruption in 1977. These eruptions resulted in thousands of casualties and considerable damage to property. In 1995 it was declared one of the “1990s decade volcano” by IAVCEI. Although the volcano remained fairly quiescent after the 1977 eruption, at the beginning of the 1990s it began to exhibit several phases of abnormal activities, such as episodes of seismic swarms, ground deformation and fissuring, and hydrothermal activities, all of which continues to the present. Past eruptions of Taal Volcano can be divided into 2 distinct cycles, depending on the location of the eruption: eruptions centered at the Main Crater (1572-1645 and 1749-1911); and eruptions occurring at the flanks (1707-1731; 1965-1977).

EMSEV cooperated with PHIVOLCS to start monitoring of this volcano since 2005. We established three continuously recording EM stations at DAK, MCE and PAN, and conducted repeat magnetic surveys. Three ordinary proton precession magnetometers were working simultaneously, which were installed by EMSEV since 2007 (see Fig. 1). We have experienced seismo-volcanic crisis twice, i.e. 2005-2006 and 2010-2011, when all the inhabitants totally evacuated from the island owing to the memory of the 1911 eruption. In particular, the 2010-2011 event was well monitored by the EM observation system by EMSEV (Zlotnicki et al., 2018, submitted to EPS). Then, a 5-year project of the MT soundings and establishment of continuous magnetic stations was performed as part of the PHIVOLCS-JICA-SATREPS Project (2010-2014). The magnetotelluric (MT) surveys brought to light the existence of a large hydrothermal reservoir underneath Volcano Island (Yamaya et al, 2013; Alanis et al, 2013). They concluded that the devastating 1911 eruption

was nothing but the collapse of the hydrothermal reservoir, which killed almost all the inhabitants with strongly acidic hydrothermal fluids. As part of the Project, new magnetometers were installed at Taal volcano. These consist of three Oberhauser-type magnetometers (installed at VTBM, VTDK and VTMC) and one fluxgate-type magnetometer (installed at VTBM). The Project also established (using magnetotelluric method) that a large hydrothermal reservoir is underneath Taal volcano and currently this is under a state of equilibrium. The state of the hydrothermal reservoir is thus monitored constantly by magnetometers.

In early 2015, remarkable resistivity changes were detected by the flux-gate magnetometer at VTBM during an earthquake swarm occurred in Taal volcano. The location of these earthquakes appears to be in the approximate location of the hydrothermal reservoir. See Fig. 2. The hydrothermal reservoir (HTR) is considered to be the aggregate of interconnected cracks filled with two-phase (gas and liquid) fluids in host rocks. During the earthquake swarm, the HTR should have been pressurized owing to the increase in the gas phase. This is reasonably expected by the observations during the 2010-2011 activity (Arpa et al., 2013), although we have no data of CO₂ emission during this period. Fig. 3 shows the apparent resistivity changes observed at VTBM. Such anomalous changes should be most probably caused by gas/liquid ratio variations in the HTR, which modifies the electric currents flowing into Taal volcano from South China Sea (Yamaya et al., 2013; Alanis et al., 2013). It is not resulted from EM induction, but conduction effect. We will also investigate if the total geomagnetic field may have varied as was the case of the 2010-2011 crisis.

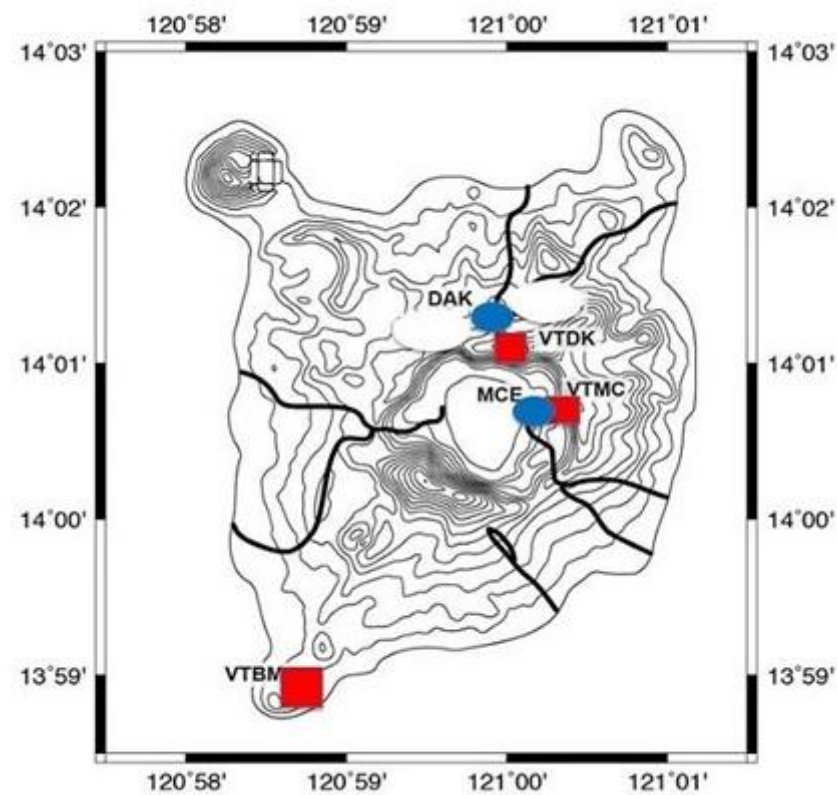


Fig. 1. Distribution of EM observation stations on Volcano Island of Taal Volcano.

February 2015

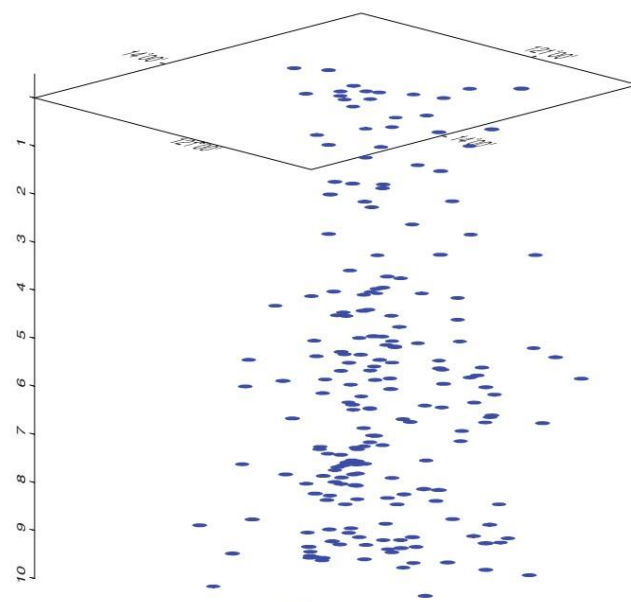


Fig. 2. Distribution of earthquakes underneath Taal volcano during February, 2015.

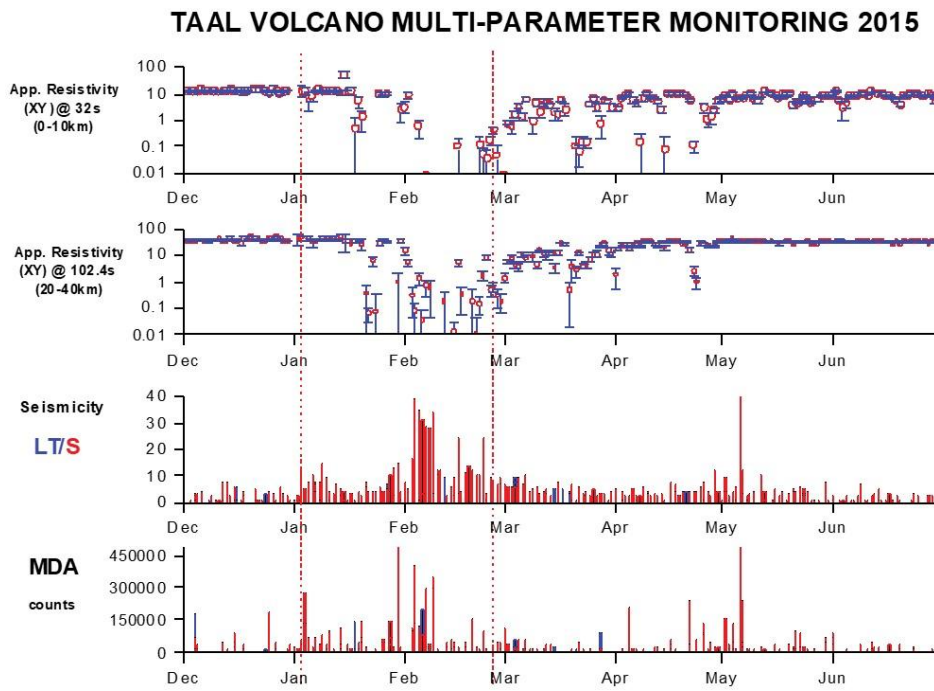


Fig. 3. Changes in the apparent resistivity observed at VTBM station during the year 2015. Upper two graphs show the apparent resistivity for 32 sec and 102.4 sec period, which are computed using standard RRRMT. The third graph shows seismicity, i.e. daily number of earthquakes.

Model for generation of geomagnetic perturbation in the ionosphere due to tsunami

V.M. Sorokin¹, A.K. Yashchenko¹, V.V. Surkov^{1,2}

¹*Pushkov Institute of Terrestrial Magnetism, Ionosphere and Radio Wave Propagation of the Russian Academy of Sciences (IZMIRAN), Moscow, Troitsk, Russia, sova@izmiran.ru;* ²*JSC "Research-and-Production Corporation "Precision Systems and Instruments", Moscow, Russia, surkovvadim@yandex.ru*

We study the mechanism for geomagnetic field perturbation associated with tsunami wave propagation. The source of perturbation is assumed to be electric currents in sea medium and the ionosphere. The electric current in the sea medium is due to the tsunami-produced wave motion of the seawater immersed in the geomagnetic field while the ionospheric current is due to acoustic-gravity wave (AGW) propagating from the atmosphere into the ionosphere. The AGW radiates into the atmosphere due to vertical displacements of seawater surface during tsunami wave propagation. Although the ionospheric conductivity is much smaller than seawater conductivity, the current in the ionosphere can be greater than that in the seawater due to an exponential increase in the amplitude of the upward propagating AGW. We deduce a spatial distribution of the geomagnetic perturbations generated by the electric current flowing in the seawater and ionosphere and take into account their mutual induction. The electric current in the ionosphere may greatly affect the geomagnetic field perturbations resulted from tsunami wave propagation. With the increase in the horizontal scale of tsunami wave and in the sea medium depth, the AGW-induced ionospheric current can enhance the perturbation amplitude observed on the ground by the factor of several units. Taking the dayside ionospheric parameters, the amplitude of geomagnetic perturbations caused by tsunami wave is estimated to be about 1 – 10 nT. In the nighttime conditions a height-integrated conductivity of the ionospheric plasma decreases by an order of magnitude that declines significantly a role played by the ionospheric currents. In our model, the ionospheric electric current due to AGW is completed through the conjugate ionosphere by virtue of filled-align currents, which makes for excitation of transversal components of magnetic and electric fields at altitudes of the upper ionosphere and magnetosphere. The amplitude of magnetic and electric fields as well as the field-align current in the ionosphere can reach values of the order of 10 nT, 10 mV/m and 10^{-8} A/m², correspondingly. We can conclude that these estimates provide a possibility for monitoring of tsunami wave by virtue of cosmic techniques.

Ground-Based Geomagnetic Signature related to the Mw 8.1 Earthquake (Chiapas, Mexico), on September 8-Th 2017

D.A. Stănică¹, D. Stănică²

¹Institute of Geodynamic of the Romanian Academy, Bucharest, Romania, armand@geodin.ro; ²Institute of Geodynamic of the Romanian Academy, Bucharest, Romania, dstanica@geodinj.ro

A great Mw8.1 earthquake, generated at 72km depth, struck offshore of Chiapas, Mexico on September 8-th 2017, at 04:49 UTC. The earthquake was intensively felt in Guatemala City and at about 1000 km in Mexico City where important damages at the international airport and some hospitals have been observed. This earthquake occurred on the subduction zone boundary between oceanic Cocos plate and North America plate where, during the time, a very large seismicity has been generated. In the last decade, the long-term real time ground-based geomagnetic observations realized in the seismic active Vrancea zone (Stanica D.A and Stanica D, 2011; 2018), together with supplementary studies regarding the Mw9.0 Tohoku earthquake, on March 11, 2011 and Mw8.3 Chile, on September 16, 2015 (Stanica et.al.2015; 2016), have enlarged our knowledge about the possible inter-relations between the pre-seismic anomalous phenomena and the final stage of the earthquakes nucleation. Consequently, to identify the geomagnetic signatures associated to this very large earthquake, in this paper, we have analysed the data collected on the interval August 1 – September 26, 2017 at the Geomagnetic Observatories Teoloyucan (TEO)-Mexico and Tucson (TUC)-USA, the last being taken as reference one (Fig.1). The pre-seismic anomalous signal is postulated to be due to the electrical conductivity changes, most probably associated with the earthquake-induced tectonic stress, followed by rupture and electrochemical processes deployed along and nearby the subduction zone. To identify the pre-seismic geomagnetic signals related to Mw8.1 earthquake it is necessarily to obtain information about: (i) polarization parameter (BPOL), which is expressed as: $BPOL(f)=Bz(f)/\sqrt{Bx^2(f)+By^2(f)}$, should be time invariant in non-seismic condition and it becomes unstable before the onset a seismic event; (ii) Strain effect-related to the pre-seismic geomagnetic signals. As regards the distance at which the strain effect is able to generates a pre-seismic electromagnetic signal, we used the following relation $R(km) = 10^{0.5M-0.27}$, where: R is epicentral distance and M is earthquake magnitude (Morgunov and Malzev, 2007). As the strain effect of the Mw8.1 Chiapas earthquake is felt at $R \approx 6000$ km, in our particular case the distances between

earthquake epicentre and the both observatories (TEO and TUC) are about 1000km and 3000 km (TUC), respectively, so that the condition to identify a pre-seismic anomalous signal is fulfilled.

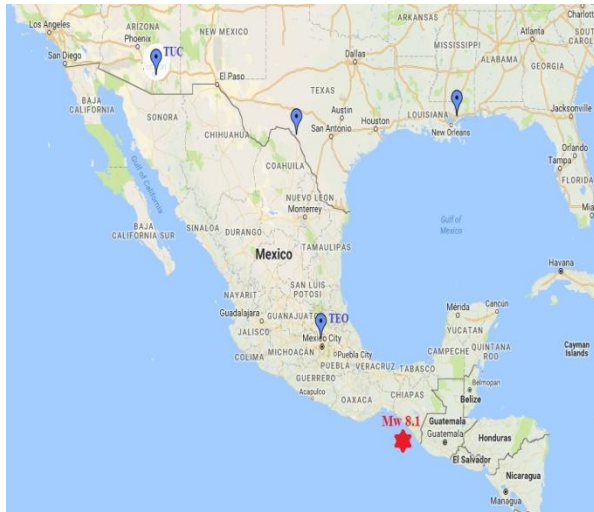


Fig. 1

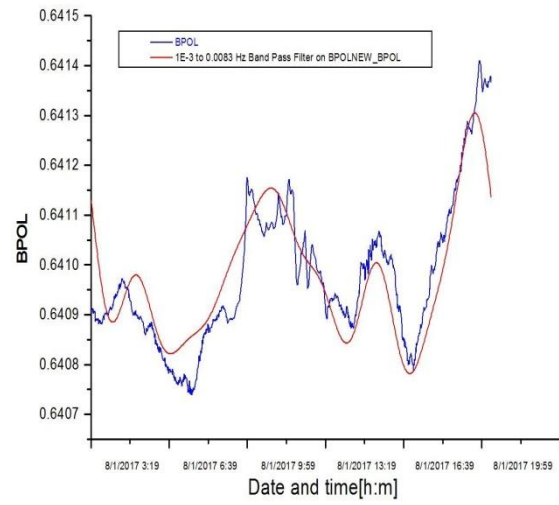


Fig. 2

Further on, by using a FFT band-pass filter analysis in the ULF range (Fig.2), the daily mean distribution of the polarization parameter BPOL and its standard deviation (STDEV) are performed for TEO (Fig. 3) and TUC (Fig.4).

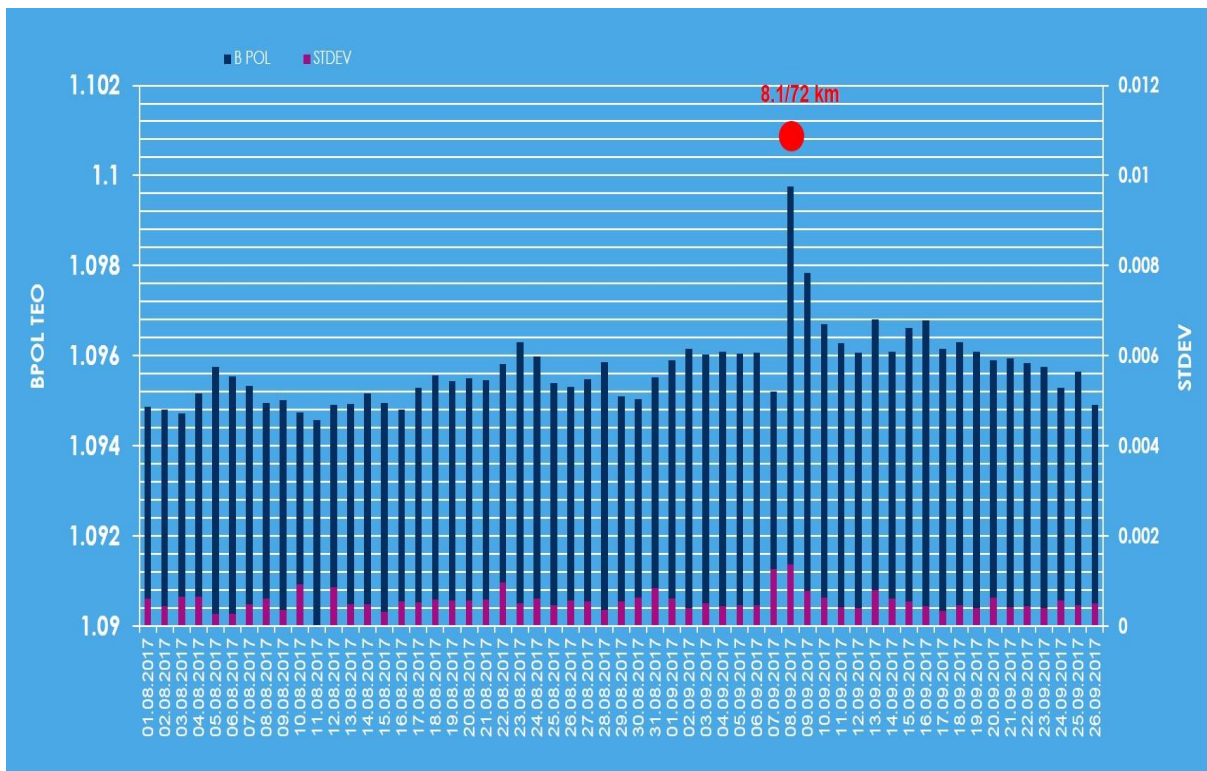


Fig. 3 Daily mean distribution of the BPOL (blue bar) and STDEV (read bar) carried out for the observatory TEO on the interval August-September, 2017

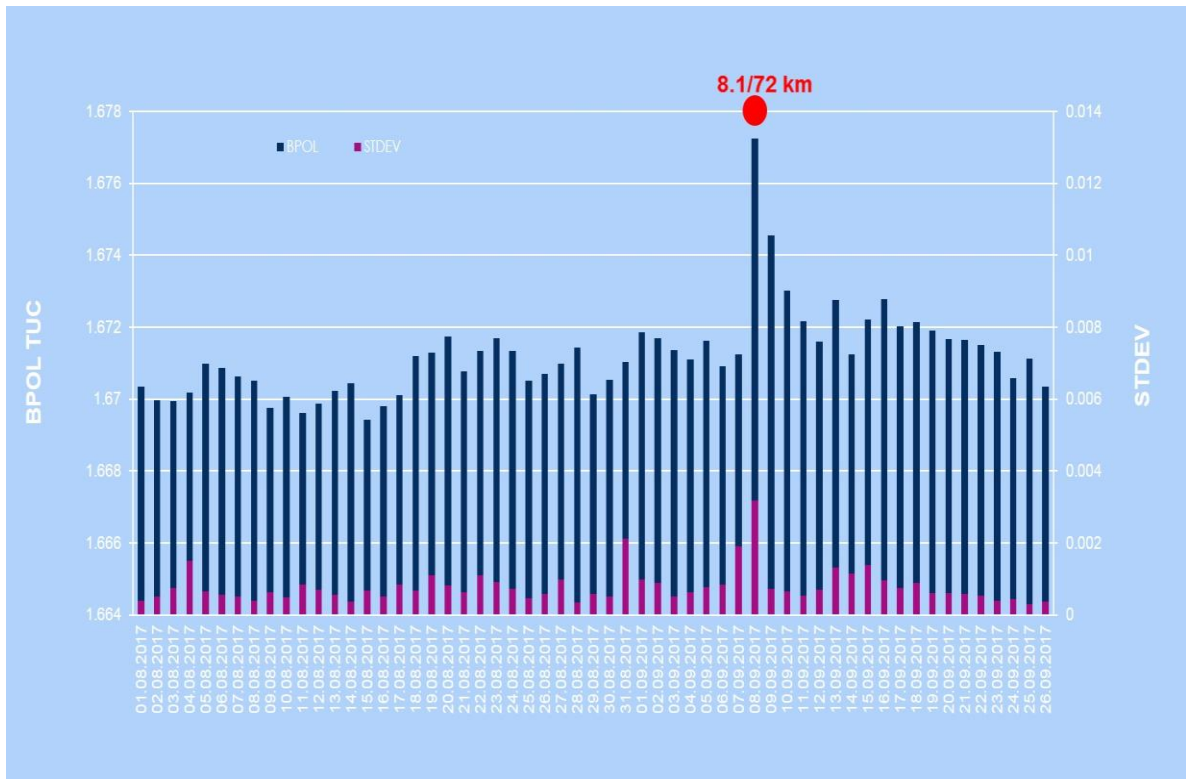


Fig. 4 Daily mean distribution of the BPOL and STDEV for the observatory TUC carried out for the observatory TUC on the interval August-September, 2017

The distributions of the BPOL and STDEV presented in Figure 3 and Figure 4 emphasize on September 8, 2017 very large anomalies (1.095 TEO and 1.677 TUC), suggesting the presence of a co-seismic effect, these results motivate us: (i) to explore in details BPOL for three consecutive days September 7, 8 and 9 (Fig. 5 and Fig. 6); to realise a differential analysis between the both observatories TUC and TEO, by using as a reference one the TEO observatory, and the final result is shown in Fig. 7.

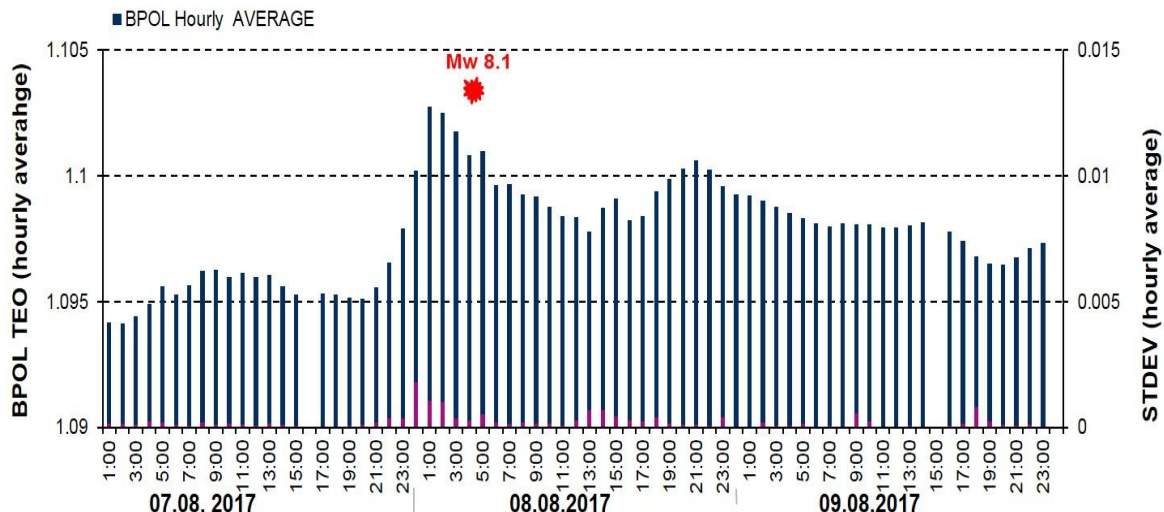


Fig. 5. Hourly mean distribution of the BPOL (TEO) on the interval September 07- 08, 2017

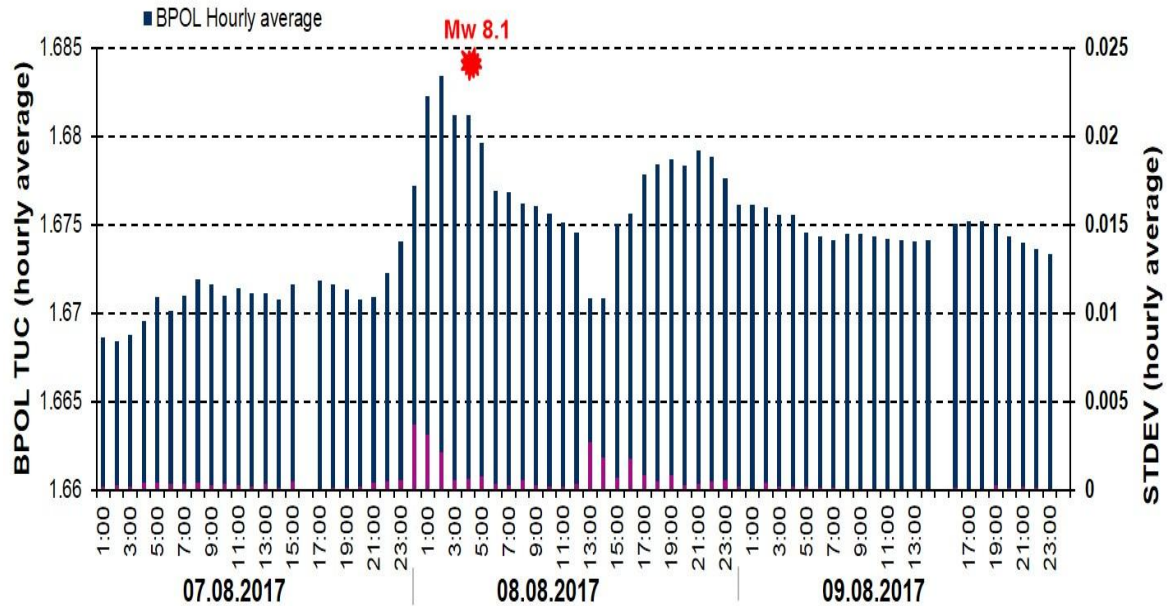


Fig. 6. Hourly mean distribution of the BPOL (TUC) on the interval September 07- 08, 2017

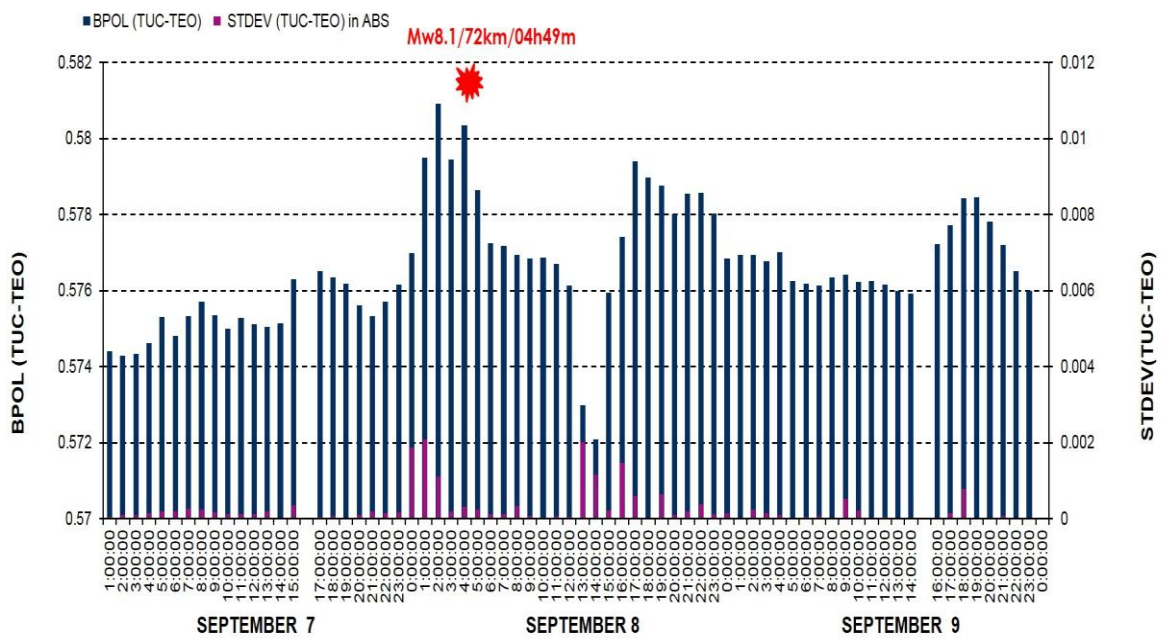


Fig. 7. BPOL (TUC-TEO) time series on the interval September 07- 09, 2017

The proposed methodology, regarding the distribution of the BPOL (TUC-TEO), provides adequate information to identify, starting with hour 1:00 on September 7-th, an anomalous behaviour and, the lead time was about 4 hours before the onset of the M8.1 Chiapas, Mexico earthquake. The anomalous distributions, observed all days' interval (September 8-9) are related to the aftershocks occurrence having magnitude higher than 5.

Identification and Prediction of Destructive Earthquakes

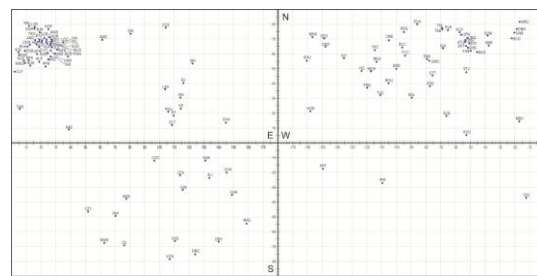
X. Zeng¹, Y. Zeng¹, L. Shi¹, J. Zeng¹

¹Huizhou sandong, Guangdong, China, e-mail: hzsxbao@126.com

On the basis of the theory of seismic structural burst dynamics and the theory of seismic precursor hydrodynamics, this paper focuses on the identification of 12 cases of near M8 earthquakes since 2016, the method of computer calculating the magnitude and epicenter, showing the bright prospect of earthquake prediction and pre earthquake warning.

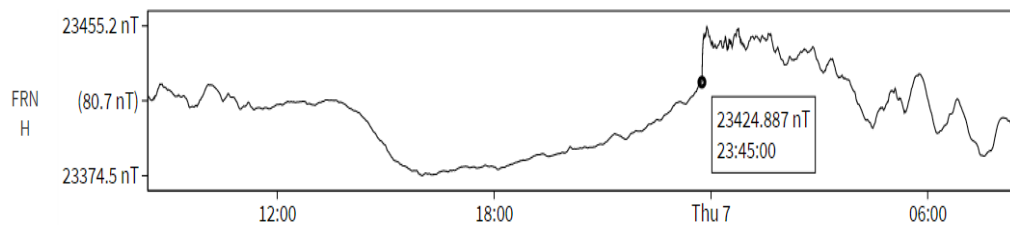
1 Electro-magnetic Stations all over the World

The monitoring of earthquake precursors, including Guangdong Huizhou and Wuhan geoeletro stations, geomagnetic stations in Chinese Academy of Sciences, the United States, Canada, Australia, France, Norway, Finland and Russia etc. see below fig.



2 Global Response of Great Earthquakes

For example: In response to the Mexico 8.1 earthquake, the FRN Geomagnetic Observatory (H) in the United States, see fig. below:



The response time t for 12 strong earthquakes, see Table1.

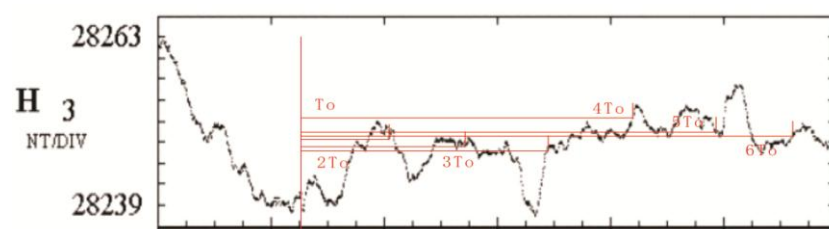
Table 1 Three factors and the response time t for 12 strong earthquakes

Name	M	Seismic time /UTC	Epicenter	Depth /km	t/h
1 South Pacific	7.8	2016-03-02 12:49:48	4.9S/94.3E	24.0	51.6
2 Ecuador	7.8	2016-04-16 23:58:37	0.37N/79.9W	19.2	45.1
3 Mariana	7.7	2016-07-29 21:18:26	18.5N/145.5E	212.4	67.7
4 New Zealand	7.8	2016-11-13 11:02:59	42.7S/173.1E	22	49.77
5 Solomon	7.8	2016-12-08 17:38:46	10.7S/161.3E	41	53.1
6 New Guinea	7.9	2016-12-17 10:51:13	4.5S/153.4E	103	52.8
7 Papua New Guinea	7.9	2017-01-22 04:30:23	6.2S/155.1E	136.0	45.7
8 Russia	7.7	2017-07-17 23:34:14	54.5N/168.8E	11.7	41.6
9 Mexico	8.1	2017-09-08 04:49:21	15.1N/93.7W	69.7	29.1
10 Iraq	7.3	2017-11-12 18:18:17	34.9N/45.9E	23.2	65.9
11 Honduras	7.6	2018-01-10 02:51:31	17.5N/83.5W	10.0	44.1
12 Alaska	7.9	2018-01-23 09 : 31:42	56.0N/149.07W	25.0	47.5

3 Computer processing of seismic elements

3.1 Resonance period and magnitude

The resonance period determining the magnitude is a period of completion of a cycle wave (2π , 360°) is expressed in T_0 . The resonance wave cycle is independent of the diagnostic method and is not affected by the motion. Such as: (1)South Pacific (Indonesia)7.8, 2016-03-02 12:49:48 outbreak, 2016-02-24(24h) BJ recorded its typical structure and resonance cycle, see Fig. 7 below:



The magnitude is calculated according to the formula (1), TO in min.

$$M = 4.14 \cdot \lg T_O - 1.486 \quad (1)$$

3.2 Epicentral distance and time difference of fast and slow wave

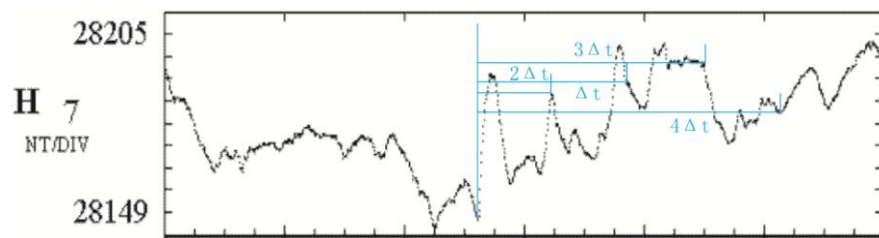
Tidal or magnetic force formed resonance wave with shock wave characteristics, to be a fast wave and slow wave, their time difference deciding distance of epicentral. Due to the magnetic resonance wave, the fast speed of up to 9368km/h, for a particular earthquake, fast wave at nearly the same time reaching to the global geomagnetic station, The epicenter distance ΔX was calculated by the formula (2):

$$\Delta X = 6.312\Delta t - 14.331 \quad \dots \dots \dots \quad (2)$$

In witch the ΔX in expansion the figure of the latitude and longitude, 1mm = 112.12km; the Δt in the geomagnetic time wave figure, 1h = 5.385mm.

For example:(10) Iraq7.3 (7.8BJ), 2017-11-12 18:18:17 outbreak, 34.9N/45.9E;

2017-11-09 (24h) BJ recorded of wave time difference, see Fig. 12 below:



3.3 Epicenter

The determination of the epicenter requires at least three epicenter distances determined by the monitoring stations. As follow four epicenter maps of the strong earthquakes, which are made by computer.

(2) Ecuador M7.8 (4) New Zealand (BJ) M7.8

2016-04-16 23:58:37, epicenter 0.37N/79.9W 2016-11-13 11:02:59, epicenter
42.7S/173.1E

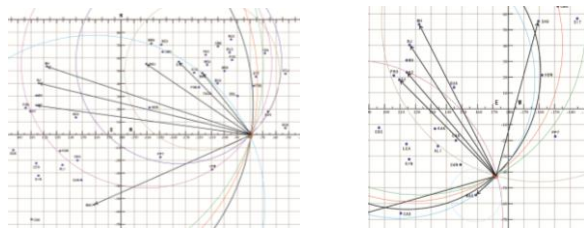


Fig. 15 Ecuador M7.8 epicenter chart Fig.16 New Zealand (BJ) M7.8 epicenter chart

(7) Papua New Guinea M7.9

(8) Russia M7.7

2017-01-22 04:30:23, epicenter 6.2S/155.1E 2017-07-17 23:34:14, epicenter
54.5N/168.8E

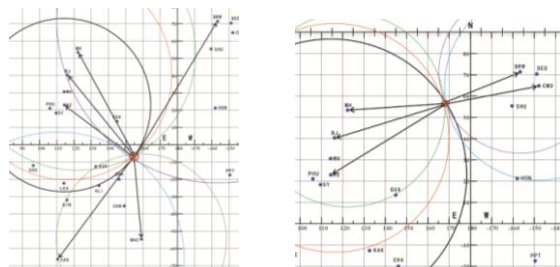


Fig.17 Papua New Guinea M7.9 epicenter chart Fig.18 Russia M7.7 epicenter chart

The computer can accurately produce the epicenter map, which provides a rapid operation method for accurate prediction of strong earthquakes and pre earthquake early warning.

4 The typical seismic prediction

The 7.7 magnitude earthquake in Russia was accurately predicted: Magnitude, 7.7; Epicenter: 53 N 168.5 E; Shock time(UTC): 2017-07-17. The monitoring results of the US Geological Survey are M7.7, 54.466°N 168.822°E, 2017-07-17 23:34:14.

5 The theoretical basis of earthquake prediction

After the Wenchuan earthquake, Xiongfei Zeng team to invest in breakthrough of earthquake theory and prediction technology, in ten years of arduous struggle, “The Fluid Dynamics Theory of Seismic Structure” and “The Prediction Method of Resonant Cell – Explosion Chimney” have been established finally. These results are based on the discovery of the existence of seismic structures known as “Seismic Occlusion Body(SOB)”, see fig. 23. These structures are physical entities. Seismic processes are the process of energy storage, triggering and releasing (burst) of the seismic structure. It has the inherent volume, pressure and temperature. For the geoelectric and geomagnetic wave the existence of the resonance

period is the natural property of such structure, so it has nothing to do with the monitoring means.

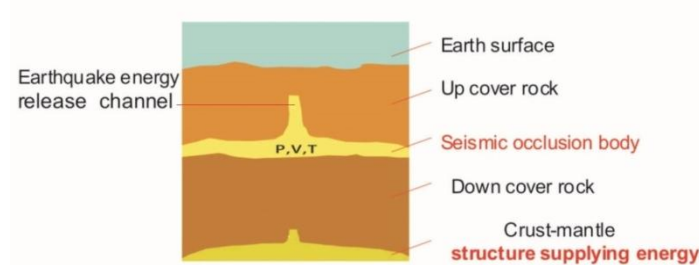


Fig. 23 Seismic occlusion body(SOB)system

Acknowledge

Geomagnetic information of this study, mainly originated from BJ, MH, SY and ZS of the Chinese Academy of Sciences, the U.S. Geological Survey, Canada and Australia, Norway geomagnetic station, Finland, Russia and France and other stations, author pays tribute to the great dedication of these international shared stations, and gives the most sincere thanks.

References

- [1] Fuye Qian, Biru Zhao. The Impending Geoelectric Precursors to the Wenchuan MS 8.0 Earthquake and Methods of Earthquake Impending Prediction by Using HRT Wave. *Science in China (Issue D) Earth Sciences*, 2009,39(1):11-23
- [2] Xiongfei Zeng. Theory of seismic structure burst and short-term and imminent prediction[J]. *Earth Science Frontiers*. 2013 Vol.20 No.6 001-014
- [3] Xiongfei Zeng, Yan Zeng. The fluid dynamics theory for earthquake precursors and prediction[c]//. Lanzhou: EMSEV-2016 Workshop, 25.August 2016.
- [4] Xiongfei Zeng, Yan Zeng, Jiang Zeng. The seismic prediction method of resonant cell – explosion chimney and its application[c]//. Wuhan: The 13th China International Geo-Electromagnetic Workshop, 9. November 2017.

Chapter 3

*Investigation of active faults and volcanoes
based on satellite remote sensing*

New perspectives on regional and national scale surface deformation analysis through advanced space-borne radar interferometry techniques

R. Lanari¹

¹IREA-CNR, Napoli, Italy, lanari.r@irea.cnr.it

The investigation of Earth's surface deformation phenomena plays a key role for the comprehension of several processes of great interest for science and society, especially from the perspective of further understanding the Earth System and its impact on human activities. In this framework, Differential Synthetic Aperture Radar Interferometry (DInSAR) [1] is a well-established microwave remote sensing technique able to investigate surface displacements affecting wide areas, through the generation of spatially dense deformation maps with centimeter to millimeter accuracy. To this aim, DInSAR exploits the phase difference (i.e. interferogram) between pairs of SAR images acquired at different times but with nearly the same illumination geometry and from sufficiently close flight tracks, whose separation is typically referred to as baseline.

Recently, DInSAR has evolved from the analysis of single deformation episodes towards the study of the temporal evolution of the detected displacements through the generation of deformation time series, by benefitting from the availability of long-term SAR data archives collected since 1992, as those acquired from the ESA ERS-1/2 and ENVISAT satellite systems. Accordingly, in the past decades several advanced DInSAR techniques have been developed, based on a proper combination of a set of multi-temporal interferograms relevant to an area of interest, in order to compute the deformation time series. Among these techniques, the one referred to as Small BAseline Subset (SBAS) algorithm [2] generates LOS-projected deformation time series and corresponding mean deformation velocity maps with millimeter accuracy [3], at different spatial scales [4] and with multi-sensor data [5], by properly combining DInSAR interferograms characterized by small temporal and spatial baselines between the acquisition orbits, in order to mitigate the noise (decorrelation) effects [6].

During the last decades, the development of advanced DInSAR approaches has been boosted by the consequent technological progress, oriented toward the development of new SAR satellite missions, characterized by different frequency bands, spatial resolutions, revisit

times and ground coverages. In this context, the DInSAR scenario relevant to the last 25 years is characterized by the large disposal of SAR data acquired by the previously mentioned, long-term C-band ESA archives (e.g. ERS-1/2 and ENVISAT), the C-band RADARSAT-1/2 data sequences, those provided by the L-band ALOS-1/2 systems and by the new generation X-band SAR sensors, such as the COSMO-SkyMed (CSK) and TerraSAR-X (TSX) constellations. Moreover, starting from 2014, a massive and ever increasing data flow acquired over large part of the Earth on a regular basis is supplied by the C-band Sentinel-1 (S-1) constellation, developed within the framework of the European Copernicus Programme and composed of two twin satellites (Sentinel-1A and Sentinel-1B) that collect SAR data in continuity with the first generation ERS-1/2 and ENVISAT missions. The S-1 constellation is specifically designed for interferometric applications over land, since it guarantees both short spatial (less than 250 m) and temporal (down to 6 days in the case of two operating satellites) baselines. Furthermore, the S-1 sensors exploit an innovative acquisition mode referred to as Terrain Observation with Progressive Scans (TOPS) [7], used to acquire S-1 Interferometric Wide Swath (IWS) scenes, which guarantees a very large spatial coverage (about 250 km), thus allowing to operate with a global coverage acquisition strategy. It is worth noting that the whole S-1 archive is available with a free and open access data policy, thus easing the data access and enlarging the scientific community benefitting from its exploitation, opening new research perspectives to understand Earth's surface deformation dynamics at national/continental scale.

All these SAR systems have enabled us to collect, over the past 25 years, huge SAR data archives that have permitted to continuously investigate surface displacements over a wide temporal and spatial extent, with different spatial resolutions and revisit times. In this context, a massive data volume will be supplied in the next few years, and petabytes of DInSAR measurements have to be archived, processed and handled, so that the DInSAR scenario is moving toward a Big Data challenge, with a strong impact on the data storage and the computational requirements needed to efficiently generate and exploit the advanced DInSAR products. Accordingly, in order to take advantage of the performance of the current SAR sensors, it is crucial to develop innovative and effective solutions, able to properly deal with the transfer, the storage, and, above all, the processing of such huge SAR data archives.

Within this framework, an advanced parallel computing solution of the SBAS processing chain, referred to as Parallel Small BAseline Subset (P-SBAS), has been recently developed [8]. The P-SBAS approach implements a complete advanced DInSAR processing chain (starting from either RAW or SLC data and ending with deformation time series generation)

and exploits distributed computing architectures (such as cluster and GRID infrastructures) also encompassing different parallelization strategies (both multi-nodes and multi-cores), with good scalable performance. In this work, we present an efficient and automatic interferometric processing chain implementation based on the P-SBAS algorithm, specifically devoted to the generation of Sentinel-1 IWS DInSAR products. The S-1 P-SBAS processing chain is capable to automatically ingest Sentinel-1 SLC SAR images and carry out several interferometric processing steps, such as image co-registration, interferogram generation, and phase unwrapping, in order to finally compute in an efficient and systematic way the deformation time series and the corresponding mean displacement velocity maps relevant to very extended areas. In particular, we take advantage of the intrinsic characteristics of the TOPS acquisition mode of the Sentinel-1 IWS data that consists of a series of independent bursts, which can be therefore considered as separate acquisitions. This allows us to deploy an appropriate parallelization strategy for some major steps of the proposed P-SBAS interferometric chain, making use of distributed computing architectures.

However, within such a Big Data scenario, we have to consider some drawbacks deriving from the massive processing that will inevitably follow the expected huge SAR data flow provided by the S1 constellation; indeed, in-house High Performance Computing (HPC) infrastructures can be very expensive in terms of procurement, maintenance, and upgrading. To overcome this issue, the use of Cloud Computing (CC) environments, as for the case of the Amazon Web Services (AWS) CC environment, may represent a promising solution, for both resource optimization and performance improvements, implying a further push towards the use of such a technology also in scientific applications and operational contexts, as well.

In this work, we present the results relevant to the national scale surface deformation analysis performed over the Italian peninsula through the S-1 P-SBAS processing chain. In particular, we show the deformation time series and the corresponding mean velocity maps generated by processing through the P-SBAS approach the whole Sentinel-1 data archive acquired along descending orbits over Italy (more than 3000 S-1 IWS scenes) during the March 2015 - April 2017 time interval. Such a national scale analysis has been entirely carried out by exploiting the AWS Elastic Cloud Computing (EC2) platform, in order to evaluate the P-SBAS scalability performance achievable within a CC infrastructure when dealing with huge SAR data volumes.

Acknowledgments

This work was supported by the Italian Civil Defense Protection Department, the ESA's GEP

project, the EPOS-IP project of the European Union Horizon 2020 research and innovation program (grant agreement 676564), the I-AMICA (PONa3_00363) project, and the IREA-CNR/Italian Ministry of Economic Development DGS-UNMIG agreement. Sentinel-1 SAR data are copyright of Copernicus (2016); the DEMs of the Italian territory are acquired through the SRTM archive.

References

- [1] A. K. Gabriel, R. M. Goldstein, and H. A. Zebker, “Mapping small elevation changes over large areas: Differential interferometry,” *J. Geophys. Res.*, 94, B7, 9183–9191, 1989
- [2] P. Berardino, G. Fornaro, R. Lanari, and E. Sansosti, “A new Algorithm for Surface Deformation Monitoring based on Small Baseline Differential SAR Interferograms”, *IEEE Trans. Geosci. Remote Sens.* 40, 11, 2375-2383, 2002.
- [3] F. Casu, M. Manzo, and R. Lanari, “A quantitative assessment of the SBAS algorithm performance for surface deformation retrieval from DInSAR data”, *Remote Sens. Environ.*, 102, 3/4, 195–210, 2006
- [4] R. Lanari, O. Mora, M. Manunta, J. J. Mallorquì, P. Berardino, and E. Sansosti, “A small-baseline approach for investigating deformations on full-resolution differential SAR interferograms”, *IEEE Trans. Geosci. Remote Sens.*, 42, 7, 1377–1386, 2004
- [5] A. Pepe, E. Sansosti, P. Berardino, and R. Lanari, “On the Generation of ERS/ENVISAT DInSAR Time-Series Via the SBAS Technique,” *IEEE Geosci. Remote Sens. Lett.*, 2, 3, 265–269, 2005
- [6] H. A. Zebker and J. Villasenor, “Decorrelation in interferometric radar echoes,” *IEEE Trans. Geosci. Remote Sens.*, 30, 5, 950-959, 1992
- [7] R. Torres, P. Snoeij, D. Geudtner, D. Bibby, M. Davidson, E. Attema, P. Potin, B. Rommen, N. Flouri, M. Brown, I. Navas Traver, P. Deghaye, B. Duesmann, B. Rosich, N. Miranda, C. Bruno, M. L’Abbate, R. Croci, A. Pietropaolo, M. Huchler, F. Rostan, “GMES Sentinel-1 mission”, *Remote Sens. Environ.*, 120, 9-24, 2012
- [8] F. Casu, S. Elefante, P. Imperatore, I. Zinno, M. Manunta, C. De Luca, and R. Lanari, “SBAS-DInSAR Parallel Processing for Deformation Time-Series Computation,” *IEEE J. Sel. Top. Appl. Earth Obs. Remote Sens.*, 7, 8, 3285–3296, 2014

From ERS-1 to Sentinel-1: 25 years of radar interferometry investigations on the Neapolitan active volcanic district surface deformations

M. Bonano^{1,2}, F. Casu², C. De Luca², R. Lanari², M. Manunta², M. Manzo², G. Onorato², I. Zinno²

¹IMAA-CNR, Tito Scalo (PZ), Italy, manuela.bonano@imaa.cnr.it; ²IREA-CNR, Napoli, Italy, bonano.m, casu.f, deluca.c, lanari.r, manunta.m, manzo.mr, onorato.g, zinno.i@irea.cnr.it

Differential Synthetic Aperture Radar Interferometry (DInSAR) has already demonstrated over the past decades its capabilities to effectively study and follow deformation phenomena related to natural events, such as earthquakes, volcano unrest phases and landslides, as well as to anthropic hazards associated with ground water exploitation, oil/gas extraction and storage, and tunnelling activities [1], [2]. The DInSAR technique is able to generate spatially dense deformation maps of extended areas with centimeter/millimeter accuracy, by exploiting the phase difference (i.e. differential interferogram) between pairs of SAR images, collected over the same area at different epochs (temporal baseline) and with different orbital positions (spatial baseline), where the topography-related phase component has been properly accounted for and removed by means of an external Digital Elevation Model (DEM).

Thanks to its capability to produce spatially dense maps of the surface displacements, DInSAR has progressively emerged as an effective, non-invasive tool in civil protection scenarios, with limited monitoring costs with respect to the traditional in-situ surveys. However, to overcome the limitations related to the use of single differential interferograms (i.e. inaccuracies of the external DEM, atmospheric disturbances etc), in the past 25 years several advanced DInSAR approaches have been developed. They are based on the exploitation of large sequences of SAR images collected over an investigated area and properly combined to generate the corresponding DInSAR interferograms, with the aim to follow the temporal evolution of the detected displacements via the generation of deformation time series. Among these methods, the advanced DInSAR technique referred to as Small Baseline Subset (SBAS) algorithm [3], [4] has proven to be an effective tool able to carry out multi-scale and multi-sensor analyses of surface deformation, providing insights on the spatial and temporal characteristics of the detected displacements at both regional (medium resolution analysis) and local (full resolution analysis) spatial scales. The SBAS approach relies on an appropriate combination of a large number of differential interferograms

produced by SAR interferometric data pairs characterized by short temporal and spatial baselines, in order to limit the noise (decorrelation) effects. Benefiting from the generated small baseline interferograms, the SBAS approach allows retrieving mean deformation velocity maps and corresponding time series for each coherent pixel with an accuracy of about 1-2 mm/year for what concerns the mean deformation velocity information and 5-10 mm for the single deformation measurement [5], [6].

The widespread use and application of advanced DInSAR approaches throughout the scientific community are also fostered by the development of new SAR sensors and satellite missions, characterized by different frequency bands, spatial resolution, revisit times and ground coverage. The DInSAR scenario is nowadays characterized by a steady increase in the availability of satellite SAR systems since 1992, starting from the "first-generation" C-band SAR missions (ERS-1/2 and ENVISAT of the European Space Agency and RADARSAT-1 of the Canadian Space Agency), moving to the "second-generation" SAR constellations, specifically the X-band COSMO-SkyMed (CSK) and TerraSAR-X (TSX) systems, which are particularly appropriate to investigate the space-time characteristics of the detected deformation phenomena at the scale of single buildings, as well as to monitor the temporal evolution of the displacements also in presence of small rates, fast-varying and non-linear deformation phenomena.

The recent launch (2014) of the C-band Sentinel-1 (S1) constellation, developed within the framework of the European Copernicus Programme, is pushing toward the present Earth Observation scenario to up-to-date research and monitoring frontiers, opening new possibilities to the investigation of surface deformation phenomena at the national/continental scale, thanks to the innovative acquisition mode referred to as Terrain Observation with Progressive Scans (TOPS) [7] specifically designed for advanced DInSAR applications. In particular, such a C-band system allows generating SAR images with a spatial resolution comparable to that of the ERS and ENVISAT satellites, but with a remarkable increase in the range coverage (about 250 km). Moreover, the reduced revisit time (6 days) ensured by the fully operative Sentinel-1A and Sentinel-1B twin satellites permits to systematically generate highly coherent interferometric products over very wide areas. The impact of the Sentinel-1 systems in the scientific community is further enhanced by the global coverage acquisition strategy and the "free and open access" data distribution policy.

This work is aimed at providing a comprehensive overview on how the availability of data gathered by such SAR systems has been impacting the DInSAR scenario since 1992 and how it is opening new perspectives in the Earth Observation monitoring activities relevant to

surface deformation phenomena in a real active volcanic context. In particular, we concentrate on the Neapolitan active volcanic district, including three volcanic complexes, i.e. the Campi Flegrei Caldera, the Mt. Somma-Vesuvius and the Ischia Island, which have been continuously “observed” from different satellite SAR systems working at different wavelengths since 1992. Thanks to this long-term SAR data archive available for this area, the Neapolitan active volcanic district represents a unique case study to demonstrate the key role played by the advanced DInSAR measurements for the comprehension of the physical processes responsible for the retrieved surface deformation patterns, providing a fundamental support also in the operational use of radar interferometry as a monitoring tool in civil protection scenarios.

In this work, we first highlight the capabilities offered by the SBAS-DInSAR technique to effectively study the long-term behaviour of deformation phenomena related to volcanic risk, through the generation of very long time series retrieved by exploiting the nearly 20-year SAR archive collected by the ERS-1/2 and ENVISAT ESA sensors between 1992 and 2010. Subsequently, we show the advantages arising from the use of SAR data collected by the more recent X-band COSMO-SkyMed constellation (2009-2018) for what concerns the assessment and mitigation of volcanic risk; indeed, thanks to their reduced revisit time and improved spatial resolution, the CSK SAR images allow us to follow the detected displacements with a great level of spatial and temporal details, also in presence of limited spatial extent deformations and rather fast dynamics. Finally, we investigate the capabilities of the new C-band Sentinel-1 constellation (2015-2018) to carry out advanced DInSAR analyses over the studied area. The reduced revisit time of the system (down to 6 days), together with the limited spatial baselines and the wide area coverage open new possibilities to systematically generate highly coherent interferometric products of very wide areas. Moreover, the availability of systematic SAR acquisitions collected from both ascending and descending passes over the investigated area allows detecting, in addition to the LOS ground deformation, the vertical and East-West components of the surface displacements, thus opening new monitoring perspectives to investigate Earth’s surface deformation dynamics.

Acknowledgments

This work has been supported in the framework of the DPC-IREA Agreement and DPC-INGV Agreement 2012–2021. The contents of this paper represent the authors' ideas and do not necessarily correspond to the official opinion and policies of the Italian Department of Civil Protection. This work was supported by the Italian Civil Defense Protection Department, the ESA's GEP project, the EPOS-IP project of the European Union

Horizon 2020 research and innovation program (grant agreement 676564), the I-AMICA (PONa3_00363) project, and the IREA-CNR/Italian Ministry of Economic Development DGS-UNMIG agreement. Sentinel-1 SAR data are copyright of Copernicus (2016) the COSMO-SkyMed data have been supplied by the Italian Space Agency (ASI), and they have been acquired through a dedicated acquisition plan. The DEMs of the Italian territory are acquired through the SRTM archive

References

- [1] A. K. Gabriel, R. M. Goldstein, and H. A. Zebker, "Mapping small elevation changes over large areas: Differential interferometry," *J. Geophys. Res.*, 94, B7, 9183–9191, 1989
- [2] D. Massonnet, and K. L. Feigl, "Radar interferometry and its application to changes in the Earth's surface," *Rev. Geophys.*, 36, 441-500, 1998
- [3] P. Berardino, G. Fornaro, R. Lanari, and E. Sansosti, "A new Algorithm for Surface Deformation Monitoring based on Small Baseline Differential SAR Interferograms", *IEEE Trans. Geosci. Remote Sens.* 40, 11, 2375-2383, 2002.
- [4] R. Lanari, O. Mora, M. Manunta, J. J. Mallorquí, P. Berardino, and E. Sansosti, "A small-baseline approach for investigating deformations on full-resolution differential SAR interferograms", *IEEE Trans. Geosci. Remote Sens.*, 42, 7, 1377–1386, 2004
- [5] F. Casu, M. Manzo, and R. Lanari, "A quantitative assessment of the SBAS algorithm performance for surface deformation retrieval from DInSAR data", *Remote Sens. Environ.*, 102, 3/4, 195–210, 2006
- [6] M. Bonano, M. Manunta, A. Pepe, L. Paglia, and R. Lanari, "From previous C-Band to New X-Band SAR systems: assessment of the DInSAR mapping improvement for deformation time-series retrieval in urban areas", *IEEE Trans Geosci Remote Sens* 51(4), 1973–1984, 2013
- [7] R. Torres, P. Snoeij, D. Geudtner, D. Bibby, M. Davidson, E. Attema, P. Potin, B. Rommen, N. Flouri, M. Brown, I. Navas Traver, P. Deghaye, B. Duesmann, B. Rosich, N. Miranda, C. Bruno, M. L'Abbate, R. Croci, A. Pietropaolo, M. Huchler, F. Rostan, "GMES Sentinel-1 mission", *Remote Sens. Environ.*, 120, 9-24, 2012

Swarm satellite constellation to study the possible effect of large earthquakes to the ionosphere

A. De Santis¹, D. Marchetti¹, G. Cianchini¹, R. Di Giovambattista¹, L. Perrone¹, A. Piscini¹, A. Ippolito¹, C. Cesaroni¹, L. Spogli^{1,3}

¹ *Istituto Nazionale di Geofisica e Vulcanologia, Via di Vigna Murata 605, Rome 00143, Italy* Contacting author: angelo.desantis@ingv.it

Within the SAFE project, funded by ESA in 2015-2016, we have started to analyse possible effects in ionosphere of seismic activity, known as Lithosphere-Atmosphere-Ionosphere Coupling (LAIC) effects. During the project, we analysed 12 large and intermediate earthquakes showing that the use of Swarm data, integrated by ground observations (e.g. seismic and ionosonde measurements), is very important to better understand the preparatory phase of large earthquakes in the world. The positive results have convinced ESA to approve an extension (e-SAFE) of one year (presently ongoing and ending in 2019). The e-SAFE project, together with an ASI founded project, Limadou-Science, continues to show that there is a possible influence of lithospheric activity on the magnetic field and on the electron density measurements taken by Swarm satellites.

In this presentation, we will show some examples of anomalous magnetic and electron density Swarm tracks that precede some M6+ earthquakes in the world and are potential seismic precursors of them.

Finally, we will show an automatic validation / correlation of the anomalies detected by Swarm satellites with the earthquakes occurrences showing some statistically significant concentrations of magnetic field and electron density anomalies that anticipate the earthquakes by around 85, 60, 20 and 10 days.

Investigating the possible correlation of atmospheric ozone variability with earthquakes: The case of Greece

M.N. Efstathiou¹, P.K. Varotsos¹

¹*Climate Research Group, Division of Environmental Physics and Meteorology, Faculty of Physics, National and Kapodistrian University of Athens, University Campus Bldg. Phys. V, Athens 15784, Greece
GR email: sovarotsos@hotmail.com*

Recently, Efstathiou [1] attempted to evaluate the association of the total ozone column (TOZ) variability with the eight major earthquakes that occurred during 2001–2010, in Greece. According to the results obtained, TOZ maxima or minima observed before or after an earthquake, did not appear to be significantly related to the seismic event.

Varotsos et al. [2] examined the seismo-atmospheric anomalies around the time and the epicentre of some of the major earthquakes occurred in Greece during the period 2001-2015. They used daily values of aerosol optical depth (AOD) and TOZ in the time window between 25 days before, and 14 days after each of these seismic events. For some of the earthquakes, the extreme values of $\Delta(\text{AOD})$ and $\Delta(\text{TOZ})$ appeared exceeding the upper bound ($M + 2 \times \text{IQR}$). Nevertheless, in other cases there was no unusual anomaly around the epicentre of the earthquake.

We herewith tried to verify the results extracted from the two above-mentioned studies, by applying another statistical analysis. In particular, we have applied a conventional statistical analysis as well as a receiver operating characteristic (ROC) curve analysis to graphically investigate the connection between TOZ fluctuations and the major recent earthquakes in Greece during the period 2001-2017. Our study was divided in two periods 2001-2010 and 2011-2017 to take into account the temporal change in TOZ scaling properties that may affect the reliability of TOZ as a precursor to seismic tool for earthquake forecasts.

TOZ daily time-series of the TOZ over each earthquake epicenter were created by the NASA Giovanni website (<http://disc.sci.gsfc.nasa.gov/giovanni>).

Our first step was to apply a conventional statistical analysis in order to detect the possible existence of unexpected TOZ fluctuations in the time-window of 2 weeks before and after the earthquake dates. If a TOZ value was outside the interval $(\mu - 2\sigma, \mu + 2\sigma)$, it was considered as a maximum or minimum, where μ and σ represent the mean and standard deviation of the total TOZ data set, correspondingly, over all the years 2001-2017 (excluding the year of the

earthquake), for the location and the time-window of each earthquake event, separately. Table 1 lists the 13 earthquakes.

Table 1. Earthquakes with $M_w \geq 6.0$ during 2001-2017 (Geo-Dynamic Institute of the National Observatory of Athens-GI-NOA, United States Geological Survey -USGS)

Earthquake	Date	Epicentre (°N, °E)	Depth (Km)	Magnitude (M_w)
1	26 July 2001	39.05, 24.35	19	6.5
2	14 August 2003	38.79, 20.56	12	6.2
3	8 January 2006	36.21, 23.41	69	6.7
4	6 January 2008	37.11, 22.78	86	6.2
5	14 February 2008	36.50, 21.78	41	6.9
6	14 February 2008	36.22, 21.75	38	6.5
7	20 February 2008	36.18, 21.72	25	6.2
8	8 June 2008	37.98, 21.51	25	6.4
9	1 April 2011	35.54, 26.63	60	6.0
10	16 June 2013	34.35, 24.99	12	6.0
11	24 May 2014	40.29, 25.4	27	6.9
12	17 Nov 2015	38.8, 20.4	10	6.5
13	12 June 2017	38.85, 26.33	10	6.4

Apart from this conventional statistical analysis, we also applied ROC curve analysis, for the period 2001-2010 and the period 2011-2017, separately. An ROC space is defined as a false positive rate (FPR) and true positive rate (TPR) as x and y axes, respectively, which depicts relative offsets between true positive and false positive [3]. Then, TPR and FPR denote:

$$\text{TPR} = \frac{\Sigma \text{ true positive}}{\Sigma \text{ condition positive}} \text{ and } \text{FPR} = \frac{\Sigma \text{ false positive}}{\Sigma \text{ condition negative}} \quad (1)$$

It finally turned out that there was no statistically significant correlation between the TOZ values and these earthquake events and the extracted values of Matthews correlation coefficient returns indicated a disagreement between prediction and observation [4].

In summary, we examine here whether the TOZ extreme values can be a precursor tool for predicting an earthquake. We focus on the strong seismic events in Greece ($M_w \geq 6.0$) during 2001-2017. We separate our investigation in two periods, namely 2001-2010 and 2011-2017, to take account the different scaling properties in the temporal TOZ variability during these periods. We apply both conventional and ROC statistical analysis to the daily TOZ values obtained from satellite observations in the two-week time window before and after each of the

seismic events. The main conclusion from the above analysis is that no statistically significant correlation of the TOZ values with the occurrence of an earthquake exists, thus TOZ time variability cannot be used as a precursor for earthquakes.

References

- Efstathiou M, Rem Sens Lett **3** (N.3), 181-190, 2012.
- Varotsos CA, Efstathiou MN, Cracknell AP, Acta Geophys **65** (N.4), 659-665, 2017.
- Fawcett T, Patt Recog Lett **27** (N.8), 861-874, 2006.
- Boughorbel S, Jarray F, El-Anbari M, PLoS One **12** (N.6), e0177678, 2017.

Is there a precursory signal of the surface air-temperature variability for earthquakes?

M.N. Efstathiou¹, P.K. Varotsos¹

¹*Climate Research Group, Division of Environmental Physics and Meteorology, Faculty of Physics, National and Kapodistrian University of Athens, University Campus Bldg. Phys. V, Athens 15784, Greece
GR email: sovarotsos@hotmail.com*

A number of scientists have suggested that characteristic features of a few components of the climate system (e.g. atmospheric constituents and meteorological parameters) are closely linked to earthquakes (e.g. [1], [2]).

However, two recent publications Efstathiou [3] and Varotsos et al. [4] did not detect any unexpected total ozone column (TOZ) variability or unusual fluctuations in aerosol optical depth before and after recent major earthquake events (with magnitude ≥ 6) that occurred in Greece. In fact, Efstathiou [1] examined the TOZ variability in the time window between 14 days before and after the eight major earthquakes of the 2001-2010 period, in Greece, but did not detect statistically significant correlation. Similarly, Varotsos et al. [4] studied five major earthquakes that occurred in Greece (on dates: 26/7/2001, 14/8/2003, 8/1/2006, 14/2/2008 and 17/11/2015) in connection with possible unusual changes in aerosol optical depth and TOZ in the time window between 25 days before, and 14 days after each of these seismic events. In most cases no unusual anomaly around the epicentre of the earthquakes has been observed.

In this paper we investigate whether the surface air-temperature (SAT) variability in a 2 week time window before and after a major earthquake is associated with the seismic event.

For this purpose, the daily SAT values that were generated from the NASA Giovanni website (<http://disc.sci.gsfc.nasa.gov/giovanni>) were used for each earthquake epicentre for the major earthquakes that occurred in Greece during 2011-2017 (see Table 1).

We analyzed SAT data employing conventional and modern statistical tests, and we found that there was no statistically significant extreme value of SAT (at a 95% confidence level), in the 14 days time window preceding each earthquake event that occurred in Greece during 2011–2017. In the case of the third and fourth events, an extreme SAT value occurred 10-11 days after the seismic event, so it could not be considered as a precursor signal. Any SAT anomaly regardless of whether preceded or followed by earthquakes may be due to several

other factors of meteorological and physico-chemical nature, that take place in the Earth - Atmosphere system [e.g., 2, 5, 6, 7,8].

Table 1. Earthquakes with $M_w \geq 6.0$ during 2001-2017 (Geo-Dynamic Institute of the National Observatory of Athens-GI-NOA, United States Geological Survey -USGS)

Earthquake number	Date	Epicentre (°N, °E)	Depth (Km)	Magnitude (M_w)
1	1 April 2011	35.54, 26.63	60	6.0
2	16 June 2013	34.35, 24.99	12	6.0
3	24 May 2014	40.29, 25.4	27	6.9
4	17 November 2015	38.8, 20.4	10	6.5
5	12 June 2017	38.85, 26.33	10	6.4

By summarizing, in this work we focus on the SAT values throughout the period 2011-2017 and search for a potential association of their variability with major earthquakes in Greece. The main finding drawn is that there is no statistically significant correlation of the SAT changes with the earthquakes.

References

- Akhoondzadeh M, Adv Space Res **55**, 1754–1763, 2015.
- Ganguly ND, J Atmos Sol-Terr Phys **140**, 16–22, 2016.
- Efstathiou M, Rem Sens Lett **3** (N.3), 181-190, 2012.
- Varotsos CA, Efstathiou MN, Cracknell AP, Acta Geophys **65** (N.4), 659-665, 2017.
- Tertyshnikov AV, Phys. Solid Earth **31**, 789–794, 1996.
- Chmyrev V, Smith A, Kataria D. Nesterov B, Owen C., Sammonds P,...Vallianatos, F, Advances in Space Research **52** (N.6), 1135-1145, 2013.
- Pulinets SA, Ouzounov D, Ciraolo L, Singh R, Cervone G, Leyva A., ...Kotsarenko A, Annales Geophysicae **24** (N.3), 835-849, 2006.
- Varotsos PA, Sarlis NV, Skordas ES, Lazaridou MS, Tectonophysics **589**, 116-125, 2013.

Investigating volcanic ash phenomena from space by means of Himawari-8 data

A. Falconieri¹, F. Marchese¹, N. Pergola¹, V. Tramutoli²

¹*Institute of Methodologies for Environmental Analysis (IMAA), Italian Research Council (CNR), Tito Scalo (PZ) Italy, alfredo.falconieri@imaa.cnr.it.*; ²*University of Basilicata, School of Engineering, Via dell'Ateneo Lucano 10, 85100, Potenza, Italy*

In November 2017, after several years of quiescence the Mt. Agung (Indonesia) erupted, emitting volcanic ash causing a temporary air traffic in Indonesia. A few months later (i.e. on 19 February 2018) an intense explosive eruptions occurred at Mt. Sinabung (Indonesia), which was sporadically active since 2010, emitting an ash cloud reaching an altitude of 5-7 km above sea level. In this work, we investigate those volcanic phenomena from space, assessing the potential of a known RST (Robust Satellite Techniques) based algorithm specifically developed to detect ash clouds in providing reliable and accurate information about ash dispersion in atmosphere by exploiting the high-temporal resolution (10 min) and the spectral features of Himawari-8. The AHI (Advanced Himawari Imager) sensor aboard the new Japanese geostationary satellite offers in fact improved features than imagers of previous MTSAT (Multi-functional Transport Satellites) series, which should guarantee further improvements in the identification, monitoring and characterization of ash phenomena from space. Results of this study show that coupling RST performance to Himawari-8 observations ash clouds emitted by aforementioned volcanoes could effectively be identified and tracked from space. Moreover, starting from the estimates of ash-cloud top height performed using a largely accepted literature method, the mass eruption rate has been also estimated for Mt. Agung explosive eruption. These outcomes show that if Himawari-8 data are properly used they could provide an important contribution for the early identification and continuous monitoring of ash events affecting East Asia and Western Pacific region.

Correlations between VAB electron loss detected by NOAA and strong seismic activity used to improve forecasting of $M \geq 6$ earthquakes

C. Fidani¹

¹*Central Italy Electromagnetic Network, Fermo, Italy, c.fidani@virgilio.it*

To correlate seismic activity with NOAA data, a Ntuple was created which contains earthquake data including: event time, location, magnitude and depth. The values of the corresponding L-shells of the earthquake epicentres projected to different altitudes were also calculated by the same methodology used for particles and included in the Ntuples. This was done to determine the possibility of a physical link between earthquakes and particle fluxes and their space-time locations. The earthquake list was downloaded from the Earthquake Center of United States Geological Survey (USGS) at <http://neic.usgs.gov/neis/epic/epic.html>, and has been adjusted to eliminate foreshocks and aftershocks.

NOAA data consisted in binary files which were stored in Ntuples where the time step was 8 seconds. From July 1, 1998 to December 31, 2014, binary data were downloaded from NOAA (<http://www.ngdc.noaa.gov/stp/satellite/poes/dataaccess.html>) and examined to exclude uncorrected instrument operations through their corresponding flags. Furthermore, the electron counting rates were corrected for proton contamination using software downloaded from the Virtual Radiation Belt Observatory (<http://virbo.org/POES#Processing>). In order to include the geomagnetic and extraterrestrial influences on the particle fluctuations, the counting rates data were associated to daily averages of the geomagnetic Ap index and SID (<http://www.aavso.org/solar-sids>), as well as three hour averages of the Ap index (<ftp://ftp.ngdc.noaa.gov/STP/GEOMAGNETICDATA/APSTAR/apindex>).

Plot in Figure 1 reports the statistical correlation calculated over more than 16 years of data collecting the time difference between strong earthquake occurrence and electron burst detection $T_{EQ} - T_{EB}$ from -72 to 72 hours. The distribution shapes and average values (in red) were compared with standard deviations (in yellow) of correlation events, evidencing super-poissonian distributions. Note that, based on super-poissonian fitting of correlation distribution a significant correlation peak appeared between 2 and 3 hours of positive time difference, which means that the electron burst was observed before the corresponding

earthquake. The peak at 2 - 3 hours started to be significant when considering earthquake epicentre projections above 1,400 km altitudes.

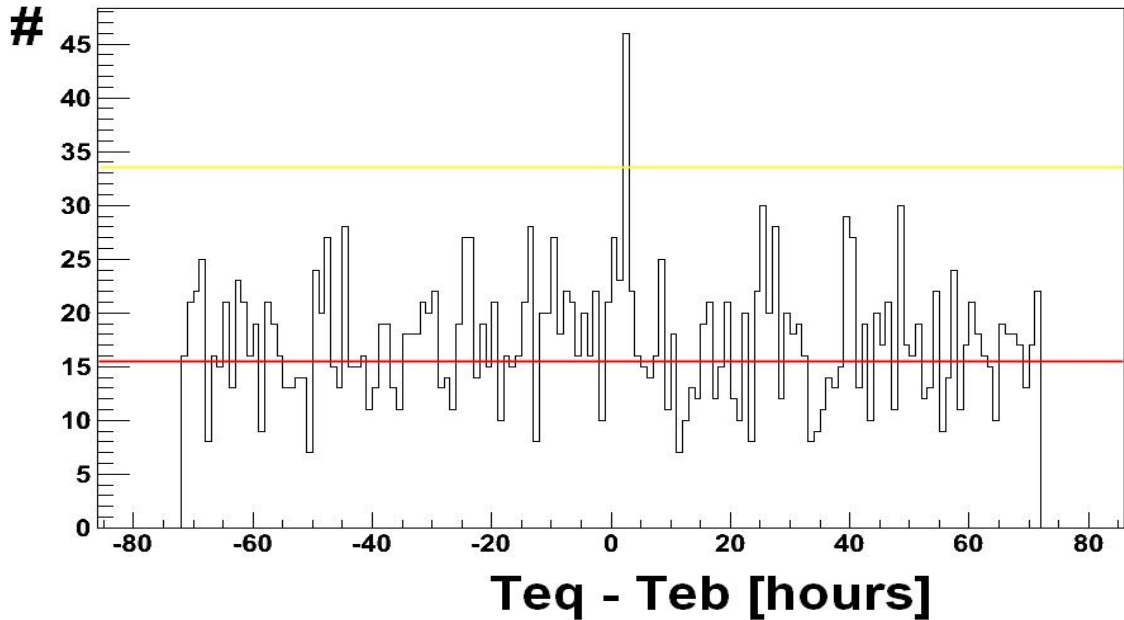


Fig. 1. The correlation between strong earthquakes and electron burst calculated over 144 hours, the significant peak is above the threshold of 99% in yellow, the average is the red line.

Correlation peak significance was also calculated taking into account solar influence. It was made by dividing the peak magnitude minus average value, by the variance. Results are shown in Figure 2 left, where the number of sigma distributions are depicted for various earthquake altitude projections using the Ap index threshold seasonally modulated or the Ap index constant threshold equal to 18. These values were chosen based on past studies. The Ap index constant threshold permitted to obtain up to 5 sigma of peak significance above the average value, as well as Ap index seasonally modulated, shown in Figure 2 right permitted to obtain up to 6 sigma of peak significance above the average value.

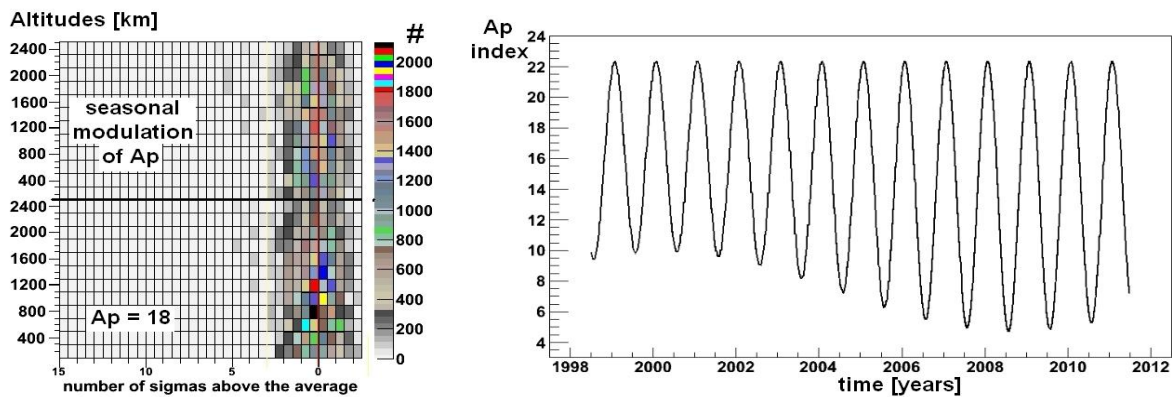


Fig. 2. The correlation significance, in terms of sigma on the left, where colours define the number of correlation events, was calculated for different Ap index thresholds; both maximum numbers of sigma were obtained for 2,400 km earthquake altitude projections.

Epicentre locations having earthquakes correlated with electron bursts were concentrated in both the Indonesian and Philippine Regions (Fidani, 2015). As was shown, positions could be linked in a causal way with some kind of electron disturbances occurring several hours before the main shocks. In fact, by taking into account that electrons drift eastwards and that the earthquake epicentres were located west of the electron burst detection positions, a causal connection between them can be supposed. In turn, if any kind of signal was emitted around the earthquake epicentres, it could have reached the ionosphere above the epicentres. Therein, it would have perturbed electron motions and electron bursts that would have been detected some time after. Indeed, based on electron energies detected by NOAA particle telescopes, it was calculated to be of the order of at least 2 - 7 hours, thus the perturbation process would have occurred at least 4 - 10 hours before the earthquakes (Fidani, 2015).

Magnetic pulses detected during the Norcia seismic swarm (Orsini and Fidani, 2017 and 2018), culminated with a main-shock of $Mw = 6.6$ occurred on October 30, 2016, gave new interest to the physical process which could be the link between earthquakes and electron bursts. The physical interaction consists in magnetic fluctuations coupled with charged particles which are able to modify pitch angles of electron motions inside the Van Allen Belts. Pitch angle variations generate variations in bouncing altitudes of charged particles, with a consequent presence of greater fluxes of electrons at satellite altitudes. However, the correlation above regarding earthquakes which occurred in the Indonesian and Philippine Regions are located at different geographical coordinates and, overall, at different geomagnetic coordinates. This implicates that, if magnetic pulses are able to reach the ionosphere, different interaction times occur with different populations of Van Allen Belts for Italian earthquakes with respect to those concerning the above correlation.

If such a causal connection exists between earthquakes and electron bursts, a question can be raised: could the 2 - 3 hours correlation be used for strong earthquake forecasting? The answer to this question can be positive if the probability calculation of a strong earthquake over the next 2 - 3 hours refers to Indonesia or the Philippines. Probability can be calculated throughout the relation between covariance and cross correlation (Fidani, 2018)

$$P(EQ|EB) = P(EQ) + \text{corr}(EQ, EB)\sqrt{P(EQ)[1-P(EQ)][1-P(EB)]}/P(EB), \quad (1)$$

where EQ and EB indicate earthquake and electron burst events, respectively. Which means that, if a correlation exists between earthquakes and electron bursts, and the time difference is chosen to be that of correlations between earthquake and electron burst events,

the probability of a strong earthquake is increased of a term proportional to the correlation.

References

- Fidani C.; 2015: Particle precipitation prior to large earthquakes of both the Sumatra and Philippine Regions: a statistical analysis, *Journal of Asian Earth Science*, 114, 384-392.
- Fidani C.; 2018: Improving earthquake forecasting by correlations between strong earthquakes and NOAA electron bursts. *Terr. Atmos. Ocean. Sci.*, 29, 117-130.
- Orsini M. and Fidani C.; 2017: Magnetic perturbations observed around the October 30, 2016, Norcia, 36th GNGTS, Novembrer 14 – 16, 2017, Trieste, 316-318.
- Orsini M. and Fidani C.; 2018: Modelling magnetic pulse swarms that anticipated the 2016 Norcia, and 2017 Capitignano, Central Italy earthquakes, EMSEV 2018, September 17 – 21.

On the potential of Robust Satellite Techniques (RST) to investigate TIR signatures associated to impending earthquakes

N. Genzano¹, C. Filizzola², M. Lisi¹, N. Pergola², V. Tramutoli¹

¹*School of Engineering, University of Basilicata, Potenza, Italy; nicogenzano@gmail.com;* ²*Institute of Methodologies for Environmental Analysis of the National Research Council, Tito Scalo (PZ), Italy*

Since '80, the space-time fluctuations of TIR radiation measured by satellite record have been considered as a possible precursor of seismic events (see Tramutoli et al., 2015). As proposed by several authors (Qiang et al., 1991; Tramutoli et al., 2001, 2013) the appearance of anomalously high TIR records near the place and the time of earthquake occurrence could be related to the increase of green-house gas (such as CO₂, CH₄, etc.) emission rates.

Up to now, several methodologies have been proposed study the different phases of seismic events with the purpose to highlight satellite thermal anomalies due to earthquake events. Among these, also the general change detection approach named RST (Robust Satellite Techniques, Tramutoli 1998,2007) has been successfully used in tens of earthquakes happened in the last 40 years.

In this work, the good abilities of RST methodology to discern anomalous TIR signals possible related to seismic events from the normal variability of TIR signal due to other causes (e.g. meteorological), have been exploit to study the “nocturnal heating” effect, associated by Bleier et al. (2009) to seismic activity. In particular, we will show results achieved studying the seismic phases of recent earthquakes occurred in Italy (e.g. Amatrice earthquake, August 24, 2016, Mw 6.0) and in Japan (e.g. Kumamoto earthquake, April 16, 2016; Mw 7.0).

Monitoring Mt. Etna thermal activity by means of RST_{VOLC} system

F. Marchese¹, A. Falconieri¹, T. Lacava¹, G. Mazzeo¹, N. Pergola¹, V. Tramutoli²

¹*Institute of Methodologies for Environmental Analysis (IMAA), Italian Research Council (CNR), Tito Scalo (PZ) (Italy); francesco.marchese@imaa.cnr.it.*; ²*University of Basilicata, School of Engineering, Via dell'Ateneo Lucano 10, 85100, Potenza (Italy).*

The RST_{VOLC} algorithm, which is based on the well-established RST (Robust Satellite Techniques) multi-temporal approach, has been developed to detect and monitor volcanic thermal anomalies from space. The algorithm was originally tested with good results using infrared AVHRR (Advanced Very High Resolution Radiometer) data. Afterwards, it was implemented on MODIS records showing a high potential in detecting low-level hot spots, like those preceding the Mt. Asama (Japan) September 2004 eruption. In this study, we present some results achieved monitoring the recent Mt. Etna (Sicily; Italy) thermal activity integrating both AVHRR and MODIS observations in near real time. In particular, we show results achieved investigating the paroxysmal events of Mt. Etna of May 2016, as well as the hot degassing activity occurring from a small vent opening within the Voragine (VOR) crater since August 7. The temporal fluctuations of volcanogenic radiant flux indicate that after the intense paroxysmal events of May 2016 some interesting changes in the intensity of thermal emissions took place at the monitored volcano, preceding the high-temperature degassing activity from VOR. Those changes in thermal activity, which are consistent with information provided by independent high spatial resolution satellite data (i.e. Sentinel-2 MSI and Landsat 8-OLI), confirm that RST_{VOLC} may give an important contribution for the early identification of weak phases of thermal unrest even in areas well monitored by ground-based systems.

Pre-earthquake chain processes in occasion of the 2016-2018 seismic sequence in Central Italy from ground and space observations

D. Marchetti¹, A. De Santis^{1,3}, A. Piscini¹, S. D'Arcangelo², F. Poggio³

¹*Istituto Nazionale di Geofisica e Vulcanologia, Via di Vigna Murata 605, Rome 00143, Italy
dedalo.marchetti@ingv.it;* ²*Facultad Física (UCM), Avd. Complutense, s/n. 28040 – Madrid ,Spain;* ³*Università Gabriele D'Annunzio – Chieti, Italy*

We present in this talk the magnetic and climatological analysis to search for possible electromagnetic and atmospheric effects in the preparatory phase of the 2016-2018 Central Italy seismic sequence. The major events occurred on 24 August 2016 (Amatrice earthquake, Mw 6.0), 30 October 2016 (Norcia mainshock, Mw6.5) and 18 January 2017 (four M5+ events close to Campotosto-Visso). The seismic sequence is still ongoing.

The work will show the approach we defined and introduced in the framework of SAFE (ESA funding Agency) and LIMADOU-Science (ASI funding agency) Projects as applied to this case study. It will concern the analysis of electromagnetic data from the Swarm three satellites by ESA, combined with the observations from the INGV magnetic observatories of L'Aquila and Duronia for investigating the preparatory phase of the earthquakes sequence. The study is also integrated with the combined analysis of some atmospheric parameters, such as skin temperature, total column water vapour and total aerosol thickness comparing the values preceding the seismic sequence with the historical time series of the previous years.

Our results combined /compared also with those provided by other works show a certain synchronicity of the different physical parameters, forming a chain of processes pointing toward the imminent earthquakes.

The experience learnt by these analyses could be very useful for the investigation of the future CSES satellite data related to next large earthquakes.

This work is partly funded by the European Space Agency under “SAFE” Project and by the Italian Space Agency under “Limadou-Science” Project.

Integration of field surveys and remote sensing techniques for seismic damage assessment

A. Masi¹, L. Chiauzzi¹, G. Nicodemo¹

¹School of Engineering, University of Basilicata, Potenza, Italy, angelo.masi@unibas.it;
giuseppe.nicodemo@unibas.it

After a natural disaster, such as an earthquake, accurate and rapid information on the damage caused is of crucial importance for rescue and relief operations and to better utilize available resources for repair and recovery. Seismic damage assessment of urban areas is the key in the emergency management of post-earthquake. Rapid identification of damage distribution is fundamental for Civil Protection during the management of the first emergency phase in order to identify priorities in planning the usability inspections. Generally, the evaluation of damage and the estimation of building usability are performed by means of a building-by- building survey based on a form filled out by expert technicians during the days and weeks following the event (Masi et al., 2016). When the affected area is large, conventional methods of information gathering are slow and incompatible with immediate relief. In this framework, many studies have been carried out worldwide in order to identify, in the immediate aftermath of an earthquake, the damage distribution through remote sensing approaches. The acquisition, interpretation and use of data from remote sensing allow to gather information over a wide area quickly and independently of the situation on the ground (Chesnel et al., 2007). The occurrence of recent damaging earthquakes and the huge availability of satellite images have offered a unique opportunity to make progress towards the aim of rapid post-disaster damage mapping (Saito and Spence, 2004a). Indeed, a variety of sensors are available to acquire a huge volume of remotely sensed image data at different spatial resolutions and with temporal coverage before and after a disaster event. Therefore, the main goal is to integrate the field surveys data with remote sensing data for rational planning of emergency and rescue operations and damage assessment studies. The integration of remote sensing data and damage information collected in the field can effectively streamline, accelerate and increase the volume and diversity of data captured during post-disaster reconnaissance (Saito and Spence, 2004b; Yamazaki et al. 2004). In this paper, after the Ml=6.0 (GdL INGV 2016) earthquake occurred in Central Italy on August 24, 2016, optical images were taken in order to have a first idea of the damage distribution in the

villages located in the epicentral area (Copernicus 2016). The damage distribution of Amatrice village obtained from remote sensing approach has been compared with field data collected in the aftermath of the August 24 event (Santarsiero et al., 2016). The comparison between remote sensing and field data underlines that the identification of the areas with the higher percentage of severely damaged and collapsed buildings can be effectively achieved through remote sensing. On the contrary, dealing with the areas with lower damage levels can be more complicated and requires also field data. However, availability of remote sensing information can contribute to plan usability inspections, taking into account that the buildings with heavy damage are certainly unusable.

References

- Chesnel A.L., Binet R., Wald L., (2007) *Quantitative assessment of building damage in urban area using very high resolution images*. In: 2007 urban remote sensing joint event. IEEE, pp 1–5
- Copernicus (2016) <http://emergency.copernicus.eu/mapping/list-of-components/EMSR177>
- GdL INGV 2016, Gruppo di Lavoro INGV sul terremoto di Amatrice (2016). Secondo rapporto di sintesi sul Terremoto di Amatrice MI6.0 del 24 agosto 2016 (Italia Centrale).
- Masi A., Santarsiero G., Digrisolo A., Chiauzzi L., Manfredi V., (2016) *Procedures and experiences in the post-earthquake usability evaluation of ordinary buildings*. Bollettino di Geofisica Teorica e Applicata 57(2):199–210
- Saito K., Spence R., (2004a) *Rapid damage mapping to support post-disaster recovery*. In: 13th World Conference on Earthquake Engineering, Conference Proceedings, 2004
- Saito K., Spence R., (2004b) *Rapid damage mapping using post-earthquake satellite images*. In: Proceedings of 2004 IEEE international geoscience and remote sensing symposium, 2004. IGARSS'04, vol. 4. IEEE, pp 2272–2275
- Santarsiero G., Chiauzzi L., Masi A., (2016) *Analisi del danneggiamento di edifici situati nella zona Sud del comune di Amatrice: confronto pre e post sisma del 24/08/2016 (V2)*. <http://www.reluis.it>
- Yamazaki F., Kouchi K.I., Kohiyama M., Muraoka N., Matsuoka M., (2004) *Earthquake damage detection using high-resolution satellite images*. In: Proceedings of 2004 IEEE international geoscience and remote sensing symposium, 2004. IGARSS'04, vol 4. IEEE, pp 2280–2283

Research on electron density of Swarm satellites based on DWT

K. Zhu¹, M. Fan¹, K. Li¹, C. Chi¹, Z. Yu¹

¹*Key Laboratory of Geo-Exploration Instrumentation, Ministry of Education, Jilin University, Changchun, China, zhukaiguang@jlu.edu.cn*

Earthquake could cause ionospheric disturbances according to LAIC mechanism. Satellite measurements could be used to study the earthquake precursor all over the world. In this paper, we analyzed the strong Ecuador (Mw=7.8) earthquake of 16 April 2016 by analyzing the electron density variations of Swarm satellites. In consideration of the geomagnetic indices, the potential seismic anomalies were shown on 7 and 10 days before the event. Furthermore, we applied DWT to decompose electron density data into 6 levels for these two days, and amplitude anomalies were found. Thus they could be considered as the earthquake precursors. Our results indicate that the Swarm satellites measurements could also be used in the earthquake precursor research.

1. Introduction

Earthquakes is the lithosphere, under the stress due to the plate tectonics, releases most of its energy with some rapid ruptures. Lithosphere–Atmosphere–Ionosphere Coupling (LAIC) model can explain anomalous variations which are usually named as short-term earthquake precursors. To investigate earthquake events, many scholars have analyzed the DEMETER satellite measurements by different methods and obtained some positive results (e.g. M. Akhoondzadeh, 2010; M. Parrot, 2012; X. Shen, 2012; X. Yan, 2014). Recently several researchers have already used the data of Swarm satellites to study the earthquake precursor (e.g. A. De Santis, 2017; M. Akhoondzadeh, 2018). In this paper, we would investigate the electron density data of Swarm satellites to study the Ecuador earthquake based on DWT (Discrete Wavelet Transform).

2. Data observation and anomalies detection

Ecuador earthquake occurred on 16 April 2016, 23:58:36 UTC, with a magnitude Mw 7.8 (hypocenter 0.371°N, 79.940°W). In this paper, electron density data of Swarm Alpha satellite during the period of 1st April to 30 April 2016 were processed to study Ecuador earthquake.

2.1 Geomagnetic indices

Solar geomagnetic field and geomagnetic storms could cause strong anomaly in ionospheric. We chose the geomagnetic indices Kp and Dst to reject the days of geomagnetic disturbances. And the days when Dst index $< -40\text{nT}$ and Kp index > 3 are considered high geomagnetic activity. By analyzing the geomagnetic indices for 30 days in April 2016, 2, 3, 7, 8 and 12-16 April 2016 cannot be used to study the anomalies associated with the Ecuador earthquake.

2.2 Electron density anomalies detection

This study selects electron density data of Dobrovolsky's area (1979) which located at $19.629^\circ\text{S} \sim 20.371^\circ\text{N}$ and $59.94^\circ\text{E} \sim 99.94^\circ\text{E}$.

Electron density anomalies detection is divided into the following steps. At the first step, the tracks in the study area were divided into daytime and night-time according to local time and we selected the night tracks. Then, the difference between the measured electron density and the values predicted by IRI2012 model was calculated. Next, the data were filtered by Alpha-trim filter. The filtered data are denoted as X ($m \times n$), where m indicates the number of samples, n is the number of days.

$$\mu_1 = (\sum_{i=1}^m \sum_{j=1}^n X(i,j)) / (m \times n) \quad (1)$$

$$\sigma_1 = \sqrt{\frac{1}{m \times n} \sum_{i=1}^m \sum_{j=1}^n (X(i,j) - \mu_1)^2} \quad (2)$$

Set $\text{Th1} = \mu_1 + 5\sigma_1$ as threshold, $N(i)$ ($i = 1, 2, \dots, n$) is the number of samples of the i th day that exceeds Th1.

$$\mu_2 = (\sum_{i=1}^n N(i)) / n \quad (3)$$

$$\sigma_2 = \sqrt{\frac{1}{n} \sum_{i=1}^n (N(i) - \mu_2)^2} \quad (4)$$

Set $\text{Th2} = \mu_2 + 1.5\sigma_2$. It should be noted that the Th1 and Th2 were calculated only by quiet geomagnetic days. The days that N exceed Th2 can be seen as anomalies. From the results of the first tracks we found that N of April 2, 6, 7, 9, and 13 all exceeded Th2 before the earthquake. And we rejected the April 2, 7, and 13 due to its high geomagnetic indices. Therefore, April 6 and April 9 can be considered as seismo-ionospheric anomalies and in addition, the tracks of these two days are very close to the epicenter. About the second tracks we found that N of April 2, 6 and 15 all exceeded Th2. Only April 6 is a quiet geomagnetic

day which can be seen as an anomaly day. In summary, April 6 and 9, 2016 could be considered as seismo-ionospheric anomalies associated with the Ecuador earthquake.

3. Anomalies analysis

In order to do the detailed analysis, we used the DWT to investigate the anomalous nighttime tracks of Swarm satellite on April 6 and 9. In this paper, Mallat algorithm is adopted to implement the DWT, as shown in equation (5).

$$\left\{ \begin{array}{l} A_0[x(t)] = x(t) \\ A_j[x(t)] = \sum_k H(2t - k)A_{j-1}[x(t)] \\ D_j[x(t)] = \sum_k G(2t - k)A_{j-1}[x(t)] \end{array} \right. \quad (5)$$

where $x(t)$ is the signal, j is the number of decomposition levels, A_j is the low-frequency wavelet coefficients of the signal in the j th level, D_j is the high-frequency wavelet coefficients of the signals in the j th level, and H and G are the wavelet decomposition filters.

We decomposed the anomalous electron density data of the Alpha during nighttime into 6 levels using db4 wavelet basis, which corresponding frequency ranges are lower than 0.0446Hz, 0.0446 to 0.0893Hz, 0.0893 to 0.1786Hz, 0.1786 to 0.3571 Hz, 0.3571 to 0.7143Hz, and 0.7143 to 1Hz. Then, we reconstructed the single branch from 1-D wavelet coefficients and got A_{re5} , and $D_{re5} \sim D_{re1}$. The results of the tracks during nighttime on April 6 and 9 indicate obvious anomalies at $D_{re5} \sim D_{re1}$, and then become smaller with time. Therefore, the detected anomalies on 6 and 9 April could be possibly considered as earthquake precursors related the Ecuador earthquake.

4. Conclusions

Based on DWT, we have investigated the electron density data of Swarm satellites for the Ecuador earthquake. The analysis of electron density data shows that there are obvious amplitude anomalies at the components which frequency range is from 0.0446 to 1Hz on 7 and 10 days before the earthquake obeyed the LAIC mechanism. Although the Swarm satellites data is low frequency, the high precision characteristic make it could be applied to the earthquake precursor study.

Reference

- Akhoondzadeh M., Parrot M., and Saradjian M. R., 2010. Electron and ion density variations before strong earthquakes ($M>6.0$) using DEMETER and GPS data. *Nat. Hazards Earth Syst. Sci.*, 10, 7–18, 2010.
- Akhoondzadeha M., De Santis A., Marchettib D., Piscinib A., and Cianchini G., 2018. Multi precursors analysis associated with the powerful Ecuador (MW= 7.8) earthquake of 16 April 2016 using Swarm satellites data in conjunction with other multi-platform satellite and ground data. *Advances in Space Research* 61 (2018) 248–263.
- Parrot M., 2012. Statistical analysis of automatically detected ion density variations recorded by DEMETER and their relation to seismic activity. *Annals of Geophysics*, 55, 1, 2012.
- De Santis A., Balasis G., Pavón-Carrasco F.J., Cianchini G., and Mandea M., 2017. Potential earthquake precursory pattern from space: The 2015 Nepal event as seen by magnetic Swarm satellites. *Earth and Planetary Science Letters* 461 (2017) 119–126.
- Xiangxiang Y., Xinjian S., Jinbin C., and Ji T., 2014. Statistical analysis of electron density anomalies before global $Mw\geq7.0$ earthquake (2005-2009) using data of DEMETER satellite. *Chinese Journal Geophysics*, 2014, 57(2):364-376.
- Zhima Z., Xuhui S., Jinbin C., Xuemin Z., Jianping H., Jing L., Xinyan O., Shufan Z., 2012. Statistical analysis of ELF/VLF magnetic field disturbances before major earthquakes. *Chinese Journal Geophysics*, 2012, 55(11):3699-3708.

Chapter 4

*Magnetospheric, ionospheric and
atmospheric phenomena associated with
seismic activities*

Seismo-ionospheric precursors of the 2017 M7.3 Iran-Iraq Border Earthquake and the 2018 M5.9 Osaka Earthquake observed by FORMOSAT-5/AIP

J.Y. Liu^{1,2,3}, iSTEP/CAPE groups^{1,2}

¹*Center for Astronautical Physics and Engineering, National Central University, Taoyuan City 32001, Taiwan;*

²*Graduate Institute of Space Science, National Central University, Taoyuan City 32001, Taiwan; ³Center for Space and Remote Sensing Research, National Central University, Taoyuan City 32001, Taiwan.*

FORMOSAT-5 (F5) launched on 25 August 2017 travels on a sun-synchronous orbit with 720 km altitude, 98.25-degree inclination, and 99-minute period. A science payload of AIP (advanced ionospheric probe) on board F5 probes the ion density, ion temperature, and ion velocity in the ionosphere. The mission of F5/AIP is to observe ionospheric space weather and to monitor earthquake precursors. Global ionospheric maps (GIMs) of the total electron content (TEC) derived by ground-based GNSS (global navigation satellite system) receivers act a complementary observation of seismo-ionospheric precursors (SIPs). SIPs of the 12 November 2017 M7.3 Iran-Iraq Border Earthquake and the 17 June 2018 M5.9 Osaka earthquake are detected by the GIM TEC and the F5/AIP ion density/velocity. The GIM TEC over the epicenter is employed to temporal SIPs, while the anomaly count of spatial SIPs is used to locate possible forthcoming large earthquakes. When the spatial SIP is located, the F5/AIP ion density and ion velocity are employed to confirm and find the detected SIP and possible causal mechanism. The GIM shows that the TEC significantly increase over the epicenter 8-10 days and 3 days before the 2017 M7.3 Iran-Iraq Border Earthquake and 2018 M5.9 Osaka Earthquake, respectively. The F5/AIP ion density confirms the positive SIPs of the ion velocity shows the seismo-generated electric field generated before the earthquake being essential.

Electromagnetic field observations by the DEMETER satellite in connection with the 2009 L'Aquila Earthquake

Bertello¹, M. Piersanti², M. Candidi¹, P. Diego¹, P. Ubertini¹

¹*Istituto di Astrofisica e Planetologia Spaziali, Rome, Italy. 2INFN – Sezione di Roma Tor Vergata, Rome, Italy*

On April 6, 2009, at 01:33 UT, a 6.2 Mw earthquake stroke the city of L'Aquila ($\lambda=42,21^\circ$; $\varphi=13,23^\circ$). An intense preseismic activity ($3 < M < 5$) had been observed for several months. The DEMETER satellite was operational and flew within 1 hour in local time (LT) over L'Aquila twice a day (~10 LT and ~22 LT). Electromagnetic field data from DEMETER, experiments ICE and IMSC, have been analyzed during periods in which waveform data collection was available to retrieve possible signals, connected with the earthquake and possible precursor activity. The data analysis was performed based on a new technique (ALIF, Cicone et al. 2016 and Piersanti et al. 2017). The statistical background was evaluated over four months (January – April) in 2009 and 2010 when geomagnetic activity was very low ($0 < K_p \leq 2$; Sq). On April 4, 2009, two days before the April 6, 2009 earthquake, when DEMETER flew exactly over L'Aquila at UT=20:29, an intense and very localized signal was observed at 333 Hz. Because of the very low geomagnetic activity of solar origin ($3 \leq \text{Sym-H} \leq 10$ and $\text{AE} \leq 25$) and the very quiet Ionogram, this kind of signal can be related to a pre-seismic activity. Indeed, its peculiar polarization, in terms of Poynting flux, could be associated with a horizontal current system flowing at ground, switched on by an anomalous ground impedance generated by the fault-break.

The INFREP Cooperation: Recent Results

P.F. Biagi¹, R. Colella¹, L. Schiavulli¹, A. Ermini², M. Boudjada³, H. Eichelberger³, K. Schwingenschuh³, K. Katzis⁴, M. Kachakhidze⁵, M.E. Contadakis⁶, C. Skeberis⁶, I.A. Moldovan⁷, H.G. Silva⁸

¹*Department of Physics, University of Bari, Bari, Italy (pierfrancesco.biagi@uniba.it);* ²*Department of Industrial Engineering, University of Tor Vergata, Rome, Italy (ermini@uniroma2.it);* ³*Space Research Institute, Austrian Academy of Sciences, Graz, Austria (mohammed.boudjada@oeaw.ac.at);* ⁴*Department of Computer Science and Engineering, European University Cyprus, Nicosia, Cyprus (k.katzis@euc.ac.cy);* ⁵*Saint Andrew Georgian University, Faculty of Informatics, Mathematics and Natural Sciences, Tbilisi, Georgia (kachakhidzem@gmail.com);* ⁶*Department of Surveying & Geodesy, University of Thessaloniki, Thessaloniki, Greece (kodadaki@eng.auth.gr);* ⁷*National Institute of Earth's Physics, Seismological Department, Bucharest, Magurele, Romania (iren@infp.ro);* ⁸*Renewable Energies Chair, University of Évora, IIFA, Évora, Portugal (hgsilva@uevora.pt)*

In order to investigate the precursors of earthquakes, about 10 years ago the INFREP cooperation started. INFREP is a scientific cooperation among different international research teams. The cooperation aims to build up networks for measuring different physical/chemical parameters in order to search and study effects related to the occurrence of earthquakes. Actually the network is formed by ten receivers located: two in Italy, Romania and Greece; one in Austria, Portugal, Cyprus and Georgia. The receivers, realized by an Italian factory, can measure with 1 min sampling rate the intensity of 10 radio signals in the band VLF (10-50 kHz) and LF (150-300 kHz). The data collected are transmitted every day to the server located at the Department of Physics of the University of Bari (Italy) that is the central node of the network. The different temporal trends (10 for each receiver) can be seen free in real time using the INFREP web site: infrep-eu.it, while the data bank is protected by username and password. At the purpose to reveal possible radio precursors the data are analyzed for discovering “anomalies”, that is not normal variations of the data trends. Generally, due to the different conditions of the ionosphere, the VLF/LF radio signals are less disturbed during the night than during the day. So, the analysis of the radio data is performed only on the night-time data. In INFREP the Wavelet spectra are used. Using the “Morlet function” the Wavelet transform of a time signal is a complex series that can be usefully represented by its square amplitude, i.e. considering the so-called Wavelet power spectrum. The power spectrum is a two dimensions plot that, once properly normalized with respect to the power of the white noise, gives information on the strength and precise time of occurrence of the various Fourier components which are present in the original time series. Generally, colour from blue to red

indicates increase in the power strength; so, red zones define anomalies. A software able to apply the Wavelet analysis on the radio data automatically at the end of each day has been planned and realized. The analysis is performed on the 20 days preceding each day; this day is indicated on the spectrum by a vertical white line; the part of the spectrum after the day is related to 15 days data without any frequency added to avoid border effects. At the moment the software operates on the night time data of four signals collected by each of the following receivers: Cyprus, Crete, Greece and L'Aquila (IT). The results obtained with the Wavelet analysis are protected in the INFREP web site by a further username and password.

On October 26, 2016 an earthquake with $Mw=5.9$ occurred in Central Italy, near Castelsantangelo village; after 4 days the main shock with $Mw=6.5$ occurred near Norcia small town. The two epicenters are 12 km far from each other and are located in the "sensitive" area of the INFREP network. Unfortunately, at the time of the earthquake, several receivers were out of service, so only the data from Cyprus receiver are available. Some days before the first earthquake two clear anomalies appeared one after the other in two of the ten signals, the intensity of which is collected with 1 min sampling rate by this receiver. The two signals are radiated by DHO transmitter (23.4 kHz) located in Rhauderfehn (Germany) and by ICV transmitter (20.27kHz) located in Sardinia (Italy). The 5th Fresnel zones of the radio paths brush the border of the Dobrovolsky area of the previous main shock. The anomalies seem to move in the same direction of the two epicenters.

On July 20, 2017 a strong ($Mw=6.7$) earthquake occurred offshore, near the coast of Turkey and Kos island (Greece); on August 8 an earthquake with $Mw=5.0$ occurred practically in the same zone. The focal depth was 10 km for both the events. The epicentres are inside the "sensitive" area of the INFREP network. On both the occasions, evident pre-seismic disturbances were pointed out in the DHO (23.4 kHz) signal collected by the Cyprus receiver. All the anomalies here presented, were revealed by the on-line warning system based on the Wavelet analysis, planned and realized in the frame of the INFREP cooperation.

The new algorithm for the complex modeling of seismoionospheric coupling (SIC)

P.F. Biagi¹, V.V. Grimalsky², A. Gritsay³, V.N. Fedun⁴, A. Krankowski⁵, Yu.G. Rapoport³, A. Rozhnoi⁶, M. Solovieva⁶

¹*Dept. of Phys., Univ. of Bari, Bari, Italy* ²*Autonomous Univ. of State Morelos (UAEM) Cuernavaca, Mor., Mexico* ³*Phys. Faculty, National Taras Shevchenko Univ. of Kyiv, Ukraine* ⁴*University of Sheffield, UK* ⁵*Geodyn. Res. Lab., Univ. of Warmia and Mazury, Olsztyn, Poland* ⁶*Institute of Physics of Earth, RAS, Moscow, Russia*

I. The algorithm and model

We are developing a new and general model of SIC [1-3] as a part of the coupling in the system “Lithosphere-Atmosphere-Ionosphere-Magnetosphere (LAIM/MIAL)”. An important features of a rather general model of SIC will be (1) Including the nonlinearity and the results of an active acoustic experiments into acoustic model and new quasistatic/electromagnetic model of SIC using the new method of “successive electrostatic-quasistatic-electromagnetic/MHD approximations-equivalent external sources (EQUEMES)” [4, 5], (2) Inclusion a possibility of targeting coherent-incoherent influence on the atmosphere-ionosphere and mosaic sources of acoustic and electromagnetic sources, (3) In the perspective, interference between Acoustic and Electromagnetic channels of SIC including the feedback and “trigger effects” and inclusion of the convection and hydration. It is shown that the set of incoherent acoustic pulses with the different but close frequencies (in particular, around 1 Hz) penetrate from the ground level to the altitudes of the ionospheric E region better, than a single pulse with the sum intensity, due to nonlinearity, diffraction and losses. This result is important for the understanding the mechanism of acoustic SIC channel and developing possible ways of artificial influence on the ionosphere. The details of the EQUEMES, perturbations of electron concentration and VLF waveguiding propagation modeling are presented. The new model of “Earth radius-scale” vortex MHD structures in the ionosphere is developed.

II. Results of modeling based on the proposed algorithms and signal processing

(a) Perturbations of electron concentration and the model of “Two Earths”

Perturbation of electron concentration and TEC [1, 6] modeling can be based on the equation for the electron concentration with proper boundary conditions, and then integration over an altitude. First, the electric field should be determined. In the case of wave approach, an upper boundary condition incorporates outgoing radiated waves. In the electrostatic approximation, we avoid commonly accepted upper boundary conditions $d\varphi/dz' = 0$ used somewhere on the magnetic field line field, where z' is the coordinate along the field line, because such a condition corresponds to $\sigma \rightarrow \infty$, where σ is the conductivity. Instead of this, we applied the conditions $\varphi = 0$ at $z = 0$ and at the magneto-conjugate point, if magnetic field line is closed. To mimic this condition qualitatively, we used the model of the “Two Earths” while the magnetic field lines are straight, they start at the “first Earth” and finish at the “second Earth”, similar to the regions in the neighbourhood of the first and second conjugate points, respectively. External current has been taken in the form

$$\operatorname{div}(\vec{\sigma} \vec{\nabla} \varphi) = \operatorname{div} \vec{J}^{ext}; \quad \vec{J}^{ext} \equiv J_z = J_o \times e \chi p \left[-\left((x - L_x/2)/x_q \right)^2 - \left((y - L_y/2)/y_q \right)^2 \right]; \quad x_q \square y_q \sim 100 \text{ km};$$

$J_o \sim 1 \text{ mKA/m}^2$. The modeling demonstrates that in the case of the closed field line, the penetration of the electric field from the lower atmosphere to the ionosphere is much stronger than for the closed field line. Electric field of the order of a few mV/m at the ionospheric altitudes $z = 250$ km have been obtained for the dynamical processes. Respectively, variations of the electron concentration and TEC could reach a few percent. Accounting for a possibility of the ionosphere plasma instabilities, such as, f.e. Rayleigh-Taylor instability, the value of TEC variations could reach few dozens of percent, which corresponds to the results of the observations before the strong earthquakes.

(b) Perturbation of the characteristics of VLF signal in the waveguide “Earth-Ionosphere”

The perturbation of the phases and amplitudes of electromagnetic waves (EMW) in VLF range in the waveguide “Earth-Ionosphere” have been evaluated qualitatively on the basis of the method for the derivation of the nonlinear evolution equations in layered structures (NEELS). The new analytical-numerical algorithm for VLF modeling in the Earth-Ionosphere waveguide is proposed, which includes (1) modeling the excitation and propagation of VLF waves in the waveguide “Earth-Ionosphere” using two approaches: one based on the determination of eigenmodes of the waveguide and the other one based on a beam approximation; special upper boundary conditions, based on the condition of a radiation and

determination of an equivalent tensor impedance boundary conditions, (2) determination of the perturbations of the characteristics (phases, amplitudes and polarizations) of EMW in the waveguide “Earth-Ionosphere” due to (seismogenic) inhomogeneity in the ionospheric plasma. It is shown numerically that the beam and eigenmode approaches to VLF waveguide propagation correspond to each other.

(c) An influence on the ionosphere due to AGW generated in the lower atmosphere

Such an influence is described by the models of (1) linear AGW packet in the ULF range of the seismogenic origin in the presence of the ionospheric Rayleigh-Taylor instability and (2) nonlinear AGW transformed into the ionosphere from the sound waves, generated by a ground-based parametric sound generator. The results correspond qualitatively, in particular, to the data of the scattering of electromagnetic waves (in VLF (kHz) and HF (MHz) ranges) on the ionospheric irregularities, and the formation of the neutral and ion structures in the ionosphere [4].

(d) Signal processing and electromagnetic channel of seismoionospheric coupling

The results on experimental observations of Very Low Frequency (VLF) and Total Electron Content (TEC) will be presented. Preliminary analysis of variations in the ionosphere parameters near time of large earthquakes has been carried out. We have found that Shannon entropy has the clear peculiarity in the same period as residual amplitude of VLF waves in the Earth-Ionosphere waveguide i.e. 3-4 days prior to Vrancea (Nov. 22, 2014) earthquake [5]. VLF data have been analysed with use of Shannon entropy for time interval near a strong earthquake also in the Kuril region (magnitude 8.1) on 13 January 2007. TEC variations before and after Kumamoto earthquake (magnitude 7.0) on 15 April 2016 have been also studied. Such a combined approach opens the way for the complex analysis of the electromagnetic pre-seismic events including VLF, TEC and other electromagnetic and also AGW data. Such a model has been described in detail in a series of the publication in 1998-2014.

Besides modeling VLF in the Earth-Ionosphere waveguide, the proposed method for the modeling of the penetration of the EMW through the system LAIM in the ULF range included first the combination of the linear model for EMW in the system “Lithosphere-Atmosphere-Ionosphere” with the geometrical optics approximation for the electromagnetic waves in the active magnetosphere with the amplification of EMW in the radiation belts. Then this method was significantly developed for the modeling EMW in the metamaterial

concentrator in the IR range, which can be also applied for EMW in the LAIM system.

III. Conclusions

The complex algorithms for modeling the electric–photochemistry and AGW channels of seismoionospheric coupling have been proposed. The seismogenic modifications of electron concentration and the characteristics of VLF waves in the waveguide “Earth-Ionosphere”, and AGW influence on the ionosphere have been included in the algorithm. The numerical results of using new models of VLF propagation in the waveguide “Earth-Ionosphere”, penetration of the electromagnetic waves, and electrostatic field and AGW [6] from the lower atmosphere into the ionosphere, and data processing are presented. The proposed complex algorithm and the method of data processing can be used for investigation of the ionosphere as an interface between atmosphere and magnetosphere and ionospheric modification and wave processes in the ionosphere as a sensitive indicator of the influences on the ionosphere from “below” and “above”. Such influences can be caused by the presence of powerful sources in the system LAIM (connected, e.g. with earthquakes, hurricanes, thunderstorms, strong magnetic storms etc.). Our hypothesis is that the active synergetic system “Lithosphere-Atmosphere-Ionosphere” before strong earthquakes contains the set of active “quasioptical” lenses for EMW, placed in the lower atmosphere, mesosphere and ionosphere.

References

1. Pulinets, S. (2012), Low-Latitude Atmosphere-Ionosphere Effects Initiated by Strong Earthquake Preparation Process, *Intern. J. Geophys.*, 2012, Art. ID 131842, 14 pp.
2. Sorokin, V., V. Chmyrev, and M. Hayakawa, Electrodynamic Coupling of Lithosphere-Atmosphere-Ionosphere of the Earth, Nova Science Pub. Inc, 326p, 2015.
4. Rapoport, Yu. G., O. K. Cheremnykh, V. V. Grimalsky , Yu. A. Selivanov e.a. (2014), Ionosphere as a Sensitive Indicator of Powerful Processes in the Lower Atmosphere/Lithosphere, Artificial Acoustic Influence and Space Weather, In: *EMSEV 2014, Konstancin Jeziorna, Poland, on September 21–27, 2014, Conf. Paper book*, 4 Pp.
5. Solovieva M., Rozhnoi A., Fedun V., Schwingenschuh K., Hayakawa M., Ann. Geophys., Ionospheric perturbations related to the earthquake in Vrancea area on November 22, 2014, as detected by electromagnetic VLF/LF frequency signals, 58, 5, 2015, A0552
6. Rapoport, Yu.G., Cheremnykh O.K., Koshevoy V.V., Melnik M.O., Ivantyshyn O.L., Nogach R.T., Selivanov Yu.A., Grimalsky V.V., Mezentsev V.P., Karataeva L.M., Ivchenko V.M., Milneovsky G.P., Fedun V.N., Tkachenko E.N. Ground-based acoustic parametric generator impact on the atmosphere and ionosphere in an active experiment, *Ann. Geophys.*, 2017, V. 35, P. 53–70.

Disturbances in the ionosphere above seismic and thunderstorm areas - Swarm satellite registrations

J. Błęcki¹, J. Słomiński¹, R. Wronowski¹, E. Słomińska², R. Haagmans³

¹*Space Research Centre PAS, Warsaw, Poland, e-mail:jblecki@cbk.waw.pl;* ²*OBSEE, Warsaw, Poland , e-mail: evvaes@icloud.com;* ³*ESTEC Noordwijk, Netherlands, e-mail: Roger.Haagmans@esa.int*

The observation of the magnetic field, electron density and temperature variations in Ultra and Extremely Low Frequency (ULF/ELF) registered by Swarm satellite in the ionosphere over the seismic and thunderstorm areas will be presented.

Swarm is a constellation of three satellites to measure the Earth's magnetic field and identify the sources of its variations. This mission consists of the three identical Swarm satellites (A, B, and C), which were launched on 22 November 2013 into a near-polar orbit. Swarm A and C form the lower pair of satellites flying side by side (1.4° separation in longitude) at an altitude of about 470 km (inclination angle is equal to 87.30°), whereas Swarm B is cruising at higher orbit of about 520 km (inclination angle is equal to 87.75°). They are equipped with a set of six identical instruments - absolute scalar magnetometer, vector field magnetometer, star tracker, electric field instrument, GPS receiver, and accelerometer (Olsen et al. 2013). Further we use data from vector field magnetometer to study magnetic field variations and Langmuir probe (being a part of electric field instrument) to discuss the topic of our studies.

The magnetometers installed on-board of Swarm satellites measure main magnetic field with sampling rate 50Hz (3 components and absolute value). On this way, we are looking for the ionosphere effects associated with seismic and thunderstorm activity, that are mainly seen in the variations of the electromagnetic fields in very broad frequency range from fraction of Hz up to several MHz. The registrations performed by the Swarm satellites limits our studies only to very low frequencies called ULF (ultra-low frequencies up to single Hz) and ELF (extra low frequencies). The frequency of 50Hz gives theoretically the possibility to study variations up to 25Hz, but the filter inside the instrument limits this range to 15 Hz.

Next problem of our studies is related to the extremely small values of these variations (typically fraction of nT) in comparison with the main geomagnetic field measured in tens thousands of nT. Their observation requires sensitive magnetometers for the ac component of the magnetic field and carefully selected methods of signal analysis. The use of the vector

field magnetometer on board Swarm, intended for observation of main geomagnetic field, requires application of special filtering techniques.

The used techniques gives δB_i residuals retrieval from the measured signal for three B components. Thus, δB_i is obtained as a difference between measured signal and computed best fit. In the next step FFT is applied, giving power spectrum for each component and intensity of the B field residuals, in the frequency range up to 25 Hz.

An example of the magnetic field variations spectra and changes of the electron concentration in the vicinity (around 600km) of the Vrancea earthquake epicenter 4 days before this event is shown in Fig.1 (Stanica et al.2018) . The effect presented in this case is very weak in comparison to the effect reported from DEMETER registration (Parrot et al. 2006; Błęcki et al. 2011), but clearly seen. The spectra have a maximum in the lowest part of the frequency range and correspond to the range below the oxygen ions O⁺ gyro-frequency which is of the order of 34 Hz. It can be associated with Alfvén waves.

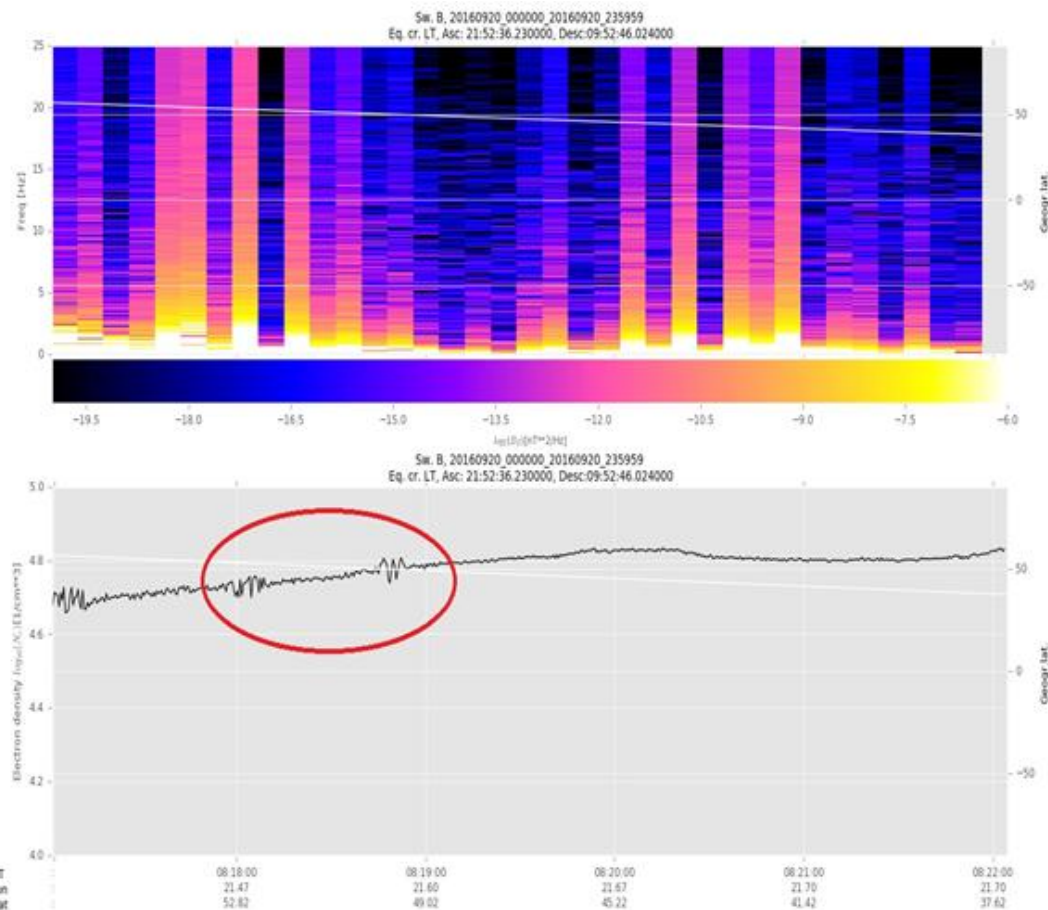


Fig.1 The spectra of the magnetic field variations (upper panel) and electron concentration registered by Swarm B satellite in the vicinity of the Vrancea zone on September 20.

Fig. 2 presents spectra of the magnetic field variations and electron concentration taken on September 23 (one day before the discussed earthquake) from half orbit crossing the Vrancea

zone.

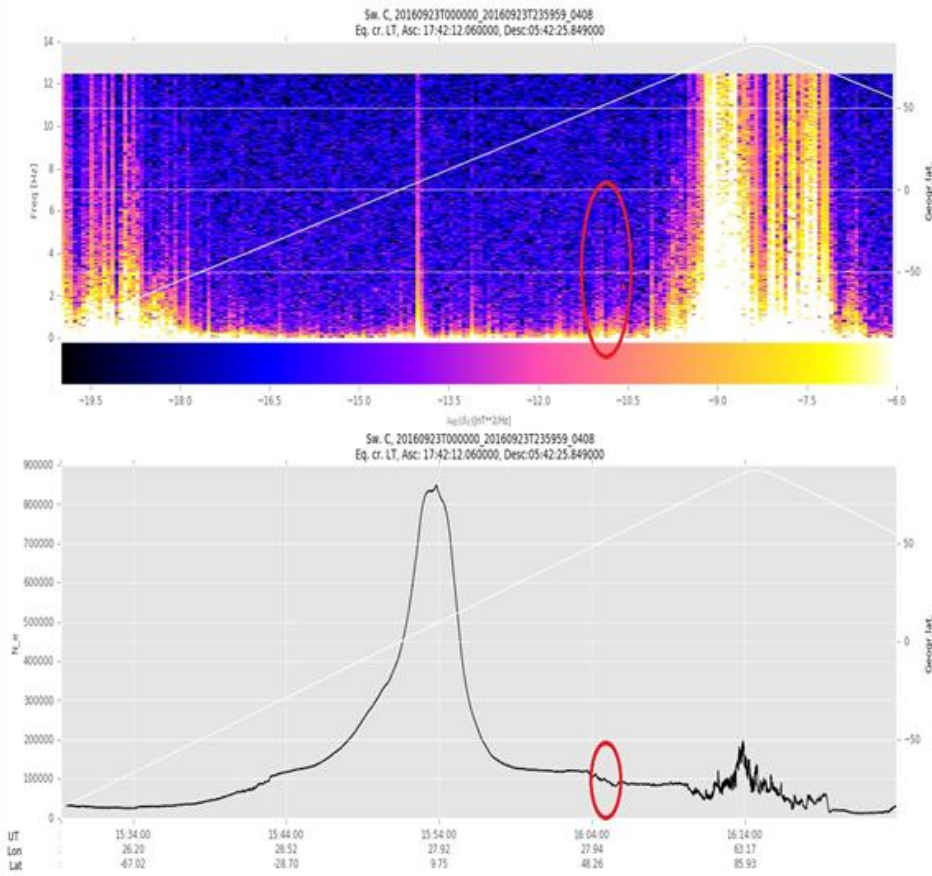


Fig.2 The same as in Fig.1, but for the September 23 and taken for entire half orbit crossing area in vicinity of the Vrancea zone.

One can see strong effects associated with high latitude regions (auroral oval, ionospheric through) in comparison with the weak variations in the vicinity (distance about 500km) of the epicenter. Closest vicinity was at 16:04UT. The disturbances are marked by red ellipses in Fig.2.

The disturbances in the ionosphere over the thunderstorm area in central Africa are presented in Fig.3 for comparison.

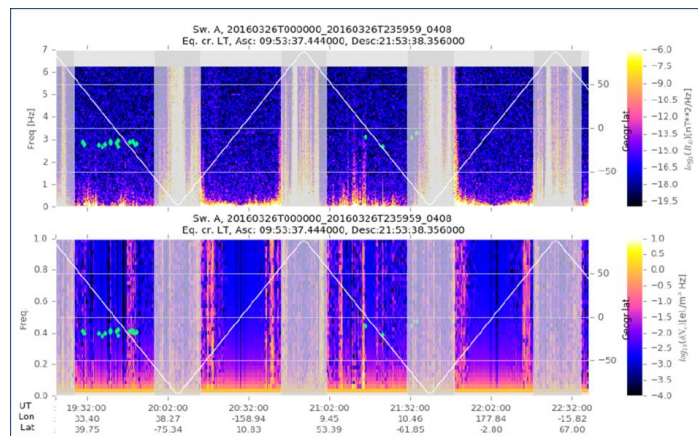


Fig.3 Time - frequency dynamic spectrograms (δBE - top panel, δNe - bottom panel) for selected

passes of Swarm A over active thunderstorm in Africa. Dynamic spectra for regions with latitudes greater than 55° N/S are masked.

References

- Błęcki J, Parrot M, Wronowski R (2011) Plasma turbulence in the ionosphere prior to earthquakes, some remarks on the DEMETER registrations, JAES, 41:450–458. doi:10.1016/j.jseae.2010.05.016.
- Olsen N, Friis-Christensen E, Floberghagen R, Alken P, Beggan CD, Chulliat A, Doornbos E, Teixeira da Encarnacao J, Hamilton B, Hulot G, van den IJssel J, Kuvshinov A, Lesur V, Lühr H, Macmillan S, Maus S, Noja M, Olsen PEH, Park J, Plank G, Püthe C, Rauberg J, Ritter P, Rother M, Sabaka TJ, Schachtschneider R, Sirol O, Stolle C, Thebault E, Thomson AWP, Tøffner-Clausen L, Velimsky, J, Vigneron P, Visser P N (2013) The Swarm Satellite Constellation Application and Research Facility (SCARF) and Swarm data products. Earth Planets Space, 65:1189–1200, doi:10.5047/eps.2013.07.001.
- Parrot M, Berthelier JJ, Lebreton JP, Sauvaud JA, Santolik O, Blecki J (2006), Examples of unusual ionospheric observations made by the DEMETER satellite over seismic regions. Physics and Chemistry of the Earth, 31: 486–495.
- Stanica D.A., D.Stanica, J.Błęcki, T.Ernst, W.Jóźwiak, J.Słomiński, Pre-seismic geomagnetic and ionosphere signatures related to the Mw5.7 earthquake occurred in Vrancea zone on September 24, 2016 Acta Geophysica 2018, <https://doi.org/10.1007/s11600-018-0115-4>.

Acknowledgments

This work was supported by grant NCN 2017/27/B/ST10/02285. We express our gratitude to ESA for access to Swarm data.

A study of the correlation between hazard of large aftershocks and GPS TEC measured after the main shock

Y. Chen¹, J.Y. Liu²

¹*Institute of Statistics, National Central University, Jhongli, Taoyuan, Taiwan, ychen5325@gmail.com;* ²*Institute of Space Science, National Central University, Jhongli, Taoyuan, Taiwan, tigerjyliu@gmail.com*

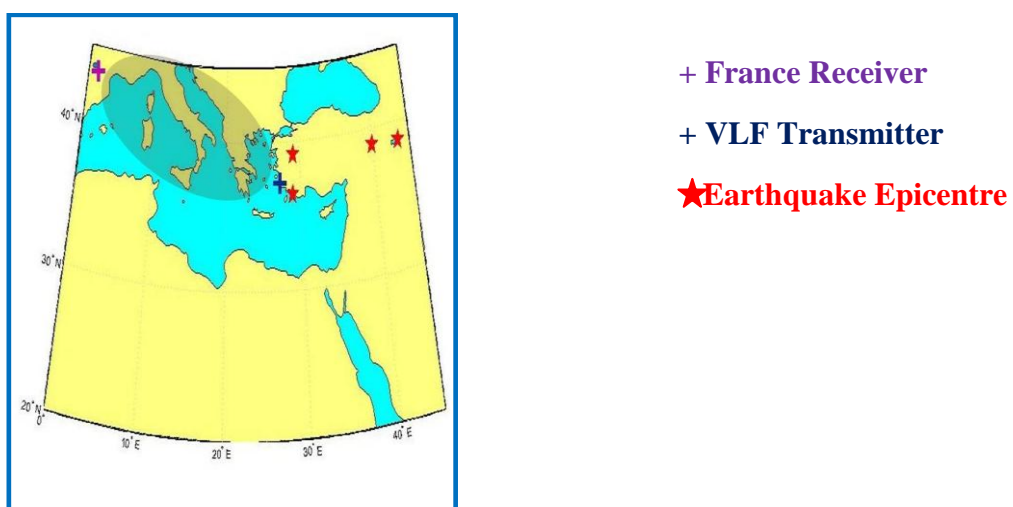
The Reasenberg-Jones (RJ) model is conventionally used to describe the time-magnitude hazard of large aftershocks. The maximum likelihood (ML) estimated RJ model is then obtained based on the aftershocks occurred within a short time after the main shock in a study region. Based on the ML estimated RJ model, the probabilities of short-term large aftershocks in the study region are finally computed. We explore herein the correlation between the aftershock probability and the GPS TEC measured daily after the 1999 Mw7.6 Chi-Chi, Taiwan, earthquake and 2008 Mw7.9 Wenchuan, China, earthquake, respectively. We also investigate how well the RJ model-based daily forecast can be improved by incorporated with the associated GPS TEC measurements.

Investigation of Very Low Frequency range of radio waves for the sub-ionospheric perturbations associate with Turkey earthquakes

Su. Choudhary¹, A.K. Gwal², G. Lather³, R. Gour⁴, J. Lohiya⁵

¹CESSS, Rabindranath Tagore University, Raisen, India, csuryansh@gmail.com; ²CCESSS, Rabindranath Tagore University, Raisen, India, ashok.gwal@gmail.com; ³Babamastnath University, Rohtak, India, glather143@gmail.com; ⁴Scope College, Bhopal, India, 4roshnigour09@gmail.com; ⁵Saduvavani College, Bhopal, India, jaish_lohia@yahoo.co.in

Investigation of Sudden Ionospheric Disturbances (SID) is being carried out by using Very Low Frequency (VLF) data from SID monitoring station of Bafa (latitude 37.24° N, longitude 27.19° E) at 23.4 kHz received at France with sampling rate is 10 sec. The radio waves are extensively used to study of Seismo-ionospheric phenomena which may possibly associate with four major earthquakes in the Turkey region. We analyse the trend of VLF signal for the whole year and compute the sunrise and sunset terminator time from it. We observe night-time fluctuation during the processes of earthquake preparation over the earthquake epicentres in the Turkey Anatolian block. We calculate the total energy accumulation by all those earthquakes for a single day and compute the effective magnitude of all the earthquakes for that day which behaves as a single quake. We computed a cross correlation between trend from the night-time fluctuation value with effective magnitude of earthquake and found that the unusual fluctuations in VLF signal strength are well correlated with earthquake magnitude and the fluctuation is maximum on few days prior to earthquake events.



Fresnel Zone along with earthquake epicenters

Development and assessment of a robust GPS-TEC data analysis (RST_{TEC}) for the identification of ionospheric perturbations possibly related to impending earthquakes: the case of L'Aquila (April 6th, 2009, M_w=6.1) earthquake.

R. Colonna¹, V. Tramutoli¹

¹*University of Basilicata, Potenza, Italy, r.robertocolonna@gmail.com;*

This work aims to propose a new approach for the detection of anomalous behaviours of the Total Electron Content (TEC) parameter in ionosphere, possibly associated to impending strong earthquakes.

The new approach proposed is defined RST_{TEC} because based on the general approach Robust Satellite Technique (RST; Tramutoli, 1998; 2005; 2007) but reformulated in order to be applicable to the TEC measurements.

The TEC measurements used in the analysis are recorded by the Global Positioning System (GPS) satellite constellation.

As first application, the RST_{TEC} approach is employed on the case study of the 2009 L'Aquila earthquake (Italy).

The focus of the approach is to compute a set of values named Δ_{TEC} in the 15 days before the earthquake, in the geographical region of the earthquake and at regular time intervals. The Δ_{TEC} values are given from the differences between the measured VTECs and their “15-day moving medians” (Liu et al., 2000, 2001, 2004). As usual, the 15-day moving medians are calculated in the same time slot and geographic area of the value under investigation.

Once this set is obtained, other sets of Δ_{TEC} are calculated in the same way and in the same days, but during the previous years. These sets are used as reference values.

In this way is possible to compare every single time slot of every single day under investigation with a reference value (in the specific case the mean) computed by using a significant sample of values related to the same time slot and to the same period of the year of the value investigated.

In this work result achieved in the case of L'Aquila (April 6th, 2009, M_w=6.1) earthquake will be discussed.

References

- Liu J. Y., Chen Y. I., Pulinet S. A., Tsai Y. B. and Chuo Y. J. 2000, "Seismo-ionospheric signatures prior to M \geq 6.0 Taiwan earthquakes", *Geophys. Res. Lett.*, 27, 3113–3116.
- Liu J. Y., Chen Y. I., Chuo Y. J., and Tsai H. F., 2001, "Variations of ionospheric total electron content during the Chi-Chi earthquake", *Geophys. Res. Lett.*, 28, 1383–1386.
- Liu J. Y., Chuo Y. J., Shan S. J., Tsai Y. B., Chen Y. I., Pulinet S. A. and Yu S. B., 2004, "Pre-earthquake ionospheric anomalies registered by continuous GPS TEC measurements", *Ann. Geophys.*, 22, 1585–1593.
- Tramutoli V., 1998, "Robust AVHRR Techniques (RAT) for environmental monitoring: theory and applications." In: Cecchi G. and Zilioli E. (eds), *Proc. SPIE, Earth Surf. Remote Sens. II*, Barcelona, Spain, Vol. 3496, pp. 101-113.
- Tramutoli V., 2005, "Robust Satellite Techniques (RST) for natural and environmental hazards monitoring and mitigation: ten years of successful applications." In: *Proc. 9th Int. Symp. Phys. Meas. Signatures Remote Sens.*, Beijing, China, XXXVI, pp. 792-795.
- Tramutoli V., 2007: "Robust Satellite Techniques (RST) for natural and environmental hazards monitoring and mitigation: theory and applications.", in: *Proc. Int. Workshop Anal. Multi-Temporal Remote Sens. Images (MULTITEMP)*, Louven, Belgium, pp. 1-6.

Observation of the Ionospheric turbulence modulation by intense seismic activity

M.E. Contadakis¹, D.N. Arabelos¹, G.S. Vergos¹

¹*Department of Geodesy and Surveying, Aristotle University of Thessaloniki*

According to the well-known Lithosphere Ionosphere Coupling (LAIC) mechanism, tectonic activity during the earthquake preparation period produces anomalies at the ground level which propagate upwards in the troposphere as Acoustic or Standing gravity waves. These Acoustic or Gravity waves affect the turbidity of the lower ionosphere, where sporadic Es-layers may appear too, and the turbidity of the F layer. Subsequently the produced disturbance starts to propagate in the ionosphere's waveguide. Thus observing the frequency content of the ionospheric turbidity in a well extended area, in space and time, around an earthquake event we will observe a decrease of the higher limit of the turbidity frequency band, as a result of the higher damping rate of the higher frequencies, as we move away from the event site. In this article we review the repeated observational accordance to these theoretical explanation, on the occasion of strong earthquakes.

Some aspects of low-latitude upper atmosphere response to impact from above and below

A. Depueva¹, V. Depuev², Yu. Ruzhin³, M. Devi⁴, A.K. Barbara⁵

¹*Pushkov Institute of Terrestrial Magnetism, Ionosphere and Radio Wave Propagation, Russian Academy of Sciences (IZMIRAN), Moscow, Troitsk, 108840, Russia, e-mail:depueva@izmiran.ru;* ²*Pushkov Institute of Terrestrial Magnetism, Ionosphere and Radio Wave Propagation, Russian Academy of Sciences (IZMIRAN), Moscow, Troitsk, 108840, Russia, e-mail:depuev@izmiran.ru;* ³*Pushkov Institute of Terrestrial Magnetism, Ionosphere and Radio Wave Propagation, Russian Academy of Sciences (IZMIRAN), Moscow, Troitsk, 108840, Russia, e-mail:ruzhin@izmiran.ru;* ⁴*Department of Physics, Gauhati University, Guwahati 781014, Assam, India, e-mail: md555gu@gmail.com;* ⁵*Department of Physics, Gauhati University, Guwahati 781014, Assam, India, e-mail: md555gu@gmail.com*

Ionospheric disturbances caused by diverse effects (in most cases, phenomena on the Sun and in the magnetosphere) have been studied for many decades. At the same time, the geographical position of the observation point is always taken into account, since the nature and characteristics of various physical processes in the ionospheric plasma depend on it. It is known that such effects from above show themselves in different ways at ionospheric heights, depending on the latitude and longitude of the observation site. For the same reason, the response in the ionosphere due to the effect from below (earthquake, eruption, tsunami, thunderstorm, etc.) is reasonable to consider taking in mind the location of the observation point and relative position of the observation point and the source of the disturbance.

The low-latitude ionosphere (belt of $\sim 30^\circ$ width to the north and south relative to the magnetic equator) has a number of special features due to the specific geometry of the geomagnetic field. They have long been well known [Fejer, 1997]. There is a unique latitude distribution of the electron concentration in the F (NmF2) region and the midday "bite-out" in the daily variation of NmF2, called the equatorial ionospheric anomaly. At altitudes of 90–110 km above the magnetic equator, in the daytime, the presence of an equatorial current jet of width $\sim 5^\circ$ is recorded. The horizontal (W-E) electric field of the electrojet and the geomagnetic field perpendicular to it (N-S) could cause the plasma to rise upward. This phenomenon is called a "fountain" effect.

Relatively long ago, the main manifestations of strong earthquakes and processes of their preparation in the large-scale structure of the low-latitude ionosphere, which differed from those observed in the mid-latitude ionosphere, were also observed [Depueva and Rotanova, 2001; Devi et al., 2012; Namgaladze et al., 2018]. Among them, one can note a

predominantly observed decrease (not an increase) of NmF2 on the eve of earthquakes; the dependence of the observed effects on the location of the epicenter relative to the magnetic equator and the observation point, etc. The listed features of the modification of the background ionosphere still require further study, additions and refinements.

The question of the behavior of the inhomogeneous structure of the low-latitude ionosphere on the eve of earthquakes remains a little studied area until now. It is known that the morphological features of low-latitude inhomogeneities in the E and F regions of the ionosphere also differ significantly from those of the mid- and high-latitude ionosphere. For example, F-spread – the manifestation of small-scale inhomogeneities on the ionograms of vertical sounding – is a regular phenomenon observed in low latitudes at night. The rarest cases of diurnal equatorial F-spread or the absence of F-spread in night conditions can serve as evidence of an irregular effect from above or below, so their study is of interest. Molchanov et al. [2004] have shown that one of the causes of ionospheric irregularities generation may be processes preceding earthquakes.

According to ground and satellite measurements, we analyzed cases of unusual behavior of F-spread in low latitudes and made assumptions about the possible causes of such anomalies. Among them, not only earthquakes, but also other impacts from above (for example, geomagnetic storms), and from below (for example, the passage of the atmospheric front) are presented.

Acknowledgement

The authors acknowledge with thanks the financial support received from the DST, India and RFBR, Russia for partial support received by them through Grant No 17-55-45094 IND_a.

Reference

- Fejer, B.G., 1997. The electrodynamics of the low-latitude ionosphere: Recent results and future challenges. *J. Atmos. Solar-Terr. Phys.*, 59, pp. 1456–1482.
- Depueva, A.Kh. and Rotanova, N.M., 2000. Modification of the low-latitude and equatorial ionosphere before earthquakes. *Geomagnetism and Aeronomy*, 40, pp. 50–54.
- Devi, M., Sarma, A.J.D., Kalita, S. et al., 2012. Adoptive techniques for extraction of pre-seismic parameters of Total Electron Content (TEC) at anomaly crest station. *Geomatics, Natural Hazards and Risk*, 3, pp. 193–206.
- Namgaladze, A., Karpov, M., Knyazeva, M., 2018. Aerosols and seismo-ionosphere coupling: A review. *J. Atmos. Solar-Terr. Phys.*, 171, pp. 83–93.
- Molchanov, O.A., Akentieva, O.S., Afonin, V.V., Mareev, E.A., Fedorov, A., 2004. Plasma density-electric field turbulence in the low-latitude ionosphere from the observation on satellites; possible connection with seismicity. *Phys. Chem. Earth.*, 29, pp. 569–577.

Atmospheric waves as Earthquake Precursive Index

M. Devi¹, A.K. Barbara¹, A. Depueva²

¹*Department of Physics, Gauhati University, Guwahati, Assam, India;* ²*Pushkov Institute of Terrestrial Magnetism, Ionosphere and Radio Wave Propagation, Moscow, 142190*

Amongst a number of adopted parameters in Earthquake (EQ) studies using EM techniques, the ionization density, Total Electron Content (TEC), VLF /VHF propagation characters are though well adopted, the atmospheric waves as precursive indices are still a debated exercise because of the complex modes of their generation and propagation. However complex the problem be , it is important to understand the processes of growth of such waves in the atmosphere triggered by EQ induced activities , because they could redistribute their momentum and energy in the environment leading to significant modification in the propagating media and may thus provide insight in to the coupling dynamics' between lithosphere to upper atmosphere. Under this background the work aims at to identify features of EQ time waves and then to examine their mode of propagation from troposphere to ionosphere and finally to explore their sources of origin. The paper started with presentation of sloping structures at the lower atmospheric heights detected prior to an EQ by Sound Detection and Ranging (Sodar) set up of Gauhati ($26^{\circ}10'N$, $91^{\circ}45'E$). These waves with periodicity of 20 min to 30 min appeared at the lower atmosphere when there was a sudden break down of night time inversion layer, a few hours prior to the EQ with epicentre near Gauhati. These structures identified as phase components of the waves also have a group feature with periodicity of about 1.5 hrs. Meteorological processes in the troposphere being strong sources leading to such phenomena which are in general associated with gravity waves, the relevant parameters like temperature, wind profiles & shears are analyzed in search of their identification. Finally the value of Froude number (Fr) is calculated by utilizing wind velocity and height at which temperature drops by half from its surface value. The calculated value of $Fr > 1$, identifies an atmospheric status where gravity wave can sustain in the background environment. The paper then extended the analysis to upper atmosphere and examines the possible development of EQ triggered waves at this altitude through GPS Total Electron Content (TEC) data monitored at Gauhati. In this connection TEC and Scintillation (1.5GHz) profiles are analyzed along with path /azimuth positions of different satellites coming in to the Field Of View (FOV) of the trans receiving geometry, for a number of EQ

events with $M > 5$. The analyses reveal that a few satellites (with specific PRN) appear beyond the normal FOV prior to an EQ and significantly azimuthal status of these satellites identifies the position of the epicentre. The TEC and scintillation magnitudes obtained from such specific satellites are observed to be relatively large and that the TEC/ Scintillation profiles are modulated by waves of periodicity about 1 to 2 hours embedded with small scale structures. These situations are shown to have association mainly with EQ modified tropospheric Radio Refractive Index (RRI) enhancing Effective Earth Radius by 18% to 20 % and that the undulations embedded in TEC profiles have origin at the troposphere. The propagation modes of the waves from lower to upper atmosphere and their parameterization are made on the basis of the lower atmospheric convective status, wind shear and its strength at the epicentre locations. The Lithospheric- Tropospheric-Ionospheric (LTI) coupling mode and topographic role in generations of such waves are brought in to the ambit of discussions.

Acknowledgement

The authors acknowledge with thanks the financial support received from the DST, India and RFBR, Russia for partial support received by them through Grant No 17-55-45094 IND_a.

Perturbation features imprinted on ionosphere by successive clusters of strong earthquakes with epicenters in the East-West Pacific zone: Role of atmospheric coupling dynamics

M. Devi¹, S. Patgiri², A.K. Barbara³, V. Depuev⁴, A. Depueva⁴, Yu. Ruzhin⁴

¹*Department of Physics, Gauhati University, Guwahati, Assam, India;* ²*Department of Physics, Gauhati University, Guwahati, Assam, India;* ³*Department of Physics, Gauhati University, Guwahati, Assam, India;*

⁴*Pushkov Institute of Terrestrial Magnetism, Ionosphere and Radio Wave Propagation, Moscow, 142190;*

The paper presents a few significant features imprinted on the ionosphere in an unique seismic environment when earthquakes ranging from 7.1 to 8.2 magnitudes occurred within two weeks period, over the Pacific zone. Amongst the events the important cases considered in this paper are earthquakes of the Chile (M=7.7 and M= 8.2), New Guinea (M=7.1) and Solomon Island (M=7.6) that occurred within April 1st to April 13th, 2014 covering 20° S to 6°S and longitude zone 150°E to 70°W. The occurrence of cluster of earthquakes prior to the events is the specialty to the cases considered here. The main data sources for the study are Global Total Electron Content (TEC) and the parameters from GPS observations taken at Guwahati, at a location in the Appleton anomaly crest region, especially when this region falls within EQ preparatory processes. The analyses show strong development of anomalous density , (more than 50% from its average values) , from a month prior to the occurrence of the major earthquake series , covering the entire Pacific zone with intense density specially along the fault lines encompassing Chile ,Solomon island and New Guinea . The Earthquake time Equatorial Anomaly (EEA) is well developed even during night hours widening the anomalous high density TEC environment from -20°N to 20°N over the longitude zone from 150°E to 70°W.

The abnormal ionization density magnitudes further indicate periodic oscillations of around 4/5 days maintaining a loose association with the cluster of earthquake events. The paper presents utilization of such features as predictor parameters for occurrence of a major earthquake. Further, to identify the epicentre positions, the GPS TEC data from Gauhati (this region comes within the EQ preparatory processes) are utilized along with azimuthal status of anomalous appearance of satellites beyond the normal Field Of View (FOV) of a trans-receiver pair. The electron content magnitudes as well as wave like undulating features of the TEC received from theses satellites are shown to have association mainly with EQ modified

tropospheric Radio Refractive Index (RRI) and that such waves have origin at the troposphere. The detailed variation of lower atmospheric structure constant LogCn^2 from 1km - 15 km is then analysed for identifying prime parameters of the lower atmosphere associating with an impending EQ. Structure constant variables being controlled by potential temperature and humidity, a drop in Log Cn^2 values by 13% to 14 % just prior to an earthquake indicates existence of a complex association between temperature and humidity in modifying tropospheric dynamics by seismic induced preparatory processes .

Finally, considering all the observed features i.e., (i) enhancement in TEC over the extended belt from 150°E to 70°W encompassing the EQ day along with cluster events , (ii) development of EEA covering $\pm 20^{\circ}$ N, (iii) anomalous appearance of satellites at the longitude zone of EQ epicentre and (ii) modification in RRI and Cn^2 , the paper explains how such changes prior to an earthquake lead to the enhancements in effective earth radius factor and hence in the FOV of the trans receiving pair. Along with this explanation, radon emission during EQ time from the lithosphere is also taken as a source to the modifications in atmospheric variabilities as well as in its conductivity. The modulation of the atmospheric electric field through conductivity changes and thereby generating environment for growth of Appleton type drift process even during night sector is invoked in the discussion. Effectiveness of such processes are substantiated through analysis of TEC parameters during EQ of similar magnitudes but in seasons (i.e. in solstices) when in general anomaly process is inactive. Lithospheric - Tropospheric - Ionospheric (LTI) coupling dynamics is put forward towards the explanations of the observed perturbations.

Acknowledgement

The authors M. Devi, A. K. Barbara, V. Depuev, A. Depueva, and Yu. Ruzhin acknowledge with thanks the financial support received from the DST, India and RFBR, Russia for partial support received by them through Grant No 17-55-45094 IND_a.

A tsunami early warning system using GNSS-TEC data

M. Kamogawa^{1,2}, T. Nagao², Y. Orihara^{1,2}

¹ Department of Physics, Tokyo Gakugei University, Tokyo, Japan, kamogawa@u-gakugei.ac.jp; ² Tokai University, Shizuoka, Japan

Tsunami-generated ionospheric plasma disturbances can be detected by measurement of the total electron content (TEC) between a satellite and its ground-based receivers in Global Navigation Satellite System (GNSS). TEC depression lasting for a few minutes to tens of minutes, i.e., tsunami ionospheric hole (TIH), is formed above the tsunami source area. According to Kamogawa et al. [*Scientific reports*, 2016], we showed the quantitative relationship between the maximum initial tsunami height and the TEC depression rate caused by the TIH. In addition, the largest TEC depressions appeared 10 to 20 minutes after the main shocks. This implies that the TIH measurement using the existing ground receiver networks could be used in an early warning system for near-field tsunamis. Applying our knowledge to space-based early warning system, we started developing the feasible warning system. As a real-time TEC data source, we used NICT Science Cloud service (sc-web.nict.go.jp) which provides real-time TEC data using 200 GPS receiver station data of GNSS Earth Observation Network System (GEONET), Japan. Once the large earthquake possibly accompanying tsunami is recognized through continuous monitoring earthquake early warning issued by the Japan Meteorological Agency, the derivation of 2-dimensional initial tsunami height distribution based on the NICT TEC data would be started. For estimating expected arrival tsunami height at the coast, we use the tsunami propagation Green's function calculated in advance. In the tremendous event, similar to the 2011 M9.0 Tohoku earthquake, our final target warning would be issued tentatively 10 minutes and precisely 23 minute after the mainshock. Although prototype of our system was already development, we will introduce our current results of space-based tsunami early warning system in the presentation.

Origin of Pre-seismic whistler wave intensity attenuation observed by DEMETER satellite

M. Kamogawa^{1,2}, T. Nagao², Y. Orihara^{1,2}, J.J. Berthelier³

¹*Department of Physics, Tokyo Gakugei University, Tokyo, Japan, kamogawa@u-gakugei.ac.jp;* ²*Tokai University, Shizuoka, Japan;* ³*LATMOS, Paris, France*

Statistical investigations using the in-situ VLF electric field data measured by DEMETER satellite have shown that a decrease of the VLF electromagnetic (EM) wave intensity around 1.7 kHz corresponding to the cut-off frequency of the Earth's-Ionosphere guide occurred within four hours before an earthquake with magnitude of more than 4.8 [Nemec et al, GRL, 2008]. This infers that the intensity decrease might be caused by the D-region height decrease in the ionosphere. To understand this phenomenon we analyzed whistler waves observed by DEMETER waveform electric field data in comparison with lightning energy data obtained by the world wide lightning location network (WWLLN). The whistler waves which travel through the ionosphere up to the satellite become good tracers for low altitude (in particular, D region) ionospheric disturbances which modifies absorption rate of the propagating EM waves. The whistler wave and parent-lightning concurrent measurements before the south Sumatra earthquake on March 2010. The event study showed that the whistler wave absorption up to a few dB a few hours prior to the earthquake was caused by a D-region electron density enhancement of about 20-30%.

D-region ionospheric precursors and its earthquake predictability

M. Kamogawa^{1,2}, T. Nagao², Y. Orihara^{1,2}, J.J. Berthelier³

¹*Department of Physics, Tokyo Gakugei University, Tokyo, Japan, kamogawa@u-gakugei.ac.jp;* ²*Tokai University, Shizuoka, Japa;* ³*LATMOS, Paris, France*

The intensity decrease of VLF electromagnetic waves observed by DEMETER satellite within 4 hours before 4.8 mainshock of global earthquakes (EQs) within 550 km epicentral distance (537 earthquakes in total) was statistically found by Němec et al. [2008; 2009] and Píša et al. [2013]. Our replicated analysis also showed that the electric field intensity of not only 1.7 kHz and but also the higher frequency decreased within 4 hours before $M \geq 4.8$ mainshocks, using the complete data set of the DEMETER, i.e., 6.5-year.data. To the contrary, the similar intensity decrease followed by the mainshock was also recognized. As the intensity decrease was also observed near the epicenter and in the large mainshock, this means that the causation between the intensity decrease and the EQ occurrence was found. In addition, the intensity decrease was caused by the D-region ionospheric disturbance, according to our other analysis. Thus, the precursor of D-region ionospheric electron density enhancement was statistically found. From our analysis, one can expect that an in-situ monitoring of VLF electromagnetic waves on the satellite will provide the EQ prediction.

Atmospheric Parameter Measurements for Earthquake Forecast at Kanto, Japan: Case studies for regional earthquakes and the 2018 Boso Slow-slip Event

H. Kojima¹, J. Omura^{2*}, C. Yoshino², K. Hattori², M. Shimo³, T. Konishi⁴, R. Furuya⁵, K. Ninagawa⁶, D. Ouzounov⁷

¹Graduate School of Science and Engineering, Chiba University, Japan; ²Graduate School of Science, Chiba University, Japan; ³Fujita Health University, Aichi, Japan; ⁴Ohyo Koken Kogyo Co., Ltd., Tokyo, Japan; ⁵Com System, Inc., Tokyo, Japan; ⁶Okayama University of Science, Okayama, Japan; ⁷Chapman University, US; *Now at Nippon Sogo Systems, Inc., Japan

The Ionospheric anomaly is one of the most promising precursory phenomena for large earthquakes. Lithosphere-Atmosphere-Ionosphere Coupling (LAIC) model has been proposed to explain these phenomena. To examine the possibility of the chemical channel of LAIC model through the monitoring of atmospheric electricity parameters, we have installed sensors for the atmospheric electric field (AEF), atmospheric ion concentration (AIC), radon concentration, radon exhalation quantity (REQ), and weather elements.

On May 17, 2018, an M5.3 earthquake with depth 50 km occurred at 7 km distance from the Asahi station. And, from around June 3, a slow slip event is started at the boundary of Philippine Sea plate and the North America Plate off the Boso Peninsula, where locates 40 km distance from Kiyosumi station. On June 12, an M4.9 earthquake with 15 km distance from Kiyosumi station. We observed that the ground Rn content increased and the atmospheric electric field decreased with these crustal phenomena. This is the observational fact of the chemical channel of LAIC.

To identify signals related to crustal activities such as earthquake and the slow slip event, changes caused by non-tectonic activities should be removed. In this aim, we performed Singular Spectrum Analysis (SSA) to the observed time series of the radon content and climatic parameters and investigated the correlation. Then we can discriminate radon variation influenced by climatic effects and estimate the Rn flux from the crust. Detailed results will be reported in our presentation.

Space weather and earthquakes

V. Novikov¹, Yu. Ruzhin², V. Sorokin², A.K. Yashchenko²

¹*Joint Institute for High Temperatures of Russian Academy of Sciences, Moscow, Russian Federation,
novikov@ihed.ras.ru*, ²*Pushkov Institute of Terrestrial Magnetism, Ionosphere and Radio Wave Propagation of
Russian Academy of Sciences, Troitsk, Moscow region, Russian Federation*

An overview of the studies of investigations of a possible impact of solar flares and geomagnetic storms on deformation processes in the Earth crust is presented. The problem of an influence of solar activity on the terrestrial processes has been considered for almost a century, its founder is A.L. Chizhevskiy, who in the 30-50th years of the last century pointed to the presence of synchronous variations of various processes in the different regions of the globe and connected these phenomena with an influence of variations of solar activity [1]. To date quite a large number of studies have been performed to find

A review of the work on the effect of solar flares and geomagnetic storms on deformation processes in the earth's crust is presented. The problem of the effect of solar activity on terrestrial processes has been considered for almost a century, its founder is AL. Chizhevsky, who in the 30-50 years of the last century pointed to the presence of synchronous variations of various processes in different regions of the globe and related it to the influence of variations in solar activity [1]. To date, quite a large number of studies have been performed to find the correlation between the Earth's seismicity and solar processes.

Results of these statistical studies are contradictory, some researchers found a direct correlation between the energy of earthquakes or their quantity and Wolf numbers [2-4], and others - anti-correlation, e.g. [5-6]. According to the studies of A.D. Sytinsky [2] there is a definite dependence of seismicity on the 11-year cycle of solar activity, which was verified by the experimental prediction of the general seismicity of the Earth and its specific regions. This author predicted the maximum manifestations of seismicity in 1963-1964, 1968-1969, 1974-1976, 1985, 1990, 1992, and 1995. He considered a distribution of the average annual total energy of earthquakes E_k and the annual numbers N_k of earthquakes of various magnitudes during 11-year cycle of solar activity for 1902-1977 period. The author noted a clear dependence of the Earth seismic activity on the phases of 11-year cycle of solar activity. High seismicity level is observed in the 1st, 3rd, and 6th year (with a probability of 0.99) after the maximum of solar activity. Nevertheless, there are opposite statements as well: 11-year cycles

of seismic activity have a significant negative correlation with cycles of solar activity and geomagnetic disturbances [5-6].

In addition, there is some skepticism in assessing the existence of such solar-terrestrial relations resulted in statistically significant seismicity variations, e.g. [7]. Nevertheless, practically all the mentioned conclusions (both optimistic and pessimistic) are based only on correlation analysis. Even when such analysis yields statistically significant results, the authors only assume that there is a possible triggering mechanism in the case of positive correlation, without attempts of understanding the physics of the possible relations, or provide the most general considerations [8]. For example, it was noted that earthquakes occur more often when the solar activity level drastically changes. During a solar flare radiation increases many times, which interacts with the Earth magnetosphere of the Earth resulted in its disturbance and occurrence of magnetic storm. The magnetic storms, in turn, may influence to the rotation speed of the Earth, intensity of telluric currents in the lithosphere that result in increase of stresses in the Earth crust [9]. Some researches, e.g. [10], connect the variations of seismic activity after solar flares with an increase of a number of cyclones that can act as a trigger due to sharp variations in atmospheric pressure during passage of their fronts over the earthquake source. Nevertheless, the estimations demonstrate that such variations are substantially lower than the level of stress variations due to lunar-solar tides whose influence on seismicity is still under discussion [11].

In the recent years a few papers were published where a hypothesis of triggering impact of geomagnetic field variations (sudden commencement storms) [12-15], as well as diurnal Sq-variations [16] was proposed. Particularly, results of statistical analysis obtained for different regions (Northern America, Central Europe, China, Japan) demonstrated an evident correlation between geomagnetic field variations and a number of earthquakes both for average diurnal cycle and for a long period of about 150 years. A hypothesis was proposed on a generation of additional stresses in the Earth crust due to the magnetic field variation [16].

At present a principal possibility of electromagnetic triggering of seismic events was verified [17] based on results of interdisciplinary research of an influence of powerful electromagnetic pulses on deformation processes in the Earth crust by the methods of statistical analysis, physical laboratory and numerical simulations, as well as field monitoring of the upper crust response to DC current injection into lithosphere including geoacoustic measurements in the wells, carried out during the last 20 years in the Institute of Physics of the Earth, Joint Institute of High Temperatures, Institute of Dynamics of Geospheres, Institute of Terrestrial Magnetism, Ionosphere, and Radio Wave Propagation, Research Station of

Russian Academy of Sciences and supported by Russian Foundation for Basic Research. New basic knowledge was obtained on the mechanisms of interactions of electromagnetic field and vibrations with rocks under subcritical stress state and on an influence of artificial electromagnetic fields in combination with natural impacts on the deformation processes in the Earth crust [17]. Along with this, it was shown [18] that solar flares can cause variations in the density of telluric currents in seismogenic faults comparable to current densities generated in the Earth crust by artificial pulse power sources used for active electromagnetic monitoring (MHD generators and electrical pulsed systems like ERGU-600). Consequently, the triggering of seismic events is possible not only by artificial sources of electric current, but also by ionospheric disturbances, such as powerful geomagnetic storms generated by solar flares. At present, various hypotheses have been proposed on generation of additional mechanical forces and stresses in the Earth crust [15, 19], on excitation of vibrations [20], and on electric stimulation of fluid migration into the fault zone [21] by external electric impacts. It should be noted that these hypotheses have only a phenomenological character without a detailed theoretical justification and experimental verification. New fundamental knowledge is needed on the mechanisms of interaction of the electromagnetic field and vibrations with rocks in the stress-strain state and on the influence of artificial physical fields in combination with natural geophysical fields on deformation processes in the Earth crust.

References

1. Chizhevsky A.L. (1976) Earth echo of solar storms. 2nd ed., Moscow, Mysl, 367 p. (in Russian).
2. Sytinsky A.D. (1987) Relationship of Earth's seismicity with solar activity and atmospheric processes. Leningrad, Gidrometeoizdat, 100 p. (in Russian).
3. Sytinsky A.D., Oborin D.A. (1997) Influence of perturbations of interplanetary medium on seismicity and atmosphere of the Earth, Geomagnetism and Aeronomy, 37, 2, 138-141.
4. Lotsinskaya, N. I. (1999), Relation of the Earthquake Global Energy to Solar Activity, Vestn. Kiev. Univ., Ser. Astron., 35, 45–50.
5. Shestopalov I.P., Smyrrenny L.N., Likin O.B. et al. (1995) Solar flares and seismic activity of the Earth // Annales Geophysic. V. 13. - Supp. 1.3. - Part 3. - P. 666.
6. Sobolev G. A., Shestopalov I.P., and Kharin E. P. (1998) Geoeffective Solar Flares and Seismic Activity of the Earth, Fiz. Zemli, 7, 85–89.
7. Love, J. J., and J. N. Thomas (2013), Insignificant solar-terrestrial triggering of earthquakes, Geophys. Res. Lett., 40, 1165–1170, doi:10.1002/grl.50211.
8. Georgieva K., Kirov B., Atanasov D.(2002) On the relation between solar activity and seismicity on different time scales, Journal of Atmospheric Electricity. 22, 3, 291-300.
9. Mazur I.I., Ivanov O.P. (2004) Dangerous natural processes. Moscow, Economics, 702 p. (in Russian).

10. Riccardi, U., J. Hinderer and J.-P. Boy (2007) On the efficiency of barometric arrays to improve the corrections of atmospheric effects on gravity data, *Phys. Earth Planet. Int.*, 161, 224-242.
11. Beeler, N. M., and D. A. Lockner (2003) Why earthquakes correlate weakly with the solid Earth tides: Effects of periodic stress on the rate and probability of earthquake occurrence, *J. Geophys. Res.*, 108(B8), 2391, doi:10.1029/2001JB001518, 2003.
12. Sobolev, G.A., Zakrzhevskaya, N.A., and Kharin, E.P. (2001) On the coupling of seismicity with magnetic storms, *Physics of the Solid Earth*, 11:62–72.
13. Zakrzhevskaya N.A., Sobolev G.A. (2002) On the seismicity effect of magnetic storms, *Izvestiya Physics of the Solid Earth* 38(4):249-261
14. Tarasov N.T., Tarasova N.V. (2002): The effect of geomagnetic storms on the seismicity//*Proc. of the 3rd International Workshop on Magnetic, Electric and Electromagnetic Methods in Seismology and Volcanology*, Moscow, Russia, 3-6 September 2002 (Institute of Physics of the Earth, Moscow), 206-208.
15. Sobolev G.A., Ponomarev A.V. (2003) *Physics of earthquakes and precursors*, Moscow, Nauka, 270 p.
16. Duma G., Ruzhin Yu. (2003) Diurnal changes of earthquake activity and geomagnetic Sq variations, *Natural Hazards and Earth System Sciences*. 3:171–177.
17. Zeigarnik V., Avagimov A., Novikov V., Rybin A., Schelochkov G., Bragin V., Sychev V., Bogomolov L., and Tarasov N. Earthquake hazard mitigation by electromagnetic influence on seismic activity: Results of forty-year field experiment on injection of DC electrical pulses into the Earth crust//*Geophysical Research Abstracts*, Vol. 20, EGU2018-15436-1, EGU General Assembly, April 9-13, 2018.
18. Sorokin V.M., Yaschenko A.K, Ruzhin Yu. Ya., Novikov V.A. Model for solar flare influence to the seismic activity// Proc. EMSEV-2012 Workshop. Gotemba, Japan. October 1–4, 2012. Abstract 3-10p.
19. Zeigarnik V.A., Avagimov A.A., Tarasov N.T. (1999) Managing earthquakes? *Science in Russia*, 2:16.
20. Bogomolov L.M. (2010) On a mechanism of electromagnetic effect on kinetics of microfractures and electrically stimulated variations of acoustic emission of rock samples, *Phys. Mesomech.* 13(3): 39-56.
21. Novikov V.A., Novikova E.O. Electromagnetic stimulation of fluid migration into fault area and earthquake triggering phenomena. *Geophysical Research Abstracts*. Vol. 16, EGU2014-12790, 2014 EGU General Assembly 2014.

Acknowledgements

The work was supported by RFBR grant No. 18-05-00255.

The lower ionospheric perturbations related to the strong earthquakes in Southern Europe in 2014 and 2016

A. Rozhnoi¹, M. Solovieva¹, P.F. Biagi², M.Y. Boudjada³, K. Schwingenschuh³, H.U. Eichelberger³, M. Hayakawa^{4,5}, V. Fedun⁶

¹Institute of Physics of the Earth, Russian Academy of Sciences, Moscow, Russia; ²Department of Physics, University of Bari, Bari, Italy; ³Space Research Institute, Austrian Academy of Sciences, Graz, Austria;

⁴University of Electro-Communications, Advanced Wireless Communications Research Center, 1-5-1 Chofu Tokyo, Japan; ⁵University of Electro-Communications, Graduate School of Informatics and Communication Engineering, Chofu Tokyo, Japan; ⁶University of Sheffield, Sheffield, UK; Contact person Rozhnoi A., email: rozhnoi@ifz.ru

The analysis reported in this paper is based on data obtained from very low/low frequency (VLF/LF) receivers deployed in Europe. VLF/LF signals from navigational or time service transmitters propagate inside the earth-ionosphere waveguide and they are reflected by the D region of ionosphere. Therefore, the received signals can provide valuable information about plasma perturbations near the upper atmosphere-lower ionosphere boundary.

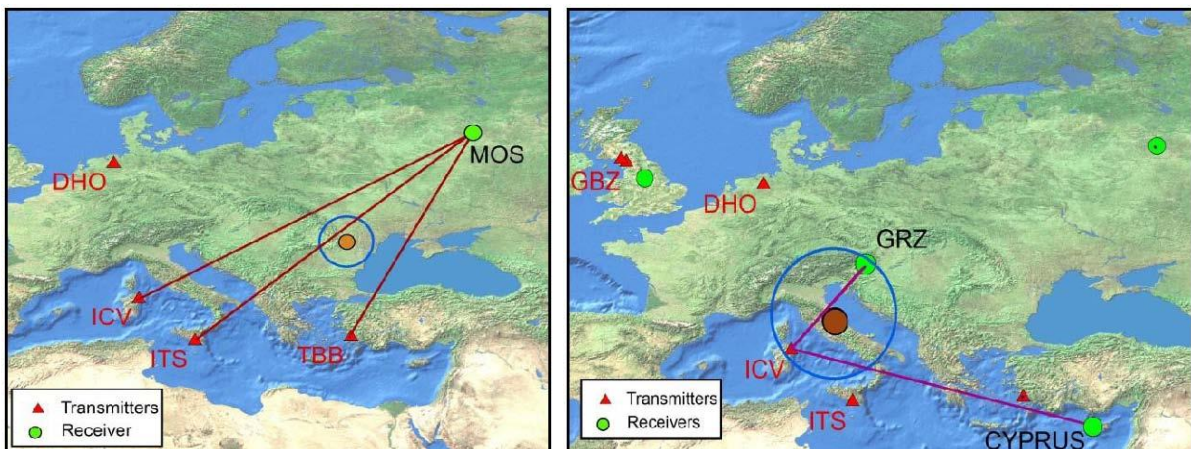


Fig. 1. The scheme of the wave paths under analysis during the Vrancea earthquake (left) and Italian earthquakes (right). The position of the UltraMSK receivers in Moscow (MOS) and Graz (GRZ) and Elettronika S.R.L. receiver in Cyprus together with several transmitters in Europe is shown. Signals from the ICV (20.27 kHz) and ITS (45.9 kHz) transmitters are analyzed in the work. Solid brown circles show the epicenters of earthquake on 22 November 2014 with $M=5.5$ (left) and two earthquakes on 26 and 30 October 2016 (right) with $M=6.1$ and 6.6 correspondingly (USGS/NEIC). The areas where the precursors of earthquake can be observed (according to Dobrovolsky) are shown by hollow blue circles.

Investigation of the VLF/LF signals associated with earthquakes in Europe has begun in the University of Bari (Italy) in 2002 (Biagi et al., 2004; 2007; 2008; Rozhnoi et al., 2009).

In this work we present the results of VLF/LF analysis in connection with the earthquake in Vrancea area on 22 November 2014 ($M=5.5$) and with the two earthquakes in the Central Italy on October 26 ($M=6.1$) and 30 ($M=6.6$) 2016.

The analysis of the earthquake in Vrancea zone is based on the data recorded by UltraMSK (<http://ultramsk.com/>) receiver in Moscow (Russia). For the analysis of Italian earthquakes were used measurements of UltraMSK receiver in Graz (Austria) and Elettronika S.R.L. receiver (Biagi et al., 2011) in Cyprus. Their positions as well as the positions of ICV (20.27 kHz) and ITS (45.9 kHz) transmitters are shown in Figure 1.

Vrancea earthquake on November 22

Vrancea zone is one of the most active seismic areas in Europe. The earthquake with $M=5.5$ (depth=39 km) (USGS/NEIC) occurred at 19:14 UT on 22 November 2014 in this area. Only the ITS transmitter signal recorded at the Moscow station crosses the earthquake preparation zone. (see Fig. 1). The area where possible precursors can be found is shown by hollow blue circle (Dobrovolsky et al., 1979). Results of the analysis are shown in Figure 2.

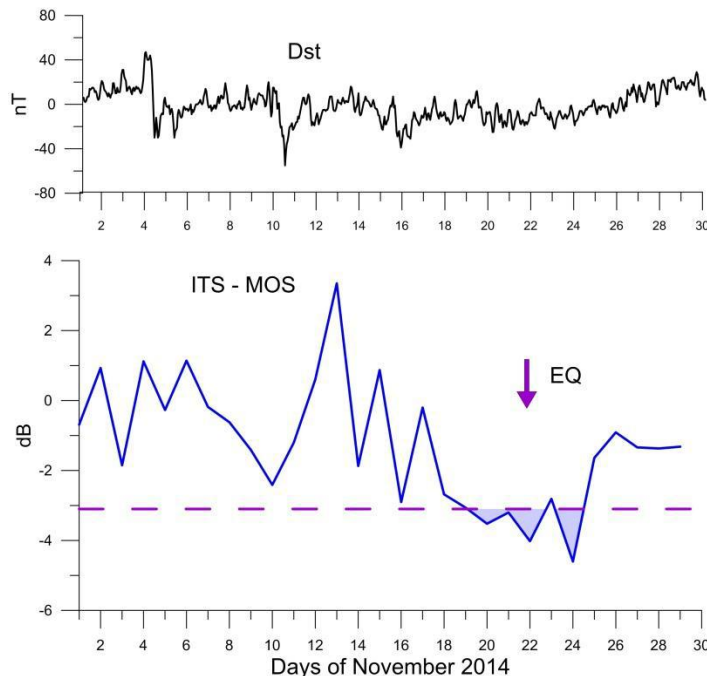


Fig. 2. The measurements of the ITS transmitter signal at the Moscow station during November 2014 (bottom panel). The averaged for nighttime residual signals of amplitude is shown. An arrow indicates the day of earthquake. Dotted line is level of two standard deviations. The filled areas highlight anomalous signal observed in Moscow. The top panel shows Dst index of magnetic activity.

Negative amplitude anomalies have been observed during 3 days before the earthquake and two days after it in the LF (45.9 kHz) signal which passed above the seismic area. No perturbations have been found for the same signal in other paths during this period. The

magnetic activity was very low ($Dst \sim 0$), so that the observed anomalies cannot be attributed to the geomagnetic environment. Not very strong proton was observed on 2-3 November and rather weak relativistic electron flux was registered on 15-16 November (EPS/GOES measurements). We have to note that strong cyclones propagated through Europe during the first ten days or so of November. Mediterranean Hurricane Qendresa was such strong as a tropical cyclone. Such strong cyclone activity in Europe can explain some decrease in the ITS signal around November 10.

Earthquakes in the Central Italy on 26 and 30 October

Two strong earthquakes occurred in October 2016 in the Central Italy (NEIC/USGS). The first earthquake took place on 26 October with $M=6.1$ (depth=10 km), the second one was registered 3 days later, on October 30 with $M=6.6$ (depth =8 km) at the same place (see Fig. 1). Three paths crossed the earthquakes preparation zone: ICV-GRZ, ICV-Cyprus and ICV-MOS. Unfortunately, the receiver in Moscow did not work during the period 22-29 October due to technical problem. The analysis of the amplitude of VLF signal in paths ICV-GRZ and ICV-Cyprus revealed negative anomalies in the signal during 3-5 days before the first earthquake (Figure 3).

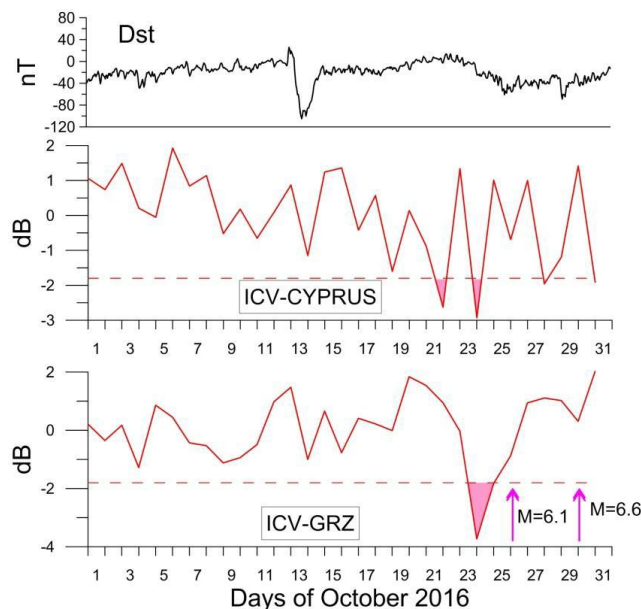


Fig. 3. Amplitude anomalies observed in the ICV-Cyprus and ICV-GRZ paths before the earthquakes in the Central Italy in October 2016. The details of representation are the same as in Fig. 2.

These anomalies can be also connected with the second earthquake. The period between two earthquakes was very short, so it is difficult to attribute the anomalies to certain earthquake. We can only say that disturbances in the VLF signal began several days before strong seismic activity in region under investigation. It should be mentioned that the

geomagnetic situation was quiet during the second part of October and no strong enough cosmic particle fluxes were observed during the period of analysis.

The recent development of the VLF/LF systems all over the world can provide useful information on the properties and position of the perturbation region in connection with seismic activity. The use of a network of observation makes it possible to separate the local VLF/LF perturbations connected with earthquakes from large-scale or global anomalies related to atmospheric circulation and space weather conditions. By utilising multi-station observations it is possible to determine the area of an impending earthquake.

References

- Biagi, P. F., R. Piccolo, L. Castellana, T. Maggipinto, A. Ermini, S. Martellucci, C. Bellecci, G. Perna, V. Capozzi, O. Molchanov, M. Hayakawa and K. Ohta (2004). VLF-LF radio signals collected at Bari (South Italy): a preliminary analysis on signal anomalies associated with earthquakes, *Nat. Hazards Earth Syst. Sci.*, 4, 685–689.
- Biagi, P. F., L. Castellana, T. Maggipinto, G. Maggipinto, A. Minafra, A. Ermini, V. Capozzi, G. Perna, M. Solovieva, A. Rozhnoi, O. Molchanov and M. Hayakawa (2007). Decrease in the electric intensity of VLF/LF radio signals and possible connections, *Nat. Hazards Earth Syst. Sci.*, 7, 423– 430.
- Biagi, P.F., L. Castellana, T. Maggipinto, D. Loiacono, V. Augelli, L. Schiavulli, A. Ermini, V. Capozzi, M.S. Solovieva, A.A. Rozhnoi, O.A. Molchanov and M. Hayakawa (2008). Disturbances in a VLF radio signal prior the $M=4.7$ offshore Anzio (central Italy) earthquake on 22 August 2005, *Nat. Hazards Earth Syst. Sci.*, 8, 1041-1048.
- Biagi, P. F., T. Maggipinto, F. Righetti, D. Loiacono, L. Schiavulli, T. Ligonzo, A. Ermini, I. A. Moldovan, A. S. Moldovan, A. Buyuksarac, H. G. Silva, M. Bezzeghoud and M. E. Contadakis (2011). The European VLF/LF radio network to search for earthquake precursors: setting up and natural/man-made disturbances, *Nat. Hazards Earth Syst. Sci.*, 11, 333–341.
- Dobrovolsky, I.R., S.I. Zubkov and V.I. Myachkin (1979). Estimation of the size of earthquake preparation zones, *Pure and Applied Geophysics*, 117, 1025-1044.
- Rozhnoi, A., M. Solovieva, O. Molchanov, K. Schwingenschuh, M. Boudjada, P. F. Biagi, T. Maggipinto, L. Castellana, A. Ermini and M. Hayakawa (2009). Anomalies in VLF radio signals prior the Abruzzo earthquake ($M=6.3$) on 6 April 2009, *Nat. Hazards Earth Syst. Sci.*, 9, 1727- 1732.

Pre-seismic Ionospheric Anomalies Detected Before the 2016 Taiwan Earthquake with $M=6.4$

K. Umeno¹, S. Goto¹, R. Uchida¹, K. Igarashi¹, C.H. Chen²

¹*Kyoto University, Kyoto, Japan, umeno.ken.8z@kyoto-u.ac.jp;* ²*National Cheng Kung University, Tainan, Taiwan, koichi0925@gmail.com*

The first clear pre-seismic ionospheric anomalies shortly before the 2016 (Southern) Taiwan intraplate earthquake with M 6.4 was detected after the careful investigation on the TEC data obtained from the GNSS stations in Taiwan by using our recently developed correlation analysis [1]. This result is important because our finding is the first pre-seismic TEC ionospheric anomalies shortly before M6 class earthquake while all the published results on similar kinds of pre-seismic ionospheric anomalies are so far restricted for targeting the earthquakes with $M \geq 7$ and our finding cannot be explained by recently proposed phenomenology that most TEC ionospheric anomalies are detected for large interpolate earthquakes with $M \geq 8$ [2]. Thus, our analysis and findings on the GNSS data strongly suggest a NEW physical model of pre-seismic process towards intraplate earthquakes together with our previous finding on pre-seismic ionospheric anomalies of 2016 Kumamoto earthquake distinguishing them with MSTID [3], which enables us to explore a NEW physical phenomenology of pre-seismic anomalies based on GNSS data analysis with potential applications to many other M6 class intraplate earthquakes such as those in Italy in 2016, 2012, 2009, 2002, 1997 and so on.

Acknowledgements

The present work are partially supported by K-opticom Corporation (K-Opticom -Kyoto Univ. collaborative research) and the Central Weather Bureau (CWB) of Taiwan (MOTC-CWB-107-E). All the details of our analysis can be found at <https://arxiv.org/abs/1806.03782>.

References

- [1] Iwata, T., and K. Umeno, “Correlation analysis of pre-seismic total content anomalies around the 2011 Tohoku-Oki earthquake”, *J. Geophysical Res. Space Physics* (2016), 121, 8969-8984.
- [2] Heki, K., and Y. Enomoto, “Mw dependence of the pre-seismic ionospheric electron enhancements”, *J. Geophysical Res. Space Physics* (2015), 120, 7006-7020.
- [3] Iwata, T., and K. Umeno, “Pre-seismic ionospheric anomalies detected before the 2016 Kumamoto earthquake”, *J. Geophysical Res. Space Physics* (2017), 122, 3.

Chapter 5

*Theoretical and laboratory studies for
understanding seismic and volcanic
phenomena*

Landslide monitoring test based on self-potential method

K.Y. Hu¹, Q.H. Huang²

¹*Department of Geophysics, Peking University, Beijing, China, huk@pku.edu.cn;* ²*Department of Geophysics, Peking University, Beijing, China, huangq@pku.edu.cn*

Rainfall and subsurface flow are crucial factors to cause landslides. Both hydrostatic effect and hydrodynamic effect could produce observable self-potential (SP) signals. Therefore, SP data could provide useful information of water flow.

In this work, we designed an SP monitoring system on Huangnibazi landslide, which is located in southwestern China. As far as we knew, the 2017 M7.0 Jiuzhaigou earthquake and the continuous rainfall jointly triggered the landslide. GPS data showed that the sliding body was a kind of creeping deformation. On this stage, precipitation infiltration and groundwater flow mainly contributed to the instability of sliding body. To further understand the possible relationship between the dynamic ground water flow and the landslide, we set two orthogonal profiles on the slope for continuous SP measurement. The SP signals were measured using 48 non-polarizable electrodes, which were connected to a digital multichannel acquisition system. We'll report the main characteristics of the SP signals after the spatio-temporal analysis of the SP data. We'll also investigate the possible relationship between water flow and landslide using the technique combining the electric charge (dipole) occurrence probability tomography and the continuous complex wavelet transformation imaging.

Integrated GPR and Structural surveys at the Consoli Palace of Gubbio (Italy)

I. Catapano¹, N. Cavalagli², F. Ubertini², F. Soldovieri¹, G. Padeletti³

¹*Institute for Electromagnetic Sensing of the Environment – National Research Council of Italy, Napoli, Italy, catapano.i@irea.cnr.it, soldovieri.f@irea.cnr.it;* ²*Department of Civil and Environmental Engineering, University of Perugia, Perugia, Italy, nicola.cavalagli@unipg.it, filippo.ubertini@unipg.it;* ³*Institute of Nanostructured Materials, National Research Council of Italy, Roma, Italy giuseppina.padeletti@ismn.cnr.it*

The Consoli Palace (Figure 1) is located in the heart of the medieval historical center of the city of Gubbio, Italy, in one of the most seismic active zones of Italy. This monument is one of the most iconic monumental buildings of Central Italy as well as the most representative monument of Gubbio. Designed by Angelo da Orvieto and Matteo Gattapone, the Consoli Palace was built in gothic style between 1332 and 1349. During the middle ages, the Palace hosted the Consuls, who were elected to control both legislative and executive branches of the government of the City. Since 1909 it has hosted the Civic Museum, with a rich collection of art masterpieces, dating back from the local ancient Umbrian time up to the XX Century. Among the treasures that are safeguarded in the Museum, the Iguvine Tablets are especially worth mentioning. The Palace has a rectangular plan of about 40x20 min dimension, an elevation of more than 60 m (from the street level up to the top of the bell-tower) and is characterized by an articulated internal distribution of volumes. In terms of constituents materials, the Palace is mainly made of calcareous stone masonry. Given the slope of the mountain on which it is erected, the Palace foundations sit above two terraces corresponding to the building's lower floors: those of the projecting southward (the “Loggia”) are placed approximately 10 m below those of the top.



Fig. 1 Aerial view of Consoli Palace (building on the left side), Piazza Grande and Gubbio Municipality (building on the right side)

The Consoli Palace shows evidence of significant structural damages in the form of existing cracks. Some of those cracks are the result of the physiological process of the masonry when subjected to the self-weight, while other cracks are likely to be associated to past and recent earthquakes. In this respect, it should be recalled that several seismic events occurred in Gubbio during the centuries, whereby the Mw5.6 Umbria earthquake occurred on April 29th 1984, with epicenter location between Gubbio and Valfabbrica, is worth to be mentioned. Figure 2 shows the crack scenarios obtained on the East and North façades after a detailed damage survey.

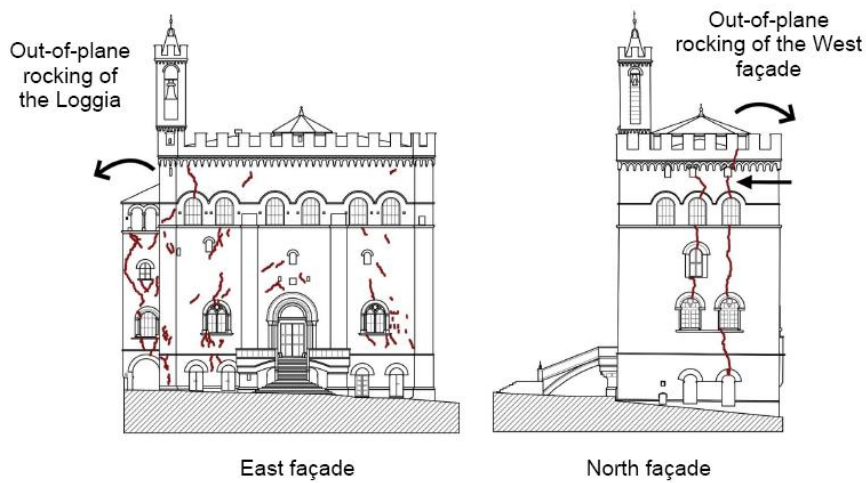


Fig. 2 Crack pattern observed on the East and North façades of the Consoli Palace.

The presence of these cracks together with the occurring material degradation phenomenon motivated the choice of the Consoli Palace as one of the test site of the HERACLES project and several sensing technologies are currently deployed to investigate and monitor its structural healthiness. Specifically, satellite, aerial, ground based and laboratory technologies are exploited to perform a multiscale characterization (from wide-area observations to local and point analysis) accounting for the several aspects occurring to define the conservation status of CH assets and the risk factors affecting them, like structural assessment, material degradation, meteorological events and climatic/anthropic conditions. The present work deals with the on-site technologies devoted to perform structural assessment and reports the surveys performed to characterize and monitor the crack affecting the wall of the cross-hall leading to the Loggia.

In order to assess the health condition of the palace, a mixed static and dynamic monitoring system has been installed and activated since July 2017. In particular, the system consists of 2 two Linear Variable Displacement Transducers (LVDTs), fixed across the two main cracks of the structure (1 data every 10 minutes), and of three accelerometers placed on

the roof level which continuously acquired the structural vibrations (sample rate of 100 Hz) to extract and check the natural frequencies of the construction [1]. Figure 3 indicated the position of the LVDT fixed on the crack near the Loggia and the time history of the relative displacement measured during all the monitoring period. The graph highlights the seasonal fluctuation of the opening/closing of the crack directly related with the local temperature data. More in detail, it has been observed an opening process of the crack with a decreasing of the temperature. This observation is justified by the material contraction correlated to the low level of temperature, which causes the opening of the crack. Nevertheless, it can be observed that the fluctuation amplitude is smaller than 1 mm, making evidence of no criticalities.

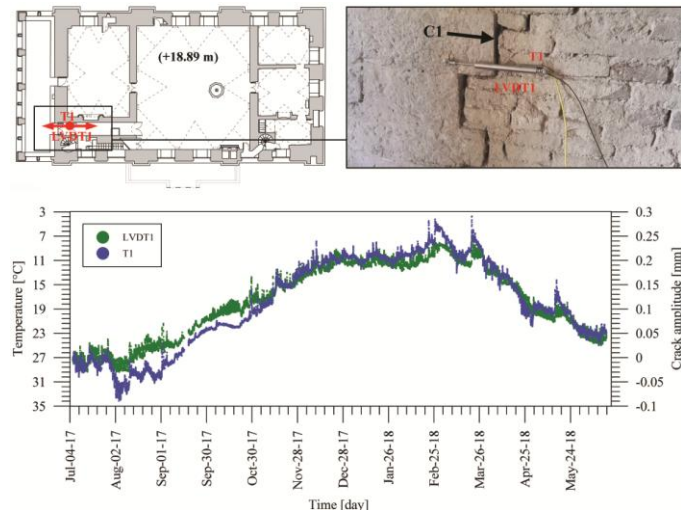


Fig. 3. Images of the LVDT1 installed across the crack and time history of the crack amplitude measured during the monitoring period.

This crack has been, also investigated by means of two GPR measurement surveys performed in July 2017 and May 2018 [2]. The GPR surveys were performed by using the IDS K2-RIS system equipped with a 2 GHz shielded antenna on an area that is about 1 m^2 wide. Specifically, the data were collected along 25 parallel traces, which were 5 cm spaced and about 90 cm long, and were processed by means of a microwave tomography based approach [2], in order to obtain focused images. This has allowed us to gather information on the geometrical features about the crack and voids occurring into the surveyed area as well as on the wall texture.

The results of the GPR survey carried out the 12th July 2017, i.e. the tomographic images referred to increasing constant depth from the air-wall interface are shown in Figure 3. Specifically, this figure shows some slices of the tomographic reconstruction referred to increasing depth from the air-wall interface, $z = 0 \text{ cm}$, to the inner part of the wall until $z = 70 \text{ cm}$, with synthetic comments explaining what they represent.

The same slices but referred to the GPR survey carried out the 8th May 2018 are very

similar, practically they are the same for the two surveys. This result corroborates that, during the period between the two surveys, there was not a significant evolution of the crack and this hints that the crack is not related to a quickly evolving structural hazard, as also highlighted by the experimental data derived by the monitoring system.

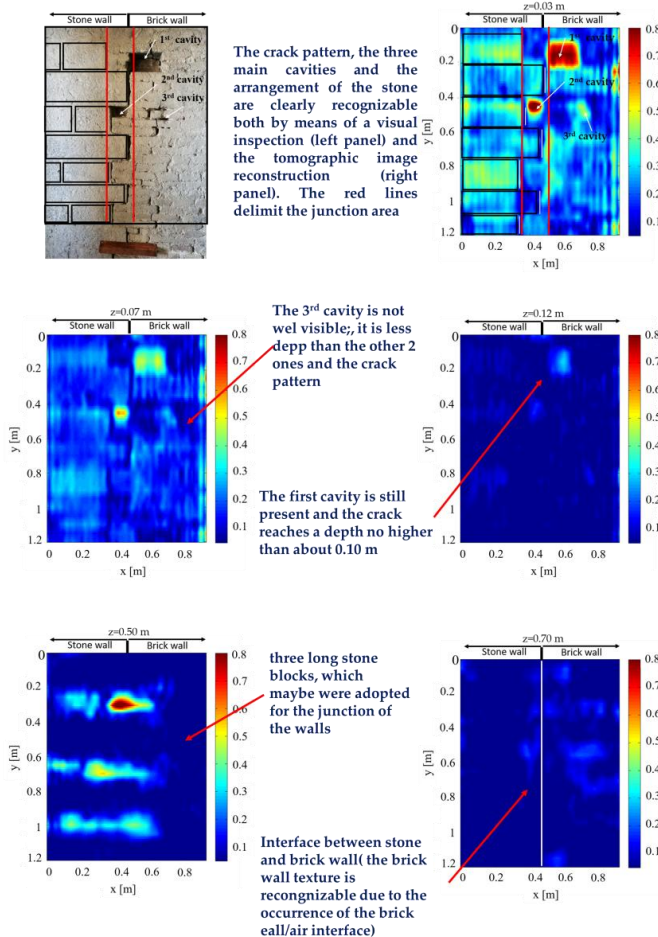


Fig 4 Image of the cracks and voids occurring on the wall of the cross-hall leading to the Loggia (upper left corner) and slices of the tomographic reconstruction for increasing constant depth from the air-wall interface, $z = 0$ m, to the inner of the wall until $z = 0.70$ m.

References

- [1]. Ubertini F., Cavalagli N., Kita A., Comanducci G. ,Assessment of a monumental masonry bell-tower after 2016 central Italy seismic sequence by long-term SHM, *Bulletin of Earthquake Engineering*, 16(2), 775-801
- [2]. Catapano I., Ludeno G., Soldovieri F., Tosti F., Padeletti G., Structural Assessment via Ground Penetrating Radar at the Consoli Palace of Gubbio (Italy). *Remote Sens.* 2018, 10, 45.

Acknowledgments

This project has received funding from the European Union's Horizon 2020 research and innovation program under grant agreement No 700395.

Modeling of gravity and magnetic anomalies to reduce the general geophysical ambiguity

M. Fedi¹

¹*Università Federico II di Napoli, c/o Dipartimento di Scienze della Terra, dell'Ambiente e delle Risorse (DiSTAR), Complesso Universitario di Monte S.Angelo, Napoli, Italy, fedi@unina.it*

Ill posedness and inherent lacking of uniqueness affect inversion of gravity and magnetic data. In general, a priori information is needed to deal with non-uniqueness. However, significant and unambiguous information may be extracted from the measured data, including the total excess mass, source geometry, boundaries or lineaments, the scaling exponent of the depth weighting function, the maximum allowed depth for the sources, the fault dip. Conversely, gravity and magnetic data may solve the ambiguity or the poor information yielded by other geophysical data, such as seismic ones, as it was shown for the Campanian Plain and the Gaeta Gulf. Two possible models are proposed within the lower/intermediate crust offshore the Campanian Plain, implying large amounts of melts and cumulates besides country rocks and a layered distribution of density or a fractal density distribution, based on the scaling exponent estimated from the gravity data.

Self-potential, Ground-tilt and Infra-Red Emission Associated with Geyser Eruptions: Implications for Monitoring Volcanic Activity.

M.J.S. Johnston¹

¹U.S. Geological Survey, Menlo Park, USA. mal@usgs.gov

Self-potential (SP), ground deformation (GD) and infrared (IR) monitoring play extremely important roles in volcano hazard assessment since they can provide valuable constraints on the depth, pressure, shape and temporal changes of both sub-surface deformation sources and surface flow patterns of hydrothermal and magmatic fluids and eruptions. However, GD in volcanic regions has usually been interpreted to result only from magma emplacement whereas recent observations of relatively rapid GD fluctuations suggest pressure transients from fluid/gas phase changes and/or hydrothermal poroelastic deformation may also contribute. Unfortunately, GD measurements that are unequivocally induced by multi-phase pressure transients with no magma involvement are rare and this has limited our ability to understand one of the major contributors to volcanic unrest. Geysers are intermittently erupting hot springs that occur when gas-rich high-temperature fluids flash to steam as a result of changing fluid/pressure/temperature conditions. These are excellent analogues to volcanoes because both systems are characterized by cyclic phenomena triggered by phase changes and fluid flow can be inferred from SP measurements. In 2009 and 2010, we documented deformation and flow in the absence of magma emplacement with measurements of SP, ground tilt (GT), IR and other parameters at “Old Faithful” and “Jones Fountain of Life” geysers in northern California and “Lone Star” geyser in Yellowstone National Park. Taking “Old Faithful” geyser as an example, the GT, SP and water outflow cycles are observed to be quasi-sinusoidal with a 4-5 minute periodicity. All are in phase except the surface eruptions. Surface eruptions occur during initial deflation about a minute after peak ground uplift and SP. The eruptions continue for about a minute with an associated small deflation/inflation pulse corresponding to the first clearing followed by recharge of the conduit. Larger-scale deformation monitoring indicates the existence of several interacting fluid pressure sources. These observations suggest that subsurface pressure transients associated with phase changes in porous and fractured media occur at relatively shallow

depths (<60m) with complex and time-variable geometry and are easily detectable with modern deformation techniques. These results are similar to observations from volcanic regions such as on Taal Volcano in the Philippines where, in 2010, a seismovolcanic crisis was preceded and accompanied by unusual changes in electric field, ground tilting, magnetic field and uplift. Thus, deformation, seismic monitoring, SP, gas, fluid flow and other continuous geophysical data may provide an effective means for identifying and separating magnetic intrusion and subsurface hydrothermal effects.

Acknowledgements

The author gratefully acknowledges the contributions to the geyser work from S. Hurwitz, R. Sohn, J. Vandemeulebrouck, L. Karlstrom and M. Rudolph and to the Taal work from J. Zlotnicki, Y. Sasai, F. Fauquet, E. Villacorte and J.M. Cordon Jr.

Multifractal analysis of telluric time series along the Hellenic Subduction Zone

G. Michas¹, J. Makris¹, F. Vallianatos¹

¹UNESCO Chair on Solid Earth Physics and Geohazards Risk Reduction, Technological Educational Institute of Crete, Chania, Crete, Greece, gmichas@hotmail.com; jpmakris@chania.teicrete.gr; fvallian@chania.teicrete.gr

The Hellenic Subduction Zone is the (HSZ) seismically most active region in western Eurasia due to subduction of the oceanic African lithosphere beneath the Eurasian plate. It exhibits complex seismotectonics and geodynamics. Long-term seismoelectromagnetic research appears to be a promising approach to study the physics of earthquakes during their preparation stage. In this framework, a number of onshore continuous magnetotelluric (MT) stations have been deployed across HSZ to investigate the geoelectric structure versus depth and possible apparent resistivity variations as well as electric and/or magnetic field transient anomalies that could be associated with seismic activity, and thus to gain insight to the criticalities of the mechanisms that precede and eventuate to fracture. These stations operated in sites selected to be of low man-made noise, and featuring optimized light-weight and small-size but robust telemetry and extended autonomy.

In this work a preliminary study the structure of recorded electric (telluric) time-series along the HSZ using multifractal analysis is presented. Such series are typically characterized by fluctuating behavior, such that multifractal analysis can enlighten the structure of the series, the local clustering effects and the heterogeneous degree of clustering, as well as the range of correlations. We perform multifractal detrended fluctuation analysis (MF-DFA) to the series to estimate the root mean-square fluctuations and the q th order fluctuation function $F_q(n)$. If the series are long-range power-law correlated, $F_q(n)$ will increase as a power-law with exponent $h(q)$, $F_q(n) \sim n^{h(q)}$ (e.g., Michas et al, 2015). For multifractal series, the exponent $h(q)$ will depend on the various values of q . Another way to characterize multifractal series is the singularity spectrum $f(a)$, where a is the singularity strength or Hölder exponent. The singularity spectrum $f(a)$ indicates the fractal dimensions of the subsets that have the same singularity strength a and gives information about the relative importance of each fractal dimension. In monofractal series the singularity strength is similar in the entire range of the set so that the singularity spectrum collapses into a single point. MF-DFA analysis reveals a range of fractal dimensions and multifractality in telluric time series along the HSZ.

References

- Kantelhardt, J. W., Zschiegner, S. A., Koscielny-Bunde, E., Havlin, S., Bunde, A., Stanley, H. E., 2002. Multifractal detrended fluctuation analysis of nonstationary time series. *Physica A*, 316, 87-114.
- Michas, G., Sammonds, P., Vallianatos, F., 2015. Dynamic multifractality in earthquake time series: Insights from the Corinth rift, Greece. *Pure and Applied Geophysics*, 172, 1909-1921.

Micro-ERT laboratory measurements for seismic liquefaction study

R. Mollica^{1,2}, R. de Franco¹, G. Caielli¹, G. Boniolo¹, G.B. Crosta², R. Castellanza², A. Villa², A. Motti²

¹National Research Council – Institute for the Dynamics of Environmental Processes, Milan, Italy,

riccardo.mollica@idpa.cnr.it; roberto.defranco@idpa.cnr.it; grazia.caielli@idpa.cnr.it;

graziano.boniolo@idpa.cnr.it; ²University of Milan-Bicocca, Department of Earth and Environmental Sciences, Milan, Italy, giovannibattista.crosta@unimib.it; riccardo.castellanza@unimib.it; alberto.villa2@unimib.it; a.motti@campus.unimib.it.

Liquefaction of soils is one of the most dangerous secondary effects of an earthquake. It deals with a drastic reduction of effective stresses and loss of bearing capacity in sandy, poorly consolidated, saturated soils. The set-up of excess pore pressure due to its rapidity (order of seconds) does not permit at the soil to dissipate these excess pressures, which accumulate inside the solid skeleton until the critical point of liquefaction is reached. At this point, the saturated sandy system acts as a pressurized non-Newtonian fluid, which loses its shear strength and causes the fracturing of neighbor units, giving the typical liquefaction phenomena at the ground surface: sand boils, linear fractures, punctual uplift of sand, deformations and significant settlements.

The liquefaction susceptibility is nowadays assessed by the so-called Simplified Approaches. These methods belong to the work of Seed and Idriss (1971) [1] and were more refined during the years by Robertson and Wride (1997) [2], Youd and Idriss (2001) [3] and Boulanger and Idriss (2014) [4]. They are based on in-situ geotechnical tests (Cone Penetration Test and Standard Penetration Test), evaluating a factor of safety (FS) given by the ratio between the Cyclic Resistance Ratio (CRR) and Cyclic Stress Ratio (CSR). The CSR is the load induced by a hypothetical earthquake, mainly depending on the local seismic hazard at site, and the CRR is the soil resistance, which depends on the soil materials and their physico-mechanical properties.

On the other hand, liquefaction susceptibility is not well discussed from the point of view of geophysical parameters. The most important works on the subject are those of Hunter (2003) [5] and Ishihara and Tsukamoto (2004) [6] which stress the importance of measuring P and S waves in order to characterize soils prone to liquefaction. By following these studies, de Franco et al. (submitted 2018) [7], suggests a first approach to attain the geophysical

susceptibility to liquefaction. They demonstrate that it is possible to identify soils prone to liquefaction by measuring their seismic velocities (v_p and v_s): the first one acts as a proxy of the degree of water saturation and the second one as a proxy of the geotechnical soil class.

In literature, using geophysical as a tool for identifying the liquefied zones after earthquakes [8,9] or the so-called Blast Tests, is presented with the aim to quantify the phenomenon [10].

The hypothesis, which we want to test in this work, is the following: during the generation of the excess pore pressures, grains of sand “vibrate” and they tend to separate from each other at each cycle of the seismic input. If so, we should observe two important variations in at least two geophysical parameters, without producing sensitive settlements or displacements: electrical resistivity and v_s velocity.

In order to validate this issue, a simple laboratory experiment has been set-up (Fig.1) to study if there were measurable resistivity variations during a dynamic loading of a saturated sandy soil.

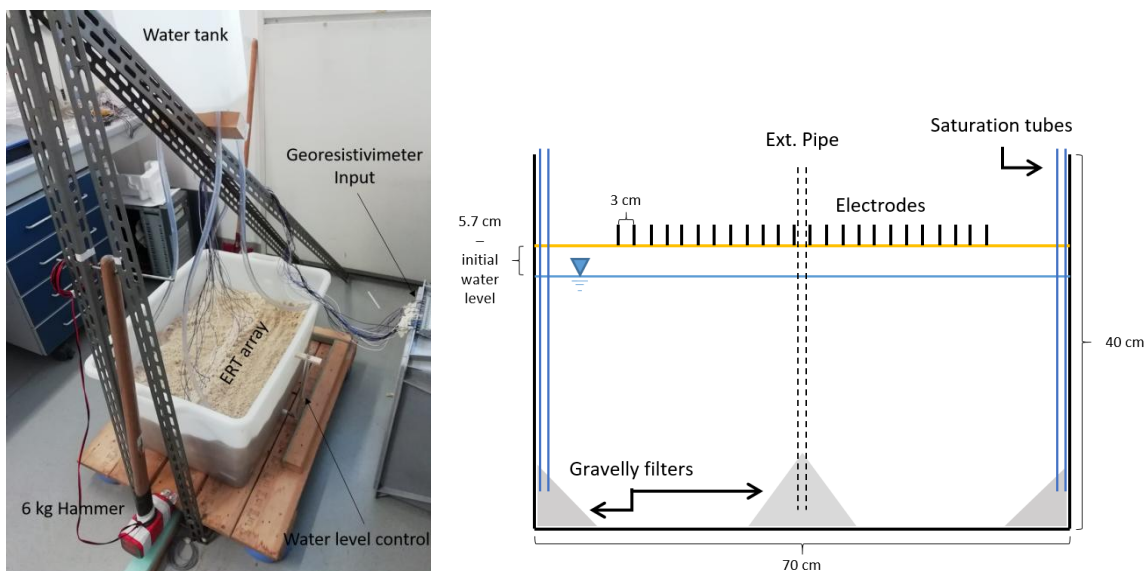


Fig. 1 The laboratory experiment

A 70x45x40 cm box is filled with fine sand (Fig. 1 right panel). The sandbox is equipped with four tubes at each angle to saturate the system gradually from the bottom. A monitoring well is installed externally to the tank to control the water level and its oscillations. The sandbox is positioned above a wood plate where a sledgehammer pendulum of 6 kg is used to hit the system generating the seismic input (Fig. 1 left panel). The peak acceleration generated by the impact is approximatively of 0.01 m/s^2 . On the surface of the sand, 24 inox steel electrodes are connected to Syscal Pro georesistivimeter for ERT measurement. Resistivity data were acquired for all the experimental steps with a Schlumberger configuration of 121

quadrupoles measured every 2 min and 10 s. The experiment was divided in four main steps:

1. Saturation step: every ERT 11 l of water was poured in the model. This step ends when the water table reaches a depth of approximatively 6 cm below ground surface;
2. Stationary step: ERT time-lapse measurements for back-ground analysis;
3. Dynamic step: the pendulum hits 7 times the system at the beginning of each ERT (once every 2 min and 10 sec). During this step, the water level increase was monitored through the external pipe.
4. Post-dynamic step: ERT time-lapse measurements of the post-dynamic pressure dissipation.

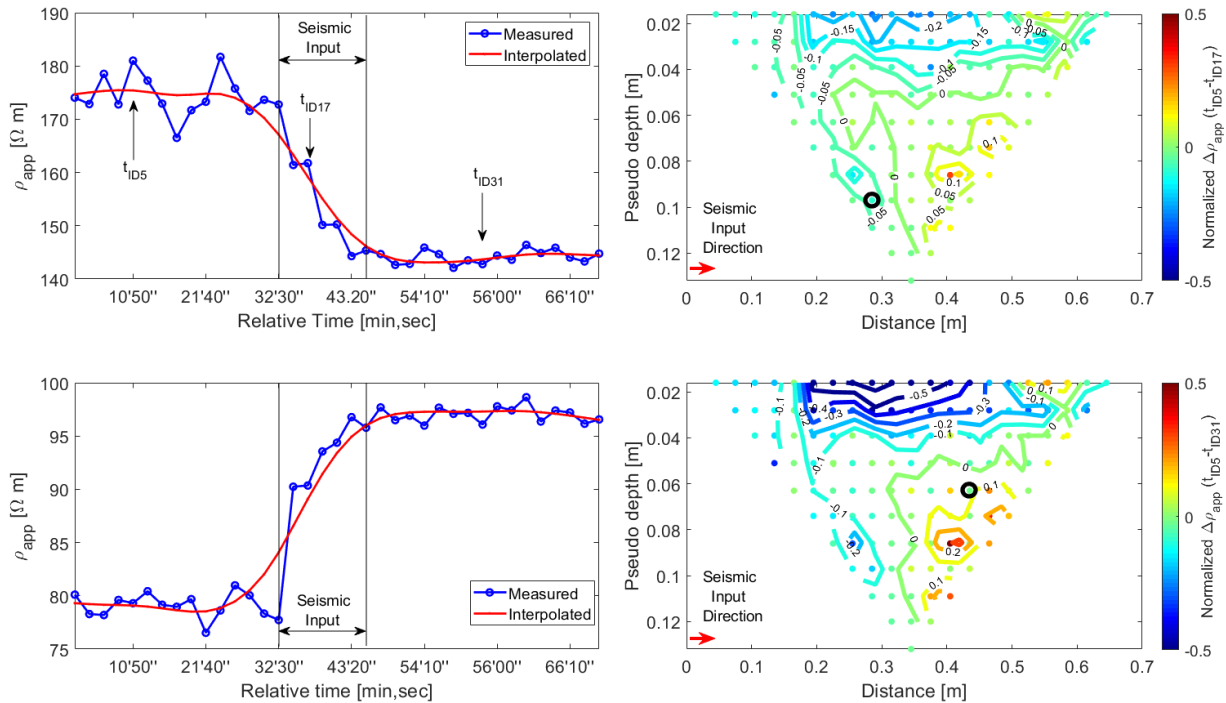


Fig. 2 ERT time-lapse measurements from step 2 to step 4. Left panels: ρ_{app} resistivity variations for the two nodes highlighted with black circles in the right panels. Right panels: ρ_{app} variations at t_{ID17} (upper) and t_{ID31} (lower) across the sandbox, normalized with respect to t_{ID5} .

The most important result obtained was reached in the Dynamic step (Fig.2). The initial water level was at a 5.7 cm depth. The starting apparent resistivity pseudo section (t_{ID5}) evidences a slight lateral variation below 10 cm depth of about 10%, while the rest of the section is quite homogeneous (<5%). The first hammer hit was at measurement time t_{ID15} . After this time, perturbations of apparent resistivity (ρ_{app}) were observed up to the seventh hammer hits (t_{ID21}). The produced variation of ρ_{app} reached 50% and it was mainly located in the upper part of the sandbox. In general, pseudo sections variations were not homogeneous. These might be due to the changes in the solid skeleton occurred after the first hit. A preliminary interpretation of the presented data could be the following: the left part of the

model exhibit excess pore pressure (negative variations), which permitted the water to flow upwards while the right part exhibits consolidation phenomena (positive variations). This interpretation could be confirmed by the increase in the average level of the water table in the external well, with a rate of 0.25 cm/hit.

These preliminary results indicate that ERT could be a suitable technique to monitor the liquefaction process.

References

- [1]Seed HB, Idriss IM. Simplified Procedure for Evaluating Soil Liquefaction Potential. *J Soil Mech Found Div* 1971;97:1249–73.
- [2]Robertson PK, Wride C (Fear). Evaluating cyclic liquefaction potential using the cone penetration test. *Can Geotech J* 1998;35:442–59. doi:10.1139/t98-017.
- [3]Youd TL, Idriss IM. Liquefaction Resistance of Soils: Summary Report from the 1996 NCEER and 1998 NCEER/NSF Workshops on Evaluation of Liquefaction Resistance of Soils. *J Geotech Geoenvironmental Eng* 2001;127:297–313. doi:10.1061/(ASCE)1090-0241(2001)127:4(297).
- [4]Boulanger RW, Idriss IM. CPT and SPT based liquefaction triggering procedures. 2014.
- [5]Hunter J. AA. Some observations of V_p , V_s , depth and porosity from borholes in water-saturated unconsolidated sediments. SAGEEP, 2003, p. 650–61.
- [6]Ishihara K, Tsukamoto Y. Cyclic strength of imperfectly saturated sands and analysis of liquefaction. *Proc Japan Acad Ser B* 2004;80:372–91. doi:10.2183/pjab.80.372.
- [7]de Franco R, Caielli G, Mollica R, Norini G, Sharon Aghib F, Di Capua A, et al. Geophysical characterization of liquefaction-prone areas: the Quistello test site, central Po Plain, Northern Italy. SUBMITTED to *Soil Dyn Earthq Eng* 2018.
- [8]Abu Zeid N, Bignardi S, Caputo R, Santarato G, Stefani M. Electrical resistivity tomography investigation of coseismic liquefaction and fracturing at San Carlo, Ferrara Province, Italy. *Ann Geophys* 2012;55:713–6. doi:10.4401/ag-6149.
- [9]Apostolopoulos G, Minos-Minopoulos D, Amolochitis G, Pavlopoulos K, Papadopoulos A. Geophysical Investigation for the Detection of Liquefaction Phenomena in an Archaeological Site, Lechaion, Greece 2013. doi:10.3997/2214-4609.20131379.
- [10]Amoroso S, Milana G, Rollins KM, Comina C, Minarelli L, Manuel MR, et al. The first Italian blast-induced liquefaction test (Mirabello, Emilia-Romagna, Italy): Description of the experiment and preliminary results. *Ann Geophys* 2017;60. doi:10.4401/ag-7415.

New algorithms as robust procedure for Geohazards climatological precursor assessment

A. Piscini¹, D. Marchetti¹, A. De Santis¹

¹*Istituto Nazionale di Geofisica e Vulcanologia, Via di Vigna Murata 605, Rome 00143, Italy*

Contacting author: alessandro.piscini@ingv.it

Abstract preference: poster

A recent study of climatological physical variables, i.e. skin temperature, water vapor and ozone, preceding several Central Italy Earthquakes, has shown a significant statistical correlation with earthquakes (Piscini et al., PAGeoph 2017).

In that paper, the CAPRI (Climatological Analysis for seismic PRecursor Identification) algorithm was introduced and it proposed a robust procedure to analyze climatological data in order to better identify the potential climatological precursors of strong earthquakes according to Lithosphere Atmosphere Ionosphere Coupling (LAIC) model (Pulinets and Ouzounov, 2011).

The present work involves some land/atmospheric parameters collected from meteo/climate big data archive starting from a date preceding the geohazards, e.g. earthquakes and volcanic eruptions, by some months, compared with its historical time series.

The simultaneous analysis of the different climatological parameters related to the world geohazards showed the presence of contemporary anomalies in all of them, thus reinforcing the idea of considering such behavior as an effective tool for an integrated system of future event prediction.

References

- Piscini, A., De Santis, A., Marchetti, D., Cianchini, G., A multi-parametric climatological approach to study the 2016 Amatrice-Norcia (Central Italy) earthquake preparatory phase, Pure and Applied Geophysics, ISSN: 0033-4553, doi: DOI: 10.1007/s00024-017-1597-8.
- Pulinets S, Ouzounov, D. (2011). Lithosphere-Atmosphere- ionosphere coupling (LAIC) model-an unified concept for earthquake precursors validation. J. Asian Earth Sci, 41(4–5):371–382.

A complexity view into the physics of precursory accelerating seismicity

F. Vallianatos¹, G. Chatzopoulos¹

¹*UNESCO Chair on Solid Earth Physics and Geohazards Risk Reduction, Technological Educational Institute of Crete, Chania, Greece (fvallian@chania.teicrete.gr)*

Strong observational indications support the hypothesis that many large earthquakes are preceded by accelerating seismic release rates which described by a power law time to failure relation. In the present work, a unified theoretical framework is discussed based on the ideas of non-extensive statistical physics along with fundamental principles of physics such as the energy conservation in a faulted crustal volume undergoing stress loading. We derive the time-to-failure power-law of cumulative energy released in a fault system that obeys a hierarchical distribution law extracted from Tsallis entropy. Considering the analytic conditions near the time of failure, we derive from first principles the time-to-failure power-law and show that a common critical exponent $m(q)$ exists, which is a function of the non-extensive entropic parameter q . We conclude that the cumulative precursory parameters are function of the energy supplied to the system and the size of the precursory volume. In addition the q -exponential distribution which describes the fault system is a crucial factor on the appearance of power-law acceleration in the seismicity. Our results based on Tsallis entropy and the energy conservation gives a new view on the empirical laws derived.

References

- Vallianatos F., Papadakis G., Michas G., 2016. Generalized statistical mechanics approaches to earthquakes and tectonics. Proc. R. Soc. A, 472, 20160497.

On the way to electromagnetic earthquake control: Results of forty-year field and lab experiments on injection of DC electrical pulses into the Earth crust

V. Zeigarnik¹, A. Avagimov¹, V. Novikov¹, A. Rybin², G. Schelochkov², V. Bragin², V. Sychev², L. Bogomolov³, N. Tarasov⁴

¹*Joint Institute for High Temperatures of Russian Academy of Sciences, Moscow, Russian Federation,
novikov@ihed.ras.ru*, ²*Research Station of Russian Academy of Sciences, Bishkek, Kirghizia*, ³*Institute of Marine
Geology and Geophysics of Far Eastern Branch of Russian Academy of Sciences, Yuzhno-Sakhalinsk, Russian
Federation*, ⁴*Schmidt Institute of Physics of the Earth of the Russian Academy of Sciences, Moscow, Russian
Federation*

An overview of the state-of-the art of pioneering research carried out in Russia on the electric/electromagnetic triggering of weak seismicity is presented. The overview covers various researches carried out in the field of artificial partial release of tectonic stresses by local electric processing of the Earth crust for earthquake hazard mitigation.

The field experiments on DC electric pulses injection were started more than forty years ago at Garm geophysical test site (Tajikistan, Pamir mountains) [18, 19] and were continued at the test site near Bishkek city, Kirgizia (Northern Tien Shan) in 1978 with application of pulsed magneto-hydrodynamic (MHD) power systems [20, 23], and later of ERGU-600 pulsed electric system (PES) powered from industrial electric line [17]. The PESs provided DC current of 600-2500 A in emitting dipole grounded into the earth crust with a distance between electrodes of about 4 km. The prime goal of the field experiments was deep electromagnetic (EM) sounding of the Earth crust for monitoring of EM precursors of strong earthquakes.

Nevertheless, after a few years of operation of MHD power systems it was found that electric pulses resulted in spatiotemporal re-distribution of local seismicity (increasing the number of weak earthquakes after DC pulse injection) [1, 16, 18-20, 23]. During forty years of the filed experiments there is clear deficit of strong earthquakes in the region under study (100 x 100 km). The results of monitoring of seismic activity by KNET seismic stations were supported by measurement of acoustic emission in the wells [13, 26], which sharply rose during the sessions of DC current injections.

The field results were verified under laboratory conditions with application of various press equipment [2-6] and spring-block sliders [7-11, 15] simulated behavior of the fault during its electric processing. Some theoretical attempts were taken to explain the

electric/electromagnetic triggering phenomena, which consider not only interaction of electric/EM-fields with stressed rocks [6, 24, 25, 27], but fluid migration under electric action [14] which may result in triggering of weak earthquakes.

Today it is clearly shown that the electric processing of the Earth crust may be used for development of advanced technology of prevention or mitigation of catastrophic earthquakes. The future research is discussed directed to application of electric processing of the seismogenic fault for transformation of "stick-slip" seismic mode to the mode of slow-slip events or creep.

References:

- Avagimov A.A., Zeigarnik V.A., and Fainberg E.B. (2005) Electromagnetically Induced Spatial–Temporal Structure of Seismicity. *Izv. Phys. Earth*, V. 41, N. 6, pp. 475–484.
- Avagimov A.A., Zeigarnik V.A., and Klyuchkin V.N. (2006) On the Structure of Acoustic Emission of Model Samples in Response to External Energy Action (2006) *Izv. Phys. Earth*, V. 42, N. 10, pp. 824–829.
- Avagimov A.A. and Zeigarnik V.A. (2008) Estimation of the Triggering Effect in Relation to Model Sample Failure. *Izv. Phys. Earth*, V. 44, N. 1, pp. 69–72.
- Avagimov A.A., Zeigarnik V.A., Okunev V.I. (2011) Dynamics of Energy Exchange in Model Samples Subjected to Elastic and Electromagnetic Impacts. *Izvestiya, Physics of the Solid Earth*, 2011, Vol. 47, No. 10, pp. 919–925
- Bogomolov L. M., Il'ichev P. V., Zakupin A. S., Novikov V.A., Okunev V.I. (2004) Acoustic Emission Response of Rocks To Electric Power Action As Seismic-Electric Effect Manifestation. *Annals of Geophysics*, 47 (1), 65–72 (2004).
- Bogomolov L. and Zakupin A. (2008). Do Electromagnetic Pulses Induce the Relaxation or Activation of Microcracking Rate in Loaded Rocks? *Solid State Phenomena*, V.137, pp. 199-208, ISSN 1662-9779.
- Chelidze T. and Lursmanashvili O. (2003) Electromagnetic and mechanical control of slip: laboratory experiments with slider system. *Nonlinear Processes in Geophysics* 10: 557–564.
- Chelidze T. and Matcharashvili T. (2003) Electromagnetic Control of Earthquake Dynamics *Computers & Geosciences*, 29, 587–593.
- Chelidze T., Varamashvili N., Devidze M., Chelidze Z., Chikladze V., and Matcharashvili T. (2002): Laboratory study of electromagnetic initiation of slip. *Ann. Geophysics*, 45 (5), 587-598.
- Chelidze T., Matcharashvili T., Gogiashvili J., Lurmanashvili O., and Devidze M. (2005) Phase synchronization of slip in laboratory slider system. *Nonlinear Processes Geophys.*, 12, 1-8.
- Chelidze T., Varamashvili N., Devidze M., Chelidze Z., Chikladze V., and Matcharashvili T. (2002): Laboratory study of electromagnetic initiation of slip. *Ann. Geophysics*, 45 (5), 587-598.
- Chelidze T., De Rubeis V., Matcharashvili, and Tosi P. (2006) Influence of strong

- electromagnetic discharges on the dynamic of earthquakes time distribution in the Bishkek test area (Central Asia). Ann. Geoph., V.49, N. 4/5, P. 961-975.
- Gavrilov V.A., Bogomolov L.M., and Zakupin A.S. (2011) Comparison of the geoacoustic measurements in boreholes with the data of laboratory and in-situ experiments on electromagnetic excitation of rocks, *Izv., Phys. Solid Earth*, V. 42, N. 11, pp. 1009–1019.
 - Novikov V., Novikova E. (2014) Electromagnetic stimulation of fluid migration into fault area and earthquake triggering phenomena. *Geophys Res Abstr* 16: EGU201-14-12790.
 - Novikov V.A., Okunev V.I., Klyuchkin V.N., Liu J., Ruzhin Yu.Ya., Shen X. Electrical triggering of earthquakes: Results of laboratory experiments at spring-block models (2017) *Earthquake Science*, May, 2017. P. 1-6, DOI: 10.1007/s11589-017-0181-8.
 - Smirnov V.B, Zavyalov A.D. (2012) Seismic Response to Electromagnetic Sounding of the Earth's Lithosphere *Izvestiya, Physics of the Solid Earth*, Vol. 48, Nos. 7–8, pp. 615–639.
 - Sychev V.N. (2008) Study of Implications of Pulsed Energy Impacts for Variations in Spatial and Temporal Distributions of Seismic Activity in Northern Tien Shan, *Cand. Sci. (Phys.–Math.) Dissertations*, Moscow: Schmidt Inst. Phys. Earth, Rus. Acad. Sci.
 - Tarasov N.T. (1997) Crustal seismicity variation under electric action. *Trans. Russ. Acad. Sci.*, 353A (3), 445-448.
 - Tarasov N.T. and Tarasova N.V., Avagimov A.A., and Zeigarnik V.A. (1999). The effect of high energy electromagnetic pulses on seismicity in Central Asia and Kazakhstan, *Volc. Seismol.*, 4-5, 152-160.
 - Tarasov N.T., Tarasova N.V., Avagimov A.A., and Zeigarnik V.A., The Change in Seismicity at the Bishkek Geodynamic Test Site under Electromagnetic Impact (2001) *Geol. Geofiz.*, V. 42, N. 10, pp. 1641–1649.
 - Tarasov N.T. and Tarasova N.V. (2004) Spatial-temporal structure of seismicity of the North Tien Shan and its change under effect of high energy electromagnetic pulses. Ann. Geoph., V.47., N.1. 199-212.
 - Tarasov N.T. and Tarasova N.V. (2011) Influence of Electromagnetic Fields on the Seismotectonic Strain Rate; Relaxation and Active Monitoring of Elastic Stresses, *Izv. Phys. Earth.*, V. 47, N. 10, pp. 937–951.
 - Zakupin A.S., Alad'ev A.V., Bogomolov L.M.; et al. (2006). Interrelation between electric polarization and acoustic emission of geomaterials specimens under conditions of uniaxial compression. *Journal of Volcanology and Seismology (Vulkanologiya i Seismologiya)*, N. 6, (December 2006), pp. 22-33, ISSN 0203-0306
 - Zakupin, A.S., Avagimov A.A., and Bogomolov L.M. (2006) Responses of Acoustis Emission in Geomaterials to the Action of Electric Pulses under Various Values of the Compressive Load, *Izv. Phys. Earth*, V. 42, N. 10, pp. 830–837.
 - Zakupin A., Bogomolov L., Mubassarova V., Kachesova G., Borovskiy B. (2012) Acoustic Emission and Electromagnetic Effects in Loaded Rocks. In: *Acoustic Emission* / Ed. W. Sikorski. InTech, Rijeka, Croatia. 2012. Ch. 8. P. 173-198. ISBN: 978-953-51-0056-0.
 - Zakupin A. S., Bogomolov L. M., Mubassarova V. A., and Il'ichev P. V. (2014) Seismoacoustic Responses to High-Power Electric Pulses from Well Logging Data at the Bishkek Geodynamical Test Area. *Izvestiya, Physics of the Solid Earth*, 2014, Vol. 50, No. 5, pp. 692–706.
 - Zakupin A.S., Bogomolov L.M., Sychev V.N., Alad'ev A.V.,et al. (2006) Relationship between the electrical polarization and acoustic emission of geomaterial specimens at uniaxial compression (2006). *Vulkanol. Seismol.*, V. 6, pp. 22–33.

Chapter 6

*Earthquake and volcano related
phenomena investigation by
multidisciplinary and multi-parametric
approaches*

Intergeospheres interaction as a source of earthquake precursor's generation

S. Pulinet¹, D. Ouzounov²

¹*Space Research Inst., Russian Acad. of Sci, Moscow, Russia, pulse1549@gmail.com;* ²*CEESMO, Chapman University, Orange, CA, USA, ouzounov@chapman.edu*

Many researches considering the origin of the earthquake precursors propose different physical mechanisms giving them the names of main physical process (or agent) involved in the precursor generation: chemical mechanism, electromagnetic mechanism, radon mechanism, AGW mechanism etc. Our conception is based on paradigm that they are not the separate mechanisms, but are the parts of the common process of inter-geospheres interaction activated at the last stage of earthquake preparation cycle. All these mechanisms work together demonstrating synergy and synchronization in space and time.

The problem of trigger is a matter of special concern. For the first time we include in our approach the trigger concept and provide some attempts to formulate the relationship between the triggers and precursors. We introduce also the notion of earthquake retarders which may delay the moment of seismic shock or abolish it at all.

We should consider also the effects not only from the underground but also from above taking into account the events of the solar activity.

Local and regional stress-forecasting from Covasna fault, Romania

A. Apostol¹, I.A. Moldovan², V. Toader³, A. Muntean⁴, A. Mihai⁵

¹*Center for Bio-Seismology Covasna, Romania, apostoland77@yahoo.com;* ²*National Institute for Earth Physics, Magurele, 077125 Ilfov, Romania, irenutza_67@yahoo.com;* ³*National Institute for Earth Physics, Magurele, 077125 Ilfov, Romania, asyst@asystech.ro;* ⁴*National Institute for Earth Physics, Magurele, 077125 Ilfov, Romania, muntean@infp.ro;* ⁵*National Institute for Earth Physics, Magurele, 077125 Ilfov, Romania, mihai.andrei@infp.ro*

The paper presents the surveillance of tectonic stress around Covasna fault in relation with slow slip events in Vrancea, Romania and also with the occurrence of local and regional earthquakes.

Slow slip events (SSE) are produced by shear slip similar to earthquakes. However, SSE have longer characteristic duration of weeks, months and up to one or two years, in this way radiating much less or no seismic energy. It was found that the seismic moment of SSE is proportional to their characteristic duration. As a result, a SSE with one year duration can release stress equivalent to a magnitude earthquake Mw around 7. Most SSE occur down-dip of the region with normal earthquakes, at about 40 km deep, and they perturb the surrounding stress field either by releasing or increasing it. SSE was recognized in many seismic active regions of the world just before, after, or in the inter-seismic periods of large earthquakes. SSE can be detected by analyzing data from a network of stations with high quality GPS data. Starting with the year 1995 such a network of 28 GPS stations has been placed in and around Vrancea seismological active region, known with historical large and destructive intermediate-depth earthquakes. The coupling between the intermediate-depth slab and the crust was regarded as weak so no large amount of stress can be transferred from the slab to the crust. The vertical and horizontal displacements signals of all GPS stations in Vrancea are very small, of the order of 1-2 mm/year. During the years 2009-2018 the stress around Covasna Fault situated at about 50 km far from Vrancea was monitored by using the bio-location methodology. It was observed that stress increased during January 2010 till November 23rd 2013. On November 23rd 2013 the bio-location data was zero and this zero has been maintained for about 14 months till January 25th 2015. This situation suggested a large SSE equivalent of an earthquake with magnitude Mw larger than 7. Another SSE has been indicated by the same method on November 23rd 2017 for 3 months and still it is going on.

We cannot tell yet if this new SSE will release or increase the stress in Vrancea at an intermediate-depth. The paper will present a comparison between GPS and bio-location results for the above-mentioned periods.

Before earthquakes and volcanic eruptions can be observed changes to the geometry of stress-aligned fluid-saturated micro cracks around faults by using a **shear-wave splitting (SWS) methodology**. A review of retrospective stress-forecasts of local and regional earthquakes based on SWS showed a relationship between the magnitude of the event and the volume of rocks in the Earth's crust with such changes in the geometry of stress-aligned micro cracks. The same relationship obtained by SWS has been highlighted in the bio-location data obtained around Covasna Fault, Romania. Bio-location is based on sensing magneto-telluric phase splitting (MTPS) an electromagnetic equivalent of seismic SWS.

Local intermediate-depth earthquakes in Vrancea, Romania, with an epicentral distance of about 40 km and a magnitude M_L of 3-4, generated bio-location anomalies with a radius of a few hundreds of meters around Covasna Fault and duration of 4-5 days only. On the other hand, regional normal-depth earthquakes in Greece and Turkey with magnitudes M_w larger than 6.5 generated similar bio-location anomalies of hundreds meters-a few kilometers but a longer duration of about 15-20 days. A large earthquake with magnitude M_w 7.3 recorded November 12, 2017 on the Iran-Iraq border showed an anomaly with duration of 20 days during July 29-August 17, 2017. Similar to the Iran-Iraq event, regional earthquakes in Greece and Turkey with magnitudes M_w larger than 6.5 have been recorded at about 90 ± 15 days from the end of bio-location anomalies recorded around Covasna Fault. If the window of time has been indicated, the location could not be predicted. A new bio-location anomaly around Covasna Fault has been recorded during April 10-April 26, 2018, with duration of 17 days and radius around Covasna Fault as large as 3 kilometers. As a result a regional earthquake with magnitude around MW 7.0 is expected in a window of time July 15-August 15, 2018. This time we are trying to estimate the location for such an event based on the shape of bio-location anomaly in correlation to a possible earthquake precursor for the main shock. The bio-location anomaly around Covasna Fault increased in radius slowly from April 10-21 then changed the slope increasing sharply April 21-24, 2018. It was expected a significant earthquake precursor somewhere in the region on April 21. Such a supposed precursor for the main shock, with a magnitude M_L 4.8, was recorded at latitude 39.95 N and longitude 23.72 E along the Northern Aegean Trough, a western continuation of the Anatolian Fault from the Marmara Sea of Turkey to the Northern Aegean Sea of Greece.

Earthquake Prediction Preparedness and Disaster Management Studies in an around Nepal region

Sh. Choudhary¹, Su. Choudhary²

¹Peoples University, Bhopal, India, shubham.mbahar@gmail.com; ²Department of physics, Rabindranath Tagore, Raisen India, csuryansh@gmail.com

India has been traditionally vulnerable to natural disaster because of its unique geo climatic condition. Earthquake has been one of recurrent phenomena. Present study observes vulnerability in Nepal region and compared its risk assessment analysis. In this results huge loss in terms of human financial environmental and livelihoods. At global level there has been considerable concerned over natural disaster. In this paper we approach and proceed new conviction and development for sustainable disaster management.

A multidisciplinary geophysical approach to unravel geothermal processes in volcanic areas

G. Currenti¹, R. Napoli¹

¹*Istituto Nazionale di Geofisica e Vulcanologia, Catania, Italy, gilda.currenti@ingv.it; Istituto Nazionale di Geofisica e Vulcanologia, Catania, Italy, rosalba.napoli@ingv.it*

We illustrate the integrated modeling assessment of various induced geophysical changes in a volcano-hydrothermal system. Continuous observations of ground deformation, gravity and geomagnetic changes have been generally carried out on many active volcanoes (e.g. Bonforte et al. 2008; Napoli et al., 2008; Currenti et al., 2009; 2014) to detect the modifications of the stress field and of the thermodynamic state related to the magmatic system preceding and accompanying volcanic unrest (Napoli et al., 2011; Currenti et al., 2011; Battaglia et al., 2008). However, also non-magmatic sources associated to the perturbation of the hydrothermal system may produce observable geophysical signals (Coco et al., 2016). In particular, the hydrothermal activity results in the heating and pressurization of hydrothermal fluids, which in turn induces changes in different geophysical parameters. Fluid circulation, temperature and pore-pressure changes necessarily induce thermal, stress and strain variations, which alter the density distribution and the magnetization of the porous media and are reflected on the ground surface in observable variations in deformation, gravity and magnetic fields. Monitoring these geophysical observables, which are the surface expressions of processes that are not directly accessible, and developing modeling tools for their interpretation are the keys to open up new perspectives in the exploration and monitoring of hydrothermal areas.

In order to investigate how hydrothermal fluid circulation may affect ground deformation, magnetic and gravity changes, a multi-parametric thermo-poroelastic simulator is proposed, which jointly solves (i) the mass and energy balance equations for a multiphase ground-water flow, (ii) the elastostatic equation for evaluating the induced deformation field and (iii) the Poisson's equations for estimating the thermo-magnetic and gravity changes. Two well-established codes, TOUGH2 for simulating fluid-flow in porous media and COMSOL Multiphysics, for solving coupled Partial Differential Equations (PDE), are linked by programming new specific subroutines for automatic sequence execution and data transfer. To illustrate the feasibility of the numerical approach, computations are designed to model the

geophysical response of the hydrothermal system of Vulcano Island to a generic unrest period. Vulcano Island has been selected as a case study since: (i) its hydrothermal activity is suitable to be described by the presented numerical approach and to show its capability; (ii) geochemical, geological and volcanological investigations have provided the required information to set up the model material parameters (Chiodini et al., 1996; Granieri et al., 2006; Federico et al., 2010; Napoli and Currenti, 2016). Moreover, several geophysical data have been acquired over the last decades at Vulcano Island using different kinds of discrete and continuous measurement techniques, which may be used to assess the simulated results. Using a model-based approach, numerical results demonstrated that detectable geophysical changes may be revealed in association with the resumption of hydrothermal activity at Vulcano Island. Under the model assumptions, a generic unrest of 1-year engenders on the ground surface low amplitude changes in all the geophysical observables (Fig.1), that are, however, above the accuracies of the modern state-of-the-art instruments (in the order of a few mm, μ Gal and tenths of nT for deformation, gravity and magnetic changes) applied in volcano monitoring. Our findings strongly support the primary role of fluid circulation in La Fossa dynamics.

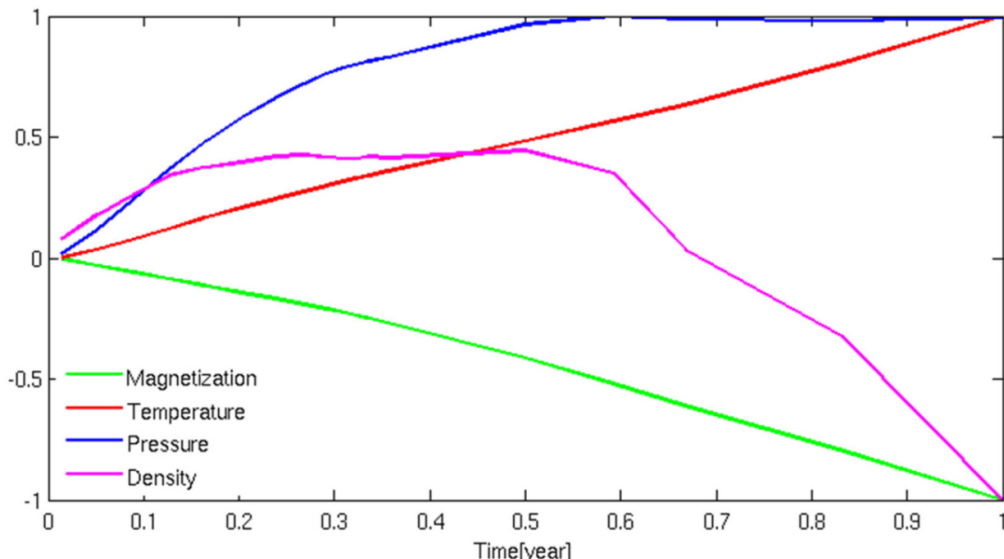


Fig 1 – Time evolution of the average normalized geophysical parameters computed over the whole domain.

References

- Battaglia, M., Gottsmann, J., Carbone, D. and Fernández, J. (2008). 4D volcano gravimetry, *Geophysics*, 73, 6, doi: 10.1190/1.2977792.
- Bonforte A., Bonaccorso A., Guglielmino F., Palano M., Puglisi G. (2008). Feeding system and magma storage beneath Mt. Etna as revealed by recent inflation/deflation cycles. *J. Geophys. Res.* 113, B05406, doi:10.1029/2007JB005334.

- Chiodini, G., F. Frondini, B. Raco, (1996), Diffuse emission of CO₂ from the Fossa crater, Vulcano Island (Italy), *Bull Volcanol.*, 58, 41–50.
- Coco, A., Currenti, G., Gottsmann, J., Russo, G. and Del Negro, C. (2016) A hydrogeophysical simulator for fluid and mechanical processes in volcanic areas, *Journal of Mathematics In Industry*, 6, 6, doi: 10.1186/s13362-016-0020-x. Comsol Multiphysics 4.3 (2012), Comsol Ab, 1356 pp, Stockholm, Sweden.
- Currenti, G. (2014) Numerical Evidences Enabling To Reconcile Gravity And Height Changes In Volcanic Areas. *Geophysical Journal International*. doi: 10.1093/Gji/Ggt507
- Currenti G., Napoli R., Di Stefano A., Greco F., Del Negro C. (2011). 3D integrated geophysical modeling for the 2008 magma intrusion at Etna: constraints on rheology and dike overpressure. *497 Physics of the Earth and Planetary Interiors*, 168, 88–96.
- Currenti, G., Del Negro C., Di Stefano, A., Napoli, R., (2009). Numerical simulation of stress induced piezomagnetic fields at Etna volcano. *Geophys. J. Int.*, 179, 1469-1476, doi: 10.1111/j.1365-5002.2009.04381.x.
- Federico, C., Capasso, G., Paonita, A., Favara, R., 2010. Effects of steam-heating processes on a stratified volcanic aquifer: stable isotopes and dissolved gases in thermal waters of Vulcano Island (Aeolian archipelago). *J. Volcanol. Geotherm. Res.* 192, 178–190. <http://dx.doi.org/10.1016/j.jvolgeores.2010.02.020>.
- Granieri, D., M. L. Carapezza, G. Chiodini, R. Avino, S. Caliro, M. Ranaldi, T. Ricci, and L. Tarchini (2006), Correlated increase in CO₂ fumarolic content and diffuse emission from La Fossa crater (Vulcano, Italy): Evidence of volcanic unrest or increasing gas release from a stationary deep magma body? *Geophys. Res Lett.*, vol. 33, L13316, doi:10.1029/2006GL026460.
- Napoli, R., and Currenti, G. (2016), Reconstructing the Vulcano Island evolution from 3D modeling of magnetic signatures. *Journal Of Volcanology And Geothermal Research* 320, 40 – 49, doi:10.1016/j.jvolgeores.2016.04.011.
- Napoli R, Currenti G, Del Negro C, Di Stefano A, Greco F, Boschi E (2011) Magnetic features of the magmatic intrusion that occurred in the 2007 eruption at Stromboli Island (Italy). *Bull Volcanol* 553 DOI 10.1007/s00445-011-0473-0
- Napoli, R., G. Currenti, C. Del Negro, F. Greco and D. Scandura, 2008. Volcanomagnetic evidence of the magmatic intrusion on 13th May 2008 Etna eruption, *Geophys. Res. Lett.*, 35, L22301, 550 doi:10.1029/2008GL035350.

Characteristics of Optical and Microwave responses of land and meteorological parameters Associated with Earthquakes

F. Jing^{1,2}, R.P. Singh¹

¹School of Life and Environmental Sciences, Schmid College of Science and Technology, One University Drive, Orange, CA 92866, USA, rsingh@chapman.edu, ²Institute of earthquake forecasting, China earthquake administration, Beijing, 100036, China, jennyfer1111@163.com

In the last two decades, land, ocean, meteorological and atmospheric parameters have been studied around the epicentral and surrounding regions. These parameters have shown anomalous behavior few days, weeks and months prior to an earthquake. Some of these parameters increase/decrease after the earthquake. The earth is complex, spatial distributions of earthquakes are characterized by geological and geophysical environment, fault types, proximity to the ocean, hydrological regime, and past seismicity etc. The Gujarat earthquake of 26 January 2001 is one of the well studied earthquakes utilizing ground, meteorological and atmospheric parameters and observed some anomalous and characteristic variations of many parameters. Similar to the Gujarat earthquake, we have analyzed satellite derived multi-parameters of land, meteorology and atmosphere of 2015 M_W7.8 Gorkha earthquake. We considered three boxes of 2°x2°, one each in Tibetan Plateau of China, Nepal and Indian region, located in different geomorphologic regions and have analyzed passive microwave brightness temperature, soil moisture, rainfall and carbon monoxide for the periods 2014-2016, one month prior and one month after the earthquake. The microwave brightness temperature at different frequencies show similar fluctuations in each grid. But the variations in box over India is observed to be different from other two boxes over the epicentral and Tibetan regions. The brightness temperature shows characteristic behaviour for different frequencies in two polarizations (horizontal and vertical) over three boxes. The characteristics over three boxes depend on the soil moisture at two different layers, surface 0-10 cm and subsurface 10-200 cm. We have also analysed some of the greenhouse gases and meteorological parameters retrieved from satellite data. An integration of information retrieved from passive microwave sensor and ground, atmospheric and meteorological parameters from optical sensor will be discussed for an early warning about an impending earthquake.

Are deep-sea fish appearances an earthquake precursor?

Y. Orihara¹, M. Kamogawa², Y. Noda³, T. Nagao⁴

¹*Institute of Oceanic Research and Development, Tokai University, Shizuoka, Japan, orihara@tsc.u-tokai.ac.jp;*

²*Department of Physics, Tokyo Gakugei University, Tokyo, Japan, kamogawa@u-gakugei.ac.jp; ³Tierra Tecnica*

*Ltd., Tokyo, Japan; ⁴Institute of Oceanic Research and Development, Tokai University, Shizuoka, Japan,
nagao@scc.u-tokai.ac.jp*

Unusual animal behavior before earthquakes (EQs) has been known as the most famous macroscopic anomaly prior to the EQs all over the world (e.g. Tributsch, 1985). The unusual animal behavior in Japan has been reported for not only inland animals such as dogs and birds but also marine species such as fish and cetaceans, some of which might be caused by the pre-seismic geo-electromagnetic change (e.g., Ikeya, 2004). Terada (1932a,b; 1933) denoted that the catch of horse mackerel around the west coast of Izu Peninsula was positively correlated with swarm EQs off the east coast of Izu Peninsula in 1930. On the other hand, Orihara and Noda (2015) concluded that a mass stranding of Melon-headed whales (*Peponocephala electra*) at the Kashima-Nada beach, Japan on March 4, 2011, i.e., seven days before the 2011 M9.0 Off the Pacific coast of the Tohoku EQ and the mainshock showed no correlation. Some reports claimed that deep-sea fish washed on shore before EQs (Rikitake, 1976; Suehiro, 1968; 1976). Deep-sea fish washing on shore has been frequently reported by the local newspaper because they are rare events. In order to statistically investigate the relationship between the deep-fish appearances and the EQs, we constructed the database based on the articles of Japanese newspapers and academic papers concerning deep-sea fish appearances. From our investigation, the correlation between the deep-sea fish appearances and the earthquakes was hardly found.

Acknowledgments

This study was supported by the Earthquake Research Institute, the University of Tokyo Joint Usage/Research Program, and the Ministry of Education, Culture, Sports, Science and Technology (MEXT) of Japan, under its Observation and Research Program for Prediction of Earthquakes and Volcanic Eruptions.

Experimental study of Radon activity associated with pre-earthquake phenomena observed in the Earth atmosphere-ionosphere environment

D. Ouzounov¹, S. Pulinets², L.C. Lee³, C.C. Fu³, V. Karastathis⁴, K. Tsinganos^{4,5}, M. Kafatos¹, N. Hatzopoulos¹, G. Eleftheriou⁴, K. Hattori⁶

¹CEESMO, Chapman University, Orange, CA, USA, Ouzounov@chapman.edu; ²Space Research Inst., Russian Academy of Sciences, Moscow, Russia, pulse1549@gmail.com; ³Institute of Earth Sciences, Academia Sinica, Taiwan, louclee@earth.sinica.edu.tw; ⁴National Observatory of Athens, Athens, Greece, karastathis@noa.gr; ⁵National and Kapodistrian University of Athens, Athens, Greece, tsingan@phys.uoa.gr; ⁶Department of Earth Sciences, Chiba University, Chiba, Japan, hattori@earth.s.chiba-u.ac.jp

We are presenting experimental data and theoretical estimates of radon measurements recorded before large earthquakes. We use radon measurements on the ground installed and coordinated in four different seismic active regions: Southern California, Taiwan, South Western Greece and South Eastern Japan. Radon measurements are obtained indirectly by means of gamma ray spectrometry of its radioactive progenies ^{214}Pb and ^{214}Bi (emitted at 351 keV and 609 keV, respectively) and also by Alpha detectors. We studied also the correlation of radon pre-earthquake anomalies with the temperature of the atmosphere boundary layer, outgoing earth infrared radiation and GPS/TEC, namely their temporal and spatial variations several days before the onset of recent earthquakes. We have found that: (i) large seismic events (M8+) could produce radon anomalies far from the epicenters, such as the 2017 M8.2 in Mexico where we observed an anomaly 3200 kilometers north (in Orange, Southern California) 6 days in advance of the main shock. (ii) Long lasting seismic swarms (as in Taiwan) could generate temporary elevation of radon levels in the near zone, but radon levels immediately return back to normal when the seismicity becomes low; (iii) the low magnitude local seismicity could produce dominant anomalies for the radon data (as in the Peloponnese, Greece). We have observed that detection of remote earthquakes is possible in case of low local seismicity.

Our data analysis in California, Taiwan, Greece and Japan suggest that pre-earthquake phase follows a general temporal-spatial evolution pattern in which radon plays a critical role in understanding the LAI coupling, involving different layers of the ionosphere, atmosphere and lithosphere. This pattern could be revealed only with multi instrument observations and has been seen in other large earthquakes worldwide.

Multi-parameter assessment of pre-earthquake atmospheric - ionospheric signals and their potential for short-term prediction

D. Ouzounov¹, S. Pulinet², J.Y. Liu³, K. Hattori⁴, P. Han⁵

¹CEESMO, Chapman University, 1 University Drive, Orange, CA 92866, USA, Ouzounov@chapman.edu;

²Space Research Inst., Russian Acad. of Sci, 84/32 Profsoyuznaya, Moscow, 117997, Russia,

pulse1549@gmail.com; ³Institute of Space science, National Central University, Chung-Li 320,Taiwan, tigerjylu@gmail.com; ⁴Department of Earth Sciences, Chiba University, Inage, Chiba, 263-8522, Japan , hattori@earth.s.chiba-u.ac.jp; ⁵Southern University of Science and Technology, Shenzhen, China,

hanpeng407@gmail.com

We apply interdisciplinary observations to study earthquake (EQ) processes, their physics and the phenomena that precede their energy release. Our approach is based on multi-sensors observations of short-term pre-earthquake phenomena preceding large earthquakes ($M > 6$). Our method for validation and are based on sensor web of several physical and environmental parameters: (i)Satellite thermal infrared radiation (STIR), (ii)electron concentration in the ionosphere (GPS/TEC), (iii) air temperature and relative humidity measurements) that were associated with earthquakes. The science rationale for multidisciplinary analysis is founded on the concept Lithosphere-Atmosphere-Ionosphere-Magnetosphere Coupling (LAIMC). To check the predictive potential of pre-earthquake signals we validate in retrospective and prospective modes. Our validation processes consist in two steps: (1) A retrospective analysis preformed over three different regions with the high seismicity-case study for M6.0 Napa 2014, M6.0 Taiwan 2016, and M7.0 Kumamoto, Japan 2016, (2) Testing of Molchan's Error Diagram (MED) for STIR and dTEC anomalies events over Japan and Taiwan. Our findings suggest that: Pre-earthquake signals follow a general temporal-spatial evolution pattern (win 1-30 days) and MED results indicate that pre-earthquake atmospheric anomalies can provide short-term predictive information for the occurrence of major earthquakes in the tested regions.

Reference

Pre-Earthquake Processes: A Multi-disciplinary Approach to Earthquake Prediction Studies, AGU Geophysical Monograph series, vol.234, AGU/Wiley, 2018, (Ed's: Ouzounov D., S. Pulinet², K.Hattori, P.Taylor)

Transient Effects in Atmosphere and Ionosphere preceding the 2015 M7.8 and M7.3 Gorkha–Nepal earthquakes

D. Ouzounov¹, A. Rozhnoi², S. Pulinets³, D. Davidenko³, M. Solovieva², V. Fedun⁴, A. Srivastava⁵, A. Rybin⁶

¹*Center of Excellence for Earth Systems Science & Observations, Chapman University, CA, USA,
Ouzounov@chapman.edu;* ²*The Schmidt Institute of Physics of the Earth, RAS, Moscow, Russia, rozhnoi@ifz.ru;*

³*Space Research Institute, RAS, Moscow, Russia, pulinets1549@gmail.com;* ⁴*University of Sheffield, Sheffield,
UK, v.fedun@sheffield.ac.uk;* ⁵*Indian Institute of Technology, Varanasi, India, asrivastava.app@itbhu.ac.in;*

⁶*Research Station RAS, Bishkek, Kyrgyzstan, rybin@gdirc.ru*

We analyze retrospectively/prospectively the transient variations of four different physical parameters of atmosphere/ionosphere during the time of M7.8 and M7.3 events in Nepal namely: (i) thermodynamic proprieties in the lower atmosphere, (ii) outgoing earth radiation (OLR) at the TOA, (ii) GPS/TEC and (iv) the very low-frequency (VLF/LF) signals at the receiving stations in Bishkek (Kyrgyzstan) and Varanasi (India). We found that in mid March 2015 a rapid augment of satellite observed earth radiation in atmosphere and the anomaly located in close vicinity to the future M7.8 epicenter reached the maximum on April 21-22. The GPS/TEC data analysis indicates an augment and variation in electron density reaching a maximum value during April 22-24 periods. A strong negative TEC anomaly in the crest of EIA (Equatorial Ionospheric Anomaly) has occurred on April 21st and strong positive on April 24th, 2015. Two VLF/LF crossing wave paths - NWC-Bishkek and JJY-Varanasi, have shown abnormal behavior of signals during on days April 21-23 several days before the first, stronger earthquake. Our continuous satellite OLR analysis revealed prospectively the new strong anomaly on May 3th, which was the reason to contemplate another large event in the area. On May 12, 2015 a M7.3 has occurred. Our results show coherence between the appearance of pre-earthquake transients effects in atmosphere and ionosphere (with a short time-lag, from hours up to few days) and the occurrence of 2015 M7.8 and M7.3 events in Nepal. The spatial characteristics of pre-earthquake anomalies were associated with large area but inside the preparation region estimated by Dobrovolsky ratio. The pre- earthquake nature of the signals in atmosphere and ionosphere were revealed by simultaneous analysis of satellite, GPS/TEC and VLF/LF observations and suggest that they follow a general temporal-spatial evolution pattern, which has been seen in other large earthquakes worldwide.

Ground geochemical observations for Earthquake and Volcano investigations: the example of the Geochemical Monitoring Network of Tuscany

L. Pierotti¹, G. Facca¹, F. Gherardi¹

¹CNR - Istituto di Geoscienze e Georisorse, Pisa, Italy, l.pierotti@igg.cnr.it; gianluca.facca@igg.cnr.it; f.gherardi@igg.cnr.it

As a part of a seismic prevention/prediction pilot project, the Regional Government of Tuscany, Italy, has financially supported the setup of a monitoring network (the Geochemistry Network of Tuscany, thereafter GNT) for studying possible geochemical precursors to seismic activity (Cioni et al., 2007). The GNT is operating since late 2002, and currently consists of six continuous automatic stations installed in the areas of highest seismic risk of Tuscany: Garfagnana, Lunigiana, Mugello, Upper Tiber Valley and Mt. Amiata (Fig. 1). Together with other monitoring networks of Tuscany (i.e. seismic, accelerometric and geodetic networks), the GNT is officially recognized by the Regional Government of Tuscany (Law n. 58 of 16 October 2009) as a “reference tool for the analysis and research on seismic risk”.

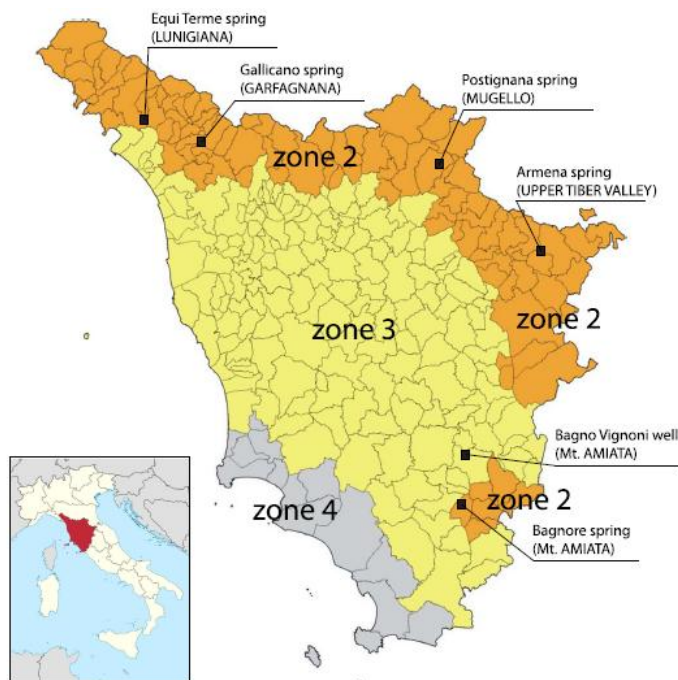


Fig. 1. Seismic classification of the Tuscany Region, Italy. Orange: seismic zone 2 (highest seismic risk level of the region), yellow: seismic zone 3, gray: seismic zone 4. Blue squares: location of the automatic stations of the Geochemical Network of Tuscany.

The IGG-CNR-Pisa continuous automatic monitoring stations (Cioni et al., 2007) are equipped with sensors for the simultaneous measurement in water of a suite of different parameters (Fig. 2), believed to be informative of the processes possibly associated to the energy release and/or the permeability variations induced by seismogenic processes (e.g. temperature, salinity, redox potential, pH, concentration of selected aqueous and/or dissolved gaseous components, as CO₂ and CH₄), to ensure cross-checking of independent signals. The measurement of CO₂ and CH₄ dissolved concentration is done with an extraction cell, where the gas is equilibrated in the headspace above the water level inside the cell, and transferred to a closed loop equipped with an I.R. spectrometer and a low-flow pump used to provide the necessary gas circulation in the loop.



Fig. 2. The IGG-CNR-Pisa continuous automatic monitoring stations: left) cupboards containing the electronics. right) Cells dedicated to physicochemical water parameters and to the concentration of dissolved gases measure.

The system was calibrated with external standard gas supply. The other parameters are calibrated with manual calibration procedures done on a monthly basis, and/or in conjunction with anomalous variations of the signals, using high precision portable instrumentation. At the same time of calibration operations, aliquots of water are collected for the in situ analysis of bicarbonates and the determination in laboratory of the main chemical constituents (Na, K, Ca, Mg, Cl, SO₄, SiO₂, F, B). Data obtained by discrete monitoring are processed with speciation programs to numerically cross-check CO₂ concentration values measured by the automatic station.

The automatic monitoring station operated with flowing water (about 5 L/min) and the monitoring is strictly continuous (1 datum every five minutes), to ensure the capability to detect abrupt and discontinuous signal variations. Data are transmitted once a day to CNR-IGG by router GPRS.

The acquisition of very long time series of several hundreds of thousands data for each station allowed to accurately and precisely define the natural geochemical baseline of the

monitored manifestations. Statistical analysis (using autocorrelations and/or Fourier techniques, etc.) highlighted short and long-term trends and/or signals periodicity due to seasonal variations and/or terrestrial tides (Gherardi & Pierotti, 2018). In each test site, geochemical data have been integrated with geological, structural and hydrogeological information to decipher the mechanisms that control the movement of underground waters (e.g. Pierotti et al., 2016), and to develop updated hydrogeological models (e.g. Pierotti et al., 2013; Gherardi & Pierotti, 2018).

Data series were analyzed then with multiple statistical techniques (Artificial Neural Networks analysis, 2σ method and by applying the Census I method) in order to identify possible anomalous variations related to seismic activity.

A number of CO₂ anomalies (Fig. 3) have been registered in different sites during the last fifteen years of active monitoring. In particular, significant anomalies in the CO₂ signal have been recognized at Gallicano over the period 2003–2013 in concomitance with three major seismic events occurred in Northern Tuscany and Emilia Romagna regions, not far from the monitoring site (Pierotti et al., 2015).

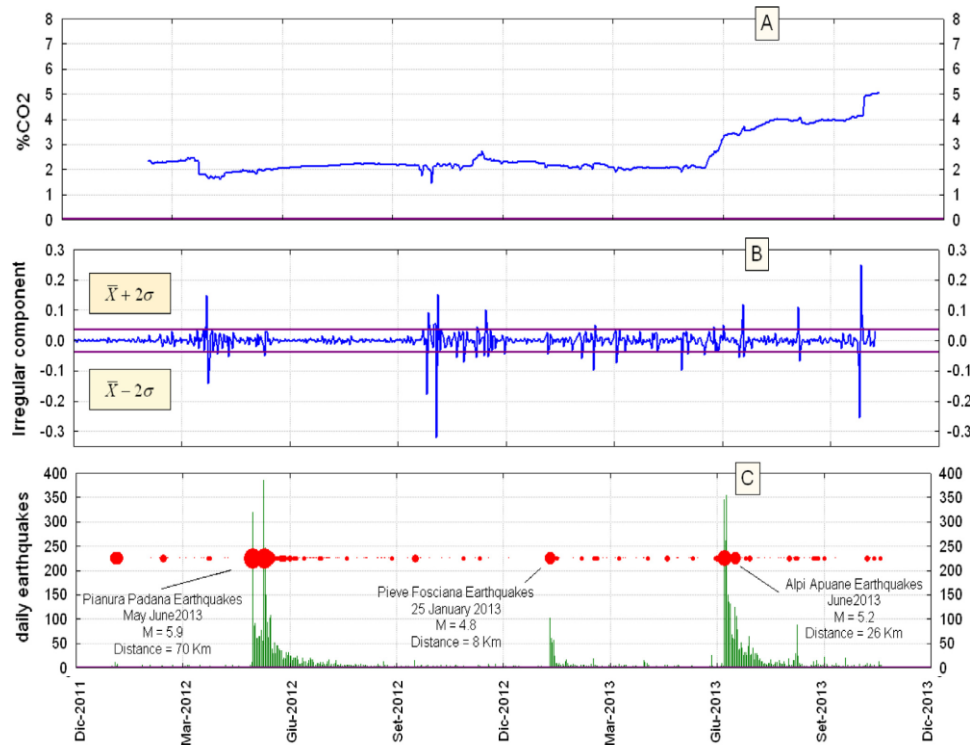


Fig. 3. CO₂ continuous signal registered at Gallicano (box A) and its irregular component after processing with Census I method (box B). The seismic activity (box C) is also given for the period December 2011–December 2013. In Box B, green bars represents the number of daily events, red dots the seismic events with $M \geq 2.5$, being the dots radius proportional to the event magnitude. (after Pierotti et al., 2015).

Similarly, at Bagnore, on the southwestern slopes of the Mt. Amiata volcano, inspection of CO₂ time series over the 2004-2015 period, revealed the existence of punctual anomalies (Fig. 4) associated with the most energetic event seismic events registered in the area within a radial distance of 40 km from the monitoring site (Pierotti et al., 2017).

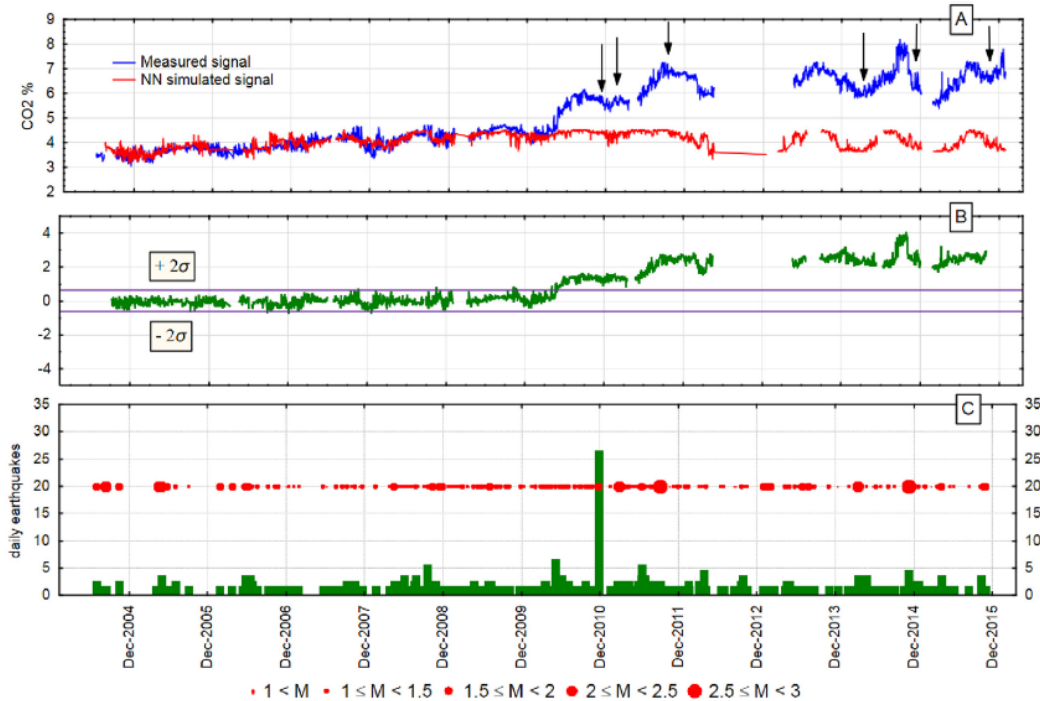


Fig. 4. CO₂ continuous signal registered at Bagnore (blue line; box A) compared with CO₂ signal simulated and forecasted by neural network (ANN; red line). (Box B) Difference between measured signal and ANN simulated signal. (Box C) Seismic activity. Seismic information from the Italian Seismological Instrumental and parametric Database (ISIDE): <http://iside.rm.ingv.it>). (after Pierotti et al., 2017).

Based on this research, CO₂ comes out as the most efficient tracer of the chemical-physical processes occurring at depth, possibly associated to the energy release and/or the permeability variations induced by seismogenic processes. The statistical processing of CO₂ continuous signal emerges as a powerful and essential tool to ensure a reliable identification of anomalies, and to possibly increase the confidence in the use of geochemical precursors of earthquakes.

References

- Cioni, R., Guidi, M., Pierotti, L., Scozzari, A., 2007. An automatic monitoring network installed in Tuscany (Italy) for studying possible geochemical precursory phenomena. Nat. Hazards Earth Syst. Sci. 7, 405–416.
- Gherardi F., Pierotti L., 2018. The suitability of the Pieve Fosciana hydrothermal system (Italy) as a detection site for geochemical seismic precursors. Applied Geochemistry 92, 166 –179.

- Pierotti, L., Botti, F., Bracaloni, S., Burresi, I., Cattaneo, M., Gherardi, F., 2013. Hydrogeochemistry of Magra Valley (Italy) aquifers: geochemical background of an area investigated for seismic precursors, Water Rock Interaction [WRI 14]. Procedia Earth Planet. Sci. 7, 697–700.
- Pierotti, L., Botti, F., D'Intinosante, V., Facca, G., Gherardi, F., 2015. Anomalous CO₂ content in the Gallicano thermo-mineral spring (Serchio Valley, Italy) before the 21 June 2013, Alpi Apuane Earthquake (M = 5.2). Phys. Chem. Earth 85–86, 131–140.
- Pierotti, L., Cortecchi, G., Gherardi, F., 2016. Hydrothermal gases in a shallow aquifer at Mt. Amiata, Italy: insights from stable isotopes and geochemical modelling. Isotopes in Environmental and Health Studies 52, 4–5, 414–426.
- Pierotti, L., Gherardi, F., Facca, G., Piccardi, L., Moratti, G., 2017. Detecting CO₂ anomalies in a spring on Mt. Amiata volcano (Italy). Physics and Chemistry of the Earth 98, 161–172.

Compatibility of different electromagnetic precursors in terms of critical dynamics

S.M. Potirakis¹, Y. Contoyiannis¹, T. Asano², A. Schekotov³, M. Hayakawa², K. Eftaxias⁴

¹*Department of Electrical and Electronics Engineering, University of West Attica, Campus 2, 250 Thivon and P. Ralli, Aigaleo, GR-12244, Athens, Greece, spoti@puas.gr, yiaconto@puas.gr;* ²*Hayakawa Institute of Seismo Electromagnetics Co. Ltd., UEC (University of Electro-Communications) Alliance Center #521, 1-1-1 Kojimacho, Chofu, 182-0026, Tokyo, Japan, asano@hi-seismo-em.jp, hayakawa@hi-seismo-em.jp;* ³*Institute of Physics of the Earth, Russian Academy of Sciences, 10 Bolshaya Gruzinskaya, 123995, Moscow, Russia, sasha.schekotov@gmail.com;* ⁴*Department of Physics, University of Athens, Panepistimiopolis, Zografos, GR-15784, Athens, Greece, ceftax@phys.uoa.gr*

A wide variety of electromagnetic (EM) phenomena possibly related with earthquake (EQ) preparation processes have been reported in the literature during the last few decades [e.g., Hayakawa and Molchanov, 2002; Pulinets and Boyarchuk, 2005; Varotsos, 2005; Molchanov and Hayakawa, 2008; Hattori, 2013; Eftaxias and Potirakis, 2013; Uyeda, 2013; Hayakawa, 2015; Eftaxias et al. 2018]. Nevertheless, EM precursors are still a highly disputed topic among scientists of different disciplines. Scientific studies related to EQ precursors, and particularly in the case of short-term prediction, are often faced with intense skepticism [Uyeda et al., 2009]. For this reason, there is a need for rigorous study of EM precursors aiming at revealing features advocating their seismogenic origin.

An interesting aspect in their study is the time-series analysis of the related observables aiming at the investigation of their statistics and any embedded dynamics which may reflect corresponding properties of EQ preparation. Based on a multidisciplinary analysis, the following four-stage model of EQ dynamics by means of precursory fracto-electromagnetic emissions (MHz- kHz EME) has recently been proposed [Eftaxias et al., 2018]:

- First stage: The initially observed MHz EM anomaly is due to the fracture of the highly heterogeneous system that surrounds the formation of strong brittle and high-strength entities (asperities) distributed along the rough surfaces of the main fault sustaining the system. The MHz EME can be described by means of a second-order phase transition in equilibrium.
- Second stage: The appearance of tri-critical behavior in the final stage of MHz EME, or in the initial stage of kHz EME, or in both, signalizes a next, distinct, state of the EQ preparation process.
- Third stage: The finally abruptly emerging strong sequence of kHz EM avalanches

originates in the stage of stick-slip-like plastic flow, namely, the fracture of asperities themselves. The burst-like kHz EME does not present any footprint of a second-order transition in equilibrium.

- Fourth stage: Finally, the systematically observed EM silence in all frequency bands before the time of the EQ occurrence is sourced in the process of preparation of the dynamical slip which results to the fast, even super-shear, mode that surpasses the shear wave speed and corresponds to the observed EQ tremor.

In this work we investigate the possible compatibility of different EM precursors in terms of the time period prior to a significant ($M \geq 5.5$) EQ during which they present critical dynamics, as well as in terms of their departure from the critical state. Specifically, we refer to the fracto-electromagnetic emissions (EME) at the MHz band, the ultra-low frequency (ULF) magnetic field variations (<10 Hz) and the sub-ionospheric very low frequency (VLF) propagation anomalies. The findings of our analysis during the last few years suggest that the EM precursors considered in this work emerge during the same spatially extensive phase of earthquake preparation, which corresponds to the first stage of the abovementioned four-stage model.

The fracture of a heterogeneous system has been suggested to follow the following timeline [Eftaxias et al., 2018, and references therein]: In the early stages of deformation, when the disordered medium is subjected to external load, the weak components break immediately and serve as nucleation centers for the growth of broken clusters. The load transferred to the nearest neighbors of broken components gives rise to further breaking. As deformation proceeds, cooperative effects appear, cracking areas cluster in space according to scale-free patterns and are dynamically interacting to each other. As the external load increases, larger clusters are formed and long-range correlations buildup through local interactions until they extend throughout the entire system. All these results advocate for a critical point interpretation of failure. The analysis of the time-series of the EM precursors presented in this work shows that these anomalies include the above mentioned critical features. Specifically, there has been detected a “critical epoch” during which the “short-range” correlations evolve into “long-range” ones, as well as the epoch of localization of the damage (departure from critical state).

Using two independent methods which are known for their ability to uncover critical dynamics, the recently proposed methods referred to as the method critical fluctuations (MCF) [Contoyiannis and Diakonos, 2000, 2007; Contoyiannis et al., 2002, 2015] and the natural time (NT) analysis [Varotsos et al., 2011], we have lately analyzed time-series of the

abovementioned precursors possibly related to a number of recent (2008-2017) significant EQs which occurred in Greece [Potirakis et al., 2015, 2016a; Contoyiannis et al., 2017], China [Hayakawa et al., 2015a] and Japan [Hayakawa et al. 2015b; Contoyiannis et al., 2016; Potirakis et al., 2016b, 2018a, 2018b, 2018c, 2018d].

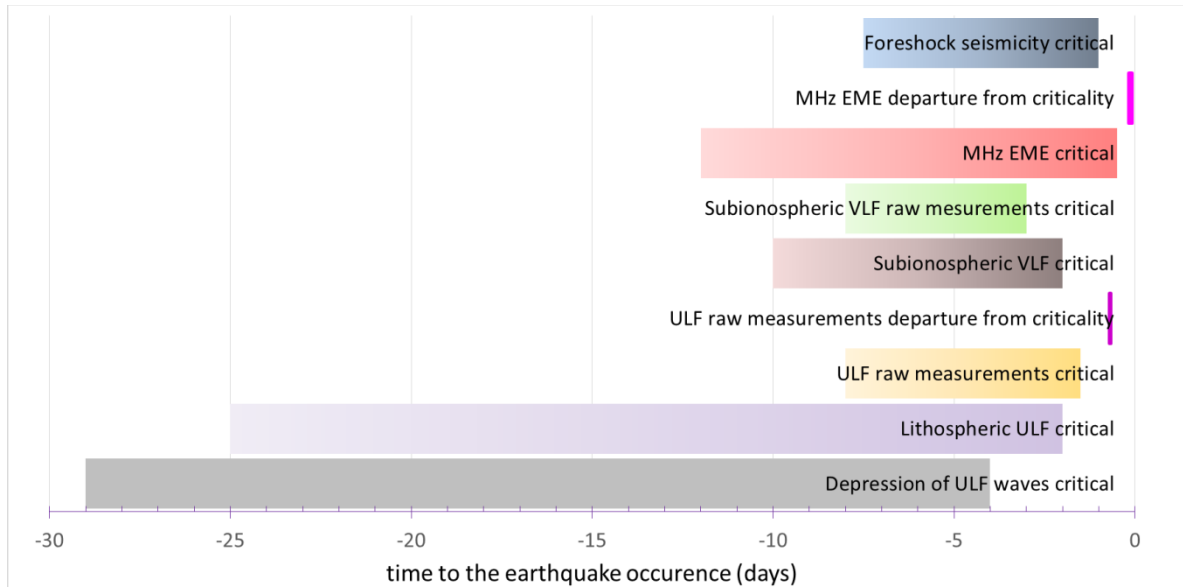


Fig. 1. Time periods prior to the EQ occurrence within which critical dynamics have been revealed in different electromagnetic precursors for recent EQs. The time period during which foreshock seismicity reached critical dynamics for some of them is also depicted, as well as the time of departure from criticality.

Our analysis results have shown that critical dynamics appear from a few days to a few weeks before the main shock (Fig. 1), while evidence for departure from criticality have been identified after the critical state even a few hours before the EQ occurrence. The aforementioned time window implies that the related EQ preparation processes happen during the same spatially extensive phase of earthquake preparation which is characterized by critical dynamics. We note that the specific time window is also compatible with the period during which foreshock seismicity has been found to reach criticality for the same EQ cases (see Fig. 1).

References

- Contoyiannis, Y., F. Diakonos, Criticality and intermittency in the order parameter space, *Phys. Lett. A* **268**, 286-292 (2000), [http://dx.doi.org/10.1016/S0375-9601\(00\)00180-8](http://dx.doi.org/10.1016/S0375-9601(00)00180-8).
- Contoyiannis, Y.F., F.K. Diakonos, Unimodal maps and order parameter fluctuations in the critical region, *Phys. Rev. E* **76**, 031138 (2007), <http://dx.doi.org/10.1103/PhysRevE.76.031138>.

- Contoyiannis, Y., F. Diakonos, A. Malakis, Intermittent dynamics of critical fluctuations, Phys. Rev. Lett. **89**, 035701 (2002), <http://dx.doi.org/10.1103/PhysRevLett.89.035701>.
- Contoyiannis, Y., S.M. Potirakis, K. Eftaxias, L. Contoyianni, Tricritical crossover in earthquake preparation by analyzing preseismic electromagnetic emissions, J. Geodynamics **84**, 40-54 (2015), <http://dx.doi.org/10.1016/j.jog.2014.09.015>.
- Contoyiannis, Y., S.M. Potirakis, K. Eftaxias, M. Hayakawa, A. Schekotov, Intermittent criticality revealed in ULF magnetic fields prior to the 11 March 2011 Tohoku earthquake (Mw=9), Physica A 452, 19–28 (2016), <http://dx.doi.org/10.1016/j.physa.2016.01.065>.
- Contoyiannis, Y., S. M. Potirakis, J. Kopanas, G. Antonopoulos, G. Koulouras, K. Eftaxias, C. Nomicos, On the recent seismic activity at eastern Aegean Sea: Analysis of fracture-induced electromagnetic emissions in terms of critical fluctuations, arXiv: 1708.00320v1 (2017), <https://arxiv.org/pdf/1708.00320>.
- Eftaxias, K., S.M. Potirakis, Current challenges for pre-earthquake electromagnetic emissions: shedding light from micro-scale plastic flow, granular packings, phase transitions and self-affinity notion of fracture process, Nonlin. Processes Geophys. **20**, 771–792 (2013), <http://dx.doi.org/10.5194/npg-20-771-2013>.
- Eftaxias, K., S.M. Potirakis, Y. Contoyiannis, Four-Stage Model of Earthquake Generation in Terms of Fracture-Induced Electromagnetic Emissions A Review, in *Complexity of Seismic Time Series: Measurement and Application*, edited by T. Chelidze, F. Vallianatos, L. Telesca (Elsevier, Oxford, UK., 2018), ISBN: 9780128131381, <https://doi.org/10.1016/B978-0-12-813138-1.00013-4> (In Press), pp. 437-502.
- Hayakawa, M., *Earthquake Prediction with Radio Techniques* (Wiley, Singapore, 2015), ISBN: 9781118770160.
- Hayakawa, M., O.A. Molchanov, (Eds.), *Seismo Electromagnetics: Lithosphere-Atmosphere-Ionosphere Coupling* (TERRAPUB, Tokyo, 2002), ISBN: 4887041306.
- Hayakawa, M., A. Schekotov, S.M. Potirakis, K. Eftaxias, Q. Li, T. Asano, An integrated study of ULF magnetic field variations in association with the 2008 Sichuan earthquake, on the basis of statistical and critical analyses, Open J. Earthq. Res. **4**, 85-93 (2015a). <http://dx.doi.org/10.4236/ojer.2015.43008>.
- Hayakawa, M., A. Schekotov, S. Potirakis and K. Eftaxias, Criticality features in ULF magnetic fields prior to the 2011 Tohoku earthquake, Proc. Japan Acad. Ser. B 91, 25-30 (2015b). <http://dx.doi.org/10.2183/pjab.91.25>.
- Hattori, K., ULF geomagnetic changes associated with major earthquakes, in *Earthquake Prediction Studies; Seismo Elecromagnetics* edited by M. Hayakawa (TERRAPUB, Tokyo, 2013), ISBN: 9784887041639, pp. 129-152.
- Molchanov, O.A., M. Hayakawa, *Seismo Electromagnetics and Related Phenomena: History and latest results* (TERRAPUB, Tokyo, 2008), ISBN: 9784887041431.
- Potirakis, S.M., Y. Contoyiannis, K. Eftaxias, G. Koulouras, C. Nomicos, Recent field observations indicating an Earth system in critical condition before the occurrence of a significant earthquake, IEEE Geosci. Rem. Sens. Lett. **12**(3), 631-635 (2015), <http://dx.doi.org/10.1109/LGRS.2014.2354374>.
- Potirakis, S.M., Y. Contoyiannis, N.S. Melis, J. Kopanas, G. Antonopoulos, G. Balasis, C. Kontoes, C. Nomicos, K. Eftaxias, Recent seismic activity at Cephalonia (Greece): a study

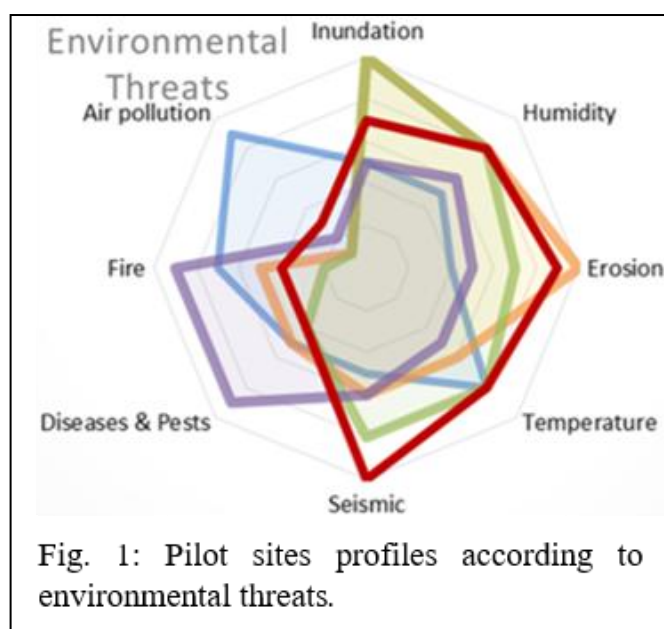
- through candidate electromagnetic precursors in terms of non-linear dynamics, Nonlin. Processes Geophys. **23**, 223-240 (2016a), <http://dx.doi.org/10.5194/npg-23-223-2016>.
- Potirakis, S.M., K. Eftaxias, A. Schekotov, H. Yamaguchi, M. Hayakawa, Criticality features in ultra-low frequency magnetic fields prior to the 2013 M6.3 Kobe earthquake, Ann. Geophysics **59**, S0317 (2016b). <https://doi.org/10.4401/ag-6863>.
 - Potirakis, S.M., A. Schekotov, T. Asano, M. Hayakawa, Natural time analysis on the ultra-low frequency magnetic field variations prior to the 2016 Kumamoto (Japan) earthquakes, J. Asian Earth Sci. **154**, 419–427 (2018a), <https://doi.org/10.1016/j.jseaes.2017.12.036>.
 - Potirakis, S.M., Y. Contoyiannis, T. Asano, M. Hayakawa, Intermittency-induced criticality in the lower ionosphere prior to the 2016 Kumamoto earthquakes as embedded in the VLF propagation data observed at multiple stations, Tectonophysics **722**, 422-431 (2018b), <https://doi.org/10.1016/j.tecto.2017.11.020>.
 - Potirakis, S.M., T. Asano, M. Hayakawa, Criticality analysis of the lower ionosphere perturbations prior to the 2016 Kumamoto (Japan) earthquakes as based on VLF electromagnetic wave propagation data observed at multiple stations, Entropy **20**, 199 (1-17) (2018c), <http://dx.doi.org/10.3390/e20030199>
 - Potirakis, S.M., Y. Contoyiannis, A. Schekotov, T. Asano, M. Hayakawa, Analysis of the ultra-low frequency magnetic field fluctuations prior to the 2016 Kumamoto (Japan) earthquakes in terms of the method of critical fluctuations, submitted (2018d).
 - Pulinets, S., K. Boyarchuk, *Ionospheric Precursors of Earthquakes* (Springer-Verlag, Berlin/Heidelberg, 2005), ISBN: 9783540208396, <http://dx.doi.org/10.1007/b137616>.
 - Uyeda, S., T. Nagao, M. Kamogawa, Short-term earthquake prediction: Current status of seismo-electromagnetics, Tectonophysics **470**(3-4), 205-213 (2009), <https://doi.org/10.1016/j.tecto.2008.07.019>
 - Uyeda, S., On earthquake prediction in Japan, Proc Jpn Acad Ser B Phys Biol Sci. **89**(9), 391–400 (2013) <http://dx.doi.org/10.2183/pjab.89.391>.
 - Varotsos, P.A., *The Physics of Seismic Electric Signals* (TERRAPUB, Tokyo, 2005), ISBN: 4887041365.
 - Varotsos, P.A., N.V. Sarlis, E.S. Skordas, *Natural Time Analysis: The New View of Time* (Springer-Verlag, Berlin/Heidelberg, 2011), ISBN: 9783642164484, <http://dx.doi.org/10.1007/978-3-642-16449-1>

A decision making system using Deep Learning for earthquake prediction by means of electromagnetic precursors

S.M. Potirakis¹, P. Kasnesis¹, C.Z. Patrikakis¹, Y. Contoyiannis¹, N.A. Tatlas¹, S.A. Mitilineos¹, T. Asano², M. Hayakawa²

¹*Department of Electrical and Electronics Engineering, University of West Attica, Campus 2, 250 Thivon and P. Ralli, Aigaleo, Athens, GR-12244, Greece; spoti@puas.gr, pkasnesis@yahoo.gr, bpatr@puas.gr, yiaconto@puas.gr, ntatlas@puas.gr, smitil@puas.gr;* ²*Hayakawa Institute of Seismo Electromagnetics Co. Ltd., UEC (University of Electro-Communications) Alliance Center #521, 1-1-1 Kojimacho, Chofu, Tokyo, 182-0026, Japan; asano@hi-seismo-em.jp, hayakawa@hi-seismo-em.jp*

When a catastrophic event such as an earthquake (EQ) occurs, general guidelines related to the specific event particular location, must be dynamically adapted in near real time by ad-hoc team of experts in order to identify the most urgent recovery actions for the specific emergency. The procedure for hazard risk management, includes several pre and post disaster interventions to be considered in the preparedness and response phases of risk management. (STORM, 2018). In the case of EQs, the pre-disaster interventions, and level of preparedness are undoubtedly the most important phases in risk management. Therefore, possible EQ prediction, could help avoid disastrous effects caused by an EQ on vulnerable structures, such as these often located in cultural heritage sites. In this work, we propose a strategy for the calculation of the probability for a significant ($M \geq 5.5$) EQ occurrence in order to be co-evaluated within a decision making mechanism which could assist in reaching a high level of



preparedness. Starting from the theoretical presentation of the methodology proposed, a practical implementation through the integration in a decision making system supported by a computer cloud infrastructure for sensory data is presented. As a reference framework under which the proposed methodology can be applied, the STORM project Cloud infrastructure has been used. STORM project (**Safeguarding Cultural Heritage through Technical and Organisational Resources Management**) project is an ongoing H2020 European research project aiming at providing critical decision making tools to all European Cultural Heritage (CH) stakeholders charged to face climate change and natural hazards (STORM, 2018). The project improves existing processes related to three identified areas: Prevention, Intervention and Policies, planning and processes, and has selected several pilots in CH sites, among which seismic risk is the most common threat, as seen in Fig. 1.

The proposed strategy presupposes the existence of a dense-enough network of VLF/LF receivers for the recording of subionospheric propagation data covering the areas of cultural interest. As an exemplary model of such a network, the network of 8 VLF/LF receivers operating during the last few years throughout Japan which receive subionospheric signals from different transmitters located both in the same and other countries is considered. Based on data collected during a three-year period of operation of the specific network for specific subionospheric propagation quantities we intend to investigate deep-learning (DL) methods for the estimation of the probability for a significant EQ to occur.

According to the conventional nighttime fluctuation method (Hayakawa, 2011), the daily (1 per day) normalized values DP^* , TR^* , and NF^* of the quantities “trend”: $TR = \sum_{N_s}^{N_e} dA(t)/(N_e - N_s)$, “dispersion”: $DP = \sqrt{(1/N_e - N_s) \sum_{N_s}^{N_e} (dA(t) - TR)^2}$, and “nighttime fluctuation”: $NF = \sum_{N_s}^{N_e} (dA(t))^2$, of the VLF/LF subionospheric propagation data are usually studied. A value exceeding the $\pm 2\sigma$ threshold ($TR^* \leq 2\sigma$, $DP^* \geq 2\sigma$, $NF^* \geq 2\sigma$) is considered a candidate precursor. The normalized values are calculated as $X^* = (X - \langle X \rangle_{\pm 15\text{days}})/\sigma_{\pm 15\text{days}}$, where $\langle X \rangle_{\pm 15\text{days}}$ and $\sigma_{\pm 15\text{days}}$ denote the mean value and standard deviation ± 15 days around the day of interest, respectively. In the abovementioned equations $dA(t)$ is the residue between the received signal amplitude $A(t)$ and an average signal amplitude $\langle A(t) \rangle$ calculated by means of a running average over ± 15 days as $dA(t) = A(t) - \langle A(t) \rangle$, and N_s and N_e are the time points of the start and end of the nighttime depending of the period of the year.

Based on the variation of the abovementioned subionospheric propagation quantities normally a prediction of an upcoming EQ determining time period, position and magnitude is made. Considering that a prediction is successful in the cases that (a) the EQ occurred ± 2 days from the predicted period, (b) the EQ epicenter was within a radius of 50km around the predicted position, and (c) the magnitude was up to 0.5 different from the predicted one, the success rate of the conventional nighttime fluctuation method is $\sim 65\%$ based on the results during the last five years.

DL is a particular branch of machine learning that is based on Artificial Neural Networks (ANNs). In contrast to other machine learning techniques, DL algorithms are capable of extracting features that are a non-linear combination of the input features and are represented in the hidden layer. Previous works based on shallow ANNs (Popova et al., 2013) have proven to be efficient in predicting seismic events based on low-frequency signal monitoring. However, in case of time-series data conventional ANNs cannot capture the local dependencies (Zeng et al., 2014).

Recurrent Neural Networks (RNNs) are a family of neural networks for processing a sequence of values (Goodfellow et al., 2016), and are applied broadly to natural language processing and time-series analysis. In particular, a value x_i depends on a set of previous n values $\{x_{i-1}, x_{i-2}, \dots, x_n\}$. This sequential dependency is represented by adding weighted connections between the hidden states h (Fig. 2A). Moreover, in order to enhance the memory of the network, a mechanism named LSTM (Long Short-Term Memory) (Hochreiter and Schmidhuber, 1997) is applied to it (Fig. 2B).

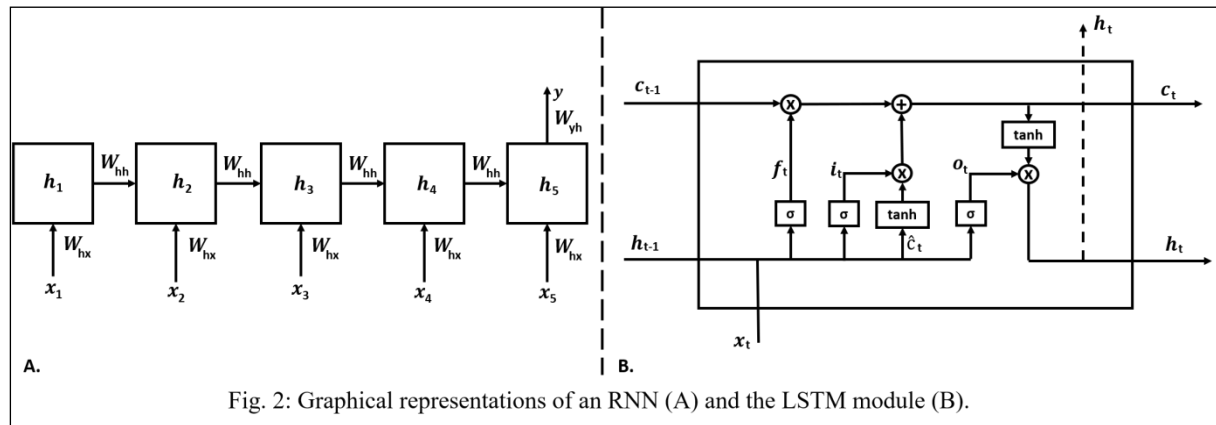


Fig. 2: Graphical representations of an RNN (A) and the LSTM module (B).

LSTM mechanism is capable of learning long-term dependencies, since it uses cell states c^t to transfer information among the hidden units h_t . Furthermore, LSTM, also, makes use of activation gates in order to forget information from the cell state (forget gate f_t), enter new

information to the cell state (input gate i_t), and pass information (output gate o_t) to the next hidden state. It should be noted, that similarly to the RNNs the values of the hidden state h_t are updated at every time step t , which in our case represents a day. The equations for representing the update of an LSTM layer are as follows:

$$f_t = \sigma(W_{fx}x_t + W_{fh}h_{t-1} + b_f) \quad (1)$$

$$i_t = \sigma(W_{ix}x_t + W_{ih}h_{t-1} + b_i) \quad (2)$$

$$o_t = \sigma(W_{ox}x_t + W_{oh}h_{t-1} + b_o) \quad (3)$$

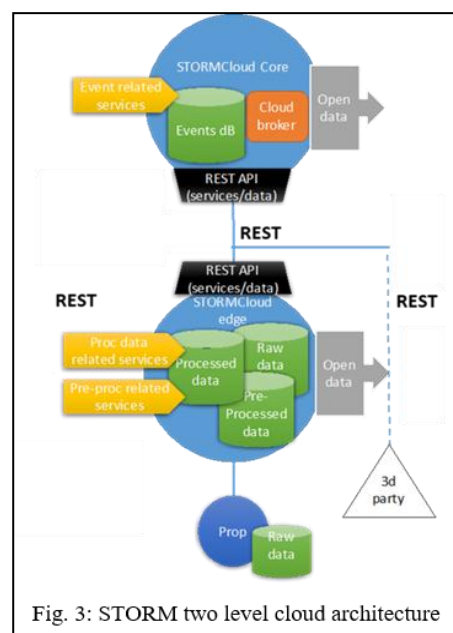
$$\hat{c}_t = \tanh(W_{\hat{c}x}x_t + W_{\hat{c}h}h_{t-1} + b_{\hat{c}}) \quad (4)$$

$$c_t = f_t * c_{t-1} + i_t \hat{c}_t \quad (5)$$

$$h_t = o_t * \tanh(c_t) \quad (6)$$

where \hat{c}_t denotes the new candidate values for the cell state, and the terms W are the weight matrices, with subscripts representing the connections between the gates and the input vector x_t . Finally, b denotes the bias term that is related to a particular gate.

Having in mind the effectiveness of the Deep RNNs on signal processing tasks (Ordóñez and Roggen, 2016), using an RNN enhanced with the LSTM cell seems to be a well-suited candidate for predicting seismic events. As it is illustrated by Fig. 2A, the per day extracted features x_t (DP^* , TR^* , and NF^*) are going to feed the LSTM layer that after being trained it will output a value y_t between 0 and 1, showing how much the subionospheric perturbations, which occurred within the previous days, are correlated with a seismic event.



Preliminary results of the proposed strategy are discussed.

Coming to the practical application of the work presented in this paper, the proposed methodology can be applied in the context of a two level architecture for the detection and

mitigation of risks, as the one adopted in STORM project (Fig. 3). The architecture using a two level cloud based infrastructure can deploy the pre-processing of data and the corresponding algorithms for seismic detection, at an edge cloud level, providing results in the form of identified risk events at a second (core-cloud) level, where they can be assessed and also evaluated across other sources for decision making.

Acknowledgment

Work presented in this paper has received funding from the European Union's Horizon 2020 research and innovation Programme under STORM project, grant agreement n°700191.

References

- STORM Project web site, available at <http://storm-project.eu>, last accessed May 10, 2018.
- Goodfellow, I., Bengio, Y., Courville, A., 2016. Deep Learning (Adaptive Computation and Machine Learning series). MIT Press. Ch. 10. pp. 373-422.
- Hayakawa, M., 2011. Probing the lower ionospheric perturbations associated with earthquakes by means of subionospheric VLF/LF propagation. *Earthq. Sci.* 24, 609–637, doi:10.1007/s11589-011-0823-1.
- Hochreiter, S., Schmidhuber, J., 1997. Long short-term memory. *Neural Computation* 9(8), 1735-1780, doi: 10.1162/neco.1997.9.8.1735.
- Ordóñez, F. J., Roggen, D., 2016. Deep convolutional and LSTM recurrent neural networks for multimodal wearable activity recognition. *Sensors* 16(1), 1-25, doi:10.3390/s16010115.
- Popova, I., Rozhnoi, A., Solieva, M., Levin, B., Hayakawa, M., Hobara, Y., Biagi, P. F., Schwingenschuh, K., 2013. Neural network approach to the prediction of seismic events based on low-frequency signal monitoring of the Kuril-Kamchatka and Japanese regions. *Annals of Geophysics* 56(3), R0328, doi:10.4401/ag-6224.
- Zeng, M., Nguyen, L. T., Yu, B., Mengshoel, O. J., Zhu, J., Wu, P. Juyong Zhang, J., 2014. Convolutional neural networks for human activity recognition using mobile sensors. In Proc. 6th IEEE Int. Conf. on Mobile Computing, Applications and Services (MobiCASE), 6-7 Nov. 2014, pp. 197-205, doi:10.4108/icst.mobicas.2014.257786.

Constraining seismic sources using electromagnetic geothermometry: Hengill volcano (Iceland) case study

V. Spichak¹, O. Zakharova¹, A. Goidina¹

¹Geoelectromagnetic Research Centre IPE RAS, Moscow, Russia, v.spichak@mail.ru

The Earth's crust in Iceland is composed of volcanic rocks with inclusions of intrusive and effusive rocks (mainly oceanic-type flood basalts, tuffs, hyaloclastites, and some felsic rocks). The high-temperature Hengill area is a triple junction zone of intersection of the Western Volcanic Zone (WVZ), the Reykjanes Peninsula Rift (RPR), and the South Icelandic Seismic Zone (SISZ), which is located in the southwest of the island (Fig.1, upper panel). The Hengill volcanic complex comprises several interconnected geothermal fields located in different directions with respect to the Mt Hengill.

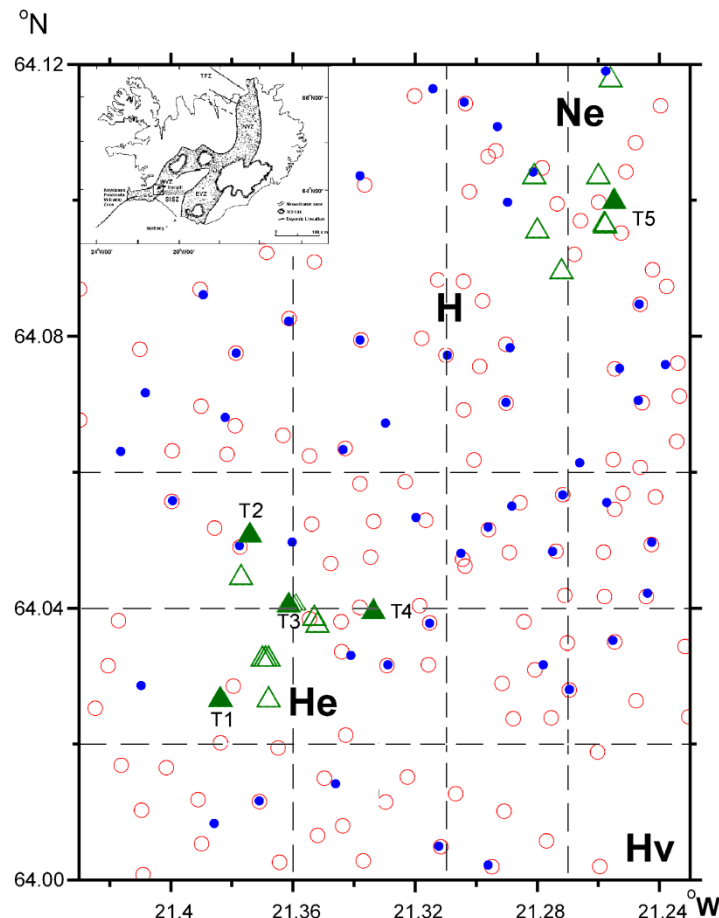


Fig. 1. Upper panel: location of the study area. Lower panel: map of the EM sites and boreholes. Circles mark TDEM sites, dots indicate MT sites, triangles mark boreholes (shaded ones mark boreholes used for EM geothermometer testing). H means Mt Hengill, He - Hellisheidi, Ne - Nesjavellir, Hv – Hveragerdi.

The stability of the spatiotemporal structure of seismicity in the region as well as the fact that seismic activity here is largely confined to the geothermally active areas while almost absent on the plate boundaries indicates that seismicity is controlled by geothermal processes which lead to the buildup of local stresses rather than by the tectonic activity caused by spreading.

A vast high-temperature geothermal area that includes the Hengill and Gresdalur central volcanoes as well as the transversal tectonic structure between them is characterized by continuous microseismicity. There is a strong negative correlation between the seismicity and faulting observed at the surface: the earthquakes are clustered around the SN or WNW-ESE azimuths but not in the SSW-NNE direction which dominates the surface geology (Fig.2). On the other hand, the seismicity spatially correlates with heat losses through the surface, which indicates that seismic activity in this region is associated with geothermal processes rather than with the plate boundary.

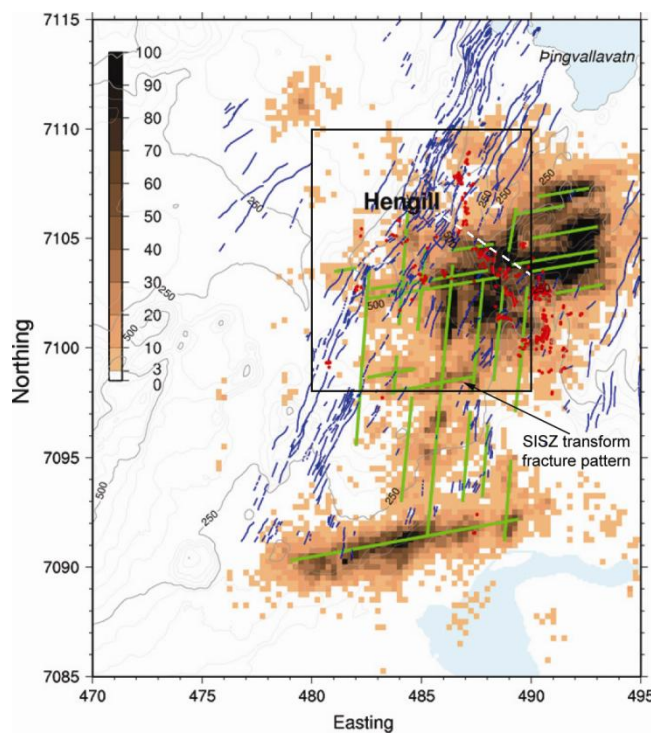


Fig. 2. Density of seismic epicentres (number within 250m x 250m bins) from 1991 to 2001 and inferred transform tectonic lineaments (light grey lines) based on the overall distribution of the seismicity (dark grey lines: faults and fissures mapped on the surface; dots: geothermal surface manifestations). (Stefansson et al., 1993). Rectangle bounds the study area, white dashed line indicates location of the Olkelduhals secondary tectonic structural trend.

The seismicity is located in the areas with electrical resistivity ranging between 15Ωm and 100Ωm (Spichak et al., 2011), which could be explained by higher porosity void of melt fractions. It is remarkable that the hypocenters cluster in the regions characterized by both

increased and decreased P-wave velocities as well as of Vp/Vs ratio (Jousset et al., 2011), which indicates that seismic velocities alone are not indicative of the seismicity pattern. Even joint analysis of the resistivity and seismic velocities data (see, for instance, above mentioned paper) does not always provide enough information, which might enable to draw conclusions on the seismicity origin.

In order to draw more justified inferences about the processes leading to earthquakes Spichak et al. (2013) have built 3D temperature model of the study area up to the depth 20km. It was constructed by means of the EM geothermometer (Spichak and Zakharova, 2015) using MT and TDEM data collected in this area (Fig. 1). The resulting temperature distribution exhibits two layers of the background temperature (one layer in the depth interval from the surface to 5-7km has a temperature below 200°C; the other layer extending to at least 20km has temperatures from 200 to 400°C. At the same time, the background temperature section which has supposedly gabbro composition, is braided by the interconnected highly conductive high-temperature channels - conduits with a diameter of 1-2km, in the central parts of which the temperature may exceed the basalt solidus.

According to this model, the heat sources for the geothermal system are probably the intrusions of hot magma composed of partly molten basalt, which rise from the depths of the mantle through the faults and fractures to the rheologically weakened layer at a depth of 10-15km and then spread laterally. On the other hand, magma which has risen up to the depths 1.5-2.5km does not form a continuous high-temperature layer, but instead cools down within shallow pockets connected with the underlying hot areas by “chimneys”.

Joint analysis of the temperature and resistivity models together with the gravity data enabled to suggest a new conceptual model of the earth crust of Icelandic type (Spichak et al., 2013). It enabled to reveal the heat sources and discriminate the locations of relict and active parts of the volcanic complex. This, in turn, explains the observed seismicity pattern by different geothermal regimes in four adjacent parts of the area separated by the deep S-N fault constrained between the meridians 21.31° and 21.33°W and a WNW-ESE diagonal band running beneath the second-order tectonic structure of Olkelduhals (Fig. 2).

In the vertical plane, most of the earthquakes in the region are known to occur in a depth interval from 2 to 5-6km. According to the crustal thermal structure discussed above the high-stress areas could be formed due to cooling in the space between the hot channels, which pass below 5-6km, and the local reservoirs at a depth of 1-2km. By correlating the projections of the hypocenters (Jousset et al., 2011; Stefansson et al., 1993) to the vertical temperature cross-sections (Fig. 3), we see that all seismic events are located in the regions where the

temperature is below 400°, which is a silica-rich gabbro solidus. This constraint is consistent with the estimates of the critical temperatures of earthquakes based on the model calculations for different mechanisms of rock deformation, behaviour of the internal friction ratio, and the character of stresses (Tse and Rice, 1986).

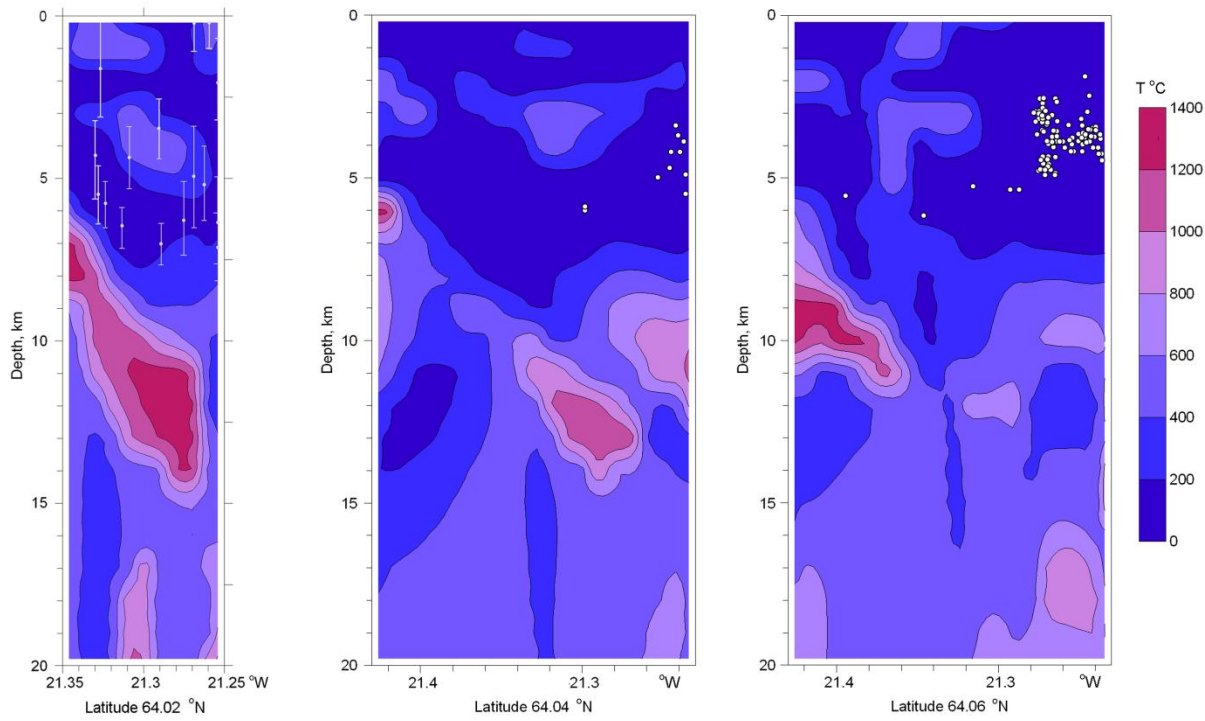


Fig. 3. Temperature cross-sections at different latitudes indicated in the Fig.1. White dots indicate the earthquake hypocenters according to Stefansson (1993) (a) and Jousset et al. (2011) (b, c).

References

- Bjarnason, I., Einarsson, P., 1991. Source mechanism of the 1987 Vatnafjoll earthquake in South Iceland. *J. Geophys. Res.* 96, 4313-4324.
- Jousset, P., Haberland, C., Bauer, K., Árnason, K., 2011. Hengill geothermal volcanic complex (Iceland) characterized by integrated geophysical observations. *Geothermics* 40, 1-24.
- Spichak, V., Goidina, A., Zakharova, O., 2011. 3D geoelectrical model of the volcanic complex Hengill (Iceland). *Trans. KRAUNZ*, 1 (19), 168-180 (in Russian with English abstract).
- Spichak V., Zakharova O., 2015. Electromagnetic geothermometry. Elsevier Inc., Amsterdam.
- Spichak, V.V., Zakharova, O.K., and Goidina, A.G., 2013. A new conceptual model of the Icelandic crust in the Hengill geothermal area based on the indirect electromagnetic geothermometry. *J. Volcanology and Geotherm. Res.*, 257, 99-112.
- Stefansson, R., Bodvarsson, R., Slunga, R., Einarsson, P., Jacobsdottir, S., Bungam, H., Gregerson, S., Hjelme, J., Kerhonnen, H., 1993. Earthquake prediction research in the South

- Iceland Seismic Zone and the SIL Project. Bull. Seismological Society of America 83, 696-716.
- Tse, S. T., Rice, J.R., 1986. Crustal earthquake instability in relation to the depth variation of frictional slip properties. J. Geophys. Res. 91 (B9), 9452-9472.

Reliability of precursor phenomena in Vrancea seismic zone

V.E. Toader¹, I.A. Moldovan¹, C. Ionescu¹, A. Marmureanu¹

National Institute for Earth Physics, Romania, asyst@asystech.ro, iren@infp.ro, viorel@infp.ro, marmura@infp.ro

We analysis the precursor phenomena in the most important seismic area in Romania called Vrancea and characterized by deep earthquakes (90 Km – 200 Km). A multidisciplinary network is concentrated in this area (Fig. 1).

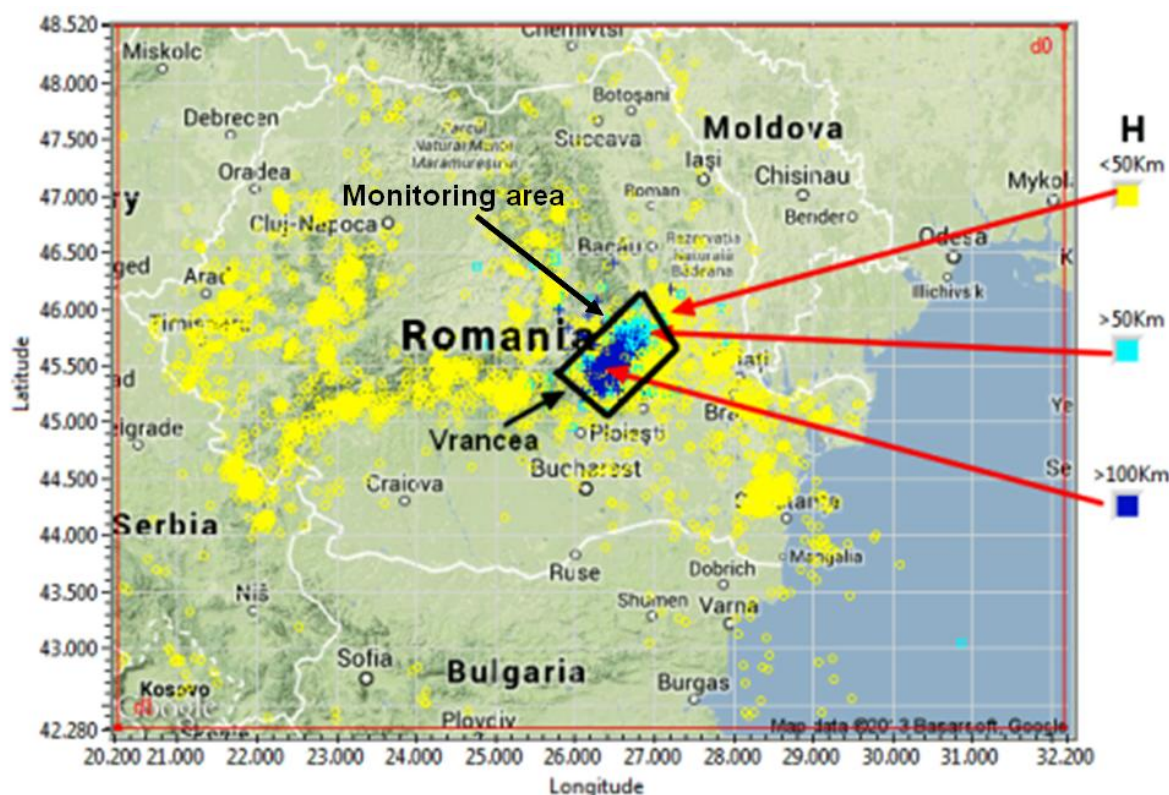


Fig. 1. Romanian seismicity, 2012 – 2018, Vrancea monitoring area

Predicting is impossible by the way it is defined, but short-term forecasting is possible. The main condition is to find locations where precursor phenomena occur and to monitor them according to their characteristics. For example, we have cases where radon emission is a precursor factor, but the electromagnetic field does not. Vrancea is an active zones with particularities generated by geological structure. In this case seismic precursors and analysis methods differ for each monitoring location. We make correlations between several measured parameters: radon concentration, CO₂, solar radiation (direct and reflected in two ranges 0.3 - 3 μm, and Far Infrared Radiation, 4.5 - 42 μm), air ionization, telluric currents, ULF radio

waves disturbance, magnetic field, temperature in borehole and acoustic waves generated by microfracturing of rocks.

An example of multidisciplinary station is presented in Fig. 2.



Fig. 2. Multidisciplinary monitoring station in Vrancioaia

We measure and correlate information from seismic equipment, infrasound, air ionisation (+ and -), radon concentration, telluric currents, solar radiation with a pyranometer, meteorological station and, acoustic (3 microphones are monitoring at 22 KHz sample rate). We recorded the reaction of animals before earthquakes in this location. A video camera monitored 3 years the sky and now the ground for observe the animal behaviour.

An example of multidisciplinary analysis is in Fig.3 that presents seismicity, evolution of radon, telluric field, CO₂, air ionization, magnetic field, meteorological data, NOAA satellite information (K_p), and seismicity in a period with 3 earthquakes around 4R. In general, we are tracking seismic activity to verify our methods, but tectonic stress does not always generate earthquakes, but it produces precursor phenomena.

The solar radiation reflected from ground can be a precursor, too. An effect of tectonic stress is the increases the ground temperature that is radiated into atmosphere. We use a net radiometer with two pyranometers and two pyrgeometers (up and low) for this monitoring.

In our example from Fig. 3 the maximum magnitude is 4.4R. We consider that a magnitude above 6.5 R highlights the precursor factors to daily and seasonal variations.

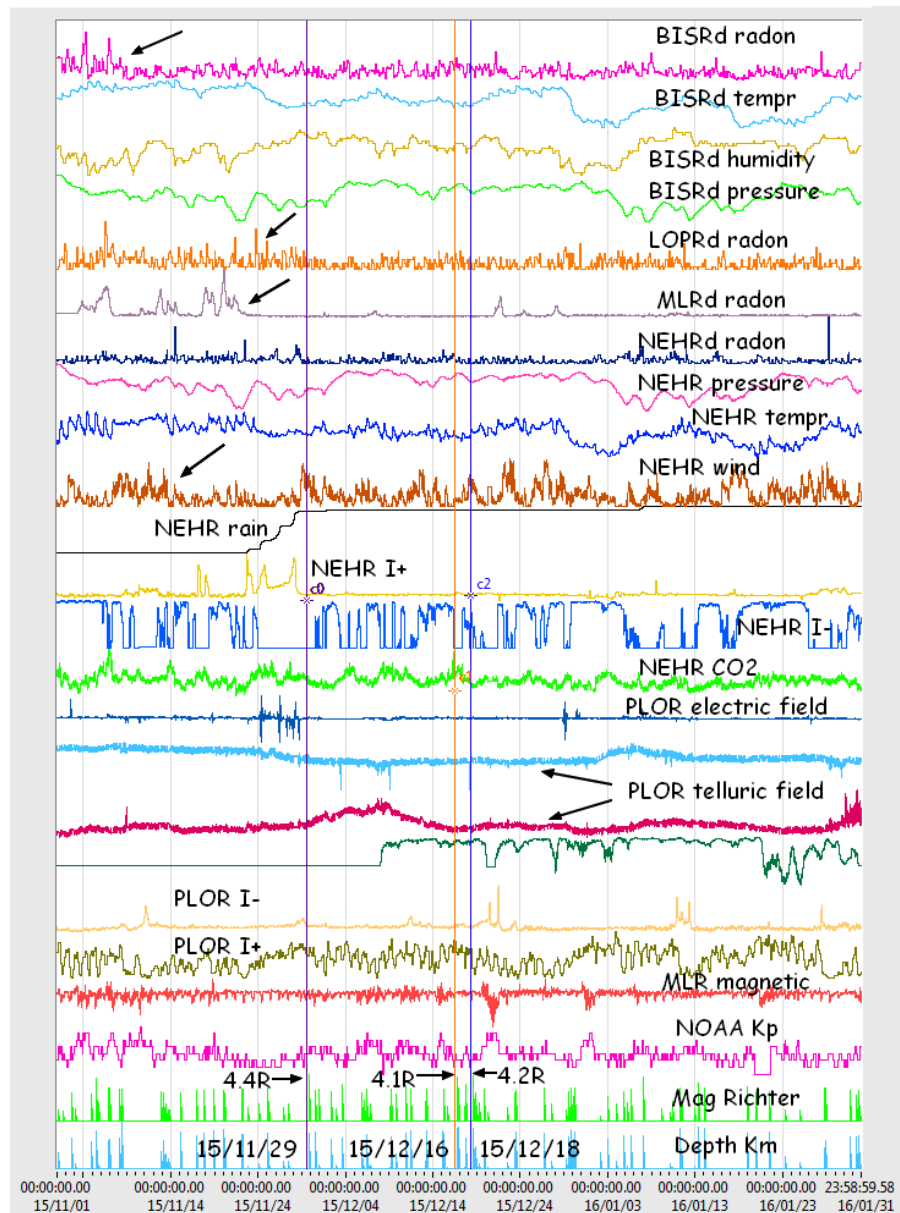


Fig. 3. Multidisciplinary monitoring

In conclusion the precursor factors are reliable only a multidisciplinary network that helps us to understand the precursor phenomena and to make forecasts. There is not a generally pattern that can help us to forecast with high probability because the geological structure of earth is not the same.

Key words: earthquake forecast, earthquake precursors, tectonic stress, multidisciplinary analysis, radon concentration, air ionization, solar radiation.

Acknowledgements

This work was supported by PN18150203 program.

Long-term air ion monitoring applied to earthquake forecasting

S. Warden¹, T. Bleier¹, K. Kappler¹

¹QuakeFinder Inc, Palo Alto, USA, corresponding author: sheldon.warden@gmail.com

Earthquake forecasting can be defined as the ability to assess the probability of an earthquake in a given area within a particular time frame: short-term earthquake forecasting, associated with time windows ranging from several minutes to several days or even weeks prior to the earthquake, is an ongoing debate among the scientific community. While there are numerous reports of both seismic and non-seismic signals measured before earthquakes, the precursory nature of these signals yet remains to be proven. In addition to pre-earthquake signals such as dilatancy-related changes in the ratio of P wave velocity to S wave velocity, anomalies in radon gas concentration or multiple types of electromagnetic perturbations spanning the entire electromagnetic spectrum, high concentrations of air ions prior to earthquakes have been reported in the literature. For instance, Hattori *et al.* (2008) monitored air ion concentration alongside radon concentration and the radiation of collected aerosols, using an array of 10 stations deployed in 2004, named the PISCO array. The authors reported an anomalous change in air ion concentration prior to the Mw7.2 Iwate-Miyagi Nairiku earthquake. Two main theories were advanced to explain anomalies in air ion concentration: the electronic charge carrier theory introduced in Freund *et al.* (2006) and a theory relating increased ionization to radon exhalation, supported by Pulinets and Davidenko (2014) and Surkov (2015).

Aside from trying to validate either of these theories, it is critical to confirm whether anomalies in air ion concentration are indeed a reliable earthquake precursor. This goes through extensive long-term monitoring of air ions in the field. An attempt at tracking outdoors air ion concentrations over several years was made by QuakeFinder, a research project carried by the aerospace company Stellar Solutions, whose goal is to develop a methodology to detect and analyze pre-earthquake electromagnetic signals in order to produce earthquake forecasts. As of April 2018, the Quakefinder array comprised 168 stations worldwide (Figure 1), each station being equipped with three feedback induction magnetometers in the 0.01-12Hz range, a horizontal 4 Hz geophone, a temperature sensor, a relative humidity sensor and two air ion sensors: one for detection of positive air ions (PAI) and one for the detection of negative air ions (NAI). These air ion counters consist of Gerdien

capacitors equipped with a fan pulling the air through the sensor plates at a calibrated rate. These lightweight handheld sensors were modified by the manufacturer AlphaLab to fulfill long-term monitoring duties: each sensor was connected to an A/D converter allowing to sample data at 50 samples for second.



Fig. 1: QuakeFinder stations location as of April 2018. Out of the 168 stations deployed worldwide, 125 are located in California, while the remaining 43 sites are installed in Peru, Chile, Greece, Taiwan and Sumatra.

In order to test the performance of our instruments and to investigate the spatial variability of air ionization, we conducted a Parallel Sensor Test (PST) at a reference station in Portola Valley, California. We first deployed two sensors side by side, 30 inches apart. The two sensors were first set to measure PAI concentration; the following day, they were switched to NAI measurement mode. We repeated the same step, but this time with sensors installed 220 inches apart. The weather was fair throughout the entire test, with no precipitation and average temperatures increasing from 10°C on 14/02 to 13°C on 17/02, well within our sensor's operating range (-10°C to 50°C). The corresponding PAI time series data are displayed in Figure 2.

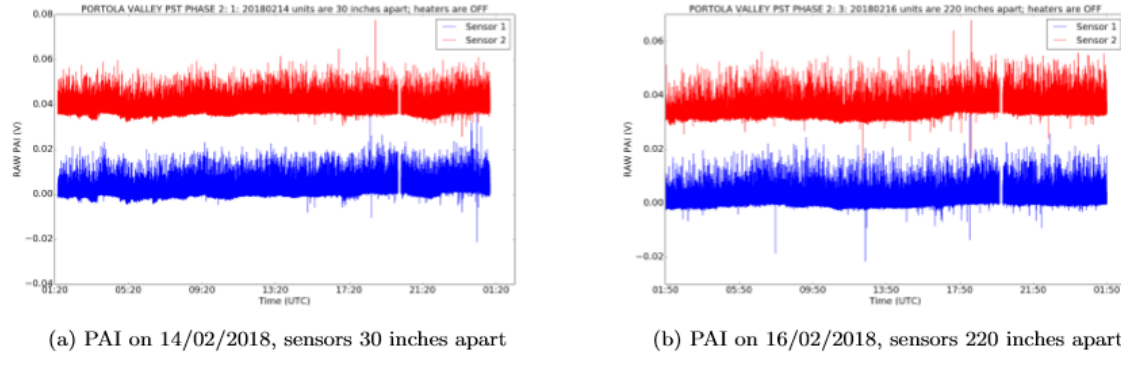


Fig. 2: PAI time series acquired during the Parallel Sensor Test (PST); we represent here the raw data in Volts (V). Output of sensor 1 is represented in blue; output of sensor 2 is displayed in red.

We computed the Pearson correlation coefficient between time series acquired using the two different sensors. The Pearson correlation coefficients confirm a good correlation between PAI time series for distances of both 30 and 220 inches between sensors ($r=0.75$ and 0.81 , respectively). While $r=0.89$ for NAI data for sensors located 30 inches apart, the correlation coefficient decreases to 0.72 when considering sensors 220 inches apart. These values are lower than the correlation coefficient of 0.97 reported by Kolarž *et al.* [2012] for their experiment conducted near the Krimml waterfall in Austria. However, it should be noted that the authors use a different type of instrument for their experiment (namely a CDI-06 unit).

We also computed the unipolarity coefficient for multiple datasets (Figure 3). The unipolarity coefficient is defined as the ratio between PAI and NAI concentrations. Unipolarity coefficient values reported in the literature are generally slightly greater than, but close to 1, due to the surface of the Earth being negatively charged (the global electric circuit).

One of our preliminary conclusions is that monitoring the unipolarity coefficient could prove an effective way to detect anomalous episodes in air ion data. Some of the pre-earthquake anomalies observed in QuakeFinder data were indeed associated with an imbalance between PAI and NAI concentrations. However, abnormal values of the unipolarity coefficient may also be due to sensor saturation, caused by condensation forming over the capacitor plates. Sensors tend to saturate more often after having been deployed in the field for extended periods of time (Bleier, personal communication). A way to circumvent this problem would be to mount heaters at the entry of the Gerdien tubes, an approach now undertaken by QuakeFinder for its next generation of stations.

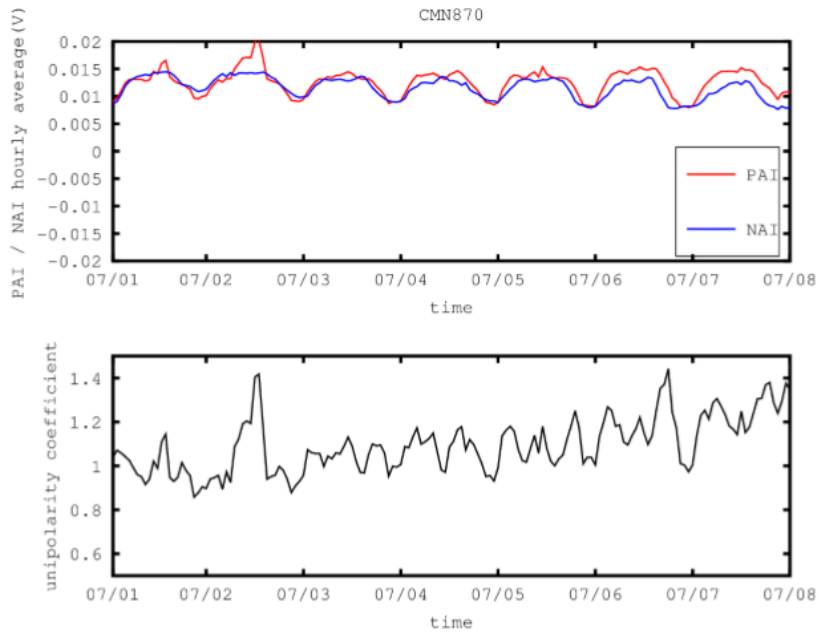


Fig. 3 (a) PAI and NAI time series from 07/01 to 07/08/2014 for station 870 (Benicia, California, USA), averaged using a 1 hour window. (b) Unipolarity coefficient.

References:

- F.T. Freund, A. Takeuchi, and B.W.S. Lau. Electric currents streaming out of stressed igneous rocks – A step towards understanding pre-earthquake low frequency EM emissions. *Physics and Chemistry of the Earth, Parts A/B/C*, 31(4-9):389– 396, January 2006. ISSN 14747065. doi: 10.1016/j.pce.2006.02.027.
- K. Hattori, K. Wadatsumi, R. Furuya, N. Yada, I. Yamamoto, K. Ninagawa, Y. I detta, and M. Nishihashi. Variation of Radioactive Atmospheric Ion Concentration Associated With Large Earthquakes. AGU Fall Meeting Abstracts, December 2008.
- P. Kolarž, M. Gaisberger, P. Madl, W. Hofmann, M. Ritter, and A. Hartl. Characterization of ions at Alpine waterfalls. *Atmospheric Chemistry and Physics*, 12 (8):3687–3697, 2012. ISSN 1680-7324. doi: 10.5194/acp-12-3687-2012
- S. Pulinets and D. Davidenko. Ionospheric precursors of earthquakes and Global Electric Circuit. *Advances in Space Research*, 53(5):709–723, March 2014. ISSN 02731177. doi: 10.1016/j.asr.2013.12.035.
- V. Surkov. Pre-seismic variations of atmospheric radon activity as a possible reason for abnormal atmospheric effects. *Annals of Geophysics*, 58(5): A0554, November 2015. ISSN 1593-5213. doi: 10.4401/ag-6808.

Progress and development trend of comprehensive prediction Method for large earthquakes in China

Z. Zeng¹, Y. Deng¹, Q. Dai¹, F. Li¹, G. Hao¹, Q. Du¹, V. Sibgatulin²

¹*China University of Geosciences, Wuhan, China, zuoxun.zeng@126.com;* ²*Special Design and Technological Bureau "Nauka", Siberian Branch of the Russian Academy of Sciences, Krasnoyarsk, Russia, ec_ropr@mail.ru*

This paper summarizes the research progress of the comprehensive prediction method and technology of large earthquakes developed in China in recent years. It includes:

1. The ultra-low frequency natural electric potential difference method with small electrode distance. The geoelectricity instrument is designed and named DD108 by ourselves. It can be used to predict the occurring time and magnitude of large earthquakes world widely.
2. The precursor signal is usually about 7 days before the occurring time of an large earthquake.

The relationship between the magnitude M and the period T of the precursory wave can be expressed as:

$$M=1.37\lg T+1.19$$

3. The geomagnetic method to predict the epicenter and magnitude with size of the abnormal geomagnetic high intensity area, abnormal amplitude and their variation among observation stations.
4. The natural electromagnetic pulse method with one or two days in advance of large earthquake for an obvious quiet period in the whole frequency bands of pulse signals.
5. The satellite gravity anomaly method with the intersection of steep gradient and active faults to predict the epicenter.
6. The geogas escaping method with the escaping center for the epicenter and escaping scale for the magnitude.
7. The geothermal method with the west edge or center point of the isolated heating region to predict epicenter and with the size of the heating area to predict the magnitude.
8. The sea surface temperature method with the isolated heating center or current "upstream" anomaly edge to predict the epicenter and with the size of the SST abnormal region to predict the magnitude.
9. The flow line method with the converging center of the air flow lines in the atmosphere

to predict the epicenter and with the size of the area involved the converging flow lines.

10. The air pressure drop method with the large scale drop center to predict the epicenter and the scale of the drop area and the decrease extent to predict the magnitude.

11. The ground tilt method combining with landslide observation. The rise side of tilt and the back side of the landslide point to the epicenter.

12. The high altitude cloud method with the shape and color of the long distant cloud to predict the magnitude, occurring time and the general direction of the epicenter.

13. The troposphere temperature method with the butterfly pattern of the troposphere temperature curves in different altitudes.

Comprehensive monitoring and prediction of big data system with the combination of different monitoring and predicting methods is the development direction of large earthquake prediction.

Acknowledgements

This paper is funded by the national natural science foundation of China (grand No. 41230206).

Author List

- Agibayev; 77
Alanis; 94
Ambrosi; 18; 20
Ammendola; 21
Anagnostopoulos; 45; 46
Apostol; 196
Arabelos; 154
Asano; 212; 217
Avagimov; 191
Avalle; 50
Aydogar; 28
Badoni; 21
Balasco; 47; 48
Barbara; 155; 157; 159
Battiston; 18; 20
Bellanova; 50; 51
Bertello; 21; 139
Berthelier; 162; 163
Besser; 28
Biagi; 83; 140; 142; 169
Błęcki; 146
Bleier; 82; 230
Bogomolov; 191
Bonano; 113
Boniolo; 185
Boudjada; 28; 140; 169
Bragin; 191
Caielli; 185
Calamita; 50; 51
Candidi; 139
Capozzoli; 72
Castellanza; 185
Casu; 113
Catapano; 176
Cavalagli; 176
Cervantes-De La Torre; 52
Cesaroni; 117
Chatzopoulos; 190
Chen CH; 173
Chen Y; 150
Cheng Y; 19
Chi; 133
Chiuzzi; 51; 131
Choudhary Sh; 198
Choudhary Su; 151; 198
Cianchini; 117
Cipollone; 21
Colella; 140
Colonna; 152
Constantin; 83
Contadakis; 140; 154
Conti; 18; 20; 21
Contin; 18; 20
Contoyiannis; 212; 217
Čop; 61
Crosta; 185
CSES-LIMADOU Collaboration; 18; 20; 21
Currenti; 199
D'Arcangelo; 130
Dai; 234
Davidenko; 206
de Franco; 185
De Luca; 113
De Santis A; 18; 20; 117; 130; 189
De Santis C; 18; 20; 21
Delva; 28
Deng; 234
Depuev; 155; 159
Depueva; 155; 157; 159
Devi; 155; 157; 159
Di Giovambattista; 117
Diego; 21; 139
Ding; 22
Du P; 24; 34
Du Q; 234
Duchkova; 66
Dyadkov; 66
Efstathiou; 118; 121
Eftaxias; 212
Eichelberger; 28; 140; 169
Eleftheriou; 204
Ellmeier; 28
Ermini; 140
Facca; 207
Falconieri; 123; 129
Fan M; 133
Fedi; 180
Fedun; 142; 169; 206

- Fidani; 68; 87; 124
Filizzola; 128
Fiorenza; 21
Fu; 204
Furuya; 164
Gallipoli; 51
Gaudiosi; 50
Genzano; 128
Gherardi; 207
Giallini; 50
Giampaolo; 72
Goidina; 222
Gonzalez-Trejo; 52
Goto; 173
Gour; 151
Grimalsky; 142
Gritsay; 142
Guan Y; 22; 25; 33
Gwal; 151
Haagmans; 146
Hagen; 28
Han J; 19
Han P; 76; 205
Hao; 234
Hattori; 76; 164; 204; 205
Hatzopoulos; 204
Hayakawa; 169; 212; 217
Hu; 175
Huang J; 16; 19; 23; 27; 32; 33; 35
Huang QH; 175
Igarashi; 173
Inbar; 77
Ionescu; 227
Ippolito; 117
iSTEP/CAPE groups; 138
Iuppa; 18; 20
Izutsu; 37
Jernej; 28
Jing; 202
Johnston; 94; 181
Kachakhidze; 140
Kafatos; 204
Kamogawa; 37; 161; 162; 163; 203
Kappler; 82; 230
Karastathis; 204
Karli; 45; 46
Kasnesis; 217
Katzis; 140
Kojima; 164
Kondo; 37
Kong; 22
Konishi; 164
Kozlova; 66
Krankowski; 142
Kuleshov; 66
Lacava; 129
Lammegger; 28
Lanari; 109; 113
Lanzo; 50
Lather; 151
Lazaridou-Varotsos; 41
Le Mouël; 38
Lee; 204
Leonhardt; 28
Li C; 24; 34
Li F; 234
Li K; 133
Li W; 23
Li X; 24; 34
Li Z; 24; 34
Lisi; 128
Liu C; 22; 25; 33
Liu G; 24; 34
Liu JY; 138; 150; 205
Lohiya; 151
Lu; 27
MacLean; 82
Magnes; 28
Makris; 183
Mancini; 50
Manunta; 113
Manzo; 113
Marchese; 123; 129
Marchetti; 117; 130; 189
Marmureanu; 227
Masciantonio; 21
Masi; 51; 131
Mazzeo; 129
Michas; 183
Mihai; 196
Mitilineos; 217
Moldovan A; 83
Moldovan IA; 83; 140; 196; 227
Mollica; 185
Moscatelli; 50
Motti; 185

- Muntean; 83; 196
Nagao; 37; 94; 161; 162; 163; 203
Napoli; 199
Nastase; 83
Nicodemo; 131
Ninagawa; 164
Noda; 203
Novikov; 165; 191
Oikonomou; 83
Omura; 164
Onorato; 113
Orihara; 37; 161; 162; 163; 203
Orsini; 87
Osteria; 18; 20
Ouyang; 35
Ouzounov; 164; 195; 204; 205; 206
Padeletti; 176
Pagliaroli; 50
Pastoressa; 47
Patgiri; 159
Patrikakis; 217
Pergola; 123; 128; 129
Perrone A; 50; 51
Perrone L; 117
PHIVOLCS EM Team; 94
Picozza; 18; 20; 21
Pierotti; 207
Piersanti; 139
Piscini; 117; 130; 189
Piscitelli; 50; 51
Poggio; 130
Pollinger; 28
Polpetta; 50
Potirakis; 212; 217
Prattes; 28
Pulinets; 195; 204; 205; 206
Rapoport; 142
Razzano; 50
Real-Ramirez; 52
Reniva; 94
Reuveni; 77
Ricci; 18; 20
Rigas; 46
Rizzo; 72
Romanenko; 66
Romano; 47; 48
Rozhnoi; 28; 142; 169; 206
Ruzhin; 90; 155; 159; 165
Rybin; 191; 206
Santarsiero; 51
Sarlis; 41
Sasai; 94
Schekotov; 212
Schelochkov; 191
Schiavulli; 140
Schneider; 82
Schwingenschuh; 28; 140; 169
Shen X; 16; 27; 28; 33; 35
Shi; 103
Shimo; 164
Sibgatulin; 234
Silva; 140
Simionato; 50
Singh; 202
Siniscalchi; 47; 48
Sirianni; 50
Skeberis; 140
Skordas; 41
Słomińska; 146
Słomiński; 146
Soldovieri; 176
Solovieva; 142; 169; 206
Sorokin; 90; 98; 165
Sottili; 50
Sparvoli; 18; 20; 21
Spichak; 222
Spogli; 117
Spyroglou; 46
Srivastava; 206
Stabile; 51
Stănică D; 99
Stănică DA; 99
Sugiura; 37
Sun; 22; 25
Surkov; 98
Sychev; 191
Tarasov; 191
Tatile; 217
Tian Z; 22
Toader; 83; 196; 227
Toma; 83
Tramutoli; 123; 128; 129; 152
Tripaldi; 48
Tsibizov; 66
Tsinganos; 204
Ubertini F; 176

- Ubertini P; 18; 20; 21; 139
Uchida; 173
Umeno; 173
Uyeshima; 94
Vallianatos; 183; 190
Vannaroni; 21
Vargemezis; 38
Varotsos; 41; 118; 121
Vergos; 154
Vignaroli; 50
Vignola; 51
Villa; 185
Wan; 19
Wang J; 28
Wang Q; 32
Wang W; 22
Wang Y; 35
Warden; 230
Wolbang; 28
Wronowski; 146
Wu; 35
Yan; 33
Yang; 16
Yashchenko; 98; 165
Yoshino; 164
Yu; 133
Yuan S; 16
Yuan X; 34
Zakharova; 222
Zeigarnik; 191
Zeng J; 103
Zeng L; 32
Zeng X; 103
Zeng Y; 103
Zeng Z; 234
Zeren; 35
Zhang A; 22; 25
Zhang J; 24; 34
Zhang X; 16; 35
Zhao S; 16; 23; 27; 35
Zheng; 22; 25
Zhou; 19
Zhu K; 133
Zhu X; 16
Zhu XH; 24; 34
Zinno; 113
Zlotnicki; 38; 94
Zoffoli; 18; 20



With the contribution of:



International Union of Geodesy and Geophysics



International Association of Geomagnetism and Aeronomy



International Association of Volcanology and Chemistry of the Earth's Interior.



International Association of Seismology and Physics of the Earth's Interior



Università degli Studi della Basilicata - Scuola di Ingegneria



Consiglio Nazionale delle Ricerche - Istituto di Metodologie per l'Analisi Ambientale



Istituto Nazionale di Geofisica e Vulcanologia



**MIBAC
Polo Museale Regionale della Basilicata**



Comune di Potenza



Comune di Marsico Nuovo



Fondazione ENI Enrico Mattei



Fondazione Ambiente Ricerca Basilicata



Parco Nazionale Appennino Lucano Val D'Agri Lagonegrese



Fondazione Matera-Basilicata 2019



Pre WiFi



TEP Car

with the contribution of



International Union
of Geodesy and
Geophysics (IUGG)



International Association
of Geomagnetism and Aeronomy



International Association of Volcanology
and Chemistry of the Earth's Interior



International Association of Seismology
and Physics of the Earth's Interior



Consiglio Nazionale
delle Ricerche

imaa
Istituto di
metodologie per
l'analisi ambientale



Università degli Studi della Basilicata
Scuola di Ingegneria



MINISTERO
DEI BENI E DELLE
ATTIVITÀ CULTURALI
E DEL TURISMO
DIREZIONE GENERALE MUSEI
POLO MUSEALE REGIONALE
DELLA BASILICATA



Fondazione Eni
Enrico Mattei



FARBAS
Fondazione Ambiente Ricerca Basilicata



MATERA 2019
OPEN FUTURE



ISBN 978-88-99432-45-4



9 788899 432454
editrice universosud